

**SYNTHESIS, CHARACTERIZATION AND BIOLOGICAL
EVALUATION OF SOME NOVEL BIOACTIVE
HYDRAZONE DERIVATIVES**



Thesis to be submitted to Bharathidasan University, Tiruchirappalli
In partial fulfillment of the requirements for the award of the degree of
DOCTOR OF PHILOSOPHY IN CHEMISTRY

By
V. PRIYADARSHINI

Ref. No: 05706/Ph.D.K2/Chemistry/Full-Time/July-2017/Date: 30.06.2017

Extn: Ref. No: 05706/Ph.D.K2/Chemistry/Full-Time/July-2017/Date: 28.09.21

Under the guidance of
Dr. K. THARINI, M.Sc., M.Ed., M. Phil., Ph.D.,



PG AND RESEARCH DEPARTMENT OF CHEMISTRY
GOVERNMENT ARTS COLLEGE
TIRUCHIRAPPALLI – 620 022
TAMILNADU, INDIA
APRIL-2022

Dr.K.THARINI. M.Sc .,M.Ed., M.Phil., Ph.D., PGDCA.,

PG & Research Department of Chemistry,

Government Arts College, Thuvakudimalai,

Tiruchirappalli-620022. Tamilnadu, India.



CERTIFICATE

This is to certify that the thesis entitled “**SYNTHESIS, CHARACTERIZATION AND BIOLOGICAL EVALUATION OF SOME NOVEL BIOACTIVE HYDRAZONE DERIVATIVES**” is a bonafide record of research work done by **Miss. V.PRIYADARSHINI** (Ref No: 05706/Ph.D.K2/Chemistry/Full–Time/July-2017/Date: 30.06.2017) Department of Chemistry, Government Arts College, Tiruchirappalli-22 under my guidance during the period **2017-2022** and that this thesis has not previously formed the basis for the award of any degree, diploma, associateship, fellowship or an similar title to the candidate. This is also to certify that the thesis represents the independent work of the candidate.

Place: Tiruchirappalli

Date:05.04.2022

(Dr. K. THARINI)

Research Supervisor

V.PRIYADARSHINI

(Ref No: 05706/Ph.D.K2/Chemistry/Full–Time/July-2017/Date: 30.06.2017)

Research Scholar

PG& Research Department of Chemistry,

Government Arts College, Thuvakudimalai,

Tiruchirappalli-620022. Tamilnadu, India.

DECLARATION

I hereby declare that the work embodied in this thesis entitled “**SYNTHESIS, CHARACTERIZATION AND BIOLOGICAL EVALUATION OF SOME NOVEL BIOACTIVE HYDRAZONE DERIVATIVES**” is a research work done by me under the supervision and guidance of **Dr. K. THARINI**, Assistant Professor, Department of Chemistry, Government Arts College, Tiruchirappalli – 620022. The thesis or any part thereof has not formed the basis for the award of any degree, diploma, fellowship or any other similar titles.

Place: Tiruchirappalli

Date: 05.04.2022

V.PRIYADARSHINI

Research Scholar

ACKNOWLEDGEMENT-

This thesis is by far the most significant accomplishment in my life and it would not have been possible without people who supported me and believed in my calibre.

I salute **GOD ALMIGHTY** and surrender all my achievements to him.

On a personal note, I have no words to express my abundant and inexplicable, affectionate gratitude to my beloved parents **Mr. S.VAITHIYANATHAN and Mrs. V.VASANTHA** for their catalytic role, moral support, colossal affection, curiosity and admiration.

First and foremost I find great pleasure in expressing my deep sense of gratitude and heartfelt thanks to my esteemed guide, **Dr. K. THARINI**, Assistant Professor, PG & Research Department of Chemistry, Government Arts College, Tiruchirappalli-22 whose continuous, exemplary guidance and supervision, constructive criticism, perfectionist attitude, constant support, kind treatment and immediate response for all necessities during the period of this research studies enabled me to carry out this work so as to reach a stage of completeness.

I am deeply indebted to **Dr. A.SIVARAJAN**, Assistant professor and Head, PG & Research Department of Chemistry, Government Arts College, Tiruchirappalli-22 for showing sustained interest and providing support throughout the period of my research work.

I am highly thankful to **Dr. S.S. ROSE MARY**, Principal, Government Arts College, Tiruchirappalli-22 for permitting me to carry out the project in the college successfully.

I express my sincere thankfulness to **Dr. D.ILANGESHWARAN**, Assistant professor, PG & Research Department of Chemistry, Rajah Serfoji Government

College (Autonomous), Thanjavur-05 for showing sustained interest and providing support throughout the period of my research work as a doctoral committee member.

I would like to express my special thanks to **Dr. S. UMAMATHESWARI**, Assistant professor, PG & Research Department of Chemistry, Government Arts College, Tiruchirappalli-22 for her valuable suggestions and encouragements and moral support during the research period as a doctoral committee member.

I would like to thank all the **teaching, non-teaching staff and Research scholars**, Department of Chemistry, Government Arts College, Tiruchirappalli-22 for their immense help, co-operation and incessant support.

I am very glad to express my sincere thanks to **SASTRA UNIVERSITY**, Thanjavur for providing NMR facility and **VINCENT SAHAYARAJ**, St. Joseph's College, Trichy for FT-IR facility.

I also wish to thank **HARMAN RESEARCH CENTER**, Thanjavur for providing facilities for biological studies.

I am indebted and owe my due respect to **Dr. U.P. ELANGO VAN M.B.B.S, Family Physician, Rasipuram** by offering me a constant help encouragement in all possible ways and his whole hearted help rendered at all times of my research work would be remembered lifelong.

I take this opportunity to express my great reverence, my sincere gratitude to **all my teachers** without whose assistance I would not have reached up to this level.

I am also to thankful **Mr. K. SUNDARESAN**, Assistant professor, Meenakshi Ramasamy College, Thathanur for his continuous support throughout my research work.

I would like to express my special thanks to **sidthantha Vithyanithi**

Mr. R. RENGASAMI, M.com., for his valuable suggestion, immense motivation and guidance for my research career.

I would like to express appreciation to my beloved uncle and Sisters **Mr. S. ELANGO VAN, Mrs. E.PORKODI** and **V. PORUTSELVI** who was always supportive throughout my research journey.

It is my duty to thank my Uncle **Mr. S. SANKARAMOORTHY** sister **Mrs. V. INDUMATHI** daughters **S. MITHRA** and **S. SAMUTHRA** without whose support, co-operation, love and warmth, this work would not have become a reality.

And finally, I am also very grateful and extend my sincere thanks to **Mr. R. APPARAJOO B.E (IT)** for his brother care during my research work.

V. PRIYADARSHINI

Synthesis, Characterization and Biological Evaluation of Some Novel Bioactive Hydrazone Derivatives

Name : V.Priyadarshini

(Ref No: 05706/Ph.D.K2/Chemistry/Full-Time/July-2017/Date: 30.06.2017)

ABSTRACT

The majority of pharmaceutical products that mimic natural products with biological activity are heterocycles. Synthetic heterocyclic compounds can and do participate in chemical reactions in the human body. Moreover, all biological processes are expressed through chemical reaction. The present study describes about the synthesis and characterization and biological studies of some novel bioactive hydrazone derivatives. The detail characterization of the compounds were carried out using FT-IR, ^1H , ^{13}C NMR spectroscopy methods.

This invitro study explores the anti-obesity properties of synthesized compounds and it can be considered as a pancreatic lipase for the management protective role in treating obesity. The insilico molecular docking study were carried out using BIOVIA Discovery Studio (DS) 2017 software. The molecular interaction analysis revealed that the BRCA1. The synthesized compound subjected to preliminary invitro thrombolytic studies by clotlysis.

Dr.K.THARINI

(Research Supervisor)

LIST OF SYMBOLS AND ABBREVIATIONS

Symbol	Abbreviation
BC	Breast cancer
b.p	boiling point
bs	broad singlet
d	doublet
dd	double doublet/doublet of doublet
FT-IR	Fourier Transform Infra red spectroscopy
Hz	Hertz
IC_{50}	Inhibitory Concentration
J	Coupling constant
2J	Geminal coupling constant
3J	Vicinal coupling constant
LBVS	Ligand Based Drug Design
m	multiplet
mL	millilitre
m.p	melting point
ppm	parts per million
q	quartet
s	Singlet
SBDD	Structure Based Drug Design
t	triplet
μg	microgram
μM	micromolar
δ	Chemical shift
$\Delta\delta$	Difference in chemical shift

CONTENTS

Chapters	Title	Page No
I	INTRODUCTION	
	1.1 Heterocyclic compounds	1
	1.2 Methods of analysis	6
	1.2.1 IR Spectroscopy	6
	1.2.2 Nucleus magnetic resonance spectroscopy	7
	1.2.3 Chromatographic techniques	7
	1.3 Invitro anti-obesity studies	8
	1.4 Insilco molecular docking study	14
	1.4.1 Docking approaches	19
	1.4.2 Complementarity in shape	19
	1.4.3 Simulation	20
	1.4.4 Drug Design using structure [SBDD]	20
	1.4.5 Applications of molecular docking	24
	1.5 Invitro Thrombolytic activity	25
	Reference	28
II	REVIEW OF LITERATURE	
	2.1 Hydrazones	34
	2.2 Invitro anti-obesity activity	44
	2.3 Insilico molecular docking	47
	2.4 Invitro thrombolytic activity	50
	Reference	54
III	SCOPE AND OBJECTIVE OF THE WORK	60
IV	MATERIALS AND METHODS	

4.1	Materials	62
4.2	Identification of compounds	
4.2.1	Melting point determination	62
4.2.2	Thin layer chromatography	63
4.2.3	FT-IR spectra	64
4.2.4	¹ H NMR and ¹³ C NMR spectra	64
4.3	Synthesis of compounds	
4.3.1	Preparation of 3-methyl-2,6-diaryl piperidine-4-one	64
4.3.2	Preparation of 3-methyl-2,6-diaryl piperidine-4-one cyanoacetylhydrazone	65
4.3.3	Preparation of N-acetyl 3-methyl-2,6-diaryl piperidine-4-one Cyanoacetylhydrazone	65
4.4	Preparation of benzaldehyde cyanoacetylhydrazone	66
4.5	Invitro anti-obesity activity	
4.5.1	Reagents	66
4.5.2	procedure	67
4.6	Insilico molecular docking	
4.6.1	Preparation of protein	67
4.6.2	Ligand preparation	68
4.6.3	Docking studies	68
4.7	Invitro thrombolytic activity	
4.7.1	Preparation of streptokinase	70
4.7.2	Collection of blood	71
4.7.3	Procedure	71
	Reference	72

V RESULT AND DISCUSSION

5.1 Synthesis of compounds (C1-C7)

5.1.1 Preparation of 3-methyl-2,6-diaryl piperidine-4-one

5.1.2 Preparation of N-acetyl 3-methyl-2,6-diaryl piperidine
4-one cyanoacetylhydrazone -

5.2 Spectral studies

5.2.1 IR spectral studies 78

5.2.2 NMR spectroscopy 79

5.3 Spectral analysis of compound N-acetyl 3-methyl-2,6-diarylpiperidine
4-one cyanoacetylhydrazone -

5.3.1 IR spectral analysis 80

5.3.2 ¹H NMR spectral analysis 82

5.3.3 ¹³C NMR spectral analysis 86

5.4 Spectral analysis of compound N-acetyl 3-methyl-2,6bis (o-bromophenyl)
piperidine-4-onecyanoacetylhydrazone

5.3.1 IR spectral analysis 92

5.3.2 ¹H NMR spectral analysis 94

5.3.3 ¹³C NMR spectral analysis 97

5.5 Spectral analysis of compound N-acetyl 3-methyl-2,6 bis(o-chloro phenyl)
piperidine-4- onecyanoacetylhydrazone

5.3.1 IR spectral analysis 100

5.3.2 ¹H NMR spectral analysis 102

5.3.3 ¹³C NMR spectral analysis 105

5.6 Spectral analysis of compound N-acetyl 3-methyl-2,6 bis (o-methylphenyl)
piperidine-4-onecyanoacetylhydrazone

5.3.1	IR spectral analysis	108
5.3.2	¹ H NMR spectral analysis	110
5.3.3	¹³ C NMR spectral analysis	113
5.7	Spectral analysis of compound N-acetyl 3-methyl-2,6 bis (p-bromo phenyl) piperidine-4-onecyanoacetylhydrazone	
5.3.1	IR spectral analysis	116
5.3.2	¹ H NMR spectral analysis	118
5.3.3	¹³ C NMR spectral analysis	121
5.8	Spectral analysis of compound N-acetyl 3-methyl-2,6 bis(p-chloro phenyl) piperidine-4- onecyanoacetylhydrazone	
5.3.1	IR spectral analysis	124
5.3.2	¹ H NMR spectral analysis	126
5.3.3	¹³ C NMR spectral analysis	129
5.9	Spectral analysis of compound N-acetyl 3-methyl-2,6 bis (o-methyl phenyl) piperidine-4-onecyanoacetylhydrazone	
5.3.1	IR spectral analysis	132
5.3.2	¹ H NMR spectral analysis	134
5.3.3	¹³ C NMR spectral analysis	137
5.10	Invitro anti-Obesity activity	
5.10.1	Pancreatic lipase inhibition activity	140
5.11	Insilico molecular docking study	
5.11.1	Insilico molecular docking study synthesized Compounds	148

5.12	Invitro thrombolytic activity	160
------	-------------------------------	-----

Part-II

5.13	Synthesis of compounds(C8-C14)	
5.13	Preparation of benzaldehyde cyanoacetylhydrazone	169
5.14	Spectral analysis of compound benzaldehyde cyanoacetylhydrazone	
5.14.1	IR spectral analysis	173
5.14.2	¹ H NMR spectral analysis	175
5.3.3	¹³ C NMR spectral analysis	178
5.14	Spectral analysis of compound o-bromo benzaldehyde cyanoacetylhydrazone	
5.14.1	IR spectral analysis	180
5.14.2	¹ H NMR spectral analysis	182
5.3.3	¹³ C NMR spectral analysis	184
5.14	Spectral analysis of compound o-chloro benzaldehyde cyanoacetylhydrazone	
5.14.1	IR spectral analysis	186
5.14.2	¹ H NMR spectral analysis	188
5.3.3	¹³ C NMR spectral analysis	190
5.14	Spectral analysis of compound o-methyl benzaldehyde cyanoacetylhydrazone	
5.14.1	IR spectral analysis	192
5.14.2	¹ H NMR spectral analysis	194
5.3.3	¹³ C NMR spectral analysis	196
5.14	Spectral analysis of compound p-bromo benzaldehyde cyanoacetylhydrazone	
5.14.1	IR spectral analysis	198
5.14.2	¹ H NMR spectral analysis	200
5.3.3	¹³ C NMR spectral analysis	202
5.14	Spectral analysis of compound p-chloro benzaldehyde cyanoacetylhydrazone	

5.14.1	IR spectral analysis	204
5.14.2	¹ H NMR spectral analysis	206
5.3.3	¹³ C NMR spectral analysis	208
5.14	Spectral analysis of compound o-methyl benzaldehyde cyanoacetylhydrazone	
5.14.1	IR spectral analysis	210
5.14.2	¹ H NMR spectral analysis	212
5.3.3	¹³ C NMR spectral analysis	214
5.10	Invitro anti-Obesity activity	216
5.11	Insilico molecular docking study	223
5.12	Invitro thrombolytic activity	229
	Reference	239
VI	SUMMARY AND CONCLUSION	240

Chapter-1

INTRODUCTION

1.1 Heterocyclic compounds

Organic synthesis is the most common method for creating chemical compounds with practical applications. Several of the millions of organic compounds have been over the last century and halves through chemical synthesis are directly linked to important applications in everyday life. Pharmaceutical that can cure or prevent diseases for example anti-fertility agent for population control, insecticides, pesticides, plant and animal hormones to increase food production and nutritional quality, polymers, fabrics, dyes, cosmetics detergents, photographic and electric items and other high technology materials used in automobile air craft and computers industries are such marvelous inventions

Organic synthesis is a subset of chemical synthesis that focuses on efficiently constructing desired organic molecules from widely available starting ingredients and reagents. Owing to the varied requirements in the areas of medicine and fine chemical industries, complexity of organic target molecules is constantly increasing and it is necessary to develop innovative techniques for forming new carbon-carbon and carbon-hetero atom bonds between functionalized moieties[1-2].

In an organic chemistry, largest families of organic compounds to be a part of the hetero cyclic compounds. In our daily life important of heterocyclic compounds are of very essential. The most complex branches of chemistry are normally heterocyclic chemistry. Synthetic heterocyclic chemistry has not only played an important role in every place of

human life and also found their application in diverse field as agriculture, polymer, medicine and various industries [3].

Studies in heterocyclic compounds are of two particular sources of interest in this subject. Firstly these are their steady streams of discovery of new heterocyclic compounds playing an important role in the metabolism of all living cells and secondly the increasing availability of intermediates suitable for the large scales production of heterocyclic compounds. Several important compounds contain heterocyclic ring for example in most of the members of the vitamin **B**-complex, alkaloids, antibiotics chlorophyll, haemin, plant pigments, amino acids, drugs, enzymes, DNA, RNA etc. A great deal of research has been carried out to synthesize new heterocycles having therapeutic value and industrial applications. Nature has chosen heterocycles as the foundation for the most important biological systems. Aromatic heterocyclic chemistry is a vast and complicated field with significant industrial and academic implications.

A number of molecules are derived from aromatic heterocycles and many pharmaceutical and agrochemical compounds are based on aromatic heterocycles. Consequently, the importance of organic chemistry has stimulated a vast amount of synthetic and theoretical work in this area. Heterocyclic compounds, both natural and synthetic and semi-synthetic, play an essential role in drug discovery and chemical biology. As a result, drug design can be thought of as an integrated whole approach that entails a number of steps, including chemical synthesis, activity-spectrum evaluation, toxicological studies, drug metabolism (i.e., biotransformation and the examine of the diverse metabolisms formed), assay procedures and galenical system and biopharmaceutics. Organic and medicinal chemistry are becoming more important fields of study. The primary objective of an organic chemist is to work towards isolation, characterization and synthesis of new compounds that

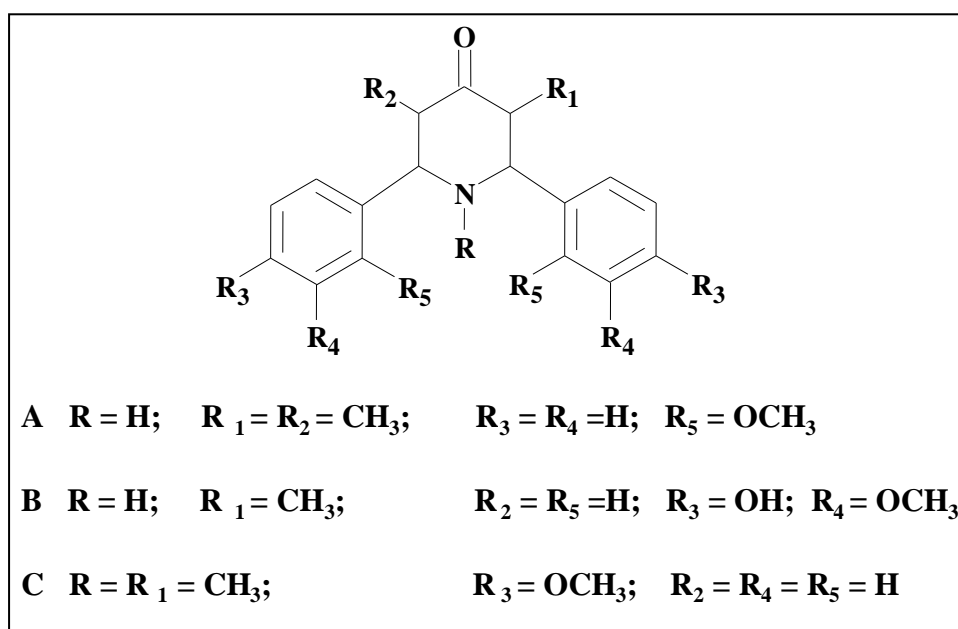
are suitable for use as drugs. Medicinal chemistry is a discipline of chemistry concerned with the formulation, production and development of pharmaceuticals. However, their N-C linkage derivatives have been utilized in medical and pharmaceutical chemistry and have been found to have a range of biological functions. Hydrazones and their derivatives are a class of compounds having several uses in organic synthesis. The carbon-nitrogen double bond chemistry of hydrazone is becoming the backbone of the condensation reaction in benzo-fused N-heterocyclics and it also represents an important class of compounds for innovative medicinal development [4].

Many publications on the conformation of different substituted 2, 6-diarylpiperidin-4-ones are available and many of them have elaborated on the conformation of 2, 6-diarylpiperidin-4-ones with or without alkyl substituents at C-3 and C-3/C-5 locations. Small compounds that operate as highly functionalized scaffolding for a variety of biologically active and medicinally powerful substances are known pharmacophores. Recently, cyanoacetyl hydrazones have attracted great attention due to their diverse biological and pharmacological properties [5-6].

Due to their vast range of biological characteristics and occurrence in a number of alkaloids, heterocyclic ring systems, notably 2,6-disubstituted piperidine nucleus, have piqued attention in the past and recent years. Extensive research on 4-piperidones has been done in the past and they are now a significant element of the molecular framework of certain major medicines due to their connection to drug production. Also, these compounds have been found to be valuable synthetic intermediates for the synthesis of variety of natural products.

Earlier reports were clearly established that the biological activities of piperidones were improved by the incorporation of the substituent at C-2, C-3 and C-6 positions.

Compounds with aromatic substituents at the C-2 and/or C-6 locations were discovered to have considerable biological activity. Similarly, presence of methyl substituent at C-2 or C-3 positions was also reported to exert significant role in enhancing their biological activities of piperidin-4-ones. Likewise, presence of phenyl or *para* substituted phenyl groups at C-2 and C-6 positions besides with/without substituents at C-3, C-5 and 'N' have wide range of antimicrobial activity. Further, blocking of its keto group has also proved to exhibit analgesic, local anaesthetic, antibacterial and antifungal activities.



2, 6-*Bis* (2-methoxyphenyl)-3,5-dimethylpiperidin-4-one. **A** and 2,6-*bis*(3-methoxy-4-hydroxyphenyl)-3-methylpiperidin-4-one **B** were shown to relieve spasm produced by histamine whereas 1,3-dimethyl-2,6-*bis*-(4-methoxyphenyl)piperidin-4-one **C** partially relieved the spasm.

Hydrazone is an organic compound with the formula $R_1R_2C=NNH_2$, generally these compounds are formed by the reaction of hydrazine with ketones and aldehyde. By adding substituted hydrazones, substituted hydrazones can be produced. Aryl hydrazones are formed by the condensation of aromatic hydrazone with carbonyl compounds. A study of the

structure of hydrazone shows it has (1) nucleophilic and amino type of nitrogen. (2) A carbon imine with both electrophilic and nucleophilic properties. (3) The inherent character of the C=N bond causes configurational isomerism and (4) In most situations, the N-H proton is acidic. These structure features give the hydrazone group its physical and chemical properties. Because of their chelating capacity and therapeutic applicability, the chemical characteristics of hydrazones have been extensively studied in a variety of disciplines. Hydrazone derivatives have attracted a great deal of interest in synthetic chemistry and considerable research on them in relation to their synthetic utility has been accomplished. Because they may easily undergo numerous ring closing processes, hydrazones have been widely investigated as reactants or reaction intermediates.

Hydrazones are medicinal compounds that are physiologically active. Hydrazone compounds with a highly reactive azomethine group (CONH-N=CH) are beneficial in the creation of novel drugs [7]. From aromatic and aliphatic compounds, many physiologically relevant hydrazone derivatives with a range of functional groups have recently been synthesized [8]. To treat illnesses with maximum therapeutic benefits and lowest toxicity, new chemicals are being created as medicines. Hydrazones have been utilized to make new heterocyclic compounds [9]. Because of their wide spectrum of biological relevance in medicinal chemistry, hydrazones have piqued the interest of medicinal chemists. Many studies have shown that hydrazone derivatives have anti-inflammatory, analgesic, antibacterial, antifungal, anticancer, antioxidant, antidepressant, antitubercular, cytotoxicity, antiamoebic, antitumor, antiplatelet, anticonvulsant, antimycobacterial, antihypertensive and antinociceptive properties [10-12]. The newly synthesized hydrazone derivatives bearing a piperidin-4-one moiety might be of potential interest or could serve as potential intermediates in medicinal chemistry. The preparation of novel hydrazone derivatives with a piperidin-4-one moiety is discussed in this paper.

The present research also confirmed that nucleophilicity affects the ease of nucleophilic substitution. All of these findings prompted the start of a research project aimed at developing novel hydrazone derivatives with a heterocyclic moiety.

1.2 Methods of Analysis

During the last few years enormous development in the field of synthetic organic chemistry has taken place due to the availability of powerful analytical techniques.

For elucidating the structure and in determining physical, chemical and biological properties, these techniques are more useful to scientists.

The spectral methods have been immense help in collection of valuable information about individual compounds. Ultraviolet, infrared and nucleus magnetic resonance spectroscopy are the most essential and significant tools among the most important spectroscopic techniques that the organic chemists now use routinely to gain information about a particular substance.

In the present study IR and NMR techniques are used to characterize the synthesized heterocyclic compounds and TLC is used to check their purity.

1.2.1 IR SPECTROSCOPY

This is one of the most widely used tools for the detection of functional groups in pure compounds and mixtures and for compound comparison.

The spectrum is obtained in minutes using a few mg of the compound which can also be recovered.

The portion of the electromagnetic spectrum between visible and microwave areas is referred to as infrared radiation. The entire molecule's IR spectrum is distinctive. Some groups of atoms create bands at or near the same frequency, regardless of the rest of the molecule's structure.

In the structural elucidation of various organic compounds especially for the presence of functional groups, IR spectral technique is very reliable.

1.2.2 Nucleus Magnetic Resonance Spectroscopy

For the structural elucidation of organic molecules, nuclear magnetic resonance spectroscopy is a useful technique. ^1H NMR and ^{13}C NMR gave configurational and conformational nature of the compounds. This technique is helpful in observing each and every proton and carbon atom separately in the compounds. A large number of synthetic as well as natural, occurring compounds have been studied by NMR spectroscopy.

1.2.3 Chromatographic Techniques

Chromatography is the most useful technique for separating and identifying a mixture of substance into its compounds. This technique is based upon the difference, in the rate of mobility of various constituents of substance through a porous medium (called stationary Phase) under the influence of some solvents or gas. Based on the nature of stationary or moving phase, chromatographic techniques are designated like paper, thin layer, column and gas chromatography.

In the present research work thin layer chromatography has been used to check the purity of the compounds.

1.3 Invitro anti-Obesity Studies

Obesity and overweight are defined as an accumulation of abnormal or excessive fat that is hazardous to one's health. The body mass index (BMI) is a basic demographic measure of obesity that is frequently used to identify persons who are overweight or obese. It is computed by multiplying a person's weight in kilograms by their height in meters squared (kg/m^2). Obesity is defined as having a BMI of 30 or higher, whilst overweight is defined as having a BMI of 25 or higher.

Obesity incidence varies by nation and is influenced by a variety of characteristics such as gender, age, educational attainment, yearly household income, work status and social class. Obesity is a very expensive health concern; the direct medical costs of overweight and obesity combined account for 5% to 10% of all health-care spending in the United States. Growth in the economy, modernization and the westernization of lifestyles (high calorie diet including processed foods higher in fats and refined sugars and decreased exercise levels) and globalization of food markets have all been suggested as factors contributing to this widespread increase in obesity. Other variables, such as hereditary predisposition, endocrine abnormalities and environmental factors, may play a role in this problem, with women being more vulnerable [13].

Over 340 million children and adolescents aged 5 to 19 were overweight or obese in 2016, with 41 million children under the age of 5 being overweight or obese. Obesity has become a global epidemic, with over 2.8 million people dying each year as a result of being overweight or obese. In the year 2019, 38 million children under the age of 5 were overweight or obese. According to the World Health Organization [14].

Overweight and obesity were predicted to be prevalent in Palestine at 58.7% and 71.3 percent among men and women, respectively. This can be attributed to several factors including decreased physical activity, increased consumption of high caloric foods,

particularly with an increase in energy coming from fat, smoking and urbanization. A cross-sectional study was carried out in Palestine to investigate the prevalence of overweight and obesity among school children aged from 6-12 years. The prevalence of overweight and obesity among male students was 13.3% and 7.9%, respectively, according to the research, while it was 13.6 percent and 4.9 percent, respectively, among female students [15].

Obesity is a common disorder usually caused by the interaction of genetic, nutritional and environmental factors. It has now become one of the most important health issues of the modern Society around the world. It is often associated with other diseases such as arteriosclerosis, Hypertension, cancer, diabetes and osteoarthritis. The incidence of obesity is increasing exponentially and it has been revealed that about 500 million adults are obese worldwide [16].

Obesity is a chronic metabolic disease caused by an energy intake-to-expend ratio that is out of balance. Obesity and overweight are characterized as abnormal or excessive fat buildup that puts one's health at danger. According to WHO, high blood cholesterol level leads to approximately 56% of cardiac disease worldwide and about 4.4 million deaths each year. Being overweight or obese should be prevented by constant exercise and dietary routines. Nevertheless, when the latter techniques fail in obtaining 10% weight loss, pharmacological treatment is required. Despite the fact that this alternative is strongly suggested, some pharmacological drugs, such as sibutramine, have had mixed effects.

Obesity is described as a buildup of fat in adipose tissue and other internal organs such as the liver, heart and skeletal muscle that is abnormal or excessive. It's a long-term carbohydrate and fat metabolism disease that puts people's health and well-being at danger. Currently available allopathic drugs used in the treatment of hyperlipidaemia are associated with a number of side effects. Licenses for drugs including amphetamine, rimonabant and sibutramine have been revoked owing to a higher risk of mental illnesses and nonfatal

myocardial infarction or stroke. Orlistat is presently the only medicine available for the treatment of obesity because of its low risk of cardiovascular events and positive benefits on diabetes control, despite the fact that it is not as effective as other weight-loss treatments. Synthetic drug use causes hyperuricemia, diarrhoea, nausea, myositis, stomach irritation and flushing, dry skin and impaired liver function. Inhibition of dietary triglyceride absorption by inhibiting pancreatic lipase has recently been proposed as a novel strategy for the treatment of obesity, as dietary triglyceride absorption is the primary source of excess calories. More effective and better-tolerated drugs should be developed which must be safe and consumed long-term in the management of obesity [17].

Weight-loss drugs are pharmacological treatments that help people lose or maintain their weight. These drugs affect one of the body's most basic functions, weight management, by affecting appetite or calorie absorption.

Dieting and physical activity remain the major therapeutic strategies for overweight and obese people. The FDA has authorized orlistat (Xenical) for long-term usage in the United States. It inhibits pancreatic lipase, which lowers intestinal fat absorption. A second medicine, rimonabant (Acomplia), operates by blocking the endocannabinoid system in a particular way. It was created based on the fact that cannabis users frequently experience hunger, which is referred to as "the munchies." It was approved in Europe for the treatment of obesity, but it was not approved in the United States or Canada due to safety concerns. In October 2008, the European Medicines Agency advised that the sale of rimonabant be halted since the hazards appear to outweigh the benefits. Sibutramine (Meridia), a drug that works in the brain to prevent neurotransmitter deactivation and so reduce hunger, was pulled from the US and Canadian markets in October 2010 owing to cardiovascular risks. Anti-obesity drugs should only be used for obesity if the advantages of the treatment outweigh the risks, due to

potential adverse effects and limited evidence of minor weight loss advantages, especially in obese children and adolescents [18-20].

Overweight and obesity, the most frequent nutritional issues caused primarily by an energy imbalance induced by an increased ratio of caloric intake to energy expenditure, are fast becoming global health hazards. More than 300 million individuals worldwide are obese, with a BMI of less than 30 kg/m² and 800 million are overweight (BMI of 25 to 29.9 kg/m²), according to the international obesity task force[21]. If nothing is done to combat this concern, this amount might double by 2025 due to the growing trend in obesity prevalence. Obesity reduces quality of life and life expectancy, as well as being a high risk factor for illnesses such type 2 diabetes, heart disease, stroke, some malignancies, osteoarthritis, liver disease, urine incontinence, sleep apnea and depression [22].

Obesity rates are rising over the world, putting a strain on national healthcare systems if not addressed. Despite progress in understanding its pathophysiology, current obesity pharmacotherapy is restricted in terms of the amount of weight reduction that may be achieved as well as the medications' safety and tolerability. Thus, discovery of new targets and therapeutic agents is a focal point for combating this epidemic. A large section of world's population relies on traditional remedies to treat various diseases. Due to its efficacy, cheap costs, simple access, ancestral expertise and absence of side effects, medicinal herbs are an essential aspect of traditional medicine practiced all over the world [23]. Generally obesity is associated with oxidative stress which results from an imbalance between the production of free radicals and an effective antioxidant system.

Natural-occurring chemicals offer a promising avenue for the development of novel anti-obesity drugs. Body weight is one of the world's most serious public health issues, both because its prevalence is steadily rising, not just in developed nations but also in low- and middle-income countries and because it is a major risk factor for a variety of chronic

illnesses. It condition in which the body contains too much fat and it can lead to a variety of health problems. Obesity must be handled since it can lead to a number of serious and even life-threatening disorders in addition to noticeable physical changes. Obesity raises the risk of diseases like type 2 diabetes, fatty liver disease, hypertension, myocardial infarction, stroke, dementia, osteoarthritis, obstructive sleep apnea and several cancers (including breast, colon and prostate), all of which contribute to a decrease in both quality of life and life expectancy. Obesity has also been linked to psychological issues including sadness and low self-esteem. It is estimated that 44% of cases of type 2 diabetes, 23% of cases of ischemic heart disease and up to 41% of some cancers are attributable to obesity/overweight (Figure 1). In total, overweight and obesity represent the fifth most important risk factor for global mortality and the deaths attributable to obesity are at least 2.8 million/year worldwide [24].

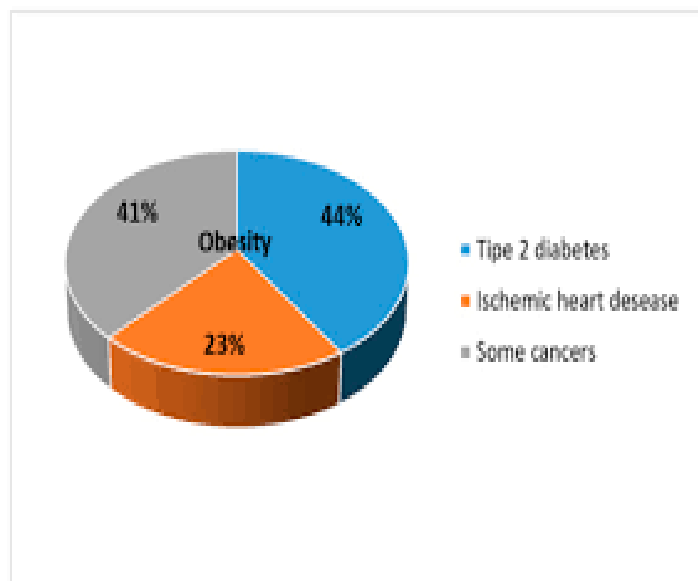


Fig.1

Reduced glutathione (GSH) is the liver's first line of defense against free radicals, as well as the preservation of protein thiols and serving as a substrate for Glutathione peroxidase (GPx). The findings showed that GSH levels were decreased in obese rats produced by a

high-fat diet, but were recovered after treatment with ATECR. Enzymatic antioxidants, like superoxide dismutase (SOD), catalase (CAT) or GPx, can scavenge reactive oxygen species (ROS) and free radicals or prevent their formation. The present study suggested decreased activities of antioxidant enzymes SOD, CAT and GPx in the liver of rats fed with high fat cafeteria diet as compared to those on normal diet and these results are in agreement with reports of earlier workers which suggest that feeding a high fat diet to experimental animals depresses their antioxidant system due to increased lipid peroxidation and formation of free radicals [24].

This study described as an abnormal buildup of body fat that has the potential to harm one's health. It has spread around the globe. Obesity is known to be related to increase risks of coronary heart diseases, hypertension, noninsulin-dependent diabetes mellitus and certain type of cancer. Obesity is caused in part by a mismatch between energy intake and expenditure. The creation of food digestion and absorption inhibitors, in an attempt to restrict energy intake through gastrointestinal processes without affecting any central systems, is one of the most significant strategies in the treatment of obesity. One of the most commonly investigated techniques for determining the potential efficacy of natural items as anti-obesity medicines is the inhibition of digestive enzymes. Therapeutic foods are renowned for having both nutritional and medicinal properties and they are used in a variety of traditional formulations. Natural products' potential for treating obesity is now virtually untapped and they might be an ideal alternative method for developing safe and effective antiobesity medications [25].

Pancreatic lipase (PL) is a pancreatic enzyme that helps the small intestine absorb triglycerides. Dietary fats are composed of about 95% triacylglycerol's (TG). Pancreatic lipase hydrolyses the water insoluble triacylglycerol's in the intestinal lumen and thereby used for the dietary fat absorption. Diet-induced obesity is treated with pancreatic lipase

inhibitors, which are regarded a useful therapeutic treatment [27]. Searching for effective lipase inhibitors in natural products is one of the screening procedures used in the identification of anti-obesity medications. Natural-source drugs are safer and more effective, despite the fact that they are also poisonous. They cause less harm than pure synthetic drugs. The search for novel natural bioactive compounds as a foundation for new drug discovery is receiving attention as previously reliable standard drugs become less effective against the emerging new strains of multiple drug resistant strains [28].

Pancreatic lipase, also known as triacylglycerol acyl hydrolase, is a lipolytic enzyme produced and released by the pancreas that aids in the digestion of triglycerides. Pancreatic lipase is responsible for the hydrolysis of 50 to 70% of total dietary lipids. It removes fatty acids from the α and α' positions of dietary triglycerides, yielding β -monoglycerides and long chain saturated and polyunsaturated fatty acids as the lipolytic products [29].

1.4 Insilico molecular docking (Breast Cancer Activity)

Cancer is a collection of illnesses that result in abnormal cell development. Chemicals, such as the synthetic compounds found in cigarette smoke and radiation, such as UV rays from the sun, are natural cancer-causing exposures that cause all cell proliferation with the ability to attack or spread to other parts of the body. Specific alterations to genes, the fundamental physical units of heredity, are to blame. Genes are organized in chromosomes, which are lengthy strands of tightly compacted DNA. Chemicals, such as the synthetic concoctions found in tobacco smoke and radiation, such as ultraviolet (UV) rays from the sun, are examples of natural cancer-causing exposures. Cancer is the most common cause of death in the world. It was responsible for 8.2 million fatalities (about 22% of all deaths not caused by infectious illnesses, according to the most recent WHO data). Treatment options vary depending on the type and stage of the tumor. The majority of treatments are

tailored to the specific condition of each patient. Be that as it may, most medications incorporate no less than one of the accompanying and may incorporate all medical procedure, chemotherapy and radiation treatment.

Breast cancer in women is a noteworthy general medical issue all through the world. It is the most widely recognized cancer among the women in developed and developing nations. It is the guideline reason for death from cancer among women all around. Breast cancer is a malignancy that starts in the breast tissue. Cancer is a category of disorders in which the cells of the body change and grow out of control. Most cancer cells eventually coalesce into a lump or mass known as a tumor, which is called for the body part where it initially occurs. The lobules, which are milk-producing organs in the breast and the ducts that link the lobules to the nipple where the majority of breast cancers start [30]. The most common and deadly type of all cancers around the globe is lung cancer which accounts for 25% of the cancer deaths every year. Among the types of lung cancer with about 1.5 million patients and less than 20% survival rate is non-small cell lung cancer (NSCLC) .

Small cell lung cancer (SCLC) and non-small cell lung cancer (NSCLC) are both included in most lung cancer statistics. SCLC accounts for around 10%–15% of all lung malignancies in general. According to the American Cancer Society's lung cancer projections for 2019, there were approximately 228,150 new instances of lung cancer in the United States, with approximately 116,440 cases in men and 111,710 cases in women. And the death toll was estimated to be at 142,670. Men accounted for 76,650 of the total, while women accounted for 66,020 [31].

After cardiovascular diseases, cancer is the second most deadly disease to the human health. Cancer is one of the seven leading causes of mortality worldwide, affecting around 14 million people each year. Due to a lack of exercise, smoking and genetic variation, the

adoption of lifestyle activities has raised the risk of cancer, particularly in developing nations, where about 82 percent of the world's population lives. Breast cancer is the most severe kind of cancer on the planet and the leading cause of cancer-related mortality in women. Globally, an estimated 1 to 1.3 million instances of breast cancer are discovered each year. Antagonistic mammary growths are triple-negative breast tumors (TNBCs) that lack the human epidermal growth factor receptor 2 (HER2), estrogen receptor (ER), and progesterone receptor (PR). TNBCs are more likely than non-TNBCs to metastasize to the central nervous system and lung. Non-TNBC cancers are more prone to spread to the bones. Due to non-enhanced inhibitory substances, such metastatic activities lower the life expectancy of TNBC patients compared to non-TNBC patients. Jo et al. recently disclosed a unique series of 2-anilinopyrimidines as anti-MDA-MB-468 cell line inhibitors. There is also evidence that reduced manifestation of thyroid hormone receptors and / or variations in thyroid hormone genes are common in cancer, suggesting that native receptors might act as tumor suppressors and that loss of recurrence of this receptor is a selective cause of cell changes and tumors. It could be the progression of transformation [32].

Estrogens control multiple physiological processes including the growth, differentiation and function of the reproductive system. The uterus, vagina, ovaries and mammary gland are the major target organs in females, whereas the testes, prostate and epididymis are the main target organs in males. Estrogen Receptors mediate the majority of estrogen's effects (ER). A high level of estrogen is linked with increased risk of Breast cancer by stimulating breast epithelial cell proliferation. Estrogens Receptor exists in two forms ER alpha and ER beta ($ER\alpha$ & $ER\beta$). $ER\alpha$ and $ER\beta$ may have different roles in the formation and progression of breast cancer. The majority of breast cancers are diagnosed by aberrant Estrogen Receptor-positive expression, which affects around 70% of initial breast cancer patients. Estrogen stimulated cell proliferation and increased tumor formation occurs, when

only ER α is present. Hence, inhibition of Estrogen Receptor alpha is a major approach to prevent the Breast cancer [33].

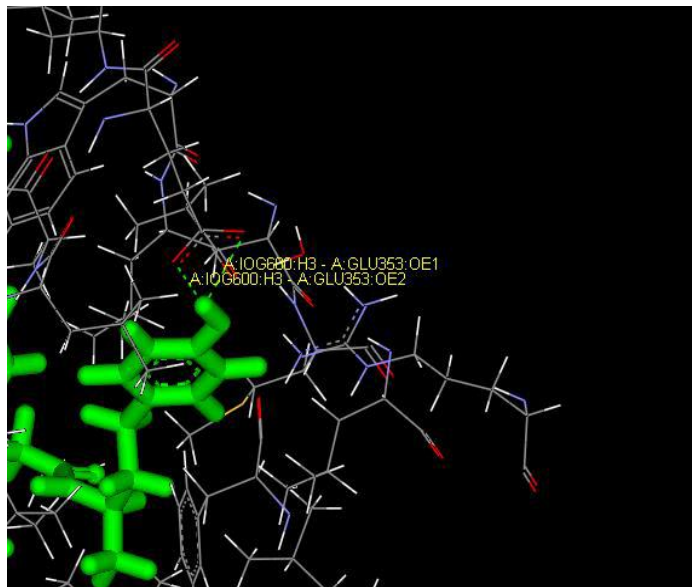


Fig.2 Interaction of human receptor with bromodeoxytospentin with a dock score16.191

Nowadays cardiovascular diseases (CD) like coronary heart disease (CHD), atherosclerosis, Hypertension and acute myocardial infarction are the main causes of death in humans. Thrombosis is one of the frequently cause of CD. Almost 20 million people are being affected by thrombotic events worldwide every year. Agents that enhance the fibrinolytic activity and inhibit thrombus formation are important for the treatment and prevention of cerebrovascular and CD. After damage or trauma, thrombin (EC.3.4.21.5) is triggered and fibrinogen begins to produce fibrin, which clogs the blood. Accumulation of fibrin in blood vessels increases thrombosis resulting in various cardiovascular diseases (CVDs) and myocardial infarction [34].

Due to its ability to anticipate the binding conformation of small molecule ligands to the correct target binding site, molecular docking is one of the most widely used approaches in structure-based drug design. Characterization of the binding behavior plays an important role in rational design of drugs as well as to elucidate fundamental biochemical processes.

To investigate complicated biological and chemical systems, pharmaceutical research has effectively included a range of molecular modeling approaches into a variety of drug development initiatives. In the identification and development of novel promising molecules, combining computational and experimental techniques has proven to be quite beneficial. Molecular docking techniques are widely utilized in contemporary drug design to investigate ligand conformations within macromolecular targets' binding sites. This approach assesses the ligand-receptor binding free energy by analyzing important steps in the intermolecular recognition process. Given the wide range of docking algorithms available today, knowing the benefits and drawbacks of each technique is critical to the creation of successful strategies and the generation of meaningful outcomes. The goal of this review is to look at current molecular docking methodologies in drug development and medicinal chemistry, as well as the advancements in the area and the importance of combining structure - and ligand-based approaches. One may think of molecular docking as a "lock-and-key" problem, where the goal is to discover the proper relative orientation of the "key" to open the "lock" (where on the surface of the lock is the key hole, which direction to turn the key after it is inserted, etc.). In this case, the protein serves as the "lock" while the ligand serves as the "key." Molecular docking is an optimization issue that explains the "best-fit" orientation of a ligand when it binds to a certain protein. Because the ligand and the protein are both flexible, a "hand-in-glove" analogy is more appropriate than a "lock-and-key" analogy. The ligand and the protein alter their shape throughout the docking process to create an overall "best-fit," and this type of conformational adjustment resulting in overall binding is referred to as "induced-fit."

1.4.1 Docking approaches

Within the molecular docking community, two techniques are particularly prominent. One method employs a matching strategy in which the protein and ligand are described as complimentary surfaces. The second technique simulates the docking process by computing the pairwise interaction energies between the ligand and the protein. Both techniques offer major benefits as well as drawbacks. These are outlined in the following paragraphs.

1.4.2 Complementarity in shape

Using geometric matching/ shape complementarity techniques, the protein and ligand are characterized as a set of features that make them dockable. Complementary surface descriptors and molecular surface descriptors are examples of these characteristics. The molecular surface of the receptor is defined in terms of its solvent-accessible surface area and the molecular surface of the ligand is characterized in terms of its matching surface description in this case. The complementarity between the two surfaces is a shape matching description that may help establish the complimentary posture of docking the target and ligand molecules. Another method is to use twists in the main-chain atoms to explain the protein's hydrophobic properties. A Fourier shape descriptor technique [35-36] is still another option. While shape complementarity-based techniques are normally rapid and reliable, they are unable to adequately describe movements or dynamic changes in ligand/protein conformations, despite recent advances allowing these methods to examine ligand flexibility. Shape complementarity approaches can scan through thousands of ligands in seconds and determine if they can bind to the protein's active site and they're typically scalable to protein-protein interactions. They're also more receptive to pharmacophore-based techniques, as they employ geometric descriptions of ligands to discover the best binding.

1.4.3 Simulation

The docking procedure is substantially more difficult to simulate. The protein and the ligand are separated by a physical distance in this method and the ligand makes its way into the active site of the protein after a particular amount of "moves" in its conformational space. Internal changes to the ligand's structure, such as torsion angle rotations, are included in the motions, as are rigid body transformations such as translations and rotations. Each of these ligand conformational changes results in a total energy cost for the system. As a result, the total energy of the system is estimated after each step. The apparent benefit of docking simulation is that ligand flexibility may be easily added, whereas shapes complementarity approaches need innovative strategies to incorporate ligand flexibility. It also reflects reality more closely, whereas shape complementary approaches are more abstract. Simulation is clearly computationally costly due to the need to explore a broad energy landscape. Docking simulation has become more realistic thanks to grid-based methodologies, optimization methods, and greater computer performance.

1.4.4 Drug Design Using Structure (SBDD)

SBDD methods (i.e., employing three-dimensional structure information obtained from biological targets) are a major aspect of modern medicinal chemistry. Molecular docking, structure-based virtual screening (SBVS), and molecular dynamics (MD) are among the most widely used SBDD strategies due to their wide range of applications in the analysis of molecular recognition events such as binding energetics, molecular interactions and induced conformational changes.

The chemical diversity available in these libraries represents the space occupied by ligands known to interact with a certain target. This sort of data is used in ligand-based drug design (LBDD) techniques. Some of the most useful LBDD approaches are ligand-based

virtual screening (LBVS), similarity searching, QSAR modeling, and pharmacophore creation. SBDD and LBDD approaches have been employed as key drug discovery tools in academia and industry due to their versatility and synergistic nature. In a range of structural, chemical and biological data analyses, combining these approaches has proved to be beneficial [37].

In pharmaceutical research and development, understanding the mechanisms by which small-molecule ligands detect and interact with macromolecules is critical (R & D). SBDD is the systematic utilization of structural data (e.g., macromolecular targets, also known as receptors), which is often collected by experimental or computational homology modeling. The goal is to create ligands with certain electrostatic and stereochemical properties that will bind to receptors with high affinity. The availability of three-dimensional macromolecular structures allows for a thorough examination of the binding site architecture, such as the existence of clefts, cavities and sub-pockets. Charge dispersion and other electrostatic characteristics can also be thoroughly investigated. Current SBDD technologies enable the creation of ligands with the properties required for effective regulation of the target receptor. High affinity ligands selectively modulate a proven drug target, interfering with certain cellular processes and resulting in the desired pharmacological and therapeutic effects. SBDD is a cyclic process that involves acquiring information one step at a time. In silico investigations are used to find possible ligands starting with a known target structure. Following these molecular modeling approaches, the most promising molecules are synthesized. Following that, several experimental platforms are used to assess biological features such as potency, affinity and effectiveness. Once active molecules have been identified, the three-dimensional structure of the ligand-receptor complex may be solved. The accessible structure enables for the study of a number of intermolecular characteristics that aid in the molecular identification process. Structural descriptions of ligand-receptor

complexes can help with binding conformations, characterization of important intermolecular interactions, characterisation of unknown binding sites, mechanistic research and the elucidation of ligand-induced conformational changes [38-39].

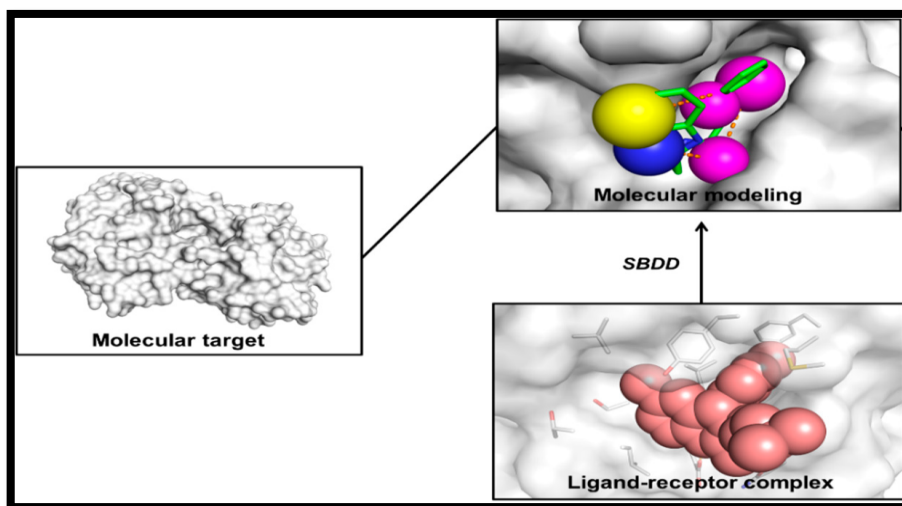


Fig. 3 Outline of SBDD

In molecular modeling investigations, the three-dimensional structure of the molecular target is used. Compounds that show promise are produced and then tested in the lab. After finding bioactive small compounds, the structure of a ligand-receptor complex may be identified. The binding complex is utilized in molecular modeling and the development of new drugs. Biological activity data is connected with structural information after a ligand-receptor complex has been discovered. As a result, the SBDD process is restarted with additional stages to integrate molecular alterations that may boost the affinity of new ligands for the binding site [40]. The outline of the SBDD process is depicted in **Figure 3**.

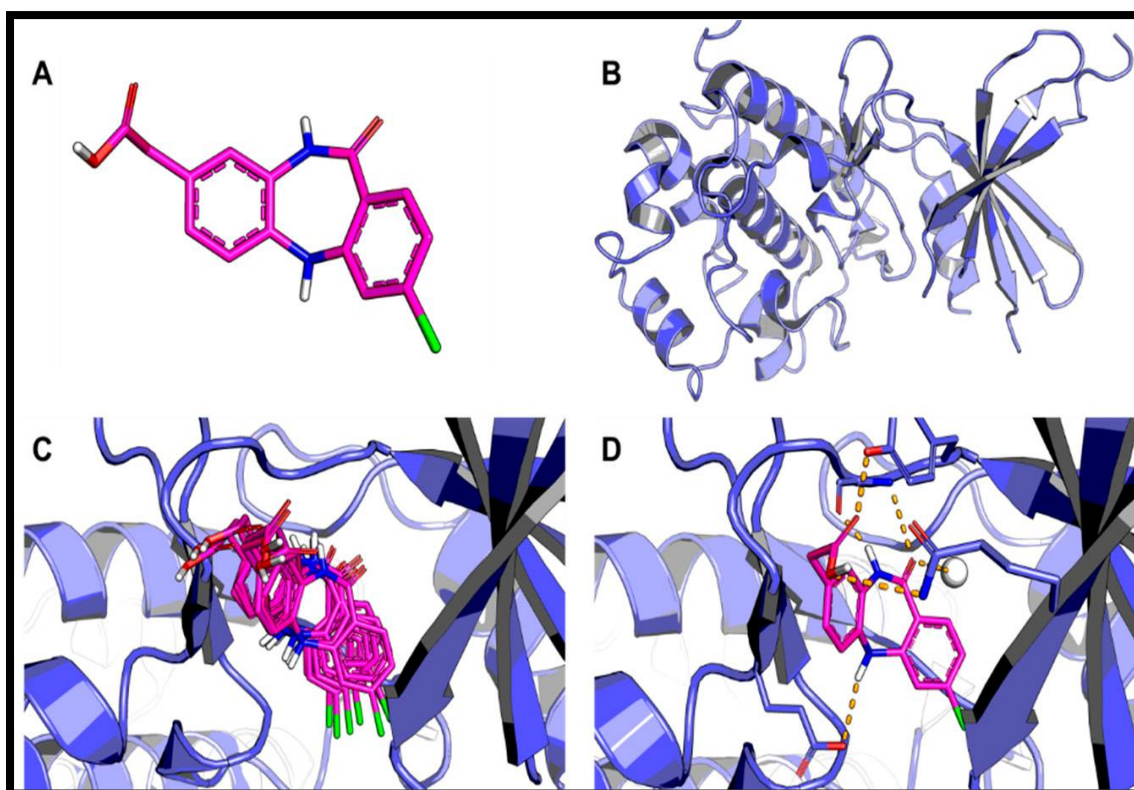


Fig 4. Outline of the molecular docking process

The molecular docking mechanism is depicted in Figure 4. (A) The ligand's three-dimensional structure; (B) the receptor's three-dimensional structure; (C) The ligand is docked into the receptor's binding cavity and the putative conformations are explored; (D) The most likely binding conformation is found, as well as the intermolecular interactions that go with it. The backbone of a protein is depicted as a cartoon. In stick depiction, the ligand (magenta in carbon) and active site residues (carbon in blue) are indicated. Water is shown as a white sphere, with dotted lines indicating hydrogen bonding. In two phases, the most likely binding conformations must be identified: (i) a precise estimate of the interaction energy associated with each of the proposed binding conformations; (ii) exploration of a vast conformational space reflecting numerous potential binding modes. These activities are carried out by molecular docking algorithms in a cyclical process in which the ligand

conformation is assessed using specified scoring functions. This approach is repeated until it converges on a solution with the lowest energy [41].

1.4.5 Applications of molecular docking

The usage of molecular docking is required for today's research. If done before the experimental stage of any inquiry, it can illustrate the viability of any job. There are a few areas where molecular docking has changed the game. Interaction studies between tiny compounds (ligands) and protein targets (which might be enzymes) can help anticipate whether an enzyme will be activated or inhibited. Such data might be used as a starting point for rational medication development. The following are some of the most common molecular docking applications:

1.4.5.1 Optimization of leads

The best orientation of a small molecule or ligand on its target can be predicted via molecular docking. It can forecast several ligand binding mechanisms in the groove of the target molecule. Knowledge gained from such type of investigations may be employed to develop more potent, selective and efficient analogs [42].

1.4.5.2 Hit Identifications

Molecular docking in conjunction with a score algorithm may be used to search large databases in order to uncover powerful drug candidates that can target the molecule of interest *in silico* [43].

1.4.5.3 Drug-DNA Interactions Studies

Chemotherapy is used in the majority of cancer treatment regimens and techniques in recent years. Despite the significant role of chemotherapy in cancer cure and control, cytotoxic mechanisms of several chemotherapeutic agents are not well characterized. Many of these anticancer chemotherapeutic drugs target nucleic acid and accessory functions as

their primary biological targets. With this in mind, researchers are continually working to understand the underlying anticancer mechanism of medications at the molecular level by examining the nucleic acid-drug interaction mode [44]. Here, molecular docking plays a significant role in the preliminary prediction of drug's binding properties to nucleic acid. The information gathered from the outcome of such investigations is helpful in the establishment of a correlation between drug's molecular structure and its cytotoxicity. Furthermore, this knowledge would be instrumental in the detection of those structural modifications in a drug that could result in sequence/structure specific binding to their target (nucleic acid). Because of non-specific binding limits medication dosage and regularity in cancer treatment, this knowledge can be used to rationally design and synthesize novel therapies with improved efficacy and fewer adverse effects. In particular, for protein-ligand docking, induced-fit-motions and flexibility of the protein will be implicated in coming years in an order to discover and design new chemotherapeutic agents. The importance of molecular docking in the pharmaceutical industry is widely understood. Computational docking simulations are now widely used at various phases of drug discovery and rational drug design techniques. As the area of molecular docking-based virtual screening will grow, its recognition will be significantly enhanced. Widely accepted and validated test data should be established to facilitate the comparisons needed to explain the new frontiers of research in this field.

1.5 Thrombolytic Activity

A thrombus (blood clot) that forms in the circulatory system owing to a lack of hemostasis produces vascular occlusion and can cause mortality in thrombolytic disorders such acute myocardial or cerebral infarction. In the technique known as thrombolysis, thrombolytic medicines are used to dissolve blood clots. To dissolve clots, thrombolytic medications such alteplase, anistreplase, streptokinase, urokinase, and tissue plasminogen activator (tPA) are commonly utilized. In recent years, it has been recognized that heart

disease is on the rise and synthetic medicine side effects are becoming an ever-increasing therapeutic concern. Almost all of the currently available thrombolytic medicines have serious flaws [45]. A pill are widely used not as they are inexpensive but in addition greater cultural acceptability, better compatibility while using skin and minimal side consequences. Herbal medicine remains be your mainstay of about 75-80% on the globe population, mainly in your establishing countries for primary health.

The dissolution (lysis) of blood clots using just pharmacological techniques is known as thrombolysis. This evidence is referred to as clot busting informally. It works by infusing analogs that influence tissue plasminogen activator (tPA), a protein that typically stimulates plasmin, to stimulate fibrinolysis by simply plasmin. Thrombolysis refers to the administration of thrombolytic medications, which are either produced by Streptococcus species or, more recently, by recombinant biotechnology, in which tPA is produced by bacteria, resulting in a recombinant tissue plasminogen activator that also contains tPA. Formation of blood clots is place for the basis of many serious disorders [46].

The term thrombus refers to the formation of a blood clot, whereas thrombosis refers to the act of obstructing blood flow via the circulatory system. After an injury, the body employs platelets and fibrin to produce a blood clot as the first stage in the healing process. Streptokinase, S-Kinase and other drugs are used to dissolve clots and treat heart attacks, strokes, deep vein thrombosis and peripheral arterial occlusion. Circulatory platelets clump together at the site of damage and constitute the most important component in thrombus formation. Thrombosis is a crucial stage of vascular illness that leads to myocardial infarction and stroke, which cause significant morbidity and death. In addition, venous thrombosis is the second leading cause of death among cancer patients. These illnesses are treated with thrombolytic medicines such tissue plasminogen activator (t-PA), Urokinase (UK), and Streptokinase (SK).UK and SK are the most often utilized thrombolytic agents in India. If

you're looking for a unique way to express yourself. They are at great risk for bleeding and severe allergic responses. Moreover, various treatments with SK are restricted due to immunogenicity. The lack of thrombolytic medicines makes developing better recombinant forms of these medications difficult. SK is utilized as a thrombolysis drug in cases of myocardial infarction (heart attack) and pulmonary embolism [47]. The illness process may have been halted, or the problems may have subsided. Thrombolytic drugs actively limit the dimensions of any clot by activating the enzyme plasminogen, which clears the cross-linked fibrin mesh. Other anticoagulants (such as heparin) reduce the "growth" of any clot (the backbone of any clot). These drugs dissolve blood clots simply by activating plasminogen, which forms the newer cleavage product called plasmin and this makes the clot soluble and subject to further proteolysis by other digestive enzymes, restoring blood flow through the occluded arteries and thrombolytic drugs that dissolve blood clots simply turn on plasminogen, which makes up the newer split product called plasmin. Plasmin is a proteolytic enzyme that breaks cross-links between fibrin molecules, which are important for the structural stability of blood clots. Because connected with such actions, thrombolytic drugs are otherwise often known as "plasminogen activator" and "fibrinolytic drug treatments". While all three kinds of medicines appear to dissolve blood clots successfully, their precise processes differ in ways that might affect their selectivity for fibrin clots. Derivatives of tPA are among the most commonly prescribed thrombolytics, particularly for coronary and cerebral vascular blockages, due to their relative selectivity for activating fibrin bound plasminogen. Thrombolytic treatment is the use of medications to break up and dissolve blood clots, which are a major cause of both heart attacks and strokes.

REFERENCES

1. Lagoja IM. Pyrimidine as constituent of natural biologically active compounds. *Chem Biodivers.* 2(1) (2005) p.1-50.
2. Katritzky AR, Ress CW, Scriven EFV, Comprehensive Heterocyclic Chemistry II. Eds. Pergamon: Oxford, U.K. (1996) p.1-9.
3. Mossaraf Hossain and Ashis Kumar Nanda, A Review on Heterocyclic: Synthesis and Their Application in Medicinal Chemistry of Imidazole Moiety, *Science Journal of Chemistry* 6(5) (2018) p 83-94.
4. Hasan MU, Arab M, Pandiarajan K, Sekar R, Marko D. *Magn.Reson.Chem.*23(1985) p.292.
5. Pandiarajan K, Sabapathy MohanRT, Krishnakumar R. *Indian J. Chem.* 26(B) (1987) p.624.
6. Pandiarajan K, Sekar R, Anantharaman R, Ramalingam V. *Indian J.Chem.*30(B) (1991) p.490.
7. Rollas S and Kucukauzes SG, *Molecules.*12 (2007) p.1910-1939.
8. Brehme R, Enders D, Fernandez R and Lassaletta JM, *European ournal of OrganicChemistry.*34 (2007) p.5629-5660.
9. Kaplancikli ZA, Altintop MD, Ozdemir A, Zitouni GT, Khan SI and Tabanca N, *Letters in Drug Design & Discovery.* 9 (2012) p.310-315.
10. Belkheiri M, Bouguernf B and Bedos-Belval F, *European Journal of Medicinal Chemistry.* 45 (2010) p.3019-3026.
11. Rajitha G, Saideepa N and Praneetha P, *Indian Journal of Chemistry.* 50 (2011) p.729-733.
12. Mohareb RM, El-Sharkawy KA, Hussein MM and El-Sehrawi HM, *Journal of Pharmaceutical Sciences and Research.* 2 (2010) p.185-196.

13. Rana M. Jamous, Salam Y. Abu-Zaitoun, Rola J. Akkawi and Mohammed S. Ali-Shtayeh, Anti-obesity and anti-oxidant potentials of selected Palestinian medicinal plants. *Evidence-based complementary and alternative medicine*. 9 (2018) p.1-21.
14. World Health Organization (WHO), World Health Organization factsheets, Obesity and overweight, (2017), <http://www.who.int/mediacentre/factsheets/fs311/en/>.
15. H. F. Abdul-Rahim, G. Holmboe-Ottesen, L. C. M. Stene et al., "Obesity in a rural and an urban Palestinian West Bank population," *International Journal of Obesity*. 27(1) (2003) p. 140–146.
16. Hafeedza Abdul Rahman, Nazamid Saari, Faridah Abas, Amin Ismail, Muhammad Waseem Mumtaz and Azizah Abdul Hamid, Anti-obesity and anti-oxidant activities of selected medicinal plants and phytochemical profiling of bioactive compounds, *International journal of food properties*. 20(11) (2017) p.2616-2629.
17. Rashmi Shivanna, Hengameh Parizadeh, Rajkumar H. Garampalli, In vitro anti-obesity effect of macrolichens *Heterodermia leucomelos* and *Ramalina celastri* by pancreatic lipase inhibitory assay, *International Journal of Pharmacy and Pharmaceutical Sciences*. 9(5) (2017) p 686-695.
18. Vinay Kumar, Uma Bhandari, Chakra Dar Tripathi, Geetika Khanna. Evaluation of antiobesity and cardioprotective effect of *Gymnema sylvestre* extract in murine model. *Indian Journal Pharmacology*. 44(5) (2012) p 607-613.
19. Mokdad A, Ford E, Bowman B, Dietz W, Vinicor F, Bales V, Marks J. Prevalence of obesity, diabetes, and obesity related health risk factors. *JAMA*. 289 (2003) p 76–79.
20. Cragg GM, Newman DJ. Natural Product Drug Discovery in the Next Millennium. *Pharm Biol* 39(1) (2001) p 8-17.

21. Moonkyu K, Jung WO, Hee KL, Hwan SC, Sang ML, Changsook K *et al.* Anti-obesity Effect of PM-F2-OB, an Anti-obesity Herbal Formulation, on Rats Fed a High-Fat Diet. *Biol Pharm Bull*, 27(8) (2004) p 1251-1256.
22. Mokdad AH, Ford ES, Bowman BA, Dietz WH, Vinicor F, Bales VS, Marks JS: Prevalence of obesity, diabetes and obesity-related health risk factors. *J Am Med Assoc* 289 (2003) p76–79.
23. Aronne LJ: Modern medical management of obesity: the role of pharmaceutical intervention. *J Am Diet Assoc.* 98 (1998) p S23–S26.
24. Neerja rani, Neeru vasudeva and Surendra and Surenra kumar kumar Sharma, Quality assessment and anti-obesity activity of stellaria media (linn.) vill, *BMC complementary&alternative medicine*, 12(145) (2012) p1-8.
25. R.B.Birari and K.K.Bhutani, Pancreatic lipase inhibitors from natural sources unexplored, *Drug Discovery Therapy.* 12 (19-20) (2007) p879-889.
26. Y.Shi and P.Burn, Lipid metabolic enzymes, emerging drug targets for the treatment of obesity, *Nature Reviews Drug Discovery.* 3 (8)(2004) p 695-710.
27. Lowe M. The triglyceride lipases of the pancreas. *J Lipid Res* 43(2002) p 2007-16.
28. Muller K. Pharmaceutically relevant metabolites from lichens. *Appl Microbiol Biotechnol*, 56 (2002) p 9-16.
29. Shanta A, Nazim U, Kazi Zahra M, Tarannur Kabir N, Fayejun N, Shermin A, Sahida A, Sajal C, Dipannita C, Nasrin A. In Silico Molecular Docking Approach of Some Selected Isolated Phytochemicals from Phyllanthus Emblic Against Breast Cancer. *Biomed J Sci & Tech Res*, 10(2) (2018) p 891-899.
30. Z. Song, Y. Ge, C. Wang, S. Huang, X. Shu, K. Liu, Y. Zhou, X. Ma, Challenges and perspectives on the development of small-molecule EGFR inhibitors against T790

- Mmediated resistance in non-small-cell lung cancer: miniperspective, *J. Med. Chem.* 59 (14) (2016) p 6580–6594.
31. A. AF.Wasfy, Synthesis and anticancer properties of novel quinazoline derivatives, *International journal of research in pharmacy and chemistry*.1 (2015) p 34-40.
32. Jaynthy C,Shanmugalakshmi G,Anusha mathan B,In silico docking studies of secondary metabolites from marine sponge *Disodermia calyx*-natural inhibitor for breast cancer, *International journal of pharmaceutical and clinical research*.10(3) (2018) p.62-64.
33. Majda Batool, Affifa Tajammal , Firdous Farhat , Francis Verpoort , Zafar A. K. Khattak , Mehr-un-Nisa , Muhammad Shahid , Hafiz Adnan Ahmad , Munawar Ali Munawar Muhammad Zia-ur-Rehman and Muhammad Asim Raza Basra, Molecular Docking, Computational and Antithrombotic Studies of Novel 1,3,4-Oxadiazole Derivatives, *Int. J. Mol. Sci.*, 19, 3606 (2018) p 2 of18.
34. . Cai W, Shao X, Maigret B, Protein-ligand recognition using spherical harmonic molecular surfaces: towards a fast and efficient filter for large virtual throughput screening, *Journal of Molecular Graphics & Modelling*. 20(4) (2002) p 313–28.
35. Morris RJ, Najmanovich RJ, Kahraman A, Thornton JM , Real spherical harmonic expansion coefficients as 3D shape descriptors for protein binding pocket and ligand comparisons, *Bioinformatics*. 21(10) (2005) p 2347–55.
36. Valasani K.R, Vangavaragu J.R, Day V.W, Yan S.S, Structure based design, synthesis, pharmacophore modeling, virtual screening, and molecular docking studies for identification of novel cyclophilin D inhibitors. *J. Chem. Inf. Mod.* 54 (2014) p 902–912.
37. Fang, Y. Ligand-receptor interaction platforms and their applications for drug discovery. *Expert Opin. Drug Discov.* 7 (2012) p 969–988.

38. Kahsai A.W, Xiao K, Rajagopal S, Ahn S, Shukla A.K, Sun J, Oas T.G, Lefkowitz R.J, Multiple ligand-specific conformations of the β 2-adrenergic receptor. *Nat. Chem. Biol.* 7 (2011) p 692–700.
39. Shoichet B.K, Kobilka B.K, Structure-based drug screening for G-protein-coupled receptors, *Trends Pharmacol. Sci.* 33 (2012) p 268–272.
40. Huang S.Y, Zou X, Advances and challenges in protein-ligand docking. *Int. J. Mol. Sci.* 11 (2010) p 3016–3034.
41. Gschwend DA, Good AC, Kuntz ID. Molecular docking towards drug discovery, *J Mol Recognit.* 9 (1996) p 175-186.
42. LG Ferreira, RN dos Santos, G Oliva, AD Andricopulo, Molecular docking and structure-based drug design strategies. *Molecules.* 20 (2015) p 13384-13421.
43. Agarwal S, Jangir DK, Singh P, Mehrotra R. Spectroscopic analysis of the interaction of lomustine with calf thymus DNA. *J Photochem Photobiol B.* 130 (2014) p 281-286.
44. Fatema Tabassum, Somaia Haque Chadni, Kamrun Nahar Mou, KM Imrul Hasif, Tareque Ahmed and Mahbuba Akter In-vitro thrombolytic activity and phytochemical evaluation of leaf extracts of four medicinal plants of Asteraceae family, *Journal of Pharmacognosy and Phytochemistry*, 6(4) (2017) p 1166-1169.
45. Mohammad Imran Hossain, Md Hossan sakib, Asif Al Mahmood, Naymul Karim, Mohammad Shahin Alam, Md. Ariful Islam, Monalisha Sharma, Study on in-vitro thrombolytic activity of methanolic extract of Mesua ferrea leaves, *International Journal of Medical and Health Research*, 1(2) (2015) 52-55.
46. Houghton PJ: The role of plants in traditional medicine and current therapy. *Journal of Alternative and Complementary Medicine* 1(2) (1995) p 131-143.

47. Rouf, S.A.; Moo-Young, M.; Chisti, Y. Tissue-type plasminogen activator: Characteristics, applications and production technology. *Biotechnology Advanced*. 14 (1996) p 239–266.

Chapter-2

REVIEW OF LITRATURE

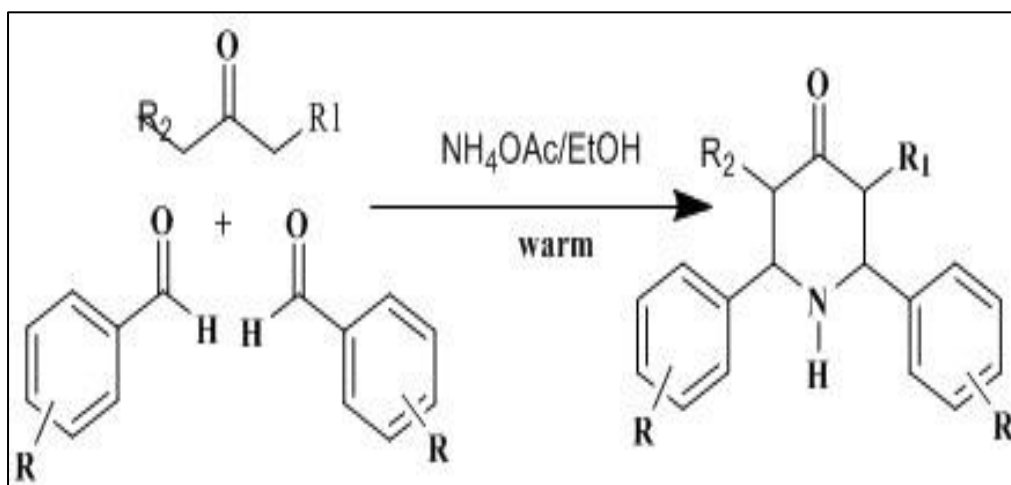
2.1 Hydrazones

Interest in the study of hydrazone has been growing because of their wide range of biological activities. Hydrazones with an azomethine -NHN=CH- are an important family of chemicals for the creation of novel drugs. As a result, several scientists have synthesized these molecules as target structures and tested their biological activity. Hydrazone and its derivatives have a lot of biological activity.

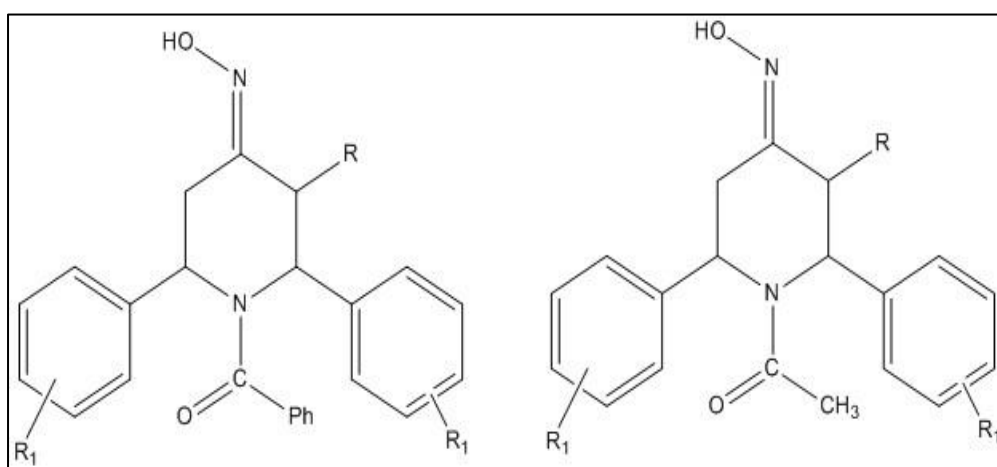
Abbas Al-Mulla [1] review heterocyclic compounds of biological relevance were screened Heterocyclic compounds are the most numerous and diverse group of organic chemicals. There are many heterocyclic compounds known today and the number is continually rising due to extensive synthetic study and their synthetic value. Heterocyclic compounds have a function in a variety of domains, including medical chemistry, biochemistry and other sciences.

The Piperidin-4-one nucleus is often generated by Mannich Reaction. An acidic proton is positioned close to a carbonyl functional group and is alkylated utilizing formaldehyde/various aldehydes, ammonia or any primary or secondary amine in the Mannich reaction. The final product is a α -aminocarbonyl molecule, sometimes known as a Mannich base. Dehydration is followed by the nucleophilic addition of an amine to a carbonyl group in this case. Noller and Baliah [2] were the first to describe a Mannich type condensation using different substituted aromatic aldehydes, ammonium acetate and ketones

in a 1:2:1 ratio with two active methylene groups, leading in the synthesis of 2, 6-diarylpiperidin-4-ones.

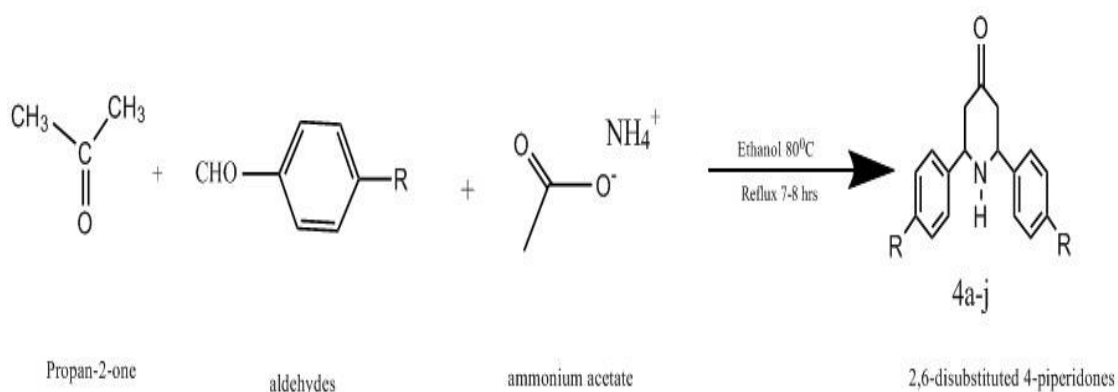


The stereochemistry of N-acetyl and N-benzoyl-2r, 6c-diphenylpiperidine-4-one oximes has been described by Pandiarajan et al.,[3].



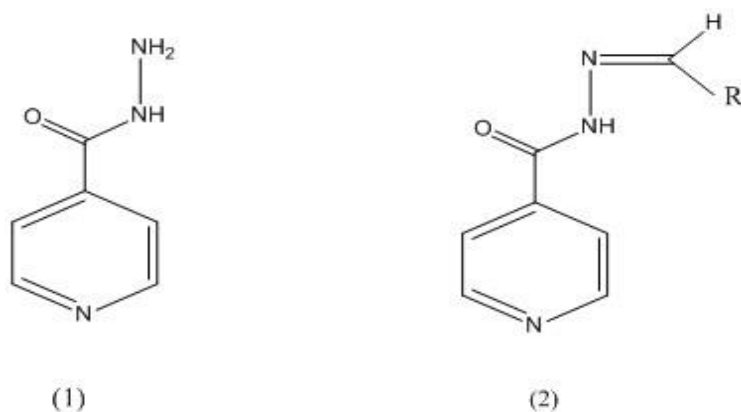
Chawla et al., [4] synthesized, characterized and tested novel 2,6-di substituted piperidine-4-one derivatives for biological activities. The substance piperidine and its derivatives have a significant influence on the medical profession owing to their wide range of pharmacological actions. Piperidine derivatives are made by reacting acetone, ammonium acetate and a substituted aromatic aldehyde in the presence of ethanol. An effort was made in this study to synthesis some new physiologically active piperidine derivatives. Spectral data

was used to characterize the structures of the freshly synthesized molecules. Antimicrobial activity was tested on the chemicals created.

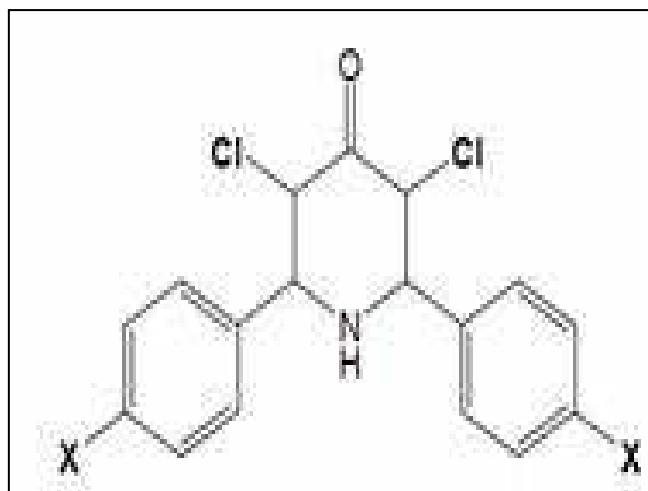


S. Saini et al., [5] reviewed the biological importance of heterocyclic chemicals studied by Mukhtyar. The pharmaceutical and agrochemical industries' keen interest in heterocycles is frequently linked to their natural occurrence.

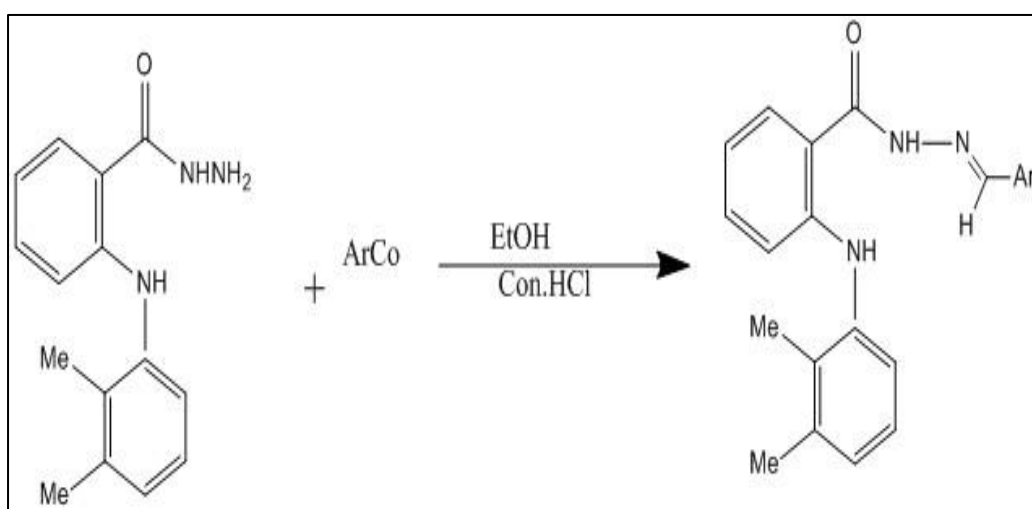
Nazia Tarannum et al., [6] conducted a systematic review on the production and biological activities of hydrazide derivatives.



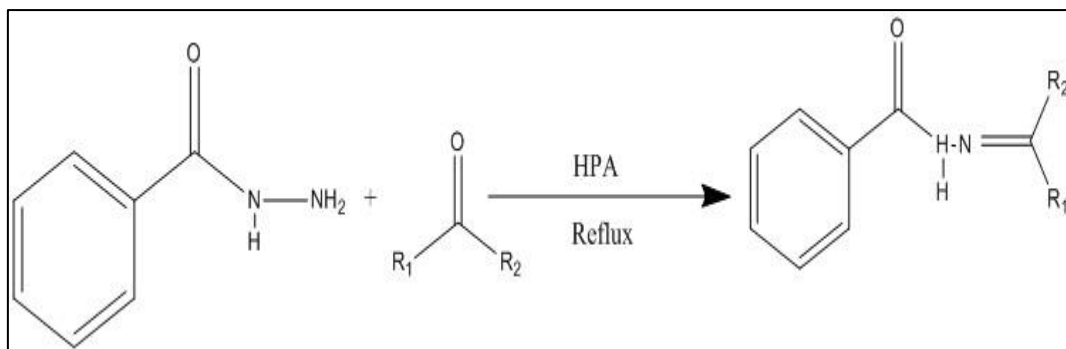
The synthesis, spectroscopic, antibacterial and molecular docking investigations of certain new 3, 5-dichloro-2, 6-diarylpiperidin-4-ones were reported by Bhakiaraj et al.,[7]. Fluoro, chloro, methoxy or methyl functions at the para position of the phenyl ring attached to the C-2 and C-6 carbons of the piperidone moiety, as well as chloro substituents at the C-3 and C-5 positions of the piperidone ring, exerted potent biological activities against antimicrobial strains at a minimum inhibitory concentration



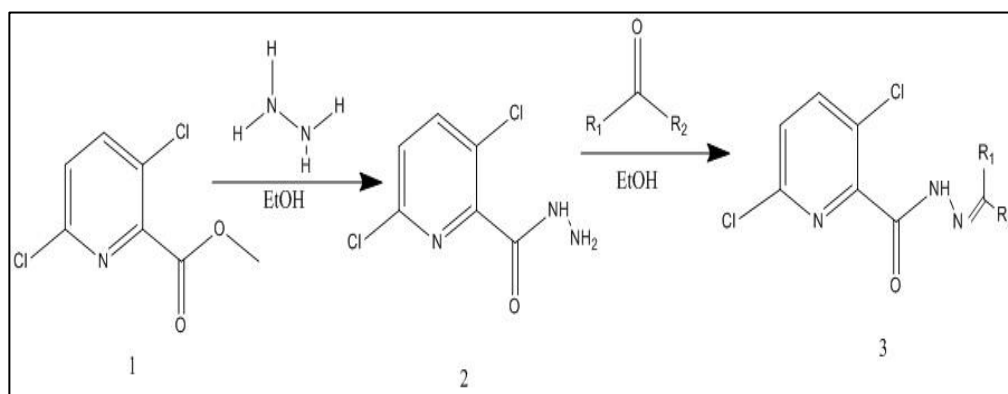
A novel series of mefenamic acid N-aryl hydrazone derivatives were prepared by Almasirad et al., [8] as per the below scheme. A mixture of aldehyde and hydrazide were treated in ethanol at 30°C in the presence of the conc. HCl as catalyst.



Sadjadi et al., [9] reported the preparation of N-acyl-benzoyl hydrazone and benzoyl hydrazone derivatives in the presence of different types keggin type of heteropolyacids like $H_3[PMO_{12}O_{40}]$, $H_4[PMO_{11}VO_{40}]$, $H_5[PMO_{10}V_2O_{40}]$, and $H_6[PMO_9V_3O_{40}]$ as catalyst in the acetonitrile solvent. Reaction mixture was filtered to recycle the catalyst.



Jie Zhang., [10] and his coworkers prepared new derivatives of hydrazone-hydrazone by reacting the compound with hydrazine hydrate in the presence of catalytic amount of H_2SO_4 in the solvent, the obtained hydrazone reacted with required carbonyl compounds to get the compound 3 using catalytic amount of acetic acid.



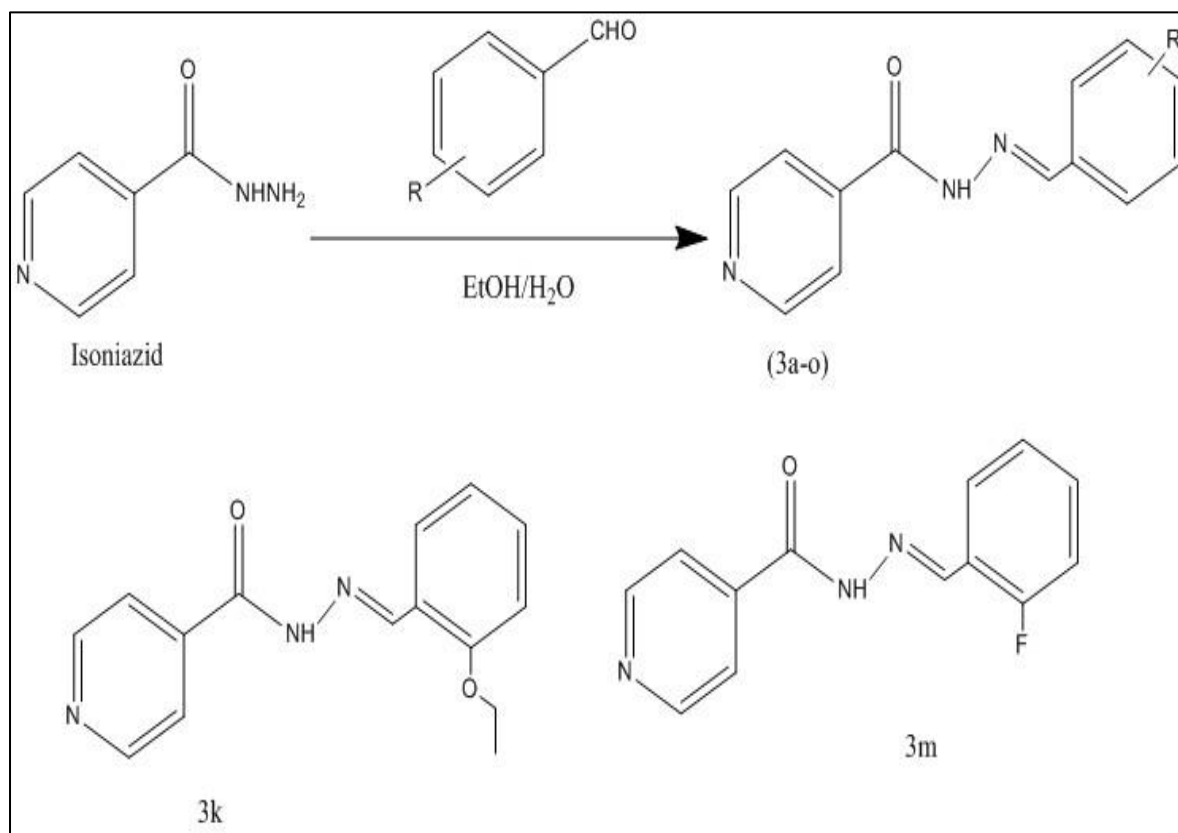
Abdel-Aal et al., [11] have reported antiviral activity of N-aryl amino acetyl hydrazones against Hapatits-A.

Nigh Singh et al., [12] have provided a brief overview of the biological actions of hydrazone derivatives. Hydrazones are found in a wide variety of bioactive heterocyclic compounds and have a wide range of biological and therapeutic uses. Many researchers have researched the production and significance of hydrazides, which are used in a variety of biological, medicinal and industrial applications. Hydrazones have been shown to have antibacterial, antimycobacterial, antidepressant, anticonvulsant, anticancer, antimalarial and

vasodilator properties, among others. Hydrazones have a number of advantages over imines, including simplicity of manufacture, enhanced hydrolytic stability and a tendency to crystallize. Hydrazones have been studied for a long time because of their beneficial properties.

Gagandeep Kaure et al., [13] a quick study of thiadiazole analogs as possible pharmacological agents; review paper has been created chemicals Due to their biological and pharmacological features, heterocyclic molecules, analogues and derivatives have recently gained a lot of attention in medicinal chemistry. The tiny and simple thiadiazole nucleus has anticancer, antibacterial, anti-inflammatory, anticonvulsant and anti-diabetic effects. These properties are also seen in its substituted derivatives. The purpose of this review is to look at the pharmacological properties of thiazole derivatives.

The synthesis and assessment of iso nicotinoyl hydrazone derivatives as anti mycobacterial and anticancer drugs was reported by Naveen Lumar HS et al., [14]. Using a tetrazolium microplate test, a novel series of iso nicotinoyl hydrazone derivatives was synthesized, described and assessed for in vitro anti mycobacterial activity against *M. tuberculosis* H37Rv and two clinical isolates (TEMA). At micro molar concentrations, some of these substances demonstrated moderate to excellent antimycobacterial action. Isoniazid (0.57 μ M), 3k, and 3m were the most potent analogues against *M. tuberculosis* H37Rv, with inhibitory concentrations of 0.59 and 0.65 M, respectively, in compared to the original drug. In addition, all of the produced compounds were tested in vitro against human colorectal cancer cell lines for anticancer potential (HCT 116).



N.Jayalakshmi et al.,[15] prepared several 2,6-diphenyl piperidine-4-ones by Mannich reaction of ethyl methyl ketone, substituted aldehyde and ammonium acetate. The synthesized compounds were tested for antibacterial, antifungal activities at various concentrations and hydrazone derivatives also possess antibacterial and antifungal activities.

P. Ball, C. H. Nicholls, and others [16] investigated the hydroxyazo compound's azo-hydrazone tautomerism. The phenomena of azo-hydrazone tautomerism in hydroxyazo compounds is discussed in connection to structural aspects such as annellation degree and substituent type and location, as well as environmental factors influenced by the media housing the tautomeric entity. Studies in solution, polymeric substrates, the crystalline solid state and the gas phase are used to examine media effects. The impact of the tautomeric

equilibrium state on chemical reactivity is studied, with an emphasis on photochemistry and acid-base behavior of tautomeric hydroxyazo dyestuffs.

Vicini et al. [17] synthesized and tested a variety of hydrazones generated from 1, 2-benzisothiazole hydrazides for antibacterial and antifungal activities. Acetophenone-4-aminobenzoyl hydrazone and 4-hydroxyacetophenone-4-amino benzoyl hydrazone and corresponding cobalt (II), Nickel (II), Zinc (II), Copper(II) and Cadmium(II) complexes were prepared by Singh.B et al.,[18] and they evaluated the antibacterial (activity of these complexes) and antifungal activities and compared with ligand hydrazone.

Bechan Sharma [19] studied hydrazones as a potential anti-HIV agent. Hydrazones are a kind of organic molecule that may be found in both chemical and biological environments. These heterocycles with nitrogen and carbon moieties provide the basic structure of a variety of physiologically intriguing compounds with antiHIV-1RT, anti-DNA polymerase and anti-RNase H properties. As a result, hydrazones function as a two-in-one small molecule that fights HIV-1. This study focuses on the characteristics and actions of hydrazones and their many chemical derivatives as anti HIV-1 agents. Hydrazones have been demonstrated to interact with viral capsid protein and prevent it from being processed completely. It belongs to the $>C=N-NH_2$ group, which has been shown to be very effective in the production of antiviral agents. A thorough search for hydrazone's various effects reveals that little is known about their interactions with viral integrase and protease activities. Based on the available data, it appears that further work is needed now to create more effective hydrazones and their derivatives against a variety of viable targets in the HIV-1 life cycle in order to prevent viral growth without causing harm to the hosts. The features and activities of hydrazones and their different chemical derivatives as antiHIV-1 compounds are highlighted in this study.

Synthesis, spectra and thermal aspects of transition metal coordination polymers with bis-hydrazones ligand has been investigated Ratiran Gomuji Chaudhary, Sudhirs. Bhyar, Smita Kharkale, Lali tmohan Jainarayan Paliwal [20] Coordination polymeric assemblies of the type $[M(dddinh)(H_2O)_2 \cdot xH_2O]_n$ [where M= Mn(II), Ni(II), and Cu(II) , x=2; and Co(II) , x=0, with (N',N''E,N',N''E)-N',N''-(1,2-diphenylethane-1,2-diylidene) diisonicotino-hydrazide (dddinh)] have been synthesized and characterized by using various spectroscopic techniques such as elemental analysis, FT-IR, diffuse reflectance spectra, magnetic measurements and thermo gravimetric analysis. All of the produced coordination polymers were given an octahedral geometry based on magnetic moment and reflectance spectral analyses Each metal ion forms a 5-member heterocyclic ring by becoming bis (bidentate) coordinated between the oxygen atom of the carbonyl group and the nitrogen atom of the amide group of the ligand, as well as two aqua ligands. Heat analysis methods were used to investigate the breakdown processes and thermal stability of these coordination polymers. The release of coordinated water and the disintegration of the backbone structure are used to explain the heat stabilities of coordination polymers (ligand). Thermal tests revealed the presence of crystallized water in all coordination polymers except Co (II), whereas coordinated water was found in other polymers.

Constatin sandra et al.,[21] have studied on xanthine derivatives (II) synthesis and antioxidant effects of some hydrazones with xanthine structure were evaluated using in vitro assays: DPPH (2,2-Diphenyl-1-picrylhydrazyl) and ABTS (2,2'-azinobis-(3-ethylbenzothiazoline-6-sulfonic acid) radical scavenging ability and total antioxidant capacity) radical scavenging ability and total antioxidant capacity) radical scavenging ability and total antioxidant capacity) radical scavenging ability and total antioxidant capacity) radical scavenging ability and total antioxidant capacity. The findings revealed that chemical modification of theophylline was linked to an increase in the antioxidant properties of the

parent molecule in general. Hydrazone c, which contains a 2-OH substituent on the aromatic ring and exhibits ABTS scavenging activity equivalent to ascorbic acid, was the most active molecule. The replacement of 3/4-OH, 4-NO₂, and 4-CN for the aromatic ring was likewise linked to increased antioxidant activities, with the corresponding derivatives possessing significant DPPH and ABTS scavenging effects as well as overall antioxidant capacity.

According to Sevim Rollas et al [22], there has been a lot of interest in developing new compounds with anticonvulsant, antidepressant, analgesic, antiinflammatory, antiplatelet, antimalarial, antimicrobial, antimycobacterial, antitumoral, vasodilator, antiviral and antischistosomiasis activities. Hydrazones with an azometine -NHN=CH- proton are an important family of chemicals for the creation of novel drugs. As a result, a number of scientists have synthesized these molecules as target structures and tested their biological effects. These findings have aided in the creation of novel hydrazones with a variety of properties.

The biological activities of hydrazine have been documented by M.Singh et al [23]. Carbonyl compound hydrazone derivatives are an important family of physiologically active chemicals. Antitumor, antibacterial, antiviral, antihypertensive, anticonvulsant, anti-inflammatory and analgesic properties, vasorelaxant activity, anticoagulant activity and anti protozoal activities, among other biological activities, have been discovered in hydrazone derivatives. During literature survey it was found that no single review is available solely on the biological activities of hydrazones. The current review compiles a list of the many biological actions that hydrazones have.

The synthesis of certain novel hydrazine derivatives containing the benzothiazole moiety has been described by Ahmet ozdemir et al., [24]. Hydrazones are a type of chemical that may be found in a wide range of products. Due to their importance in synthetic chemistry, the

present article reports the synthesis of a new series of ten compounds based on the coupling of 2-oxo-3(2H)-benzothiazoleacetic acid, hydrazide and 2-thioxo-3(2H)-benzothiazoleacetic acid, hydrazide with different aldehydes. The structures of the synthesized compounds were confirmed by elemental analyses, IR, ¹H-NMR, ¹³C-NMR and FAB+–MS spectral data.

2.2 Anti -Obesity Activity

Hajji et al., [25] used statistical methods to develop reliable QSAR models capable of predicting the inhibitory activity (CAMKK2) of a series of 32 molecules of 2-anilino, 4-aryl pyrimidines and 2,4-diaryl 7-azaindoles.

Eman Abdalla Morsi and his associates, [26] Commiphora myrrha extracts in ethyl acetate and methanol extracts were examined in vitro for their anti-diabetic and anti-obesity activities. The ethyl acetate extract of C. myrrha was shown to have anti-diabetic and anti-obesity properties, as well as being rich in chemicals that are useful in the treatment of hyperglycemia and obesity. Therefore, encourage to use this plant due to its effect is recommended to diabetes patients.

Marcos C. Carreira¹ et al., [27] the anti-obesity action of OBEX is governed by thermogenesis activation and decreased adiposity growth, according to research. Obesity has been on the rise globally in recent decades, necessitating the development of innovative and effective treatment techniques. OBEX is an anti-obesity oral dietary supplement that contains antioxidants. OBEX's effects have been studied both in vivo and in vitro. In high fat diet-fed rats, OBEX lowers weight gain by lowering adiposity growth and boosting energy expenditure in vivo, irrespective of eating habits, via activating thermogenesis in brown adipose tissue (BAT). In vitro, OBEX has anti-proliferative and anti-differentiation properties in 3T3-F442A cells. Furthermore, in mature adipocytes generated from 3T3-F442A cells,

OBEX induced a considerable reduction in lipid burden. Overall, our data indicate that OBEX protects against obesity in an obesogenic environment.

B Manimegalai et al.,[28] were screened anti-obesity properties of *Gymnema sylvestre* leaf extract were investigated. Obesity is a chronic condition of carbohydrate and fat metabolism that poses a risk to human health and well-being. It is described as adipose tissue fat buildup that is aberrant or excessive. Obesity and related diseases may benefit from the use of natural herbal supplements for weight loss. As a result, the goal of this research was to look into the phytochemical screening and anti-obesity effect of *Gymnema sylvestre* leaves extract. In ethanol and aqueous extracts of *Gymnema sylvestre* leaves, saponins, flavonoids, steroids, terpenoids, polyphenols and coumarins were detected, however tannin and triterpenoids were not. Only the ethanol extract contains alkaloids and glycosides. Only aqueous extract contains anthroquinones. According to quantitative studies, the *Gymnema sylvestre* leaves include flavonoids, saponin, phenol and terpenoid. Significant levels of flavonoids (27.29 mg/gm), saponin (37.18 mg/gm), phenol (142.00 mg/gm) and terpenoid (31.00 mg/gm) were found. The anti-obesity efficacy of *Gymnema sylvestre* was demonstrated via lipase inhibition. Overall, the results of this study show that *Gymnema sylvestre* leaves have a high concentration of phytochemicals and have anti-obesity properties.

Rashmi shivsnns et al., [29] used a pancreatic lipase inhibitory experiment to study the anti-obesity activity of macrolichens *heterodermia leucomelos* and *ramalina celastri*. They found that as the quantity of extracts increased, so did the inhibition of the enzyme. Solvent methanol showed good activity compared to ethyl acetate. The percentage of inhibition in methanol extracts of *heterodermia leucomelos* and *ramalina celastri* was 19.7-69.8 and 20.0-

86.6, respectively. At 25 mg/ml, lichen ramalina celastri inhibited enzyme lipase by 86.6 percent in methanol extract, whereas ethyl acetate inhibited enzyme lipase by 63.0 percent.

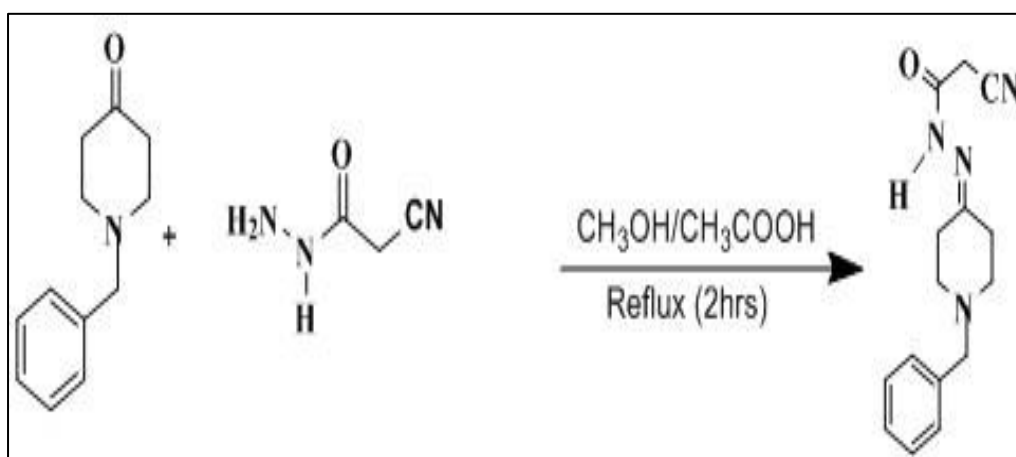
Athesh et al. [30] studied the anti-obesity potential of *Cyperus rotundus* L. Rats fed a high-fat cafeteria meal generated aqueous tuber extract. When HFCD was given to experimental rats for 40 days, it dramatically raised body weight, organ and fat pad weights, blood total cholesterol, LDL cholesterol, VLDL cholesterol, triglycerides and glucose levels, while decreasing HDL cholesterol. While ATECR therapy resulted in a dose-dependent reduction in body weight growth, organ weight of the liver, kidney and spleen, fat pad weight, and blood triglycerides, total cholesterol, LDL cholesterol, VLDL cholesterol, glucose, and a rise in HDL cholesterol. Furthermore, after treatment with varied dosages of ATECR, the levels of liver indicators such as aspartate transaminase (AST), alanine transaminase (ALT) and alkaline phosphatase (ALP), which were reported to be raised in the blood of obese rats, returned to normal. Furthermore, consuming ATECR decreased oxidative stress in rats with HFCD-induced obesity by increasing glutathione (GSH), glutathione peroxidase (GPx), superoxide dismutase (SOD) and catalase levels in the hepatic tissue.

Changhyun Roh et al., [31] the anti-obesity activity of crude plant extracts has been synthesized. Obesity is a risk factor for metabolic syndromes and promoting early adipogenesis in adipose tissue, resulting in the replacement of larger adipocytes that release inflammatory factors with tiny adipocytes, is a flexible method for treating obesity. In this work, we used in vitro enzymatic lipase activity to evaluate crude anti-obesity medicines derived from 400 plant extracts. In vitro anti-lipase activity was considerably reduced by 44 extracts from plant extracts out of 400 tested. The four plant extracts were potent in inhibiting lipid production in 3T3-L1 adipocytes, suggesting that they may be used as crude anti-obesity drugs. *Salicis Radicis Cortex* has the most fat-inhibiting action of all of them. As a result of

these findings, these four active plant extracts may be effective in the prevention or treatment of obesity.

2.3 Insilico Molecular Docking

N-(1-benzylpiperidin-4-ylidene)-2-Cyanoaceto hydrazide was synthesized by K.Tharini and K.Sundaresan et al., [32]. The molecular docking approach, according to the researchers, may be used to simulate the atomic level interaction between a small molecule and a protein, allowing them to describe small molecule behavior at target protein binding sites as well as depict fundamental biochemical processes. BIOVIA Discovery Studio (DS) 2017 software was used to conduct in silicomolecular docking investigations. When compared to typical drugs, the compound possesses a better and robust binding affinity in both proteins (2YAT and 1IR3). The CDOCKER (CHARMm-based DOCKER) methodology included in DS was used to investigate possible binding mechanisms between the ligands and this target protein. In an in silico technique, molecular docking was used to establish that comparable chemicals can attach to receptor protein therapy of breast cancer.



Jesudass Joseph Sahayarayan et.al [33] has investigated In-silico protein-ligand docking studies against the estrogen protein of breast cancer using pharmacophore based virtual screening approaches. Docking tests were carried out after comparing the screened

compounds to the recorded compounds and the data set used to create the pharmacophore sample. Glide docking scores were similarly strongly associated with prime MMGBSA scores. The consistency of the protein complex architectures is verified using molecular dynamics modeling. The complex is remarkably consistent throughout the simulation time, as seen by the RMSD, RMSF and hydrogen bond interaction results.

Estrogen receptor alpha (ER-) inhibitors such as 1,1-diphenyl-2-picrylhydrazyl, isocorilagin, kaempferol, kaempferol 3-beta-D-glucopyranoside, and quercetin might all be employed to build a breast cancer therapy. Schrodinger discovered a wide variety of docking scores during molecular docking. Isocorilagin had the best docking score against estrogen receptor alpha of all the drugs studied Nasrin Aktheret and colleagues,[34]

In silico investigations of certain 2-anilinopyrimidine derivatives as anti-triple negative breast cancer drugs were conducted by Hadiza Lawal Abdul rahman, Adamu Uzairu, and SaniUba et al., [35]. Model 4 may be utilized to produce novel 2-anilinopyrimidine derivatives with improved anti-breast cancer prediction activity and performance, according to the findings. Some 2-anilinopyrimidine derivative compounds have been shown to bind strongly to the receptor, stabilizing the receptor (TR1) as evidenced by receptor–ligand interactions, and these compounds might be the most promising TR1 inhibitors. This is a significant step forward for pharmaceutical researchers in the development of novel anti-triple-negative breast cancer therapies.

The insilico molecular design of heterocyclic benzimidazole scaffolds as potential anticancer agents was investigated by Balasubramanian Narasimhan et al., [36] The sulforhodamine B (SRB) assay was used to test the anticancer activity of synthesized benzimidazole compounds against cancer cell lines (HCT116 and MCF7) in vitro. Furthermore, utilizing CDK-8 (PDB code: 5FGK) and ER-alpha (PDB code: 3ERT) as

putative targets for anticancer action, Schrodinger-Maestro v11.5 performed a molecular docking investigation of the data set. Molecular docking data revealed that compounds 12, 16, N9, W20, and Z24 had a high docking score with greater interaction within key amino acids, which is related to their anticancer properties. Compounds 16, N9 and W20 exhibited significant ADME findings within the range of Lipinski's rule of five and Qikprop rule, suggesting that these compounds might be employed as lead molecules for the development of new anticancer medicines.

A new class of pyranoquinolinone-based compounds has been developed. Hany M. Hassanin et al.,[37] developed and synthesized Schiff's bases. They were examined for topoisomerase II (TOP2B) inhibitory activity and cytotoxicity against the MCF-7 breast cancer cell line in order to create novel anticancer drugs. Using the DISCOVERY STUDIO 2.5 program, a molecular docking research was conducted to explore their binding and functional capabilities as TOP2B inhibitors, and they demonstrated an intriguing capacity to intercalate the DNA–topoisomerase complex.. Compounds 2a, 2c and 2f had the highest docking scores (82.36 percent 29.98 kcal mol⁻¹ for compound 2a, 78.18 percent 26.98 kcal mol⁻¹ for compound 2c, and 78.65, 28.11 kcal mol⁻¹ for compound 2f) and demonstrated the most enzyme inhibition activity. The best hit compounds exhibit highly potent TOP2B inhibitors with submicromolar IC₅₀ at 5 M when compared to the reference doxorubicin.

Reetuparna Acharya et al., [38] selected furanocoumarins have been subjected to a structure-based multi-targeted Molecular Docking Analysis in the fight against breast cancer. Breast cancer is one of the world's most serious problems and the current treatment involves using partial agonists/antagonists to target hormone receptors. Tamoxifen, Trastuzumab, Paclitaxel and other powerful medications for breast cancer therapy have been linked to side effects and resistance in individuals. The study's focus was on phytochemicals that have potent inhibitory effects on eR, pR, eGfR and mtoR. Because protein-ligand interactions are

important in drug design, the current work used molecular docking. The 3D structures of ER, pR, eGfR and mtoR were docked with 23 3D PubChem structures of furanocoumarin compounds obtained from the protein data bank using Flex X. The goal of this study was to compare the in-vitro thrombolytic activity and phytochemical analyses of leaf extracts from four medicinal plants in the Asteraceae family. *Merr*, *Eclipta alba* (L) Hassk., *Emilia sonchifolia* (L.) DC., and *Spilanthes paniculata* Wall were all recognized as members of the same asteraceae family. As a consequence of our investigation, we found *Wedelia chinensis* Osbeck. *Emilia sonchifolia* (L.) DC., *Eclipta alba* (L.) Hassk., *Eclipta alba* (L.) Hassk., *Eclipta alba* (L.) Hassk., *Eclipta* Wall, *Spilanthes paniculata* *Emilia sonchifolia* (L.) DC., *Emilia sonchifolia* (L.) DC., *Emilia sonchifolia* (L.) DC., *Emilia sonchifolia* (L.) DC., *Emilia sonchifolia* (L.) DC., *Emilia sonchifolia* (L.) DC. To test anti-breast cancer activity, the Lipinski's rule of five was used to the furanocoumarins to screen for drug-likeness. Antagonist and inhibition assays for eR, eGfR and mtoR were carried out in vitro using approved procedures. The findings show that Xanthotoxol, Bergapten, Angelicin, Psoralen and Isoimperatorin had the best docking scores for breast cancer. Moreover, the in-vitro findings support the molecular docking analyses. This research implies that the selected furanocoumarins should be studied and analyzed further for breast cancer therapy and care techniques.

2.4 Invitro Thrombolytic activity

B. Vishwanathan, B.M. Gurupadayya, and colleagues [39] synthesized Thrombolytic activity of 1, 3, 4-oxadiazole derivatives. A series of 1, 3, 4-oxadiazole derivatives (3a-3q) synthesized from benzofuran were tested for thrombolytic activity in an in vitro clot lysis assay. The thrombolytic study was carried out to see if the clot lysis process could reduce the solid clot weight at concentrations of 6.25, 12.5 and 25 M strength. In vitro clot lysis for thrombolytic assessment demonstrated that the investigated compounds 3a-3q showed

considerable clot lysis when compared to the reference medication streptokinase (30,000IU). Among all the tested compounds, compound 3o, 3n and 3m exhibited potent thrombolytic activity with ED50 value of 18.8, 20.4 and 20.9 μ M, respectively.

Fatema Tabassum et al., [40] the comparative study of the thrombolytic activity and phytochemical analysis of the methanolic extract of leaves of *Wedelia chinensis* Osbeck was designed to investigate the in-vitro thrombolytic activity and phytochemical evaluation of leaf extracts of four medicinal plants from the Asteraceae family. *Merr*, *Eclipta alba* (L) Hassk., *Emilia sonchifolia* (L.) DC., and *Spilanthes paniculata* Wall. (all belonging to the same asteraceae family) were all identified. We also discovered *Wedelia chinensis* Osbeck as a result of our research. *Eclipta alba* (L) Hassk, *Emilia sonchifolia* (L.) DC., *Spilanthes paniculata* Wall, *Emilia sonchifolia* (L.) DC., *Emilia sonchifolia* (L.) DC., *Emilia sonchifolia* (L.) DC., *Emilia sonchifolia* (L.) DC. They demonstrated considerable percent of clot lysis impact with reference to Streptokinase (71.43 percent) and water, and they showed 24.48 percent, 28.71 percent, 15.19 percent and 42.77 percent clot lysis activity, respectively (2.96 percent). The presence of many phytochemicals in distinct solvent fractions was discovered by phytochemical analysis. The presence of these phytochemicals was shown to be responsible for the plants' in-vitro thrombolytic action. For the creation of new drugs, more research is required.

Monalisha Sharma et al., [41] Study on in-vitro thrombolytic activity of methanolic extract of *Mesua ferrea* leaves have been synthesized from the above study it can be concluded that the methanolic extract of *Mesua ferrea* may be a potential candidate for future thrombolytic agent. Furthermore study and isolation is needed to obtain site specific and more potent agent that causing this effect. The test was made under full concentration to develop new compounds.

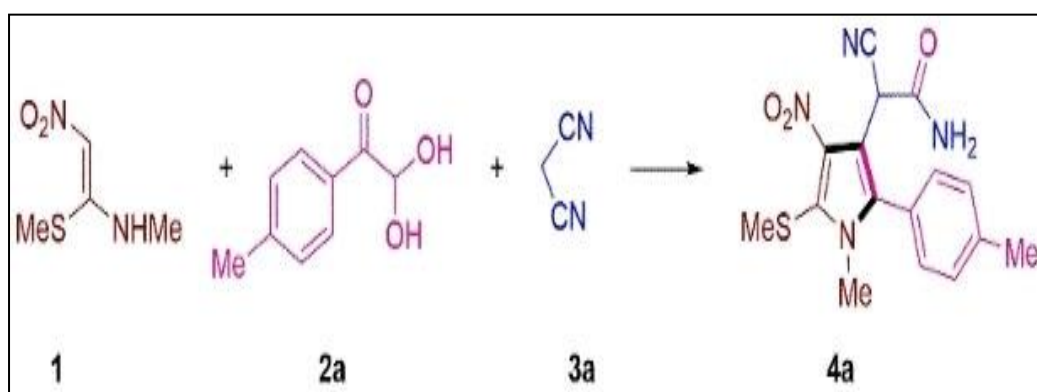
Regioselective synthesis of 2-(bromomethyl)-5-aryl-thiophene derivatives via palladium (0) catalyzed Suzuki cross-coupling reactions: as antithrombotic and haemolytically active molecules. The haemolytic and antithrombotic actions of Komal 1 Rizwan et al., [42] were investigated. The new chemicals 3f and 3i caused the most haemolysis of blood cells, with 69.7% and 33.6 percent, respectively. The chemicals' antithrombotic effect against human blood clots was determined to be modest to moderate. Clot lysis was demonstrated to be effective with compound 3i (31.5 percent).

J.P. Dupin et al., [43] New thienopyrimidinone derivatives synthesis and thrombolytic action in this paper, we describe the six-step synthesis of a series of novel benzothienopyrimidinone derivatives with significant thrombolytic action. In the pharmacological experiment, Wistar rats were anesthetized and had extracorporeal circulation superfused thrombi adhere to a strip of collagen. The thrombi's weight was continually being monitored. Six of the compounds in the series were far more potent thrombolytic agents than their thienopyridine equivalents, with effective thrombolytic doses ranging from 8 to 170 mg kg⁻¹, vs ED₃₀ values of 16000 to 20000 mg kg⁻¹ for clopidogrel and ticlopidine, respectively. This difference in the threshold thrombolytic dosage, which resulted in a three-order-of-magnitude increase in the strength of action, was followed by a prolonging of the reaction, especially with the most active molecule. Apart from that, these compounds have been proved to be synthetic thrombolytics and they need to be studied further.

Organic and aqueous extracts of *Hopea odorata* leaves were produced for antioxidant, antidiarrheal, hypoglycemic and thrombolytic activities, as well as in silico PASS prediction of its isolated components Mohammad Shah Hafez Kabir and Md. Mominur Rahman et al [44]. These findings imply that the plant might be a source of novel antidiarrheal, thrombolytic and antioxidative compounds, although it lacks antidiabetic properties. For the extracts, the PASS prediction matched the current study. More research is

needed to determine the phytoconstituents' PASS anticipated biological effects.

The In Vitro Evaluation of Pentasubstituted Pyrroles as Thrombolytic Agents and Cytotoxicity Studies on L929 Cells through a Simple and Direct Synthesis of Pentasubstituted Pyrroles by [3+4] Annulation Biguvu Balachandra and Sivakumar Shanmugam et al., [45], devised two separate procedures for the synthesis of two different polysubstituted pyrroles. The first method proceeds by the reaction of N,S-acetal, arylglyoxals and malononitrile in the presence of H₂O / PEG400 to the synthesis of 2-(2-argio-1- methyl-5-(methylthio)-4-nitro-1H-pyrrol-3-yl)-2-cyanoacetamide (4a-4p). The second technique uses methylcyanoacetate instead of malononitrile for the production of additional divergent pyrroles 2-(2-argio-1-methyl-5-(methylthio)-4-nitro-1 H-pyrrol-3-yl) acetonitrile (6a-6f) under a solvent-free, heating environment. Among the pyrroles 2-(4-methoxyphenyl) (4c), 2-(4-fluorophenyl) (4d) 2-(4-chlorophenyl) (4e), 2-(2,4-dichlorophenyl) (4f), 2-(3-chloro-4-fluorophenyl) (4g), 2-(2-bromo-4-chlorophenyl) (4h), (2-(3-bromophenyl) (4i), 2-(4-bromophenyl) (4j), (2-(4-hydroxyphenyl)(4l) and 2-(3-nitrophenyl) (4m) displayed moderate to good clot lysis. For several substances, cytotoxicity tests were also performed on L929 cells. At lower concentrations, the test derivatives 4c, 4d, 4g and 4h demonstrated good cell viability. At greater and lower concentrations, the chemical 4f demonstrated moderate to non-toxicity.



References

1. Abbas Al-Mulla, A Review: Biological Importance of Heterocyclic Compounds, *Der Pharma Chemica*, (13) (2017) p.141-147.
2. CR. Noller, V. Baliah, The preparation of some piperidine derivatives by the Mannich Reaction. *K J. Am. Chem. Soc.* 70(11) (1948) p.3853-3855.
3. K. Pandiarajan, G. Muthukumar, J. Chakkaravarthy, Conformational study of some N-acyl-2r, 6c-diphenylpiperidin-4-one oximes using NMR spectra, *Journal of Molecular Structure*. 889(1) (2008) p.297-307.
4. P. Pandey and P. Chawla Syntheses, characterization and biological Activity of novel 2,6-di substituted Piperidine-4-one derivatives, *International Journal of Pharmaceutical, Chemical and biological sciences*. 2(3) (2012) p 305-309.
5. Mukhtyar. S. Saini, Aran kumar, Jaya Dwivedi, Rakesh Singh, A Review: Biological Significances of Heterocyclic Compounds, *International Journal of Pharma Sciences and Research* 4(3) (2013) p85-94.
6. D. Bhakiaraj, T. Elavarasan, M.Gopalakrishna, Synthesis, spectral analysis, antimicrobial evaluation and molecular docking studies of some novel 3, 5-dichloro-2,6-diaryl piperidin-4-ones, *Der Pharma Chemica*. 6(5) (2014) p.243-250.
7. [Almasirad A](#), [Tajik M](#), [Bakhtiari D](#), [Shafiee A](#), [Abdollahi M](#), [Zamani MJ](#), [Khorasani R](#), [Esmaily H](#). Synthesis and analgesic activity of N-Arylhydrazone derivatives of mefenamic acid. *J Pharm Pharm Sci*. 8(3) (2005) p.419-25.
8. S.Sadjadi, Majid M. Heravi¹, Negar Mokhtari Haj, Hossein A.Oskooie, Rahim Hekmat, Heteropolyacids in synthesis of benzoyl hydrazone derivatives, *Bull. Chem. Soc. Ethiop.* 23(3) (2009) p.467-472.

9. Jie Zhang, Preparation, characterization, crystal structure and bioactivity determination of ferrocenyl-thiazole acylhydrazones, *Applied Organometallic Chemistry* ,22 (1) (2008) p.6-11.
10. Dimmock J.R, Vashistha S.C, Stables J.P, Anticonvulsant properties of various acetylhydrazone, oxamoylhydrazone and semicarbazones derived from aromatic and unsaturated carbonyl compounds, *Eur. J.Med. chem.* 35 (2000) p.24-28.
11. Abdel-Aal TM, El.sayed .A and El-Ashry.E.S.H, Synthesis and antiviral evaluation of some sugar Arylglycinoyl-hydrazones and their oxadiazidine derivatives, *Archiv der pharamazie chemistry in life science.* 339 (2006) p. 656-663.
12. Neha Singh, RituRajana, manjuKumari, Birendra Kumar Gaya, *Bio org. Med. Chem.* 3 (2016) p. 3001.
13. Gagandeep kaur, randhir singh, thiadiazole analogs as potential pharmacological agents: a brief review, *International Journal of Pharmacy and Pharmaceutical Sciences*, 6(8), (2014).
14. Naveen Lumar HS, ThigarajanParumasivan, Fatimah Jamaat, AmirinSadikun, Synthesis and evaluation of isonicotinoyl hydrazone derivatives as antimycobacterial and anticancer agents, *Medicinal chemistry Research*, 23(1) (2014) 46 Reeds.
15. Natesh Rameshkumar, Anantharaman veena, Raju ilavarasan Mandaleeswaran Adiraj, Pitchaimuthu Shanmugapandiyan and Seshaiiah krishnan Sridhar, synthesis and biological activities of 2, 6-diaryl-3-methyl-4-piperidone derivatives, *Biol. Pharm. Bull.*26(2) (2003) p.188-193.
16. N. Jayalakshmi and S. Nayandan, Synthesis characterization and pharmacological studies of selenadizole and hydrazone derivatives of 2, 6-diphenyl-4-piperidone, *Internal journal of chemical sciences.* 6(3) (2008) p. 1177-1188
17. P. Ball, C.H. Nicholls *Dyes and Pigments* (1982) 5-26.

18. Vicini.P, Zani.F, Cozzin.P, Doytchinovk.I, Hydrazone of 1, 2-benzisothiozole hydrazides, synthesis antimicrobial activity and QSAR investigation, *Eur .J.Med. Che.* 37 (2002) p.553-564.
19. Singh.B, Narang K.K, and Srivastava.R, Studies of complexe of Co(II),Ni(II), Cu(II), and Cd(II) with acetophenoene and 4-hydroxyceloptone 7-aminobenzoylhydrazone, *Inorganic and metal organic chemistry.* 33 (2003) p.1025-1036.
20. Bechan Sharma, *International Journal of Pharmacy and Pharmacetutical Sciences.* (2016) p.41-44.
21. Ratiran Gomuji Chaudhary, Sudhirs. Bhuyar, SmitaKharkale, Lalitmohan Jainarayn Paliwal, *International Journal of Pharmacy and Pharmacetutical Sciences.* (2015) 78 Reeds.
22. Constatin Sandra, Fburon, S. Routier, lenutaProfine, *International Journal of Pharmacy and Pharmacetutical Sciences.* (2016) p.171-174.
23. Sevim Rollas and S. Guniz Kucukguzel, *Bio org. Med. Chem.* (2007) p. 631-642.
24. M. Singh, NutanRaghave, *International Journal of Pharmacy and Pharmacetutical Sciences.* 3(4) (2011) p. 26-32.
25. Ahmetozdemiri, Gulhanturan-Zitouni1, ZaferAsim Kaplancikli1 and MehlikaDilekAltintopi, *J. Serb. Chem. Soc.* 77(2) (2012) p.141-146.
26. Konishi.K, Kurangano.T, Tsujikaura.T, Fungicidal activity of aromatic aldehyde pyramidinyl hydrazone, *J.Pesticide. Sciences.* 14 (1989) p.189-196.
27. Halima Hajji ,Ilam Aanouz,Khalil EL Khatabi, Tahar Lakhlifi, Mohammed Aziz Ajana, Mohammed Bouachrine, 2D-QSAR study study of the anti-obesity activity for the compounds based on 2-anilino, 4-aryl pyrimidines and 2,4 aryl 7-azanidoles using ststistical methods,*Journal of analytical sciences and applied biotechnology,*2(1) (2020) p23-31.
28. B Manimegalai and S Velavan,Evaluation of anti-obesity activity of *Gymnema sylvestre* leaves extract *Journal of Pharmacognosy and Phytochemistry* 8(3)(2019) p 2170-2173.

29. Rashmi shivanna¹, hengameh parizadeh², rajkumar h. Garampalli¹*Invitro anti-obesity effect of macrolichens heterodermia leucomelos and ramalina celastri by pancreatic lipase inhibitory assay, *International Journal of Pharmacy and Pharmaceutical Sciences*, 9(5), (2017)p 3270-3273.
30. Athesh k, divakar m, brindha p anti-obesity potential of cyperus rotundus. Aqueous tuber extract in rats fed on high fat cafeteria diet, *Asian J Pharm Clin Res*, 7(2) (2014) p 88-92.
31. Changhyun Roh * and Uhee Jung *Screening of Crude Plant Extracts with Anti-Obesity Activity, *Int. J. Mol. Sci.* 13(2012) p 1710-1719.
32. K. Tharini and K. Sundaresan, *In silico* docking studies of anti-diabetic and breast cancer activity by N-(1-benzylpiperidin-4-ylidene)-2-cyanoaceto hydrazide, *Int. J. Adv. Res.* 5(12) (2017) p601-607.
33. Jesudass Joseph Sahayarayana, Kulanthaivelu Sounder Rajan,Ramasamy Vidhyavathi, Mutharasappan Nachiappan, Dhamodharan Prabhu , Saleh Alfaraj , Selvaraj Arokiyaraj, Amalorpavanaden Nicholas Daniel In –Silico protein-ligand docking studies against the estrogen protein of breast cancer using pharmacophore based virtual screening approaches, *Saudi Journal of biological sciences* xxx (xxxx) xxx.
34. Shanta A, Nazim U, Kazi Zahra M, Tarannur Kabir N, Fayejun N, Shermin A, Sahida A, Sajal C, Dipannita C, Nasrin A. In Silico Molecular Docking Approach of Some Selected Isolated Phytochemicals from Phyllanthus Emblic Against Breast Cancer. *Biomed J Sci&Tech Res* 10(2)(2018).
35. Hadiza Abdulrahman Lawal& Adamu Uzairu& Sani Uba,QSAR, molecular docking, design, and pharmacokinetic analysis of 2-(4-fluorophenyl) imidazol-5-ones as anti-breast cancer drug compounds against MCF-7 cell line, *Journal of Bioenergetics and Biomembranes* 52(2020) p475–494.

36. Hadiza Lawal Abdulrahman*, Adamu Uzairu and Sani Uba In silico studies of some 2-anilinopyrimidine derivatives as anti-triplenegative breast cancer agents, Abdulrahman et al. Beni-Suef University *Journal of Basic and Applied Sciences* 9(13) (2020).
37. Sumit Tahlan, Sanjiv Kumar, Kalavathy Ramasamy, Siong Meng Lim, Syed Adnan Ali Shah, Vasudevan Mani and Balasubramanian Narasimhan, In-silico molecular design of heterocyclic benzimidazole scaffolds as prospective anticancer agents, *Tahlan et al. BMC Chemistry* 13(90) (2019) p 2- 22.
38. Hassanin HM, Serya RAT, Abd Elmoneam WR, Mostafa MA Synthesis and molecular docking studies of some novel Schiff bases incorporating 6-butylquinolinedione moiety as potential topoisomerase II β inhibitors, *R.Soc.opensci.* 5 (2018) p172407.
39. Reetuparna Acharya¹, Shinu chacko^{2,4}, pritha Bose¹, Antonio Lapenna³& Shakti prasad pattanayak¹ Structure Based Multitargeted Molecular Docking Analysis of Selected furano coumarins against Breast cancer ,*Scientific Reports* 9 (2019) p15743.
40. B. Vishwanathan B.M. Gurupadayya Thrombolytic activity of 1,3,4-oxadizole derivatives , *World Journal of Pharmaceutical Sciences* 3(10) (2015) p2004-2008.
41. Fatema Tabassum, Somaia Haque Chadni, Kamrun Nahar Mou, KM Imrul Hasif, Tareque Ahmed and Mahbuba Akter, In-vitro thrombolytic activity and phytochemical evaluation of leaf extracts of four medicinal plants of Asteraceae family, *Journal of Pharmacognosy and Phytochemistry*, 6(4) (2017) p1166-1169.
42. Komal Rizwan, Muhammad Zubair, Nasir Rasool, Shaukat Ali, Ameer Fawad Zahoor, Usman Ali Rana, Salah Ud-Din Khan, Muhammad Shahid, Muhammad Zia-Ul-Haq and Hawa ZE Jaafar, Regioselective synthesis of 2-(bromomethyl)-5-aryl-thiophene derivatives via palladium (0) catalyzed suzuki cross-coupling reactions: as antithrombotic and haemolytically active molecules, *Chemistry Central Journal* 8(74) (2014) p 2-8.

43. J.P. Dupin, R.J. Gryglewski, D. Gravier, G. Hou, F. Casadebaig, J. Swies, S. Chlopicki, Synthesis and thrombolytic activity Of new thienopyrimidinone derivatives, *Journal of physiology and Pharmacology* 53(4) (2002) p625-634.
44. Mohamad shah hafez kabir, Mohammed Munawar Hossain, Md. Imtiazul kabir, Shabbir Ahmad, Nishan Chakrabarty, Md.Atiar Rahman and Md.Mominur Rahuman, Antioxidant, antidiarrheal, hypoglycemic and thrombolytic activities of organic and aqueous extracts of Hopeodorata leaves and in silico PASS prediction of its isolated compounds, *BMC Complementary and Alternative Medicine*.16(474) (2016) p1-14.
45. Biguvu Balachandra and Sivakumar Shanmugam A Simple and Direct Synthesis of Pentasubstituted Pyrroles via [3+ +4] Annulation and Their In Vitro Evaluation as Thrombolytic Agents and Cytotoxicity Studies on L929 Cells, *Chemistry Select*, 3 (2018) p 2037–2044.

Chapter-3

Scope And Objective of the work

Heterocyclic systems having piperidine are found to possess better biological activity. They aroused great interest in the past and recent years due to their wide variety of biological properties and their presence in biologically active pharmaceutical ingredients.

Hydrazone and its derivatives are a class of organic synthesis compounds with a wide variety of uses. The chemistry of carbon-nitrogen double bond of hydrazone is becoming the backbone of condensation events in benzo-fused N-heterocycles and it also represents an important class of compounds for innovative medicinal development. Anti-microbial, antitubercular, anticonvulsant, analgesic, anti-inflammatory, anticancer, antifungal, antiviral, antibacterial and antimalarial actions have been claimed for a variety of hydrazone derivatives. Review of literature survey indicated that nitrogen and oxygen containing heterocycles have significant place in the development of pharmacologically important molecules.

Bioactive heterocyclic ring systems with a 2,6-diaryl-piperidine-4-one nucleus and various substituents at the 3- and 5-positions of the ring have also sparked interest due to their wide range of biological properties, including antiviral, antitumor, central nervous system, local anesthetic, anticancer and antimicrobial activities and their derivatives are also biologically important and act as neurokinins. In view of the importance and pharmacological activities of piperidin-4-one derivatives, the present topic has been chosen. Herein, the synthesis, structural characterization, *invitro* biological evaluation and molecular

docking studies of some diarylpiperidin-4-one cyanoacetylhydrazone derivatives have been carried out.

The major objectives of the present research work are as follows:

- To synthesis various substituted N-acetyl 3-methyl 2, 6-diarylpiperidin-4-one cyanoacetylhydrazone derivatives and benzaldehyde cyano acetyl hydrazone derivatives.
- To characterize the synthesized compounds using advanced analytical and spectral methods such as FT-IR, ^1H and ^{13}C NMR.
- To investigate the invitro anti obesity activity of the all synthesized compounds.
- To study the *insilico* anti breast cancer activity of the all synthesized compounds.
- To evaluate the *invitro* thrombolytic activity of the all synthesized compounds

Chapter-4

Materials and Methods

4.1. Materials

All the chemicals (solvents and reagents) were procured from Merck (India) and foreign companies (Hi-media and Sigma/Aldrich) and were used as such with no further purification and distillation. Local chemical has not been used in the research work. The purity of these chemicals was 98-99.9%.

Various substituted aldehydes and cyanoaceto hydrazide (Hi-media and Sigma/Aldrich), were used as received. The other reagent used was Sodium acetate (Merck).

Analytical grade solvents like ethanol, methanol, ethyl acetate and ethyl methyl ketone were used as such without further distillation. The synthesized compounds were scaled for yield and purified using a suitable solvent system and recrystallization.

4.2. Identification of compounds

4.2.1 Melting point determination

On a Stuart-SMP10 melting point apparatus, the melting points of the synthesized compounds were determined in open-glass capillaries and recorded in °C without adjustment. In the characterisation of an organic compound, it is an extensively employed physical constant.

4.2.2 Thin Layer Chromatography

Chromatography is an important technique to identify the formation of new compounds and also to determine the purity of the compound. Each chemical has an R_f value that is unique to it.

(i) Preparation of solvent system and saturation of chamber

The solvent system used for the development of chromatogram was prepared carefully by mixing ethyl acetate and hexane.

(ii) Application of sample

The solution of the parent compound and its target molecule were taken in small bored capillary tube and spotted at 2 cm from the base end of the plate. After spotting, the plates were allowed to dry at room temperature and transferred to chromatographic chamber containing solvent system for development.

(iii) Development of chromatogram

When the solvent front had reached a distance of 10-12 cm, plates were developed using ascending method and they were removed and dried at room temperature.

(iv) Detection of spots

The developed spots were detected by exposing them to iodine vapours.

(v) Calculation of R_f value

The R_f values of compounds were calculated using the formula

$$R_f = \frac{\text{Distance travelled by the sample}}{\text{Distance travelled by the solvent front}}$$

In all the cases, the distance travelled by the sample was found to be different from that of the parent compound spotted along with it. Thus confirming the fact that the compounds formed were entirely different from that of the parent compound. Since the entire sample gave a single spot, the compounds were taken to be free from impurities. The R_f value of compounds were reported.

4.2.3 FT-IR Spectra

IR absorption spectra were recorded in the $4,000-400\text{ cm}^{-1}$ range on a Shimadzu FT IR-8400s using KBr pellets technique. One of the most powerful analytical methods utilized is infrared spectroscopy, which allows for the identification of functional groups contained in a substance.

4.2.4 ^1H NMR and ^{13}C NMR Spectra

A Bruker AMX-300MHz spectrophotometer was used to record ^1H -NMR and ^{13}C -NMR spectra. Chemical shifts in ^1H -NMR and ^{13}C -NMR are expressed as parts per million (ppm) downfield from TMS, which serves as an internal reference. A solvent of DMSO/ CDCl_3 was used to record the spectra. The splitting patterns are denoted by the letters s, d and m which stand for singlet, doublet and multiplet respectively.

4.3 Synthesis of Compounds

4.3.1 Preparation of 3-methyl 2,6-diaryl piperidin-4-one

The 3-methyl-2,6-diarylpiperidin-4-one was made using the technique described in the literature [1-2]. In 95 percent ethanol (20ml), ammonium acetate (7.70g, 100m.mol), benzaldehyde (20.3ml, 200m.mol), and ethyl methyl ketone (14.7ml, 200m.mol) were dissolved and the solution was heated with shaking until the color changed to orange. After cooling the mixture in the tap

water, the solution was poured into ether (100ml). The ether insoluble component was filtered off and conc. HCl (14ml) was added to the filtrate. The precipitated 3-methyl 2,6-diaryl piperidin -4-one hydrochloride was separated by filtration. The hydrochloride was suspended in acetone, then drops of strong aqueous ammonia were added one at a time until a clear solution was formed. The clear solution was poured into cold water (300ml) and the solid obtained was filtered, dried and recrystallised from ethanol. Colourless crystals; m.p 102 – 103°C.

[Condensation of 2-butanone, substituted aldehydes and ammonium acetate in warm ethanol in the ratio of 1:2:1 respectively afforded the formation of various substituted 3-methyl-2,6-diarylpiperidin-4-ones.]

4.3.2 Preparation of 3-methyl-2,6-diarylpiperidin-4-one cyanoacetyl hydrazones

In methanol, a combination of substituted 3-methyl-2,6-diarylpiperidin-4-one (0.1 mol) and cyanoaceto hydrazide (0.1 mol) was refluxed for 2 hours in the presence of a few drops of concentrated acetic acid. After the completion of reaction, the reaction mixture was cooled to room temperature. The solid product formed was separated by filtration and washed with warm water and recrystallized by methanol to afford corresponding substituted 3-methyl-2,6-diarylpiperidin-4-one cyanoacetyl hydrazones.

4.3.3 Preparation of N-acetyl 3-methyl-2,6-diarylpiperidin-4-one cyanoacetyl hydrazones

3-methyl-2,6-diarylpiperidin-4-one cyanoacetyl hydrazones cyclized by 0.1 mol of acetic anhydride and recrystallized by methanol to afford corresponding substituted N-acetyl3-methyl-2,6-diarylpiperidin-4-one cyanoacetyl hydrazones.

4.4 Preparation of Benzaldehyde cyanoacetylhydrazone (BCAH)

In methanol, benzaldehyde (0.1mol), cyanoacetylhydrazide (0.1mol) and a few drops of glacial acetic acid were refluxed for two hours. The reaction mixture was cooled to room temperature once the reaction was completed. The solid product was separated by filtration and washed with warm water and recrystallized by methanol to afford Benzaldehyde cyanoacetyl hydrazone

4.5 Invitro antiobesity Activity

Pancreatic lipase activity was modified from that previously described by Kim *et al.* (2010) and Anil Kumare *et al* (2011) method. [3-4]

4.5.1 Reagents

1. Olive oil
2. Phosphate Buffer (pH 6)
3. Porcine pancreatic lipase(1 mg/mL; 0.1 mM potassium phosphate buffer (pH 6.0)
4. Acetone
5. Ethanol
6. Sodium hydroxide (0.02M)
7. Oxalic acid ((0.01M)
8. Standard: Orlistat

4.5.2 Procedure

Different concentrations of the sample (100, 200, 300, 400, and 500g/ml) were obtained and each concentration (100) was combined with 8 ml olive oil, 0.4 ml phosphate buffer and 1 ml Porcine pancreatic lipase and incubated for 60 minutes. The process was halted by adding 1.5 ml of acetone and 95 percent ethanol to the mixture (1:1). Titrating the solution against 0.02 M sodium hydroxide (standardized by 0.01 M oxalic acid) using phenolphthalein as an indicator revealed the released fatty acids, which were quantified by titrating the solution against 0.02 M sodium hydroxide (standardized by 0.01 M oxalic acid). A similar concentration of positive control as Orlistat (Standard) is used. The Lipase activity of the control was checked without inhibitor (sample). Percentage inhibition of lipase activity was calculated using the formula:

$$\text{Lipase inhibition} = A - B/A \times 100$$

where A is lipase activity, B is activity of lipase when incubated with the sample.

4.6 Insilico Molecular Docking Study

In our present study, *in silico* molecular docking studies were carried out using BIOVIA Discovery Studio (DS) 2017 software.

4.6.1 Preparation of protein

The Crystal Structure of the BRCT Domains of Human BRCA1 in Complex with a Phosphorylated Peptide from Human Acetyl-coA Carboxylase 1 (PDB ID: 3COJ) with a resolution of 1.90 was used for this investigation. Hydrogens were applied to the 3COJ protein by applying the Forcefield algorithm and then using CHARM forcefield in DS, the protein energy was reduced.

4.6.2 Ligand preparation

The molecules (synthesized compounds) and standard drug Tamoxifen were drawn in chemdraw software, subsequently, energy of the all the molecules were minimized and saved in SDF file format for further docking studies.

4.6.3 Docking study

In order to analyse the most common geometry of the protein-ligand complex, a molecular docking analysis was carried out. To understand the structural basis of these target proteins, a computational docking study was used to analyse structural complexes of the 3COJ with 7 molecules along with Schiff base compounds. The CDOCKER (CHARMm-based DOCKER) protocol integrated within DS has examined potential binding modes between the ligands and these target proteins. The CDOCKER parameter to be run was tabulated in Table 1. The algorithm flexibly provides complete ligand and employs fields of CHARMm power. The ligand binding affinity was determined using CDOCKER Interaction energy, Hydrogen bonds, binding energies, protein energy, and ligand-protein complex energy. The energy of CDOCKER is stated in negative values. More negative value energy is seen as the ligands' higher binding affinity to the target protein protein [5, 6].

The other parameter in this protocol was mentioned in **Table.1**

Table 1. Parameter of CDOCKER protocol

Input Receptor	Input/3COJ.dsv
Input Ligands	/Input/Total_min_ligands.sd
Input Site Sphere	-23.9454, 29.2003, 7.29961, 9

Top Hits	1
Random Conformations	10
Random Conformations Dynamics Steps	1000
Random Conformations Dynamics Target Temperature	1000
Include Electrostatic Interactions	True
Orientations to Refine	10
Maximum Bad Orientations	800
Orientation vdW Energy Threshold	300
Simulated Annealing	True
Heating Steps	2000
Heating Target Temperature	700
Cooling Steps	5000
Cooling Target Temperature	300
Forcefield	CHARMm
Use Full Potential	Yes

Grid Extension	8.0
Ligand Partial Charge Method	CHARMm
Random Number Seed	314159
Final Minimization	Full Potential
Final Minimization Gradient Tolerance	0
Parallel Processing	False
Parallel Processing Batch Size	25
Parallel Processing Server	Localhost
Parallel Processing Server Processes	2
Parallel Processing Preserve Order	True
Random Dynamics Time Step	0.002

4.7 Invitro Thrombolytic Activity

Thrombolytic activity determined by the method of Fatema Tabassum *et al* (2017), [7].

4.7.1 Preparation of streptokinase (SK)

The commercially supplied lyophilized SK vial of 15, 00,000 I.U. was combined appropriately with around 5 ml sterile distilled water. This solution was employed as a stock for an in vitro thrombolysis investigation, with 100 μ l (30,000 I.U) being used [8].

4.7.2 Collection of blood

1 ml of blood was placed to previously weighed sterile eppendorf tubes and allowed to develop clots from healthy human volunteers who had not used oral contraceptives or anticoagulant treatment.

4.7.3 Procedure

3ml venous blood was collected from the patient's arm and divided into four pre-weighed eppendorf tubes, which were then incubated at 37°C for 45 minutes. Following clot formation, serum was withdrawn entirely without disturbing the clot and each clot-containing tube was weighed again to calculate the clot weight (clot weight = weight of clot-containing tube minus weight of tube alone). 100µl (100g/ml) of sample was added to each eppendorf tube holding pre-weighed clot and 200µl (200g/ml) of sample was added to another eppendorf tube containing pre-weighed clot. As a negative control, 100µl of distilled water was added to the control tube. For positive control, 100µl of streptokinase (SK) was added. After that, all of the tubes were incubated at 37°C for 90 minutes to check for clot lysis. After incubation, the fluid was evacuated and the tubes were weighed again to see if there was a difference in weight after the clot was disrupted. The percentage of clot lysis was calculated from the difference in weight acquired before and after clot lysis. The formula for determining clot weight is given below.

$$\text{Clot weight} = \text{Weight of clot filled tube} - \text{Weight of empty tube}$$

$$\% \text{ of clot lysis} = \left(\frac{\text{Weight of clot after lysis}}{\text{Weight of clot before lysis}} \times 100 \right)$$

References

1. V. Baliah, R. Jeyaraman, L. Chandrasekaran, *Chem. Rev.* 83(2008) p. 379.
2. C.R. Noller, V. Baliah, *J.Am. Chem. Soc.* 70 (1948) p. 3853.
3. Kim, Y.S.; Lee, Y.M.; Kim, H.; Kim, J.; Jang, D.K.; Kim, J.H.; Kim, J.S. Anti-obesity effect of *Morus bombycis* root extract: Anti-lipase activity and lipolytic effect. *J. Ethnopharmacol.* 130 (2010) p.621–624.
4. Anil Kumar HS, Prashith Kekuda TR, Vinayaka KS, Swathi D, Venugopal TM. Anti-obesity (Pancreatic lipase inhibitory) activity of *Everniastrum cirrhatum* (Fr.) Hale (Parmeliaceae). *Pharmacognosy Journal.* 3(19) (2011) p 65-68.
5. Balasubramaniyan S, Irfan N, Senthilkumar C, Umamaheswari A, Puratchikody A. The synthesis and biological evaluation of virtually designed fluoroquinolone analogs against fluoroquinolone-resistant *Escherichia coli* intended for UTI treatment. *New Journal of Chemistry.* 44(31) (2020) p 13308-18.
6. Balasubramaniyan S, Irfan N, Umamaheswari A, Puratchikody A. Design and virtual screening of novel fluoroquinolone analogs as effective mutant DNA GyrA inhibitors against urinary tract infection-causing fluoroquinolone resistant *Escherichia coli*. *RSC advances.* 8 (42) (2018) p 23629-47.
7. Fatema Tabassum, Somaia Haque Chadni, Kamrun Nahar Mou, KM Imrul Hasif, Tareque Ahmed and Mahbuba Akter. *In-vitro* thrombolytic activity and phytochemical evaluation of leaf extracts of four medicinal plants of Asteraceae family. *Journal of Pharmacognosy and Phytochemistry.* 6 (4) (2017) p 1166-1169.
8. Prasad S, Kashyap RS, Deopujari JY, Purohit HJ, Taori GM, Dagainawala HF, HF. Effect of *Fagonia Arabica*(Dhamasa) on invitro thrombolysis. *BMC Complementary Altern.Med.* 7(1) (2007) p 36.

Chapter-5

RESULT AND DISCUSSIONS

Several bio organic chemists have attempted to study the synthesis and biological applications of heterocyclic compounds sulphonylhydrazone derivatives. Perusal of literature shows neat work on synthesis of cyanoacetylhydrazone derivatives conspicuously lacking. Hence the present study is concerned with the aim of throwing more light on the “synthesis, characterization and biological evaluation of some novel bioactive hydrazone derivatives”.

The various hydrazones which are synthesized and used for the applications may be grouped as follows:

- I. 1 to 7
- II. 8 to 14

The proposed study has been suitably designed so as to investigate the following.

5.1 Synthesis of compounds

5.1.1 Preparation of 3-methyl 2,6-diaryl piperidin-4-one

3-methyl-2,6-diarylpiperidin-4-one was prepared by adopting the literature method [1-2]. Ammonium acetate (7.70g, 100m.mol), benzaldehyde (20.3ml, 200m.mol) and ethyl methyl ketone (14.7ml, 200m.mol) were dissolved in 95% ethanol (20ml) and the solution was heated with shaking until the colour of the solution change to orange. After cooling the mixture in the tap water, the solution was poured into ether (100ml). The ether insoluble component was filtered off and conc. HCl (14ml) was added to the filtrate. The precipitated 3-methyl 2, 6-diaryl piperidin -4- one hydrochloride was separated by filtration. The hydrochloride was suspended in acetone and concentrated aqueous ammonia was added drop-wise until a clear solution was obtained. The clear solution was poured into cold water (300ml) and the solid obtained was filtered, dried and recrystallised from ethanol. Colourless crystals; m.p 102 – 103°C.

[Condensation of 2-butanone, substituted aldehydes and ammonium acetate in warm ethanol in the ratio of 1:2:1 respectively afforded the formation of various substituted 3-methyl-2,6-diarylpiperidin-4-ones.]

5.1.2 Preparation of 3-methyl-2,6-diarylpiperidin-4-one cyanoacetyl hydrazones

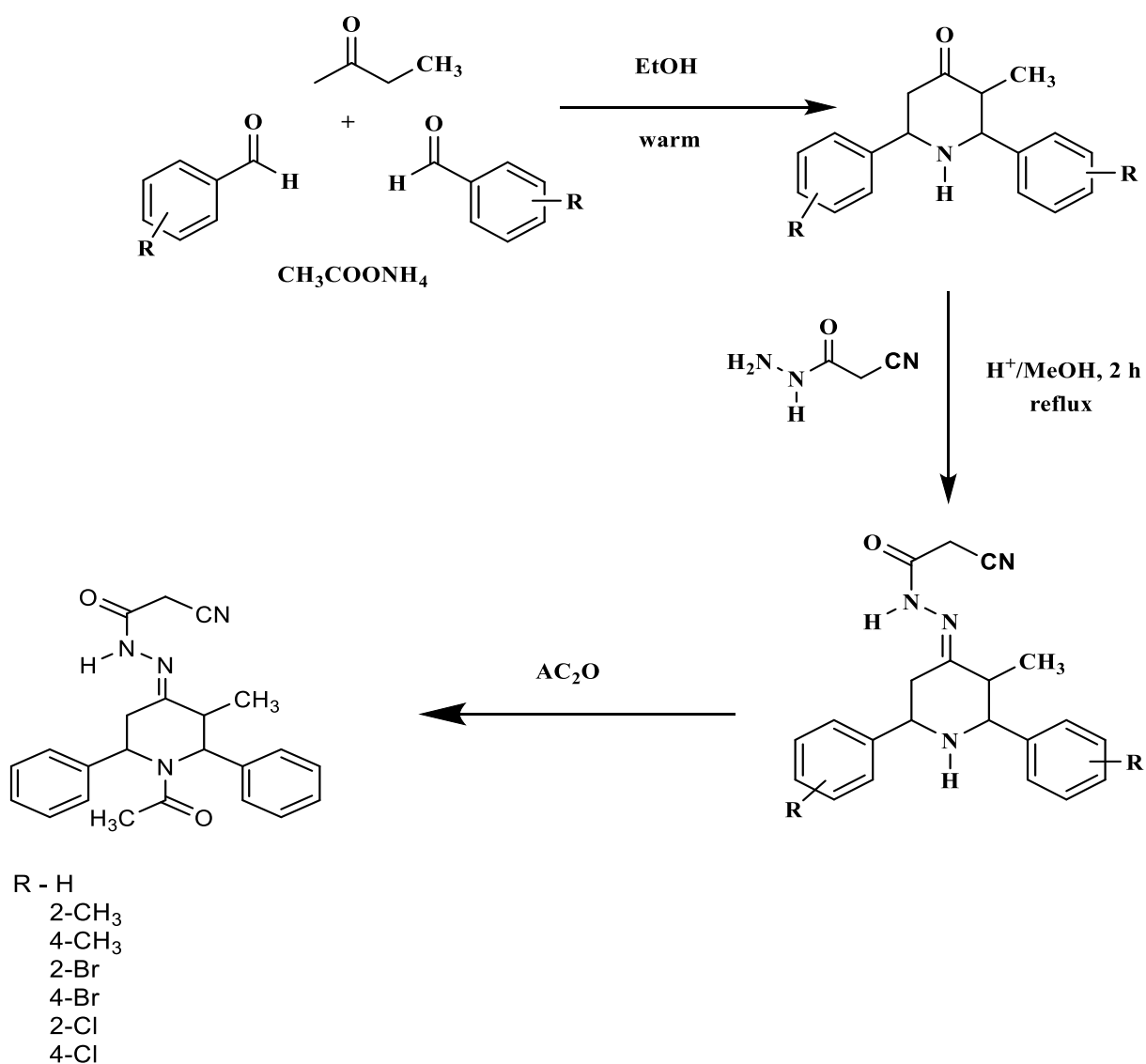
A mixture of various substituted 3-methyl-2,6-diarylpiperidin-4-one (0.1 mol), cyanoaceto hydrazide (0.1 mol) in the presence of few drops of concentrated acetic acid in methanol was refluxed for 2 hours. After the completion of reaction, the reaction mixture was cooled to room temperature. The solid product formed was separated by filtration and washed with warm water and recrystallized by methanol to afford corresponding substituted 3-methyl-2, 6-diarylpiperidin-4-one cyanoacetyl hydrazones.

5.1.3 Preparation of N-acetyl 3-methyl-2,6-diarylpiperidin-4-one cyanoacetylhydrazones

3-methyl-2, 6-diarylpiperidin-4-one cyanoacetyl hydrazones acetylated by 0.1 mol of acetic anhydride and recrystallized by methanol to afford corresponding substituted N-acetyl 3-methyl-2, 6-diarylpiperidin-4-one cyanoacetyl hydrazones.

The schematic representation of all the synthesized compounds are shown in **scheme 1**

Physical data for the synthesized compounds are shown in **Table 2**

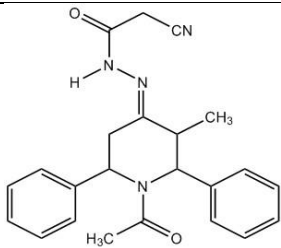
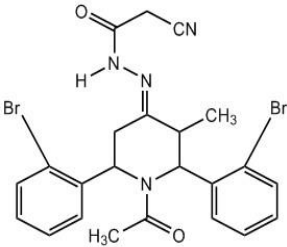


Scheme 1

The structure of all the synthesized compounds viz.,

N-acetyl 3-methyl- 2,6-diphenylpiperidin-4-onecyanoacetylhydrazone (C1),
 N-acetyl 3-methyl- 2,6 (bis-*o*-bromo phenyl) piperidin-4-one cyanoacetylhydrazone (C2),
 N-acetyl 3-methyl - 2,6 (bis-*o*-chloro phenyl) piperidin-4-one cyanoacetylhydrazone (C3),
 N-acetyl 3-methyl - 2,6 (bis-*o*-methyl phenyl) piperidin-4-one cyanoacetylhydrazone (C4),
 N-acetyl 3-methyl - 2,6 (bis-*p*-bromo phenyl) piperidin-4-one cyanoacetylhydrazone (C5),
 N-acetyl 3-methyl - 2,6 (bis-*p*-chloro phenyl) piperidin-4-one cyanoacetylhydrazone (C6),
 N-acetyl 3-methyl -2,6 (bis-*p*-methyl phenyl) piperidin-4-one cyanoacetylhydrazone (C7)
 are characterized by IR, ¹H NMR and ¹³C NMR spectral studies. The type of spectrum recorded for the synthesized compounds are listed in **Table.3**

Table.2 Physical data for the synthesized compounds

Compound	Structure	Molecular Formula	Molecular Weight	Melting point
C1		C ₂₃ H ₂₂ N ₄ O ₂	386	160-163°C
C2		C ₂₃ H ₂₆ Br ₂ N ₄ O	544	179-181 °C.

C3		$C_{23}H_{20}Cl_2N_4O_2$	454	142-145°C.
C4		$C_{25}H_{28}N_4O_2$	416	179-181°C
C5		$C_{23}H_{26}Br_2N_4O$	544	186-189°C
C6		$C_{23}H_{20}Cl_2N_4O_2$	454	148-151°C
C7		$C_{25}H_{28}N_4O_2$	416	139-141°C

Table . 3 Type of the spectrum recorded for the synthesized compounds.

Compounds	IR	¹H NMR	¹³C NMR
C1	✓	✓	✓
C2	✓	✓	✓
C3	✓	✓	✓
C4	✓	✓	✓
C5	✓	✓	✓
C6	✓	✓	✓
C7	✓	✓	✓

5.2 Spectral studies

5.2.1 IR Spectroscopy

Infrared (IR) radiation refers broadly to that part of the electromagnetic spectrum between the visible and microwave region. Of greater practical use to the field of organic chemistry is the limited portion between 4,000 and 400 cm^{-1} . Absorption bands in the spectrum result from energy changes due to molecular vibration of the stretching and bending mode of a bond. Though this absorption is quantized, vibrational spectra appear as bands rather than a line because a single vibrational energy change is accompanied by a number of rotational energy changes. Band positions in infrared spectra are presented either as wave number (ν) or wavelength (λ).

Even a very simple organic molecule can give extremely complex infrared spectrum. The organic chemist takes advantage of this complexity when he matches the spectrum of an unknown compound against that of an authentic sample. A peak-by-peak correlation is an excellent evidence for identity. It is unlikely that any two compounds except enantiomers give the same infrared spectrum.

Since the structural elucidation/identification do not solely dependent on infrared spectrum, a detailed analysis of the spectrum will not be required. In the present study, IR spectra are utilized in conjunction with other spectral data to determine molecular structure.

5.2.2 NMR Spectroscopy

Nuclear Magnetic Resonance (NMR) spectroscopy is a well-established technique for providing information about structural diagnosis of organic molecule. It involves transition of nucleus from one spin state to another state with the resultant absorption of electromagnetic radiation in the radio wave frequency region by spin active nuclei when they are placed in a magnetic field. The energy associated with NMR experiments is incapable of disrupting even the weakest chemical bond in a molecule. One dimensional NMR spectrum constitutes a plot of the frequencies of the absorption peaks versus peak intensities.

5.3 SPECTRAL ANALYSIS OF COMPOUNDS N-ACETYL -3-METHYL-2,6-DIPHENYLPYPERIDIN-4-ONE CYANOACETYLHYDRAZONE (C1)

5.3.1 IR Spectral Analysis

The IR spectrum of compound (C1) an absorption band appeared at 3269 cm^{-1} is due to N-H [1] stretching frequency. The aromatic and aliphatic C-H stretching vibrations appeared at $2935\text{-}3062\text{ cm}^{-1}$. The absorption frequency is 1894 cm^{-1} is assigned for $\text{C}\equiv\text{N}$. IR bands appeared at 1720 & 1647 are assigned for amide $\text{C}=\text{O}$ and $\text{C}=\text{N}$ stretching frequency. Among them 1720 cm^{-1} is due to $\text{C}=\text{O}$ of hydrazone moiety and 1647 cm^{-1} is observed as broad band due to the merging of stretching $\text{C}=\text{O}$ of piperidine moiety and $\text{C}=\text{N}$ stretching frequency. All the observed IR bands are supported the formation of the synthesized compounds.

All the observed IR bands are supporting evidences for the formation of compounds C1. IR spectral data of the compound C1 are shown in Table.4

Table.4 Characteristic IR stretching frequencies (cm^{-1}) of C1

Compound C1	C-H (Aliphatic and Aromatic)	N-H	$\text{C}\equiv\text{N}$	C=O (Hydrazone moiety)	C=N and C=O (Piperidone moiety)
	2935-3062	3269	1894	1720	1647

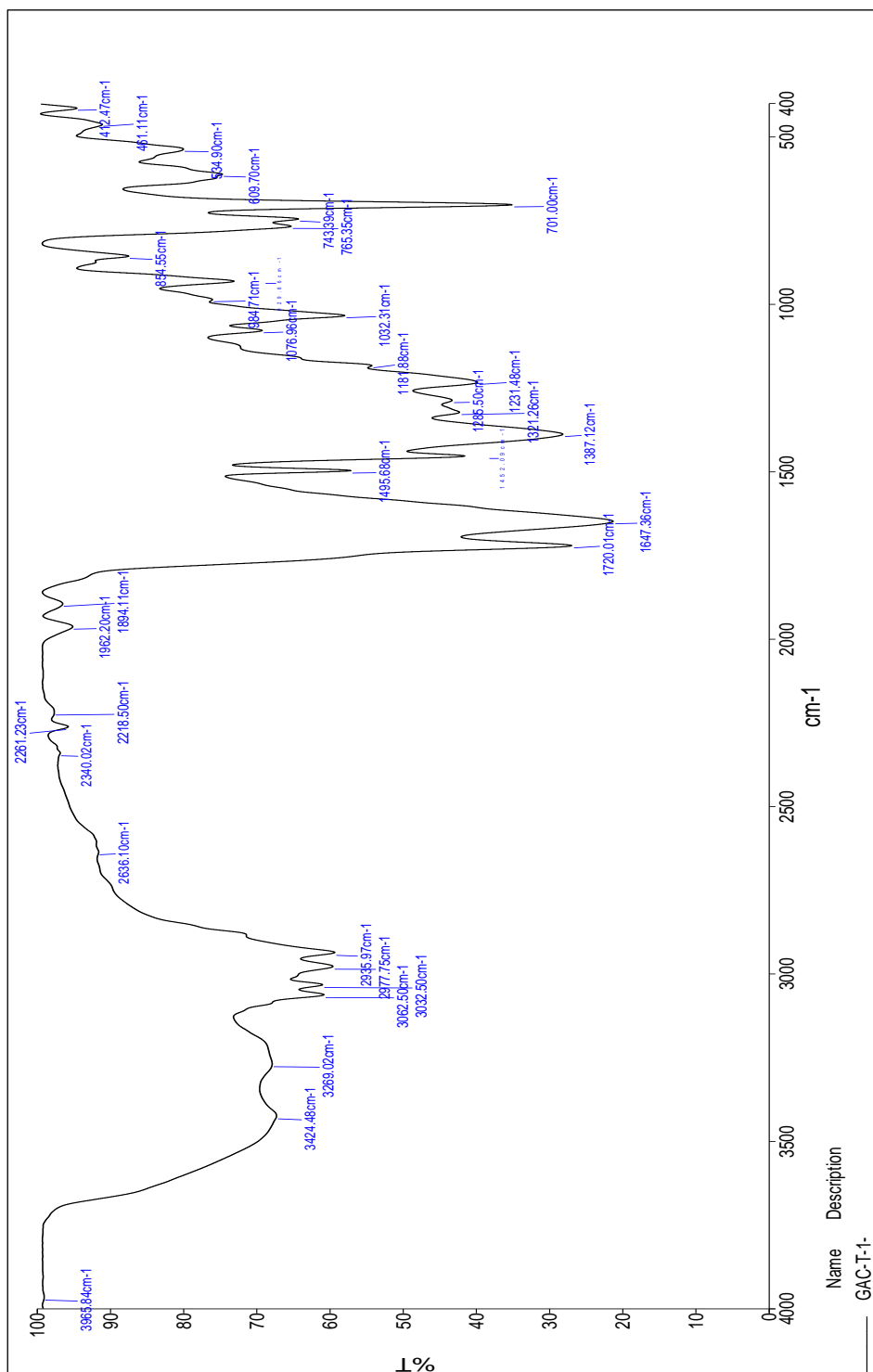


Fig. 5 IR Spectrum of compound (C1)

5.3.2 ¹H NMR Spectral analysis

The introduction of hydrazone group at the 4th position of 1-heterocyclic ketones is reported to exert a major change in chemical shifts of its acetyl group and their associated protons. ¹H NMR chemical shift values (δ , ppm) numbering of compound C1 is given in **Fig.6**.

The ¹H NMR spectral signals are assigned by their position, multiplicity and integral values and also comparing with that of parent ketone. In ¹H NMR spectrum (**Fig.7a** and **Fig.7b**), the signals appear in the range 7.50-7.26 ppm corresponding to 10 protons are due to the aromatic protons of the two phenyl groups at C-2 and C-6.

There is one broad singlet at downfield region at 9.18 ppm with one proton integral which is assigned to the N-H proton of hydrazone moiety. Moreover, two closely spaced doublets forming an AB quartet around 3.79 ppm correspond to two protons are assigned as the methylene protons of CH₂ protons of cyanoacetyl hydrazone moiety based on their spin-spin coupling constant values and 2.86 ppm CH₃ protons of acetyl moiety. The actual chemical shift values of these diastereotopic germinal protons exhibiting AB spin system of coupling was found out using second order spectral analysis.

In 3-methyl-2,6-diphenylpiperidin-4-one, the CH₃ at C-3 was reported to show its resonance at 0.84 ppm. Hence, a sharp doublet with three protons integral at 0.89 ppm ($J = 6.6$ Hz) is unambiguously assigned for the CH₃ protons at C-3.

Apart from , there are five signals in between 3.91 and 2.23 ppm, which are due to the ring protons of the piperidine moiety. They are appeared as doublet of doublets at 3.91, 2.92 and 2.23 ppm, doublet at 3.55 ppm and a multiplet at 2.58 ppm with one protons integral each. In 3-methyl-2,6-diphenylpiperidin-4-one, the doublet at 3.63 ppm with coupling

constant 10 Hz was assigned for H-2a proton and the double doublet at 4.10 ppm is assigned as H-6a proton. In fact, the doublet at 3.55 ppm with coupling constant 10.2 Hz is ascribed to H-2a proton the double doublet resonance at 3.91 ppm with vicinal coupling constants 11.7 Hz (J^3 diaxial) and 2.4 Hz (J^3 axial equatorial) is assigned to H-6a proton.

There are two double doublets at 2.23 ppm with coupling constants 11.7 Hz (J^3 diaxial) and 13.8 Hz (J^2 axial equatorial) and 2.92 ppm with coupling constants 2.7 Hz (J^3 axial equatorial) and 13.8 Hz (J^2 axial equatorial). The geminal coupling constant values suggest that those protons are present at same carbon which is assigned to methylenic protons at C-5. Furthermore, the vicinal coupling constant reveals that the double doublets at 2.23 and 2.92 ppm are due to H-5a and H-5e proton respectively. Consequently, the multiplet resonance at 2.58 ppm is ascribed to H-3a proton.

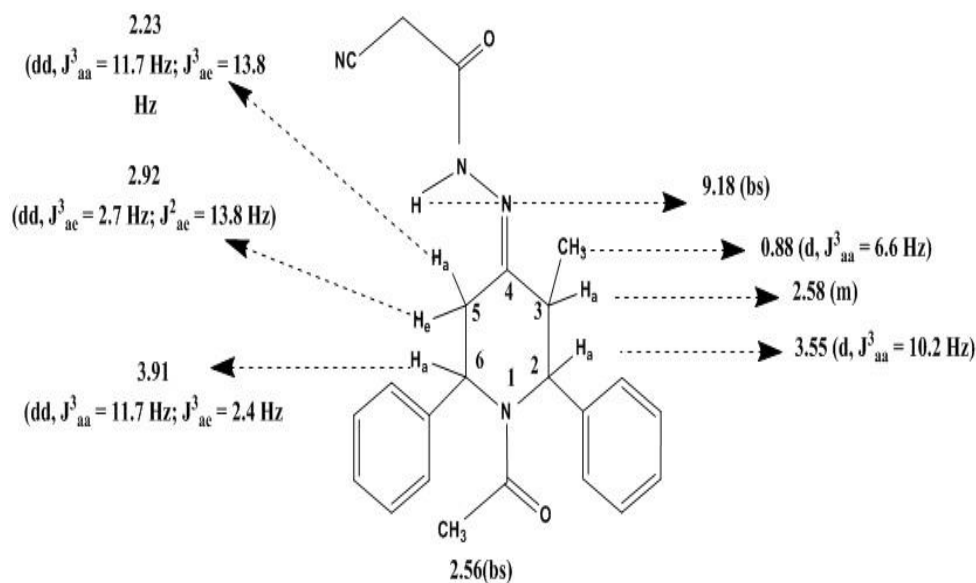


Fig. 6 ^1H NMR chemical shift values (δ , ppm) numbering of Compound C1

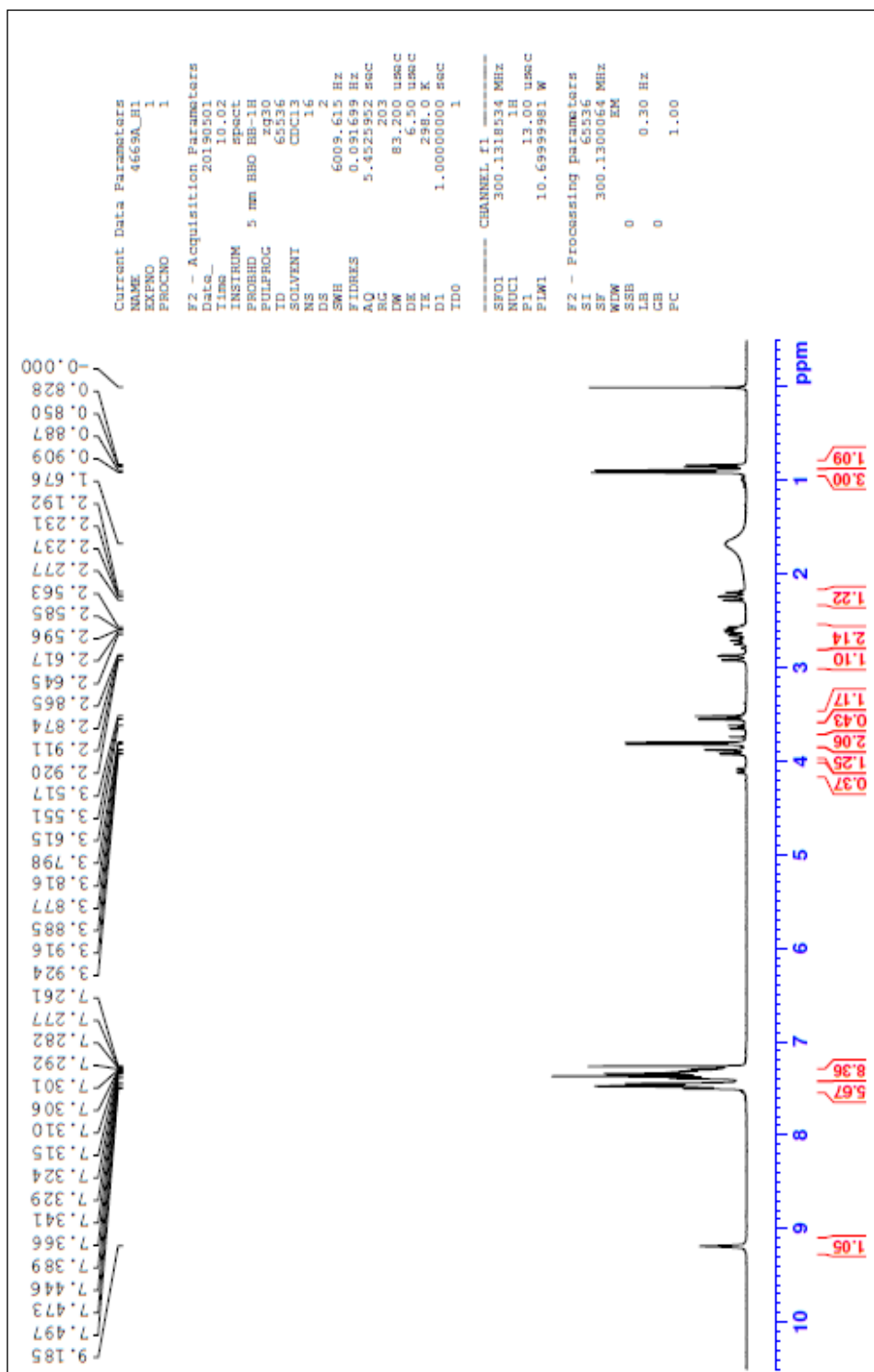


Fig. 7a ¹H NMR Spectrum of compound C1

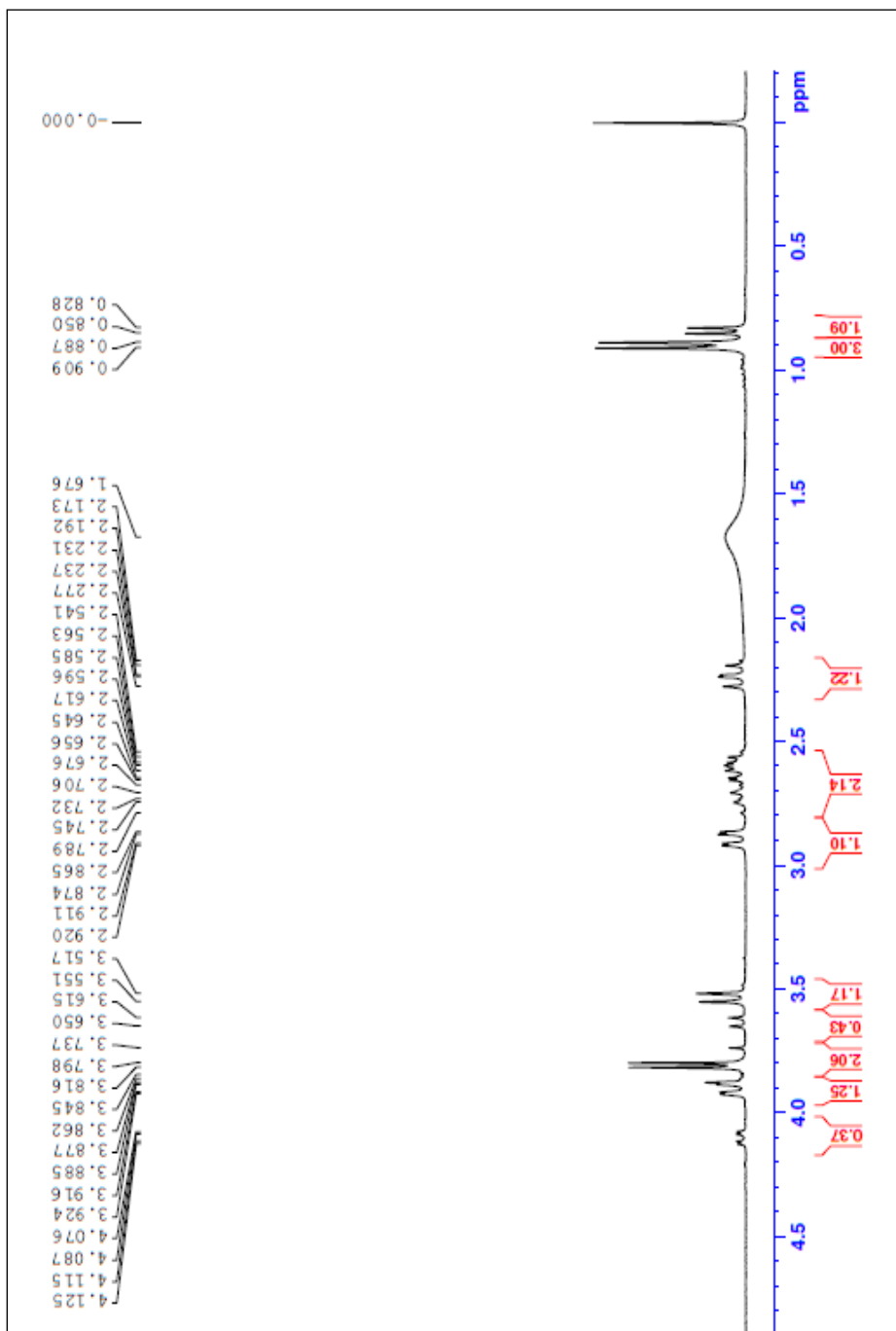


Fig. 7b ¹H NMR Spectrum of compound C1 (upfield)

5.3.3 ¹³C- NMR Spectral analysis

¹³C- NMR spectral assignments have been made based on characteristic signal positions of the functional groups and comparison with those of parent ketones.

¹³C- NMR spectra of the compound C1 depicted in (fig 8). As declared above, the ipso carbons of the phenyl rings could be simply eminent from rest of the ring carbons by their characteristic downfield absorption.

The signals at 127.93 ppm and 141.99 ppm is due to ipso carbons (C-2' and C-6' respectively) of compound C1. The signals at the region 127.82-125.90 ppm are due to other aromatic carbons. There are two less intense signals resonates at 164.41 and 158.02 ppm are characteristic for C=O (hydrazone moiety) and C=O (acetyl moiety). Hence, the signal at 156.34 and 114.29 ppm are characteristic for C=N and C≡N carbons, respectively.

The characteristic signals are appeared in the respective region for 35.70 ppm assigned for the CH₂ carbon for cyanoacetylhydrazone moiety. The 3-CH₃ proton signal appeared at 11.52 ppm and acetyl C-CH₃ resonance at 24.08 ppm.

There are four signals for piperidine ring has the chemical shifts at 68.48, 60.78, 50.04 and 44.29 ppm respectively. Among the four signals the downfield signals at 68.48 and 60.78 ppm assigned to C-2 and C-6 carbons where as the upfield signals at 50.04 and 44.29 ppm is due to C-3 and C-5 carbons. These characteristic signals are well supported our proposed structure.

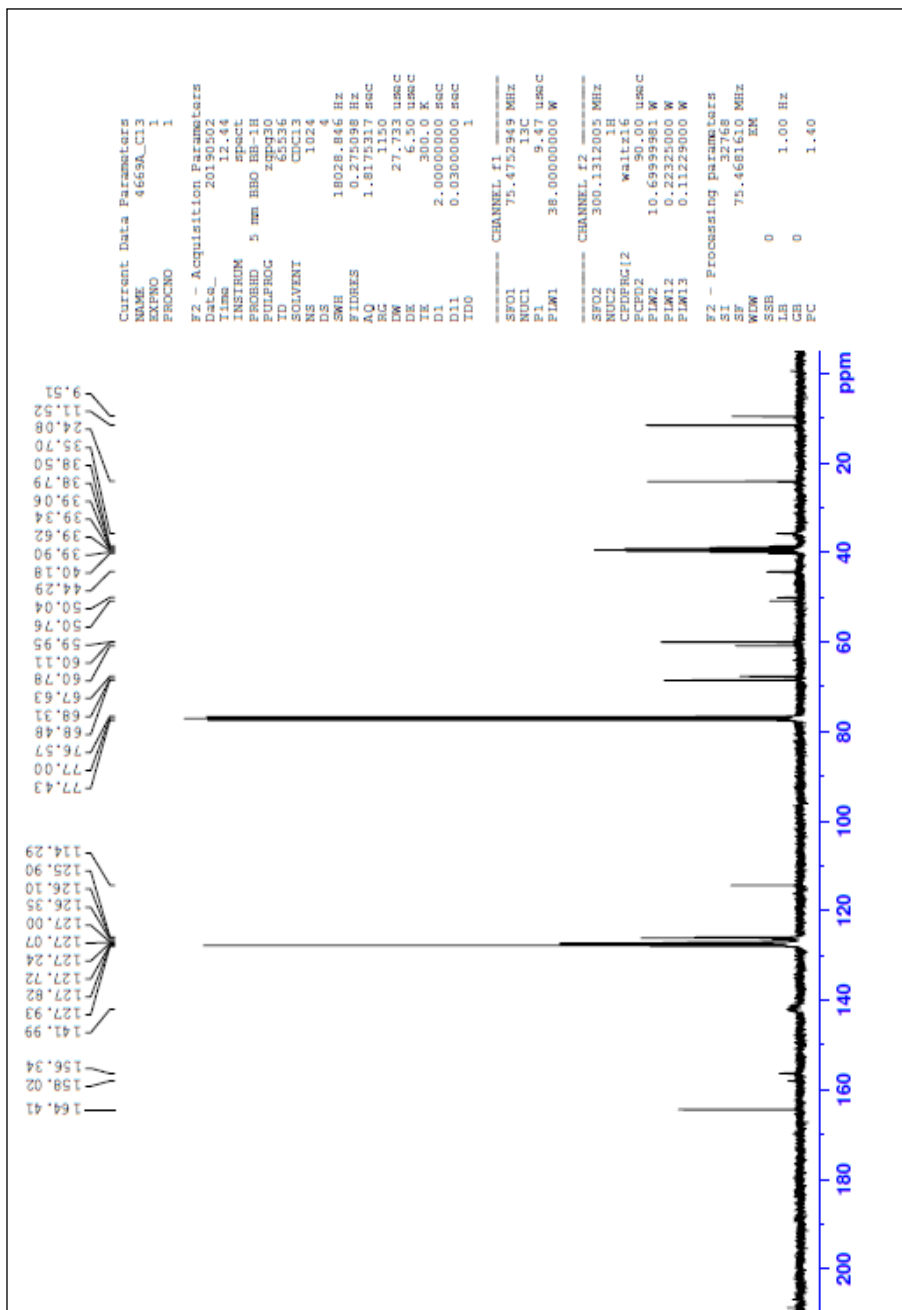


Fig. 8 ¹³C NMR Spectrum of compound C1

Conformation

Conformation of the synthesized compound **C1** is confirmed from the observed coupling constant value and magnitude of chemical shift values. All the observed coupling constant values of compound **C1** are furnished in **Table. 5**. From the **Table. 5** the coupling constant values of compound **C1** are reveals that the six membered piperidine rings exist in chair conformation with equatorial orientation of phenyl substituents at C-2, C-6 and methyl group at C-3.

Table . 5 Coupling constant values of compound C1 in Hz

Compound	$^3J_{2a,3a}$	$^3J_{5a,6a}$	$^2J_{5a,5e}$	$^3J_{5e,6a}$
C1	10.2	11.7	13.8	2.4

On hydrazone formation there are two conformations possible with the orientation of C=N-NH bond whether *syn* to C-5 are C-3 carbon. To fix the orientation of C=N-NH bond the proton chemical shift values are compared with parent ketone (3-methyl 2,6- diphenyl piperidin-4-one) and the chemical shift differences are given in **Table 6**.

Table. 6 Proton chemical shift values of parent Piperidone and synthesized compounds [δ (ppm)]

Compound	H-2a	H-3a	H-5a	H-5e	H-6a	3-CH ₃
Parent	3.63	2.68	2.74	2.83	4.10	0.84
C1	3.55	2.58	2.23	2.92	3.91	0.88
C2	3.62	2.56	2.62	2.20	3.97	0.89
C3	2.59	3.54	2.23	2.92	3.92	0.88
C4	3.49	2.57	2.20	2.83	3.87	0.89
C5	4.06	2.70	2.24	3.43	4.40	0.97
C6	3.51	2.53	2.18	2.98	3.91	0.89
C7	3.10	2.57	2.39	3.07	3.89	0.92
Parent-C1	0.08	0.10	0.51	- 0.09	0.19	- 0.04

Negative sign denotes shielding

From the **Table. 6**, the deshielding of H-5e proton reveals that the C=N-NH bond is *syn* to the C-5 bond. Hence, the conformation of the compound N-acetyl, 3-methyl 2,6- diphenyl piperidin-4-one is chair conformation with axial orientation of all the substituents at C-2, C-3 and C-6 and the C=N-NH bond *syn* orientation with C-5 carbon (**Fig. 9**)

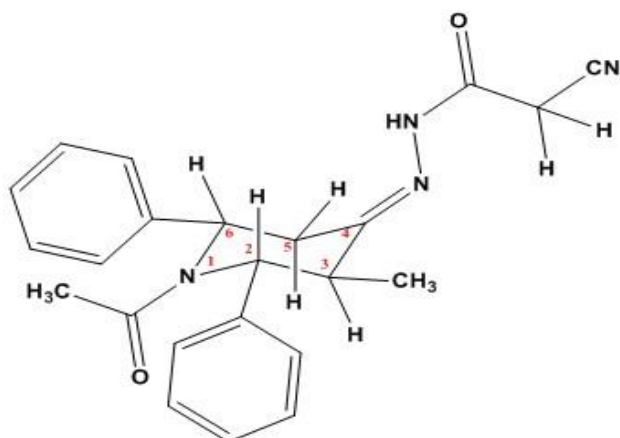


Fig. 9

A structural isomer, or constitutional isomer, is a type of isomer in which molecules with the same molecular formula have different bonding patterns and their atomic organisations, as opposed to stereoisomers, in which molecular bonds are always in the same order and only spatial arrangement differs. Since diatomic halogens can only stretch one way, and that one way is totally symmetric, there is no change or production of a dipole moment.

The synthesized hydrazones have been obtained the *syn*-conformers were determined. The *syn* conformers depend on the strength of intramolecular hydrogen bond. From the observed coupling constant values, the synthesized compound exists as structural isomers. (In the synthesis, we used the substitute aldehyde at various position. p-Br, o-Br, p-Cl, o-Cl, p-CH₃, o- CH₃).

Analytical and spectral data of compound C1 is given in **Table.7**

TABLE. 7 ANALYTICAL AND SPECTRAL DATA OF C1

MF: C ₂₃ H ₂₂ N ₄ O ₂	M.Pt. 160-163°C	Yield(%) : 85.51	M.W: 386
IR (cm⁻¹): 3062-2935 (C-H Aliphatic & Aromatic stretching), 1720 (C=O), 1647 (C=O & C=N), 2261 (C≡N), 3269 (N-H).			
¹H NMR (δ ppm) : 7.49-7.26(m, 10H, Aromatic Protons), 9.18 (b s, 1H, N-H Hydrazone Moiety), 3.79 (q, 2H, CH ₂ –Protons in hydrazone moiety), 2.87(3H, CH ₃ –Protons in acetyl moiety), 0.88 (d, J = 6.6Hz, 3H, 3-CH ₃), 3.91 (dd, J ³ _{a,e} = 2.4Hz, J ³ _{a,a} = 11.7Hz, 1H, H-6a), 3.55 (d, J ³ _{a,a} = 10.2Hz, 1H, H-2a), 2.23 (dd, J ³ _{a,e} =13.8Hz, ³ _{a,a} =11.7 Hz, 1H, H-5a), 2.92 (dd, J ³ _{a,e} = 2.7 Hz, J ² _{a,e} = 13.8Hz, 1H, H-5e), 2.58 (m, 1H, H-3a Proton).			
¹³C NMR (δ ppm) : 127.93(C-2 ipso carbon), 141.99(C-6 ipso carbon), 127.82-125.90 (Aromatic carbons),164.41 (C=O), 158.02(Ace C=O), 156.34(C= N), 114.29 (C≡N), 34.70 (CH ₂ carbon of cyanoacetyl hydrazone moiety) , 68.48 (C-2), 60.78 (C-6), 50.04 (C-3), 24.29 (C-5), 11,52 (3-CH ₃),24.08(O=C-CH ₃).			

5.4 SPECTRAL ANALYSIS OF COMPOUNDS N-ACETYL -3-METHYL-2,6 BIS(O-BROMOPHENYL PIPERIDIN -4-ONE CYANOACETYLHYDRAZONE (C2)

5.4.1 IR Spectral Analysis

The IR spectrum of compound (C2) an absorption band appeared at 3026 cm^{-1} is due to N-H stretching frequency. The aromatic and aliphatic C-H stretching vibrations appeared at $2977\text{--}2927\text{ cm}^{-1}$. The absorption frequency is 2260 cm^{-1} is assigned for $\text{C}\equiv\text{N}$. IR bands appeared at 1720 & 1647 are assigned for amide $\text{C}=\text{O}$ and $\text{C}=\text{N}$ stretching frequency. Among them 1720 cm^{-1} is due to $\text{C}=\text{O}$ of hydrazone moiety and 1647 cm^{-1} is observed as broad band due to the merging of stretching $\text{C}=\text{O}$ of piperidine moiety and $\text{C}=\text{N}$ stretching frequency. All the observed IR bands are supported the formation of the synthesized compounds.

All the observed IR bands are supporting evidences for the formation of compounds C2. IR spectral data of the compound C2 are shown in **Table.8**

Table.8 Characteristic IR stretching frequencies (cm^{-1}) of C2

Compound C1	C-H (Aliphatic and Aromatic)	N-H	$\text{C}\equiv\text{N}$	C=O (Hydrazone moiety)	C=N and C=O (Piperidone moiety)
	2977-2927	3026	2260	1720	1647

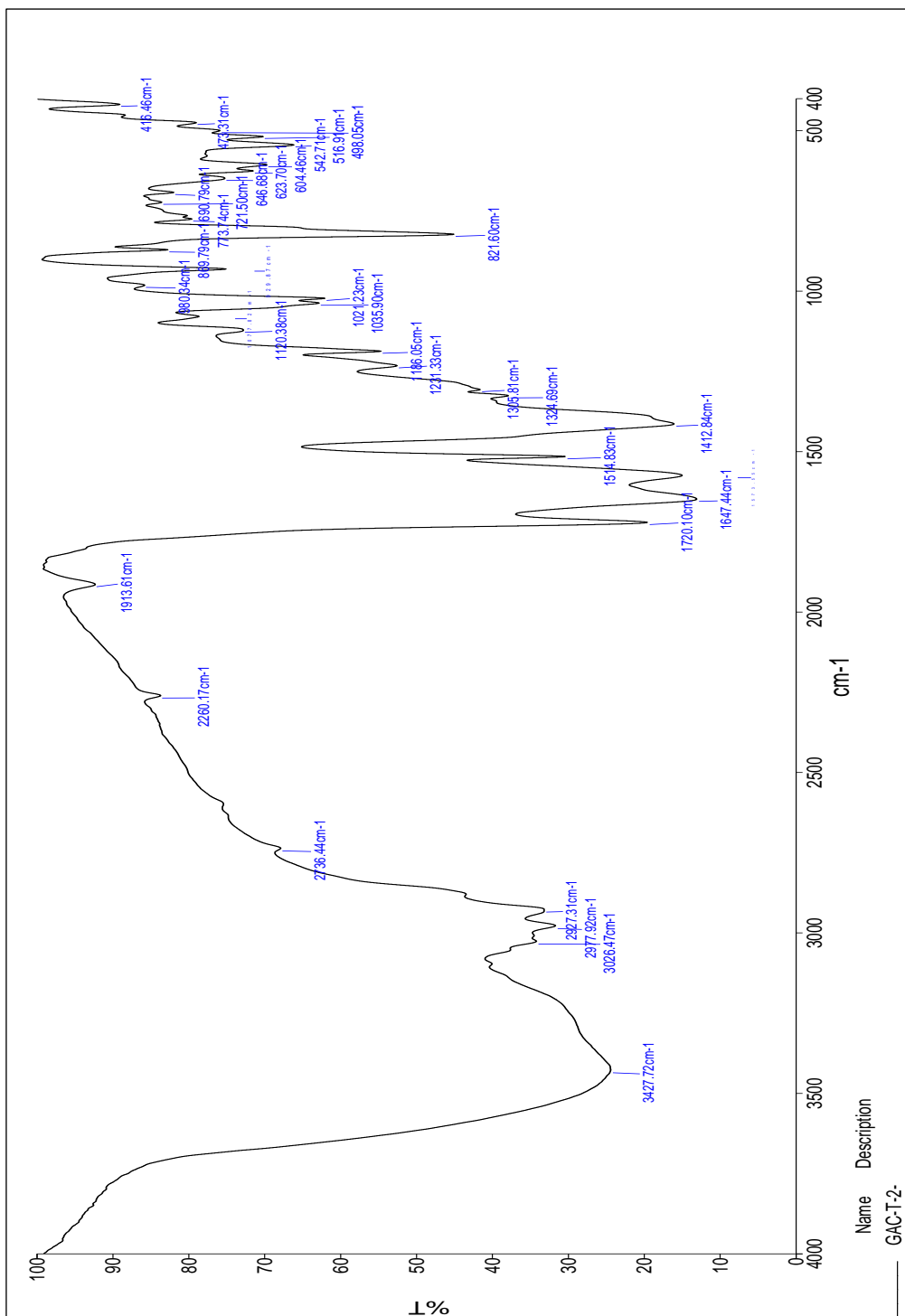


Fig. 10 IR Spectrum of compound (C2)

5.4.2 ¹H NMR Spectral analysis

The ¹H NMR spectral signals are assigned by their position, multiplicity and integral values and also comparing with that of parent ketone. In ¹H NMR spectrum (**Fig.11**), the signals appear in the range 7.59-7.36 ppm corresponding to 8 protons are due to the aromatic protons of the two phenyl groups at C-2 and C-6.

There is one broad singlet at downfield region at 10.07 ppm with one proton integral which is assigned to the N-H proton of hydrazone moiety. Moreover, two closely spaced doublets forming an AB quartet around 3.71 ppm correspond to two protons are assigned as the methylene protons of CH₂ protons of cyanoacetyl hydrazone moiety based on their spin-spin coupling constant values and 2.15 ppm CH₃ proton of acetyl moiety. The actual chemical shift values of these diastereotopic germinal protons exhibiting AB spin system of coupling was found out using second order spectral analysis.

In 3-methyl-2,6-diphenylpiperidin-4-one, the CH₃ at C-3 was reported to show its resonance at 0.84 ppm. Hence, a sharp doublet with three protons integral at 0.91 ppm (J = 6.6 Hz) is unambiguously assigned for the CH₃ protons at C-3.

Apart from, there are five signals in between 3.97 and 2.20 ppm, which are due to the ring protons of the piperidine moiety. They are appeared as doublet of doublets at 3.97, 2.62 and 2.20 ppm, doublet at 3.62 ppm and a multiplet at 2.56 ppm with one protons integral each. In 3-methyl-2,6-diphenylpiperidin-4-one, the doublet at 3.63 ppm with coupling constant 10 Hz was assigned for H-2a proton and the double doublet at 4.01 ppm is assigned as H-6a proton. Infact, the doublet at 3.62 ppm with coupling constant 9.9 Hz is ascribed to H-2a proton the double doublet resonance at 3.97 ppm with vicinal coupling constants 12.0 Hz (J³ diaxial) and 3 Hz (J³ axial equatorial) is assigned to H-6a proton.

There are two double doublets at 2.20 ppm with coupling constants 12.0 Hz (J^3 diaxial) and 12.3 Hz (J^2 axial equatorial) and 2.62 ppm with coupling constants 3 Hz (J^3 axial equatorial) and 12.0 Hz (J^2 axial equatorial). The geminal coupling constant values suggest that those protons are present at same carbon which is assigned to methylenic protons at C-5. Furthermore, the vicinal coupling constant reveals that the double doublets at 2.20 and 2.62 ppm are due to H-5a and H-5e proton respectively. Consequently, the multiplet resonance at 2.56 ppm is ascribed to H-3a proton.

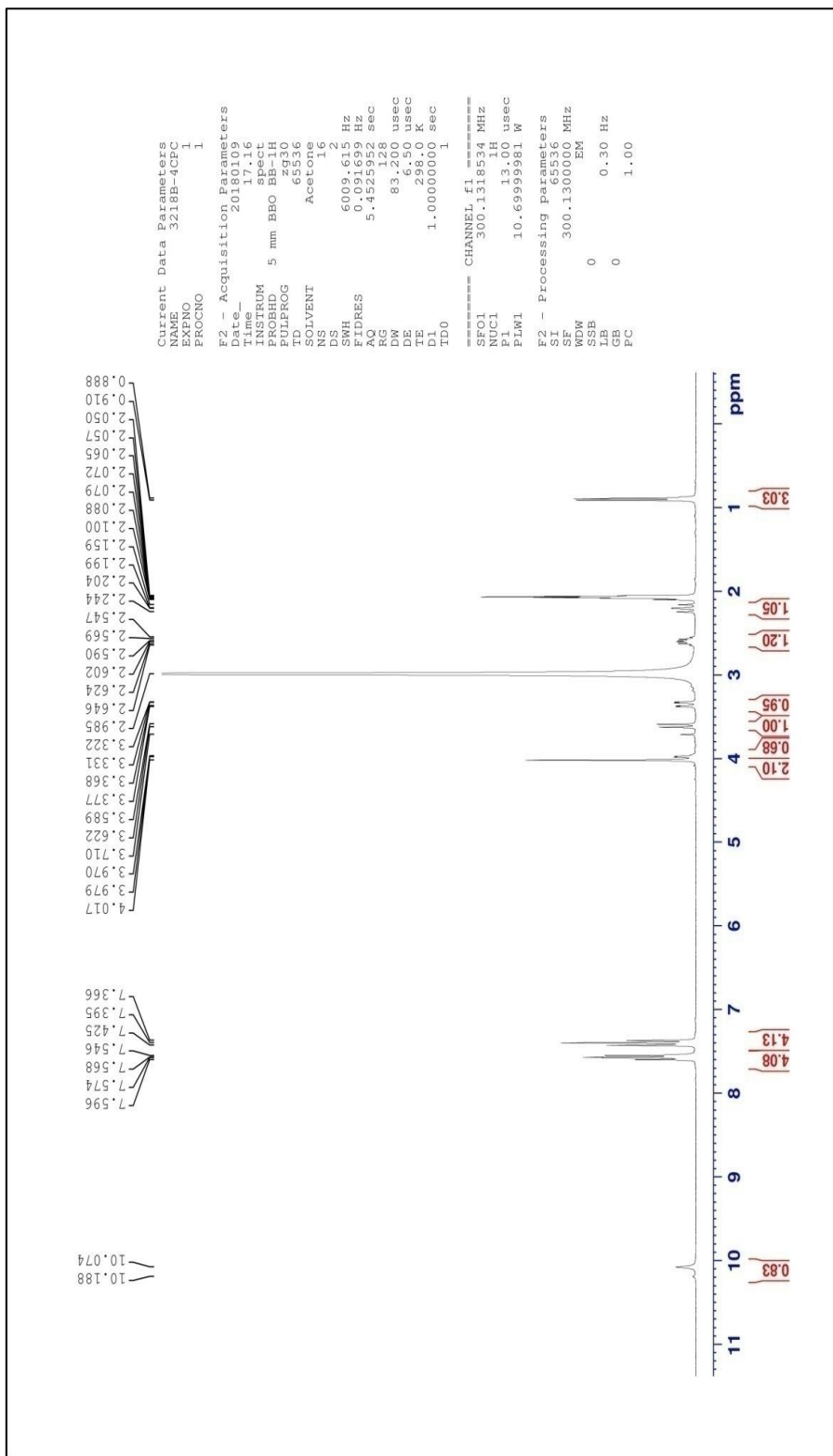


Fig. 11 ¹H NMR Spectrum of compound (C2)

5.4.3 ¹³C- NMR Spectral analysis

¹³C- NMR spectral assignment has been made based on characteristic signal positions of the functional groups and comparison with those of parent ketones.

¹³C- NMR spectra of the compound C2 depicted in (fig 12). As declared above, the ipso carbons of the phenyl rings could be simply eminent from rest of the ring carbons by their characteristic downfield absorption.

The signals at 142.01 ppm and 142.78ppm is due to ipso carbons (C-2' and C-6' respectively) of compound C2. The signals at the region 128.30-132.68 ppm are due to other aromatic carbons. There are two less intense signals resonates at 205.59 and 165.08 ppm are characteristic for C=O (hydrazone moiety) and C=O (acetyl moiety). Hence, the signal at 155.76 and 115.05 ppm are characteristic for C=N and C≡N carbons, respectively.

The characteristic signals are appeared in the respective region for 156.34 ppm assigned for the CH₂ carbon for cyanoacetylhydrazone moiety. The 3-CH₃ proton signal appeared at 11.66 ppm and acetyl C-CH₃ resonance at 24.10 ppm.

There are four signals for piperidine ring has the chemical shifts at 68.36, 59.77, 44.86 and 35.83 ppm respectively. Among the four signals the downfield signals at 68.36 and 59.77 ppm assigned to C-2 and C-6 carbons where as the upfield signals at 44.86 and 35.83 ppm is due to C-3 and C-5 carbons. These characteristic signals are well supported our proposed structure.

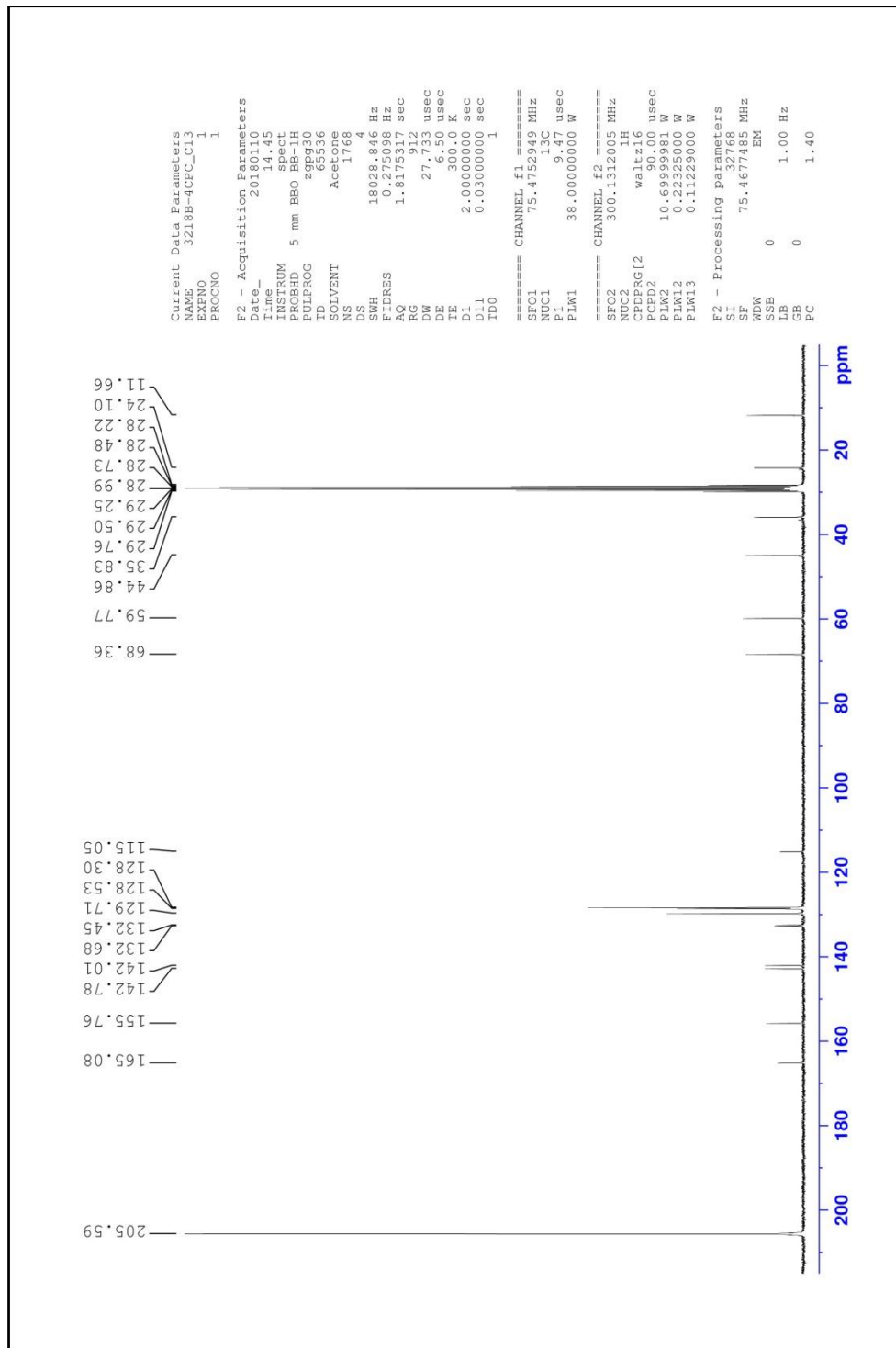
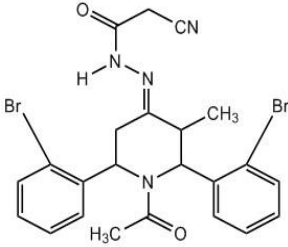


Fig. 12 ¹³C NMR Spectrum of compound C2

Analytical and spectral data of compound C2 is given in **Table.9**

TABLE. 9 ANALYTICAL AND SPECTRAL DATA OF C2

MF: C ₂₃ H ₂₀ Br ₂ N ₄ O ₂	M.Pt. 179-181°C	Yield (%) : 80.56	M.W : 544
<p>IR (cm⁻¹): 2977-2927 (C-H Aliphatic & Aromatic stretching), 1720 (C=O), 1647 (C=O&C=N), 2260 (C≡N), 3269 (N-H).</p>			
<p>¹H NMR (δ ppm) : 7.59-7.36(m, 8H, Aromatic Protons), 10.07 (b s, 1H, N-H Hydrazone Moiety), 3.71 (q, 2H, CH₂ –Protons in hydrazone moiety), 3.32(3H, CH₃ –Protons in acetyl moiety), 0.89 (d, J = 6.6Hz, 3H, 3-CH₃), 3.97 (dd, J³_{a,e} = 3.0 Hz, J³_{a,a} = 12.0Hz, 1H, H-6a), 3.62 (d, J³_{a,a} = 9.9Hz, 1H, H-2a), 2.20 (dd, J³_{a,e} = 12.3Hz, J³_{a,a} = 12.0 Hz, 1H, H-5a), 2.62 (dd, J³_{a,e} = 3.0 Hz, J²_{a,e} = 12Hz, 1H, H-5e), 2.56 (m, 1H, H-3a Proton).</p>			
<p>¹³C NMR (δ ppm) : 142.01(C-2 ipso carbon), 142.78(C-6 ipso carbon), 128.30-132.68 (Aromatic carbons),205 (C=O), 165.08(Ace C=O), 155.76 (C=N), 115.05 (C≡N), 28.22 (CH₂ carbon of cyanoacetyl hydrazone moiety) , 68.36 (C-2), 59.77 (C-6), 44.86 (C-3), 35.83 (C-5), 11.66 (3-CH₃),24.10 (O=C-CH₃).</p>			
			

5.5 SPECTRAL ANALYSIS OF COMPOUNDS N-ACETYL -3-METHYL-2,6 BIS(O-CHLORO PHENYL PIPERIDIN -4-ONE CYANOACETYLHYDRAZONE (C3)

5.5.1 IR Spectral Analysis

The IR spectrum of compound (C3) an absorption band appeared at 3205 cm^{-1} is due to N-H stretching frequency. The aromatic and aliphatic C-H stretching vibrations appeared at $3855\text{-}2935\text{ cm}^{-1}$. The absorption frequency is 2263 cm^{-1} is assigned for $\text{C}\equiv\text{N}$. IR bands appeared at 1619 & 1591 are assigned for amide $\text{C}=\text{O}$ and $\text{C}=\text{N}$ stretching frequency. Among them 1619 cm^{-1} is due to $\text{C}=\text{O}$ of hydrazone moiety and 1591 cm^{-1} is observed as broad band due to the merging of stretching $\text{C}=\text{O}$ of piperidine moiety and $\text{C}=\text{N}$ stretching frequency. All the observed IR bands are supported the formation of the synthesized compounds.

All the observed IR bands are supporting evidences for the formation of compounds C3. IR spectral data of the compound C3 are shown in **Table.10**

Table.10 Characteristic IR stretching frequencies (cm^{-1}) of C3

Compound C1	C-H (Aliphatic and Aromatic)	N-H	$\text{C}\equiv\text{N}$	C=O (Hydrazone moiety)	C=N and C=O (Piperidone moiety)
	3855-2935	3205	2263	1619	1591

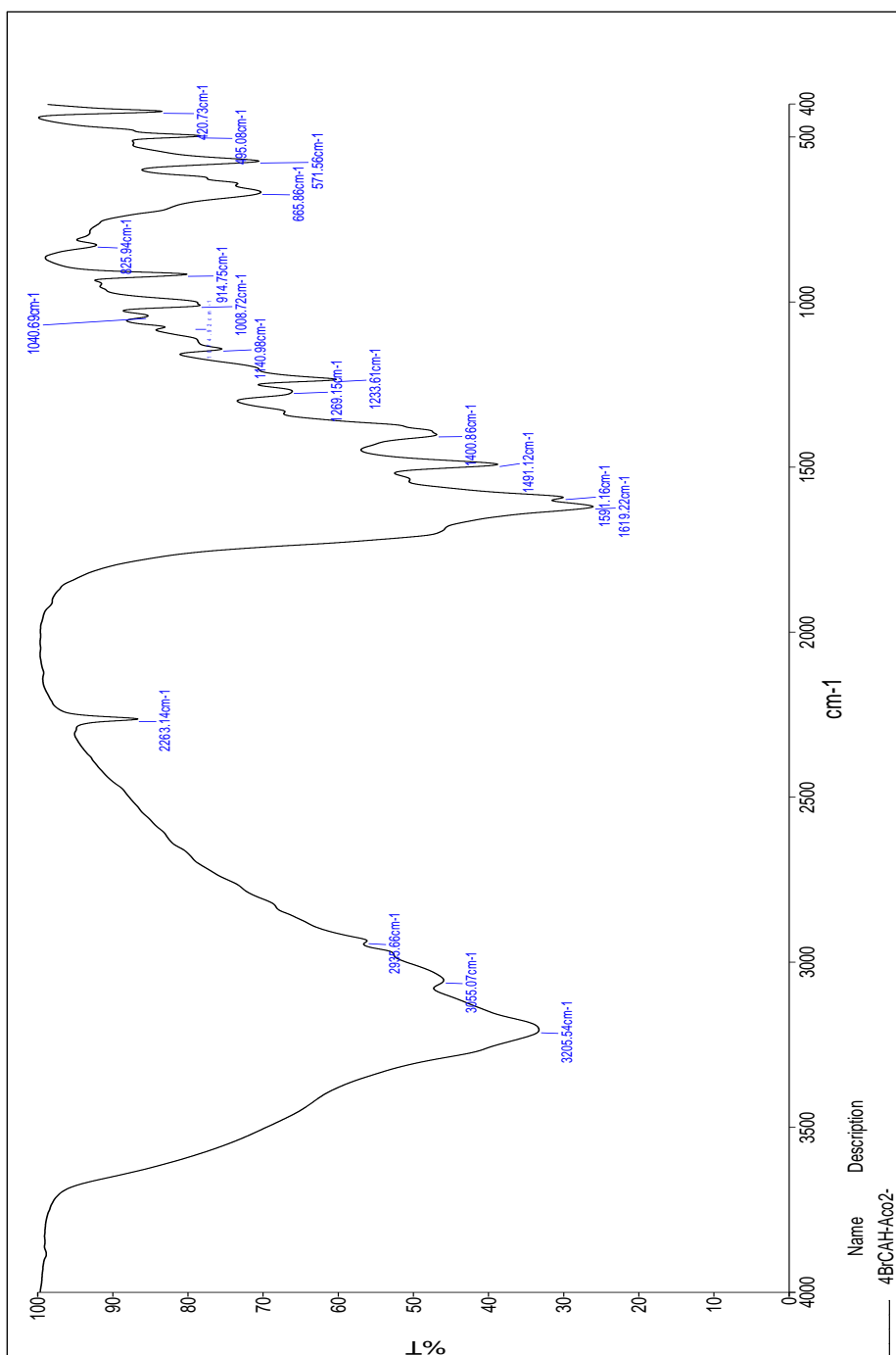


Fig. 13 ¹H NMR Spectrum of compound C3

5.5.2 ¹H NMR Spectral analysis

The ¹H NMR spectral signals are assigned by their position, multiplicity and integral values and also comparing with that of parent ketone. In ¹H NMR spectrum (**Fig.14**), the signals appear in the range 7.50-7.26 ppm corresponding to 8 protons are due to the aromatic protons of the two phenyl groups at C-2 and C-6.

There is one broad singlet at downfield region at 9.24 ppm with one proton integral which is assigned to the N-H proton of hydrazone moiety. Moreover, two closely spaced doublets forming an AB quartet around 3.73 ppm correspond to two protons are assigned as the methylene protons of CH₂ protons of cyanoacetyl hydrazone moiety based on their spin-spin coupling constant values and 1.59 ppm CH₃ proton of acetyl moiety. The actual chemical shift values of these diastereotopic germinal protons exhibiting AB spin system of coupling was found out using second order spectral analysis.

In 3-methyl-2,6-diphenylpiperidin-4-one, the CH₃ at C-3 was reported to show its resonance at 0.84 ppm. Hence, a sharp doublet with three protons integral at 0.88 ppm (J = 6 Hz) is unambiguously assigned for the CH₃ protons at C-3.

Apart from , there are five signals in between 3.92 and 2.23 ppm, which are due to the ring protons of the piperidine moiety. They are appeared as doublet of doublets at 3.92, 2.92 and 2.23 ppm, doublet at 2.59 ppm and a multiplet at 3.54 ppm with one protons integral each. In 3-methyl-2,6-diphenylpiperidin-4-one, the doublet at 3.63 ppm with coupling constant 10 Hz was assigned for H-2a proton and the double doublet at 4.10 ppm is assigned as H-6a proton. Infact, the doublet at 3.54 ppm with coupling constant 9 Hz is ascribed to H-2a proton the double doublet resonance at 3.92 ppm with vicinal coupling constants 12 Hz (J³ diaxial) and 3 Hz (J³ axial equatorial) is assigned to H-6a proton.

There are two double doublets at 2.23 ppm with coupling constants 12 Hz (J^3 diaxial) and 12 Hz (J^2 axial equatorial) and 2.92 ppm with coupling constants 3 Hz (J^3 axial equatorial) and 12 Hz (J^2 axial equatorial). The geminal coupling constant values suggest that those protons are present at same carbon which is assigned to methylenic protons at C-5. Furthermore, the vicinal coupling constant reveals that the double doublets at 2.23 and 2.92 ppm are due to H-5a and H-5e proton respectively. Consequently, the multiplet resonance at 2.59 ppm is ascribed to H-3a proton.

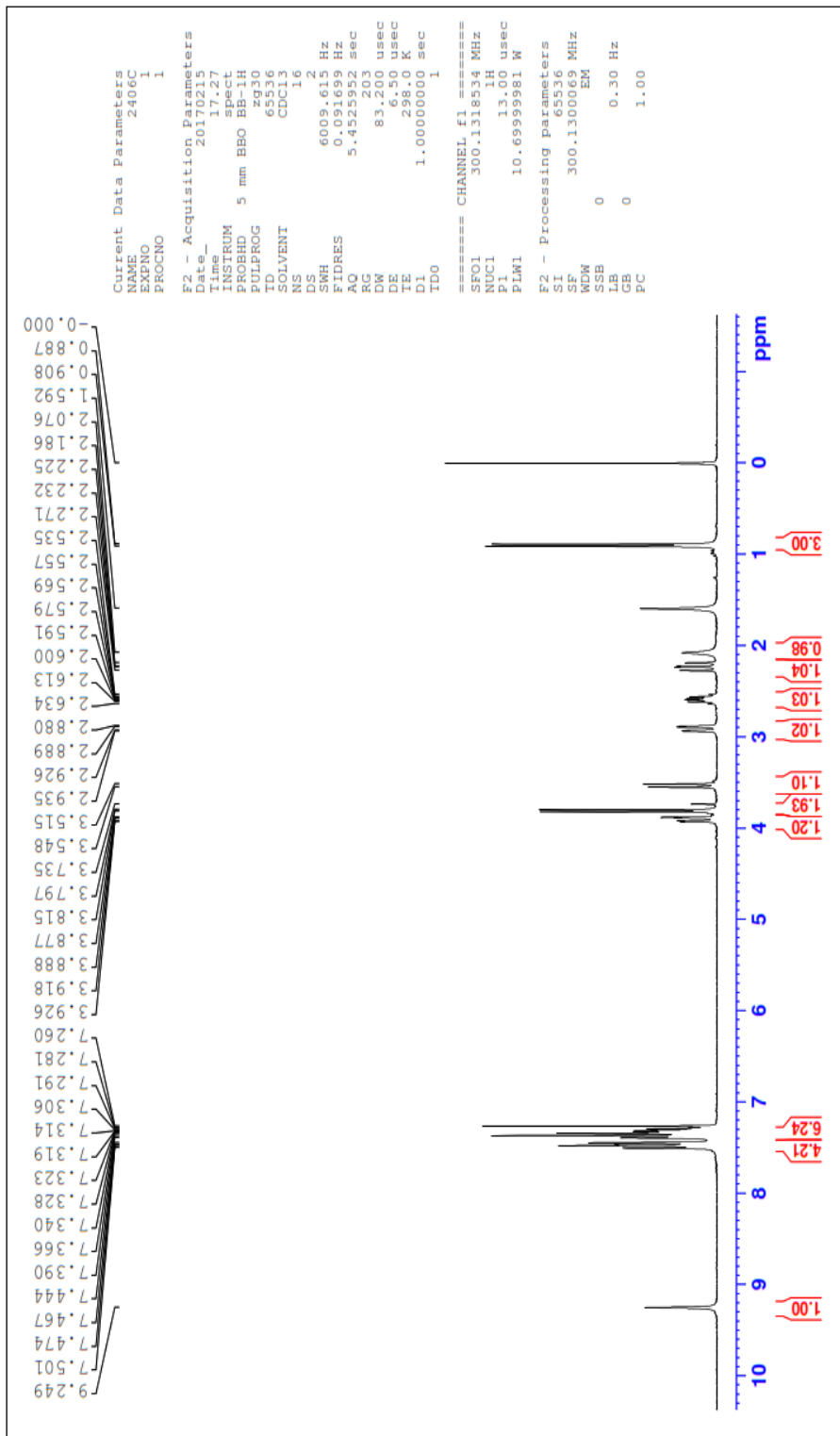


Fig. 14 ¹H NMR Spectrum of compound C3

5.5.3 ¹³C- NMR Spectral analysis

¹³C- NMR spectral assignments have been made based on characteristic signal positions of the functional groups and comparison with those of parent ketones.

¹³C- NMR spectra of the compound C3 depicted in (fig 15). As declared above, the ipso carbons of the phenyl rings could be simply eminent from rest of the ring carbons by their characteristic downfield absorption.

The signals at 139.98 ppm and 140.49 ppm is due to ipso carbons (C-2' and C-6' respectively) of compound C3. The signals at the region 126.49-135.31 ppm are due to other aromatic carbons. There are two less intense signals resonates at 164.48 and 162.28 ppm are characteristic for C=O (hydrazone moiety) and C=O (acetyl moiety). Hence, the signal at 158.05 and 114.35 ppm are characteristic for C=N and C≡N carbons, respectively.

The characteristic signals are appeared in the respective region for 24.16 ppm assigned for the CH₂ carbon for cyanoacetylhydrazone moiety. The 3-CH₃ proton signal appeared at 11.15 ppm and acetyl C-CH₃ resonance at 19.20 ppm.

There are four signals for piperidine ring has the chemical shifts at 56.12, 44.89, 38.52 and 34.56 ppm respectively. Among the four signals the downfield signals at 44.89 and 56.12 ppm assigned to C-2 and C-6 carbons where as the upfield signals at 38.52 and 34.56 ppm is due to C-3 and C-5 carbons. These characteristic signals are well supported our proposed structure.

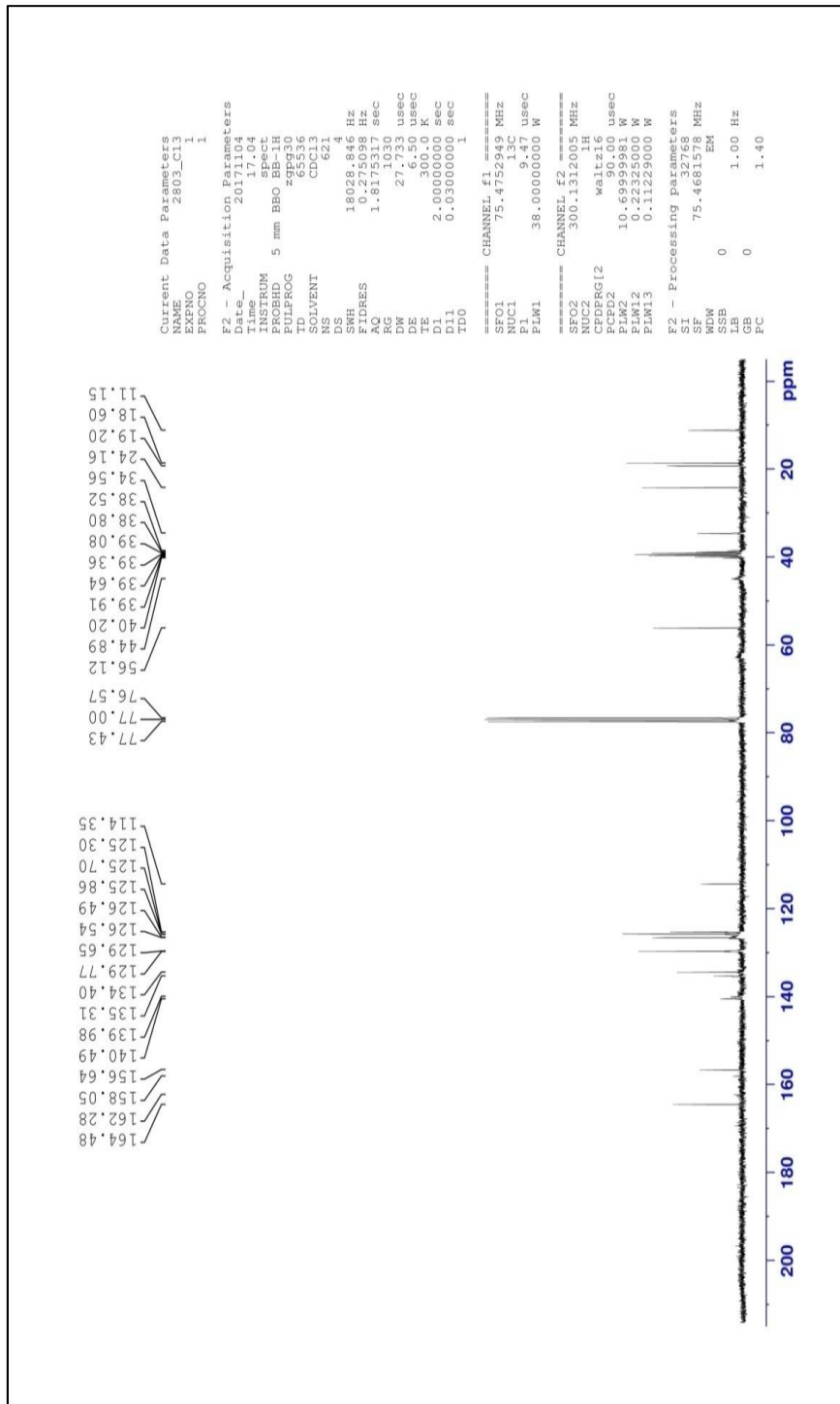
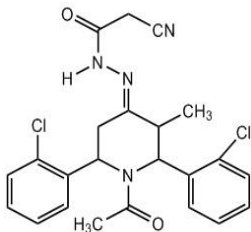


Fig. 15 ¹³C NMR Spectrum of compound C3

Analytical and spectral data of compound C3 is given in **Table.11**

TABLE. 11 ANALYTICAL AND SPECTRAL DATA OF C3

MF: C ₂₃ H ₂₀ Cl ₂ N ₄ O ₂	M.Pt. 142-145°C	Yield (%) : 86.59	M.W : 454
IR (cm⁻¹): 3855-2935 (C-H Aliphatic & Aromatic stretching), 1619 (C=O), 1591 (C=O & C=N), 2261 (C≡N), 3205 (N-H).			
¹H NMR (δ ppm) : 7.50-7.26(m, 8H, Aromatic Protons), 9.24 (b s, 1H, N-H Hydrazone Moiety), 3.73 (q, 2H, CH ₂ –Protons in hydrazone moiety), 2.93(3H, CH ₃ –Protons in acetyl moiety), 0.88 (d, J = 6 Hz, 3H, 3-CH ₃), 3.92 (dd, J ³ _{a,e} = 3 Hz, J ³ _{a,a} = 13 Hz, 1H, H-6a), 2.59 (d, J ³ _{a,a} = 9 Hz, 1H, H-2a), 2.23 (dd, J ³ _{a,e} = 12Hz, J ³ _{a,a} = 12 Hz, 1H, H-5a), 2.92 (dd, J ³ _{a,e} = 3 Hz, J ² _{a,e} = 12 Hz, 1H, H-5e), 2.54 (m, 1H, H-3a Proton).			
¹³C NMR (δ ppm) : 139.98(C-2 ipso carbon), 140.49(C-6 ipso carbon), 129.77-125.70 (Aromatic carbons),164.48 (C=O), 162.28(Ace C=O), 158.05 (C=N), 114.35 (C≡N), 24.16 (CH ₂ carbon of cyanoacetyl hydrazone moiety) , 44.89 (C-2), 56.12 (C-6), 38.52 (C-3), 34.56 (C-5), 11.15 (3-CH ₃),19.20(O=C-CH ₃).			

5.6 SPECTRAL ANALYSIS OF COMPOUNDS N-ACETYL -3-METHYL-2,6 BIS(O-METHYLPHENYL PIPERIDIN -4-ONE CYANOACETYLHYDRAZONE (C4)

5.6.1 IR Spectral Analysis

The IR spectrum of compound (C4) an absorption band appeared at 3066 cm^{-1} is due to N-H stretching frequency. The aromatic and aliphatic C-H stretching vibrations appeared at $3024\text{-}2977\text{ cm}^{-1}$. The absorption frequency is 2261 cm^{-1} is assigned for $\text{C}\equiv\text{N}$. IR bands appeared at 1619 & 1591 are assigned for amide $\text{C}=\text{O}$ and $\text{C}=\text{N}$ stretching frequency. Among them 1716 cm^{-1} is due to $\text{C}=\text{O}$ of hydrazone moiety and 1650 cm^{-1} is observed as broad band due to the merging of stretching $\text{C}=\text{O}$ of piperidine moiety and $\text{C}=\text{N}$ stretching frequency. All the observed IR bands are supported the formation of the synthesized compounds.

All the observed IR bands are supporting evidences for the formation of compounds C4. IR spectral data of the compound C4 are shown in **Table.12**

Table.12 Characteristic IR stretching frequencies (cm^{-1}) of C4

Compound C4	C-H (Aliphatic and Aromatic)	N-H	$\text{C}\equiv\text{N}$	C=O (Hydrazone moiety)	C=N and C=O (Piperidone moiety)
	3024-2977	3066	2261	1716	1650

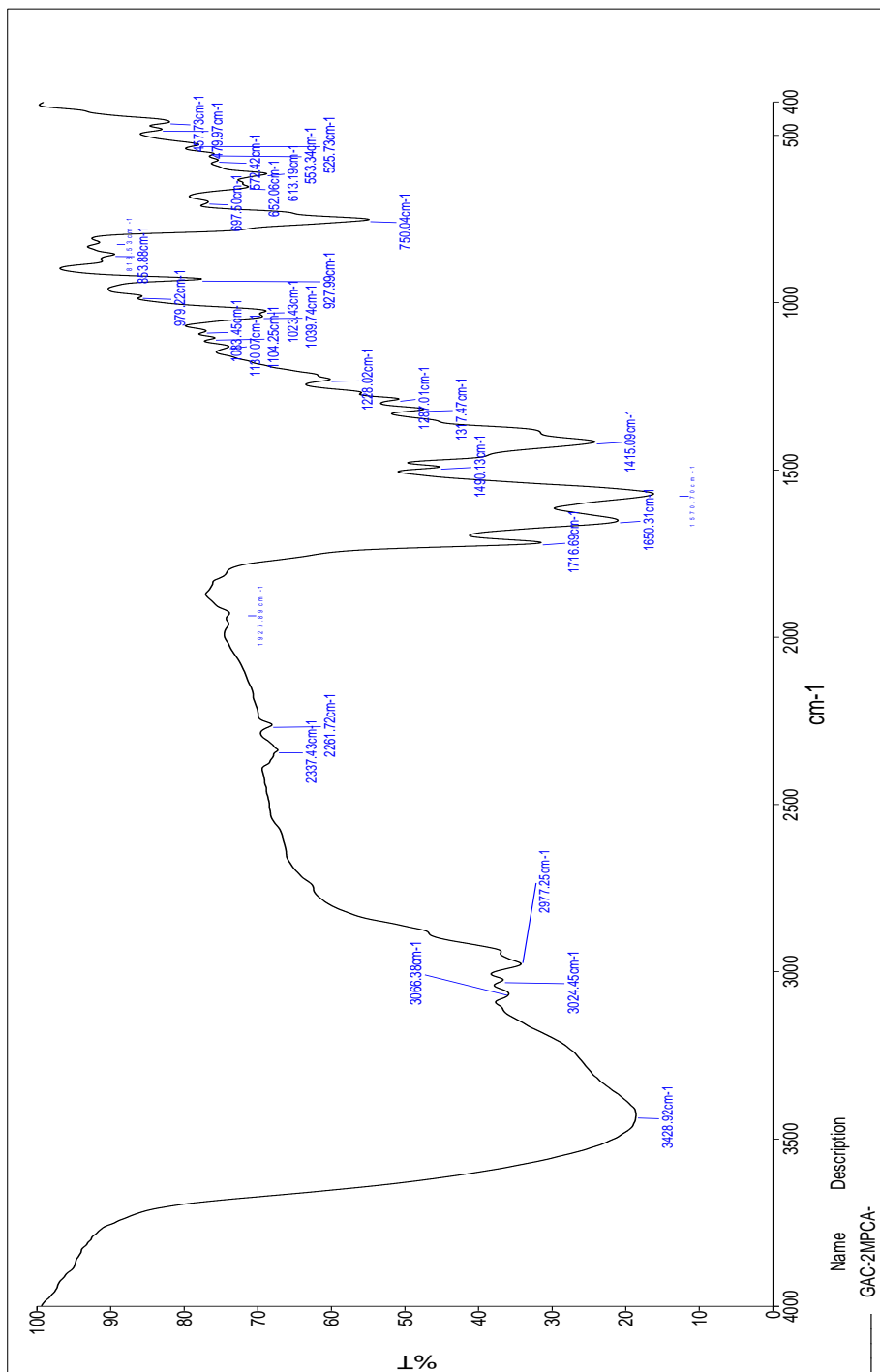


Fig. 16 IR Spectrum of Compound C4

5.6.2 ¹H NMR Spectral analysis

The ¹H NMR spectral signals are assigned by their position, multiplicity and integral values and also comparing with that of parent ketone. In ¹H NMR spectrum (**Fig.17**), the signals appear in the range 7.36-7.14 ppm corresponding to 8 protons are due to the aromatic protons of the two phenyl groups at C-2 and C-6.

There is one broad singlet at downfield region at 9.01 ppm with one proton integral which is assigned to the N-H proton of hydrazone moiety. Moreover, two closely spaced doublets forming an AB quartet around 3.73 ppm correspond to two protons are assigned as the methylene protons of CH₂ protons of cyanoacetyl hydrazone moiety based on their spin-spin coupling constant values and 2.15 ppm CH₃ proton of acetyl moiety. The actual chemical shift values of these diastereotopic germinal protons exhibiting AB spin system of coupling was found out using second order spectral analysis.

In 3-methyl-2,6-diphenylpiperidin-4-one, the CH₃ at C-3 was reported to show its resonance at 0.84 ppm. Hence, a sharp doublet with three protons integral at 0.89 ppm (J = 6.6 Hz) is unambiguously assigned for the CH₃ protons at C-3.

Apart from , there are five signals in between 3.87 and 2.20 ppm, which are due to the ring protons of the piperidine moiety. They are appeared as doublet of doublets at 3.87, 2.83 and 2.20 ppm, doublet at 3.49 ppm and a multiplet at 2.57 ppm with one protons integral each. In 3-methyl -2,6-diphenylpiperidin-4-one, the doublet at 3.63 ppm with coupling constant 10 Hz was assigned for H-2a proton and the double doublet at 4.10 ppm is assigned as H-6a proton. Infact, the doublet at 3.49 ppm with coupling constant 10.2 Hz is ascribed to H-2a proton the double doublet resonance at 3.87 ppm with vicinal coupling constants 12 Hz (J³ diaxial) and 6Hz (J³ axial equatorial) is assigned to H-6a proton.

There are two double doublets at 2.20 ppm with coupling constants 6 Hz (J^3 diaxial) and 12 Hz (J^2 axial equatorial) and 2.83 ppm with coupling constants 6 Hz (J^3 axial equatorial) and 13.5 Hz (J^2 axial equatorial). The geminal coupling constant values suggest that those protons are present at same carbon which is assigned to methylenic protons at C-5. Furthermore, the vicinal coupling constant reveals that the double doublets at 2.20 and 2.90 ppm are due to H-5a and H-5e proton respectively. Consequently, the multiplet resonance at 2.57 ppm is ascribed to H-3a proton.

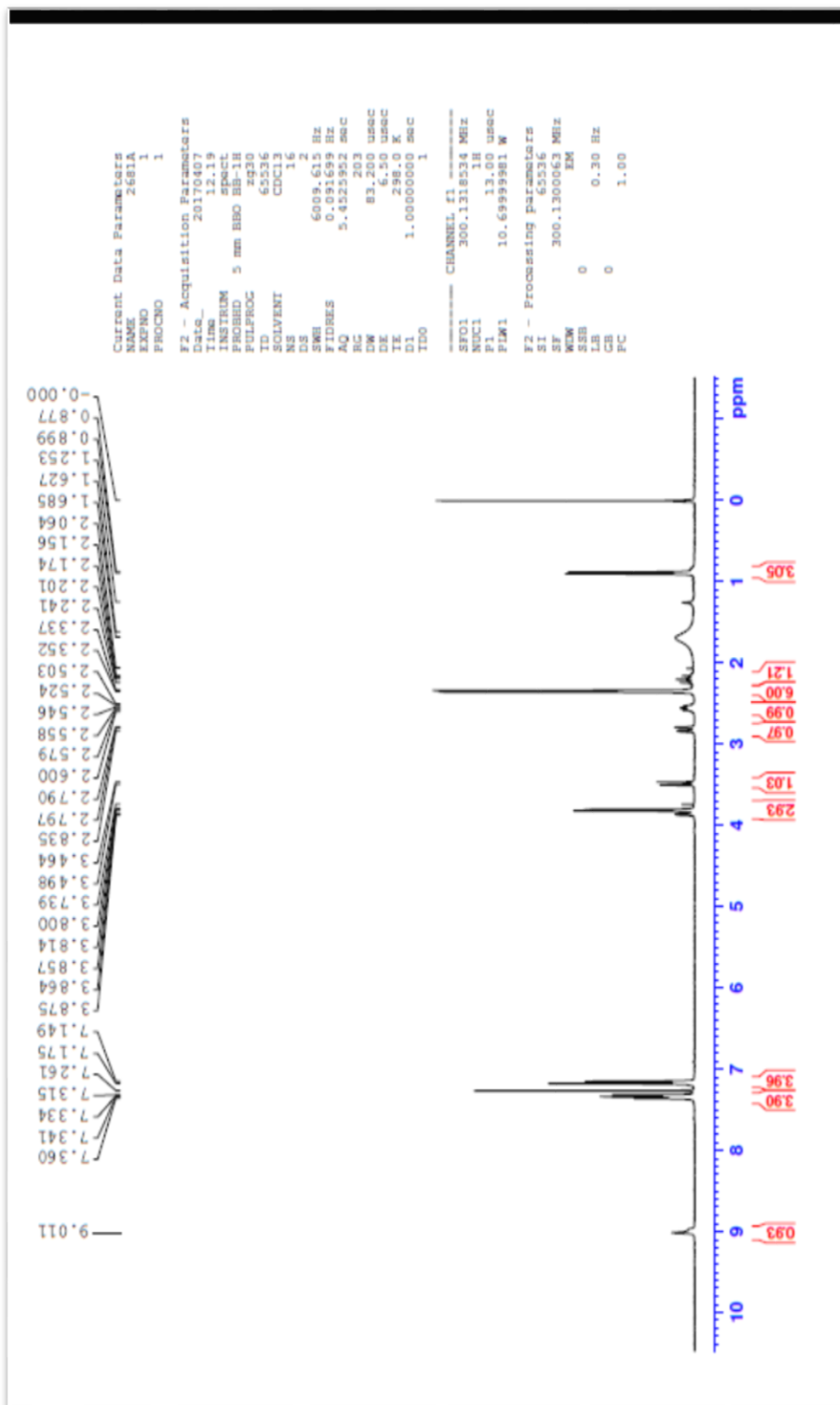


Fig. 17 ¹H NMR Spectrum of compound C4

5.6.3 ¹³C- NMR Spectral analysis

¹³C- NMR spectral assignments have been made based on characteristic signal positions of the functional groups and comparison with those of parent ketones.

¹³C- NMR spectra of the compound C4 depicted in (fig 18). As declared above, the ipso carbons of the phenyl rings could be simply eminent from rest of the ring carbons by their characteristic downfield absorption.

The signals at 139.83 ppm and 139.33 ppm is due to ipso carbons (C-2' and C-6' respectively) of compound C1. The signals at the region 126.26-129.38 ppm are due to other aromatic carbons. There are two less intense signals resonates at 164.94 and 164.87 ppm are characteristic for C=O (hydrazone moiety) and C=O (acetyl moiety). Hence, the signal at 158.07 and 114.13 ppm are characteristic for C=N and C≡N carbons, respectively.

The characteristic signals are appeared in the respective region for 24.56 ppm assigned for the CH₂ carbon for cyanoacetylhydrazone moiety. The 3-CH₃ proton signal appeared at 12.10 ppm and acetyl C-CH₃ resonance at 21.13 ppm.

There are four signals for piperidine ring has the chemical shifts at 68.92, 60.46, 45.34 and 36.14 ppm respectively. Among the four signals the downfield signals at 68.92 and 60.46 ppm assigned to C-2 and C-6 carbons where as the upfield signals at 36.16 and 45.34 ppm is due to C-3 and C-5 carbons. These characteristic signals are well supported our proposed structure.

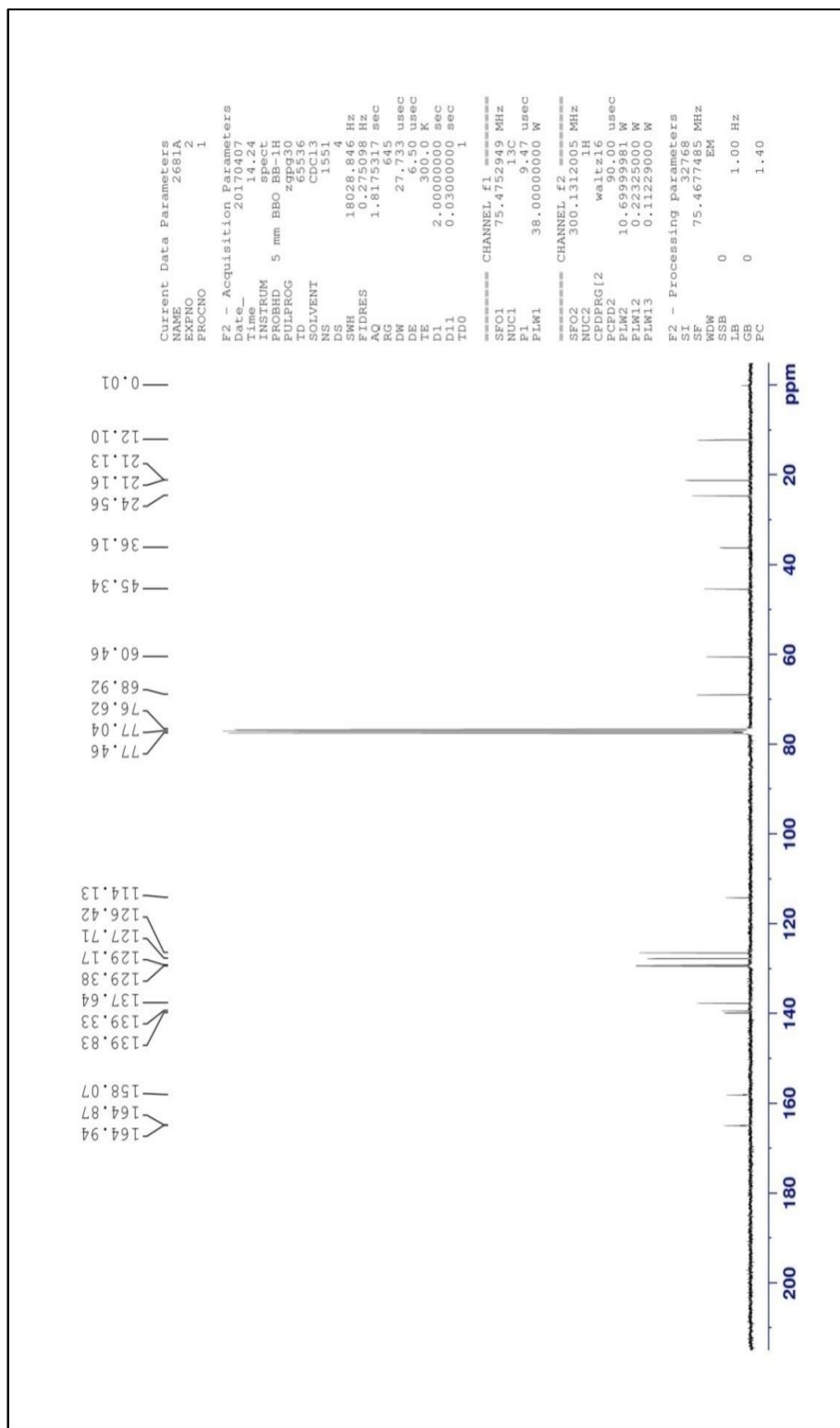
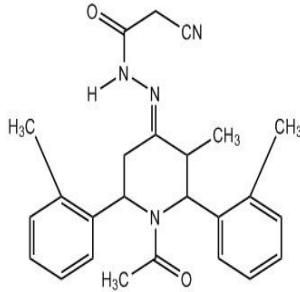


Fig. 18 ¹³C NMR Spectrum of compound C4

Analytical and spectral data of compound C4 is given in **Table.13**

TABLE. 13 ANALYTICAL AND SPECTRAL DATA OF C4

MF: C ₂₅ H ₂₈ N ₄ O ₂	M.Pt. 130-133°C	Yield (%) : 80.69	M.W : 416
IR (cm⁻¹): 3024-2977 (C-H Aliphatic & Aromatic stretching), 1716 (C=O), 1650 (C=O & C=N), 2261 (C≡N), 3066 (N-H).			
¹H NMR (δ ppm) : 7.36-7.14(m, 8H, Aromatic Protons), 9.01 (b s, 1H, N-H Hydrazone Moiety), 3.73 (q, 2H, CH ₂ –Protons in hydrazone moiety), 2.33(3H, CH ₃ –Protons in acetyl moiety), 0.89 (d, J = 6.6 Hz, 3H, 3-CH ₃), 3.87 (dd, J ³ _{a,e} = 6 Hz, J ³ _{a,a} = 12 Hz, 1H, H-6a), 3.49 (d, J ³ _{a,a} = 10.2 Hz, 1H, H-2a), 2.20 (dd, J ³ _{a,e} =13.5 Hz, J ³ _{a,a} = 12 Hz, 1H, H-5a), 2.83 (dd, J ³ _{a,e} = 6 Hz, J ² _{a,e} = 13.5Hz, 1H, H-5e), 2.57 (m, 1H, H-3a Proton).			
¹³C NMR (δ ppm) : 139.33(C-2 ipso carbon), 139.83(C-6 ipso carbon), 126.42-137.64 (Aromatic carbons),164.94 (C=O), 164.87(Ace C=O), 158.07 (C=N), 114.13 (C≡N), 24.56 (CH ₂ carbon of cyanoacetyl hydrazone moiety) , 68.92 (C-2), 60.46 (C-6), 36.16 (C-3), 45.34 (C-5), 12.10 (3-CH ₃),21.13(O=C-CH ₃).			

5.7 SPECTRAL ANALYSIS OF COMPOUNDS N-ACETYL -3-METHYL-2,6 BIS(P-BROMO PHENYL)PIPERIDIN -4-ONE CYANOACETYLHYDRAZONE (C5)

5.7.1 IR Spectral Analysis

The IR spectrum of compound (C5) an absorption band appeared at 3183 cm^{-1} is due to N-H stretching frequency. The aromatic and aliphatic C-H stretching vibrations appeared at $3099\text{-}2862\text{ cm}^{-1}$. The absorption frequency is 1823 cm^{-1} is assigned for $\text{C}\equiv\text{N}$. IR bands appeared at 1823 & 1570 are assigned for amide $\text{C}=\text{O}$ and $\text{C}=\text{N}$ stretching frequency. Among them 1823 cm^{-1} is due to $\text{C}=\text{O}$ of hydrazone moiety and 1570 cm^{-1} is observed as broad band due to the merging of stretching $\text{C}=\text{O}$ of piperidine moiety and $\text{C}=\text{N}$ stretching frequency. All the observed IR bands are supported the formation of the synthesized compounds.

All the observed IR bands are supporting evidences for the formation of compounds C5. IR spectral data of the compound C5 are shown in **Table.14**

Table.14 Characteristic IR stretching frequencies (cm^{-1}) of C5

Compound C5	C-H (Aliphatic and Aromatic)	N-H	$\text{C}\equiv\text{N}$	C=O (Hydrazone moiety)	C=N and C=O (Piperidone moiety)
	3099-2862	3183	1823	1681	1570

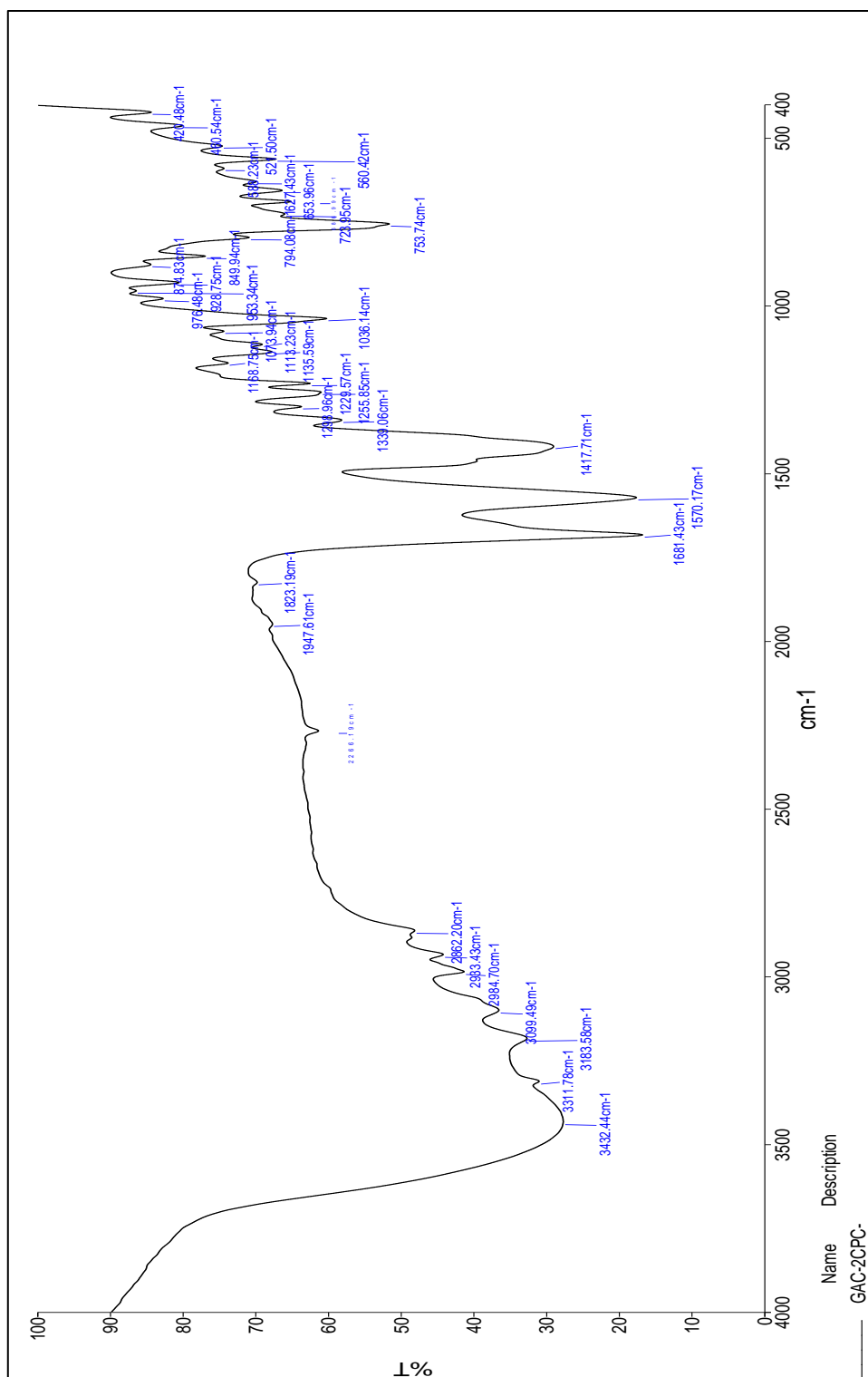


Fig. 19 IR Spectrum of compound C5

5.7.2 ¹H NMR Spectral analysis

The ¹H NMR spectral signals are assigned by their position, multiplicity and integral values and also comparing with that of parent ketone. In ¹H NMR spectrum (**Fig.20**), the signals appear in the range 7.46-7.30 ppm corresponding to 8 protons is due to the aromatic protons of the two phenyl groups at C-2 and C-6.

There is one broad singlet at downfield region at 10.09 ppm with one proton integral which is assigned to the N-H proton of hydrazone moiety. Moreover, two closely spaced doublets forming an AB quartet around 3.73 ppm correspond to two protons are assigned as the methylene protons of CH₂ protons of cyanoacetyl hydrazone moiety based on their spin-spin coupling constant values and 2.15 ppm CH₃ proton of acetyl moiety. The actual chemical shift values of these diastereotopic germinal protons exhibiting AB spin system of coupling was found out using second order spectral analysis.

In 3-methyl-2,6-diphenylpiperidin-4-one, the CH₃ at C-3 was reported to show its resonance at 0.84 ppm. Hence, a sharp doublet with three protons integral at 0.97 ppm (J = 6.6 Hz) is unambiguously assigned for the CH₃ protons at C-3.

Apart from, there are five signals in between 4.40 and 2.24 ppm, which are due to the ring protons of the piperidine moiety. They are appeared as doublet of doublets at 4.40, 3.43 and 2.24 ppm, doublet at 4.06 ppm and a multiplet at 2.70 ppm with one protons integral each. In 3-methyl-2,6-diphenylpiperidin-4-one, the doublet at 3.63 ppm with coupling constant 10 Hz was assigned for H-2a proton and the double doublet at 4.10 ppm is assigned as H-6a proton. Infact, the doublet at 4.06 ppm with coupling constant 10.2 Hz is ascribed to H-2a proton the double doublet resonance at 4.40 ppm with vicinal coupling constants 11.7 Hz (J³ diaxial) and 2.7 Hz (J³ axial equatorial) is assigned to H-6a proton.

There are two double doublets at 2.24 ppm with coupling constants 11.7 Hz (J^3 diaxial) and 13.8 Hz (J^2 axial equatorial) and 3.43 ppm with coupling constants 2.7 Hz (J^3 axial equatorial) and 14.1 Hz (J^2 axial equatorial). The geminal coupling constant values suggest that those protons are present at same carbon which is assigned to methylenic protons at C-5. Furthermore, the vicinal coupling constant reveals that the double doublets at 2.24 and 2.43 ppm are due to H-5a and H-5e proton respectively. Consequently, the multiplet resonance at 2.70 ppm is ascribed to H-3a proton.

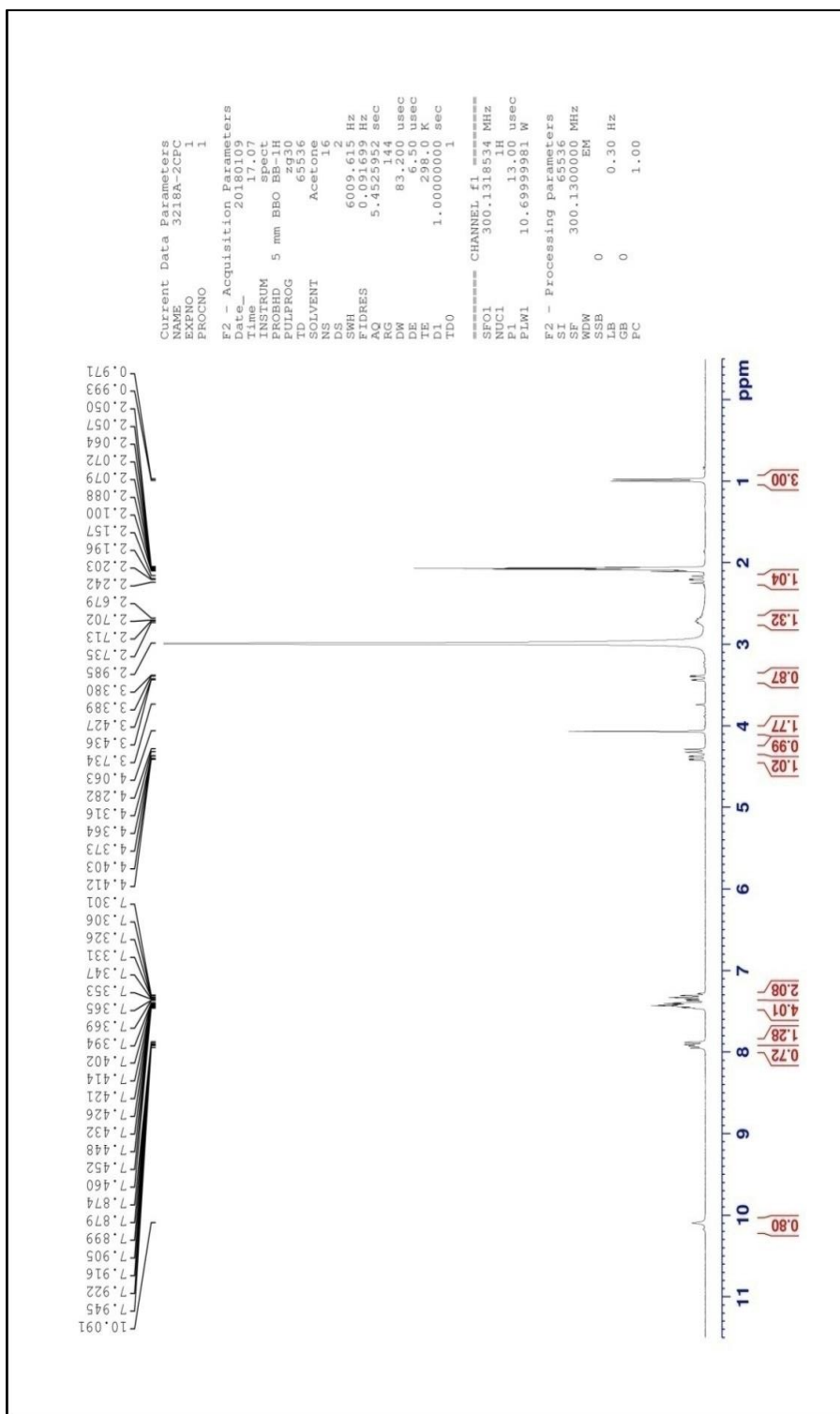


Fig. 20 ¹H NMR Spectrum of compound C5

5.7.3 ¹³C- NMR Spectral analysis

¹³C- NMR spectral assignments have been made based on characteristic signal positions of the functional groups and comparison with those of parent ketones.

¹³C- NMR spectra of the compound C5 depicted in (fig 21). As declared above, the ipso carbons of the phenyl rings could be simply eminent from rest of the ring carbons by their characteristic downfield absorption.

The signals at 140.37 ppm and 140.67 ppm is due to ipso carbons (C-2' and C-6' respectively) of compound C1. The signals at the region 127.51– 129.27 ppm are due to other aromatic carbons. There are two less intense signals resonates at 205.57 and 165.09 ppm are characteristic for C=O (hydrazone moiety) and C=O (acetyl moiety). Hence, the signal at 154.98 and 115.08 ppm are characteristic for C=N and C≡N carbons, respectively.

The characteristic signals are appeared in the respective region for 28.21 ppm assigned for the CH₂ carbon for cyanoacetylhydrazone moiety. The 3-CH₃ proton signal appeared at 11.14 ppm and acetyl C-CH₃ resonance at 24.17 ppm.

There are four signals for piperidine ring has the chemical shifts at 63.31, 56.55, 45.29 and 34.00 ppm respectively. Among the four signals the downfield signals at 56.55 and 63.31 ppm assigned to C-2 and C-6 carbons where as the upfield signals at 34.00 and 45.29 ppm is due to C-3 and C-5 carbons. These characteristic signals are well supported our proposed structure.

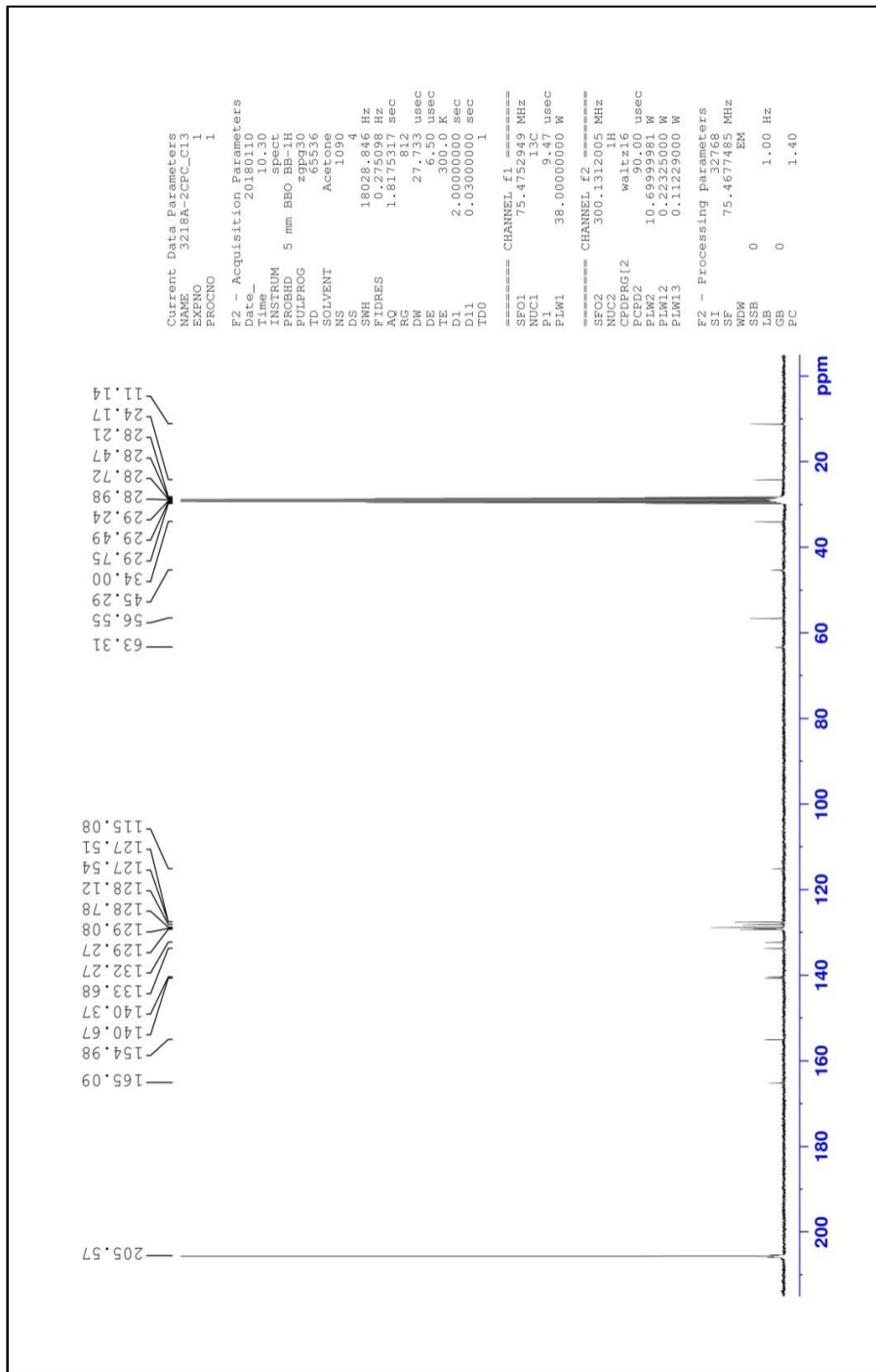
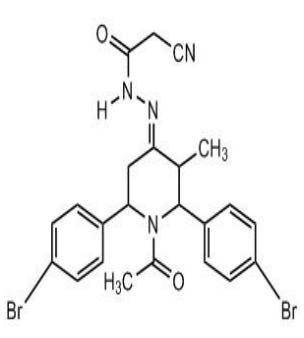


Fig. 21 ¹³C NMR Spectrum of compound C5

Analytical and spectral data of compound C5 is given in **Table.15**

TABLE. 15 ANALYTICAL AND SPECTRAL DATA OF C5

MF: C ₂₃ H ₂₀ Br ₂ N ₄ O ₂	M.Pt. 186-189°C	Yield (%) : 78.86	M.W : 544
IR (cm⁻¹): 3099-2862 (C-H Aliphatic & Aromatic stretching), 1681 (C=O), 1570 (C=O&C=N), 1823 (C≡N), 3183 (N-H).			
¹H NMR (δ ppm) : 7.49-7.26(m, 8H, Aromatic Protons), 10.09 (b s, 1H, N-H Hydrazone Moiety), 3.73 (q, 2H, CH ₂ –Protons in hydrazone moiety), 2.98(3H, CH ₃ –Protons in acetyl moiety), 0.97 (d, J = 6.6Hz, 3H, 3-CH ₃), 4.40 (dd, J ^{3_{a,e}} = 2.7Hz, J ^{3_{a,a}} = 11.7Hz, 1H, H-6a), 4.06 (d, J ^{3_{a,a}} = 10.2Hz, 1H, H-2a), 2.24 (dd, J ^{3_{a,e}} = 13.8Hz, J ^{3_{a,a}} = 11.7 Hz, 1H, H-5a), 3.43 (dd, J ^{3_{a,e}} = 2.7 Hz, J ^{2_{a,e}} = 14.1Hz, 1H, H-5e), 2.70 (m, 1H, H-3a Proton).			
¹³C NMR (δ ppm) : 140.37(C-2 ipso carbon), 140.67(C-6 ipso carbon), 129.27-127.51 (Aromatic carbons),205.57 (C=O), 165.09(Ace C=O), 154.98 (C=N), 115.08 (C≡N), 28.21 (CH ₂ carbon of cyanoacetyl hydrazone moiety) , 56.55 (C-2), 63.31 (C-6), 34.00 (C-3), 45.29 (C-5), 11.14 (3-CH ₃) 24.17(O=C-CH ₃).			

5.8 SPECTRAL ANALYSIS OF COMPOUNDS N-ACETYL -3-METHYL-2,6 BIS(P-CHLOROPHENYL)PIPERIDIN -4-ONE CYANOACETYLHYDRAZONE (C6)

5.8.1 IR Spectral Analysis

The IR spectrum of compound (C6) an absorption band appeared at 3286 cm^{-1} is due to N-H stretching frequency. The aromatic and aliphatic C-H stretching vibrations appeared at $2980\text{-}2937\text{ cm}^{-1}$. The absorption frequency is 2261 cm^{-1} is assigned for $\text{C}\equiv\text{N}$. IR bands appeared at 1716 & 1642 are assigned for amide $\text{C}=\text{O}$ and $\text{C}=\text{N}$ stretching frequency. Among them 1716 cm^{-1} is due to $\text{C}=\text{O}$ of hydrazone moiety and 1642 cm^{-1} is observed as broad band due to the merging of stretching $\text{C}=\text{O}$ of piperidine moiety and $\text{C}=\text{N}$ stretching frequency. All the observed IR bands are supported the formation of the synthesized compounds.

All the observed IR bands are supporting evidences for the formation of compounds C6. IR spectral data of the compound C6 are shown in **Table.16**

Table.16 Characteristic IR stretching frequencies (cm^{-1}) of C6

Compound C6	C-H (Aliphatic and Aromatic)	N-H	$\text{C}\equiv\text{N}$	C=O (Hydrazone moiety)	C=N and C=O (Piperidone moiety)
	2980-2937	3286	2261	1716	1642

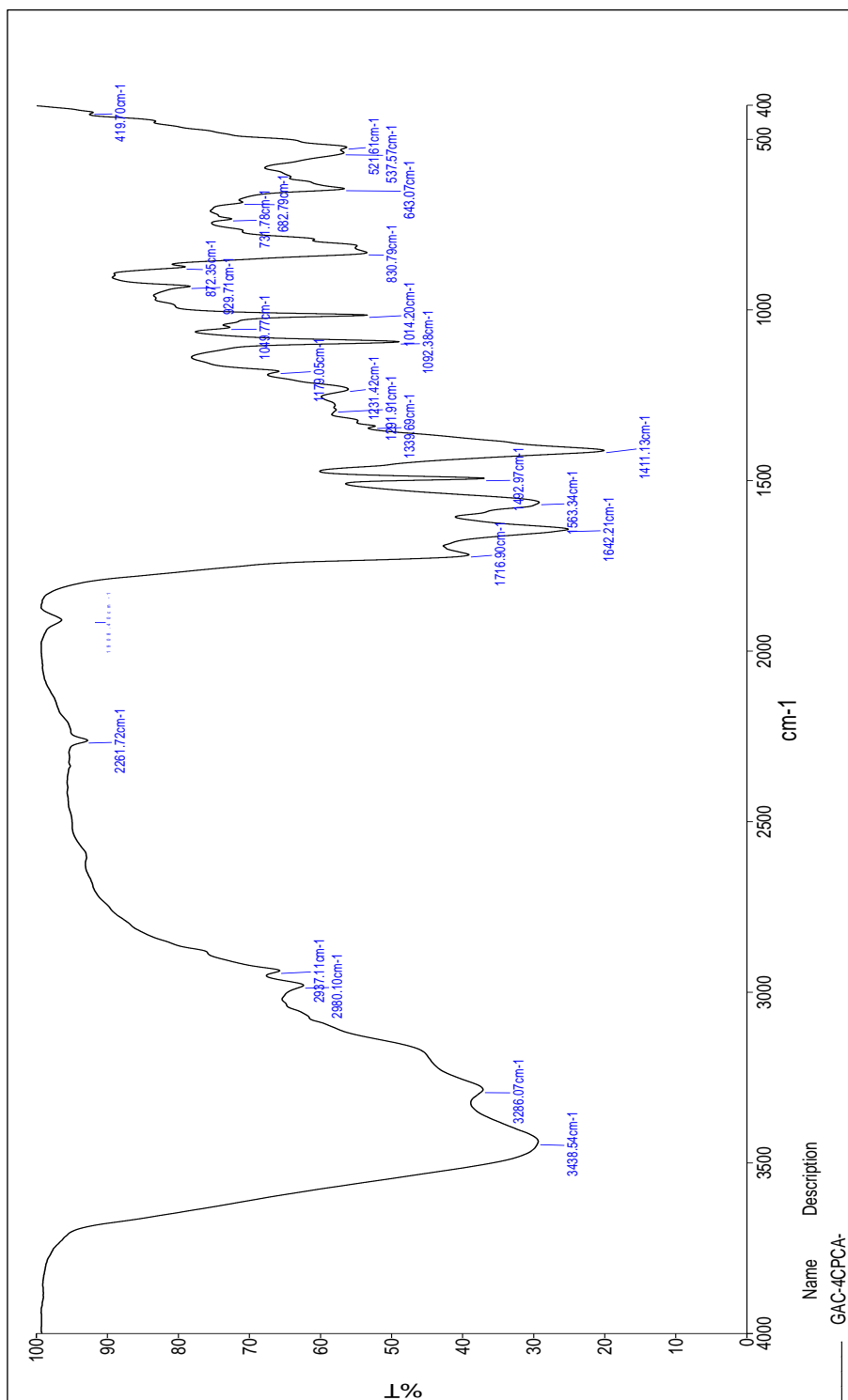


Fig. 22 IR Spectrum of compound C6

5.8.2 ¹H NMR Spectral analysis

The introduction of hydrazone group at the 4th position of 1-heterocyclic ketones is reported to exert a major change in chemical shifts of its acetyl group and their associated protons. ¹H NMR chemical shift values (δ , ppm) numbering of compound C1 is given in **Fig.6**.

The ¹H NMR spectral signals are assigned by their position, multiplicity and integral values and also comparing with that of parent ketone. In ¹H NMR spectrum (**Fig.23**), the signals appear in the range 7.51-7.26 ppm corresponding to 8 protons is due to the aromatic protons of the two phenyl groups at C-2 and C-6.

There is one broad singlet at downfield region at 9.83 ppm with one proton integral which is assigned to the N-H proton of hydrazone moiety. Moreover, two closely spaced doublets forming an AB quartet around 3.71 ppm correspond to two protons are assigned as the methylene protons of CH₂ protons of cyanoacetyl hydrazone moiety based on their spin-spin coupling constant values and 2.15 ppm CH₃ proton of acetyl moiety. The actual chemical shift values of these diastereotopic germinal protons exhibiting AB spin system of coupling was found out using second order spectral analysis.

In 3-methyl-2,6-diphenylpiperidin-4-one, the CH₃ at C-3 was reported to show its resonance at 0.84 ppm. Hence, a sharp doublet with three protons integral at 0.89 ppm ($J = 6$ Hz) is unambiguously assigned for the CH₃ protons at C-3.

Apart from, there are five signals in between 3.91 and 2.18 ppm, which are due to the ring protons of the piperidine moiety. They are appeared as doublet of doublets at 3.91, 2.98 and 2.18 ppm, doublet at 3.51 ppm and a multiplet at 2.53 ppm with one protons integral each. In 3-methyl-2,6-diphenylpiperidin-4-one, the doublet at 3.63 ppm with coupling

constant 10 Hz was assigned for H-2a proton and the double doublet at 4.10 ppm is assigned as H-6a proton. Infact, the doublet at 3.51 ppm with coupling constant 9.9 Hz is ascribed to H-2a proton the double doublet resonance at 3.91 ppm with vicinal coupling constants 10.8 Hz (J^3 diaxial) and 2.1 Hz (J^3 axial equatorial) is assigned to H-6a proton.

There are two double doublets at 2.18 ppm with coupling constants 12 Hz (J^3 diaxial) and 13.8 Hz (J^2 axial equatorial) and 2.98 ppm with coupling constants 2.4 Hz (J^3 axial equatorial) and 13.8 Hz (J^2 axial equatorial). The geminal coupling constant values suggest that those protons are present at same carbon which is assigned to methylenic protons at C-5. Furthermore, the vicinal coupling constant reveals that the double doublets at 2.18 and 2.98 ppm are due to H-5a and H-5e proton respectively. Consequently, the multiplet resonance at 2.53 ppm is ascribed to H-3a proton.

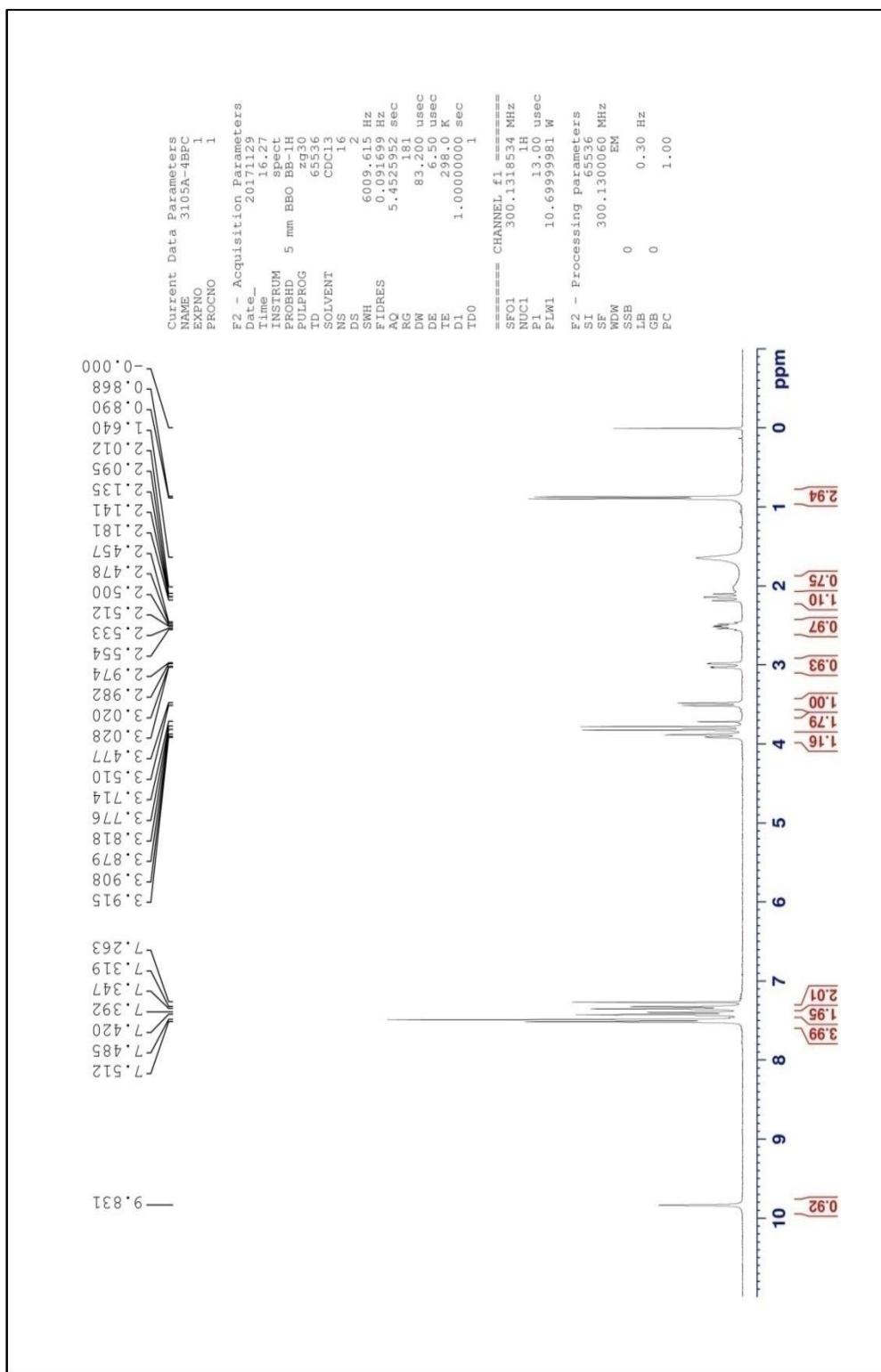


Fig. 23 ¹H NMR Spectrum of compound C6

5.8.3 ¹³C- NMR Spectral analysis

¹³C- NMR spectral assignments have been made based on characteristic signal positions of the functional groups and comparison with those of parent ketones.

¹³C- NMR spectra of the compound C6 depicted in (fig 24). As declared above, the ipso carbons of the phenyl rings could be simply eminent from rest of the ring carbons by their characteristic downfield absorption.

The signals at 130.75 ppm and 140.78 ppm is due to ipso carbons (C-2' and C-6' respectively) of compound C6. The signals at the region 120.55-130.75 ppm are due to other aromatic carbons. There are two less intense signals resonates at 164.36 and 155.48 ppm are characteristic for C=O (hydrazone moiety) and C=O (acetyl moiety). Hence, the signal at 141.63 and 114.18 ppm are characteristic for C=N and C≡N carbons, respectively.

The characteristic signals are appeared in the respective region for 35.72 ppm assigned for the CH₂ carbon for cyanoacetylhydrazone moiety. The 3-CH₃ proton signal appeared at 11.31 ppm and acetyl C-CH₃ resonance at 23.96 ppm.

There are four signals for piperidine ring has the chemical shifts at 67.56, 58.98, 44.27 and 40.08 ppm respectively. Among the four signals the downfield signals at 58.98 and 67.56 ppm assigned to C-2 and C-6 carbons where as the upfield signals at 44.27 and 40.08 ppm is due to C-3 and C-5 carbons. These characteristic signals are well supported our proposed structure.

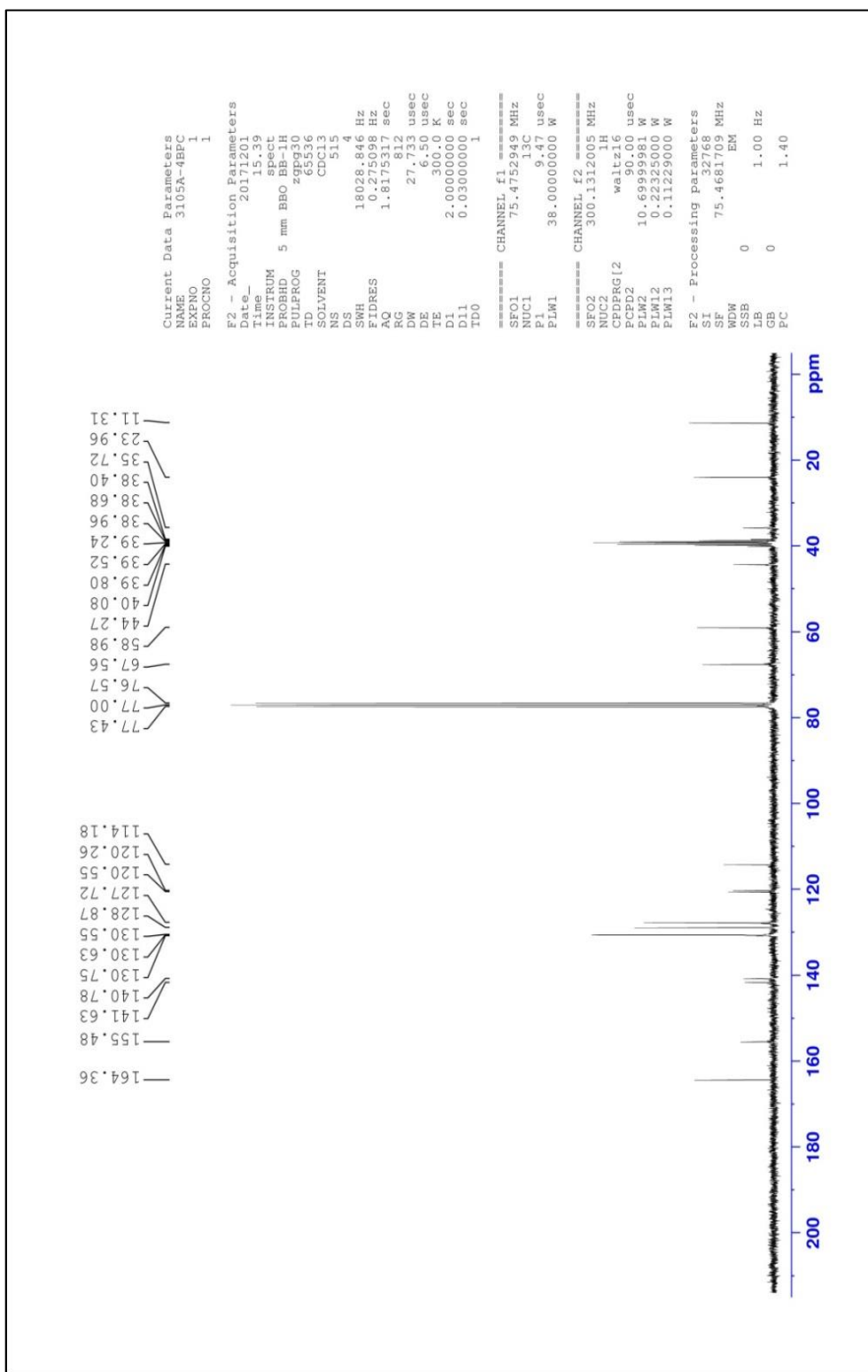
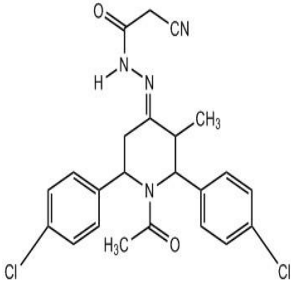


Fig. 24 ¹³C NMR Spectrum of compound C6

Analytical and spectral data of compound C6 is given in **Table.17**

TABLE. 17 ANALYTICAL AND SPECTRAL DATA OF C6

MF: C ₂₃ H ₂₀ Cl ₂ N ₄ O ₂	M.Pt. 148-151°C	Yield (%) : 80.56	M.W : 454
IR (cm⁻¹): 2937-2980 (C-H Aliphatic & Aromatic stretching), 1716 (C=O), 1642 (C=O&C=N), 2261 (C≡N), 3286 (N-H).			
¹H NMR (δ ppm) : 7.51-7.26(m, 8H, Aromatic Protons), 9.83 (b s, 1H, N-H Hydrazone Moiety), 3.71 (q, 2H, CH ₂ –Protons in hydrazone moiety), 3.77(3H, CH ₃ –Protons in acetyl moiety), 0.89 (d, J = 6 Hz, 3H, 3-CH ₃), 3.91 (dd, J ³ _{a,e} = 2.1Hz, J ³ _{a,a} = 10.8 Hz, 1H, H-6a), 3.51 (d, J ³ _{a,a} = 9.9 Hz, 1H, H-2a), 2.18 (dd, J ³ _{a,e} = 13Hz, J ³ _{a,a} = 12 Hz, 1H, H-5a), 2.92 (dd, J ³ _{a,e} = 2.4 Hz, J ² _{a,e} = 13.8Hz, 1H, H-5e), 2.51 (m, 1H, H-3a Proton).			
¹³C NMR (δ ppm) : 130.75(C-2 ipso carbon), 140.78(C-6 ipso carbon), 120.26-130.63 (Aromatic carbons),164.36 (C=O), 155.48(Ace C=O), 141.63 (C=N), 114.29 (C≡N), 35.72 (CH ₂ carbon of cyanoacetyl hydrazone moiety) , 58.98 (C-2), 67.56 (C-6), 44.27 (C-3), 40.08 (C-5), 11.31 (3-CH ₃),23.96(O=C-CH ₃).			

5.9 SPECTRAL ANALYSIS OF COMPOUNDS N-ACETYL -3-METHYL-2,6 BIS(P-CHLOROPHENYL)PIPERIDIN -4-ONE CYANOACETYLHYDRAZONE (C7)

5.9.1 IR Spectral Analysis

The IR spectrum of compound (C7) an absorption band appeared at 3184 cm^{-1} is due to N-H stretching frequency. The aromatic and aliphatic C-H stretching vibrations appeared at $3098\text{-}2936\text{ cm}^{-1}$. The absorption frequency is 2267 cm^{-1} is assigned for $\text{C}\equiv\text{N}$. IR bands appeared at 1674 & 1568 are assigned for amide C=O and C=N stretching frequency. Among them 1674 cm^{-1} is due to C=O of hydrazone moiety and 1568 cm^{-1} is observed as broad band due to the merging of stretching C=O of piperidine moiety and C=N stretching frequency. All the observed IR bands are supported the formation of the synthesized compounds.

All the observed IR bands are supporting evidences for the formation of compounds C7. IR spectral data of the compound C7 are shown in **Table.18**

Table.18 Characteristic IR stretching frequencies (cm^{-1}) of C7

Compound C1	C-H (Aliphatic and Aromatic)	N-H	$\text{C}\equiv\text{N}$	C=O (Hydrazone moiety)	C=N and C=O (Piperidone moiety)
	3098-2936	3184	2267	1674	1568

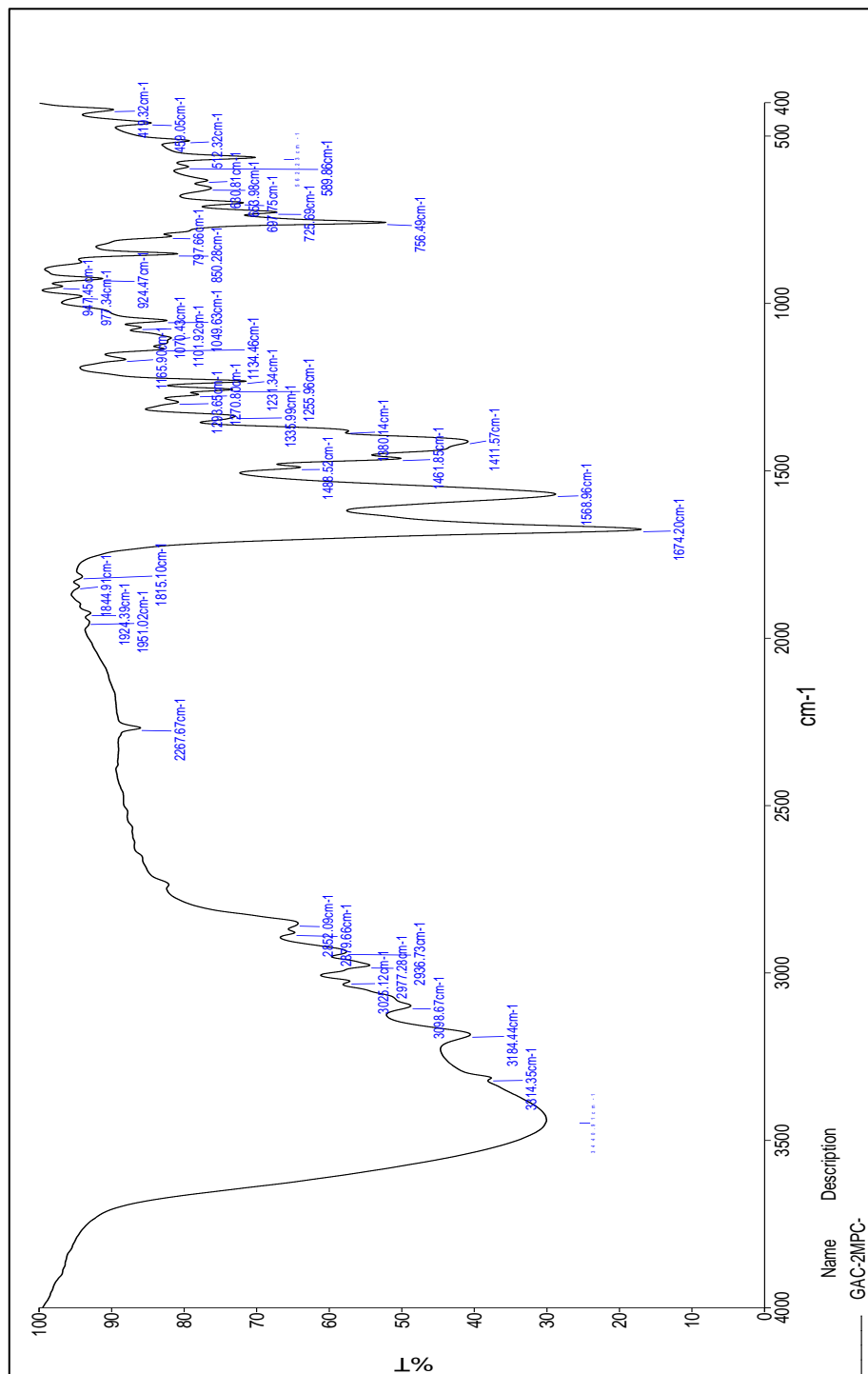


Fig. 25 IR Spectrum of compound C7

5.9.2 ¹H NMR Spectral analysis

The ¹H NMR spectral signals are assigned by their position, multiplicity and integral values and also comparing with that of parent ketone. In ¹H NMR spectrum (**Fig.26**), the signals appear in the range 7.36-7.26 ppm corresponding to 10 protons are due to the aromatic protons of the two phenyl groups at C-2 and C-6.

There is one broad singlet at downfield region at 9.24 ppm with one proton integral which is assigned to the N-H proton of hydrazone moiety. Moreover, two closely spaced doublets forming an AB quartet around 3.79 ppm correspond to two protons are assigned as the methylene protons of CH₂ protons of cyanoacetyl hydrazone moiety based on their spin-spin coupling constant values and 2.15 ppm CH₃ proton of acetyl moiety. The actual chemical shift values of these diastereotopic germinal protons exhibiting AB spin system of coupling was found out using second order spectral analysis.

In 3-methyl-2,6-diphenylpiperidin-4-one, the CH₃ at C-3 was reported to show its resonance at 0.84 ppm. Hence, a sharp doublet with three protons integral at 0.89 ppm (J = 6.3 Hz) is unambiguously assigned for the CH₃ protons at C-3.

Apart from , there are five signals in between 3.91 and 2.23 ppm, which are due to the ring protons of the piperidine moiety. They are appeared as doublet of doublets at 3.92, 2.88 and 2.23 ppm, doublet at 3.54 ppm and a multiplet at 2.57 ppm with one protons integral each. In 3-methyl-2,6-diphenylpiperidin-4-one, the doublet at 3.63 ppm with coupling constant 10 Hz was assigned for H-2a proton and the double doublet at 4.10 ppm is assigned as H-6a proton. Infact, the doublet at 3.54 ppm with coupling constant 9.9 Hz is ascribed to H-2a proton the double doublet resonance at 3.92 ppm with vicinal coupling constants 11.4 Hz (J³ diaxial) and 3.3 Hz (J³ axial equatorial) is assigned to H-6a proton.

There are two double doublets at 2.23 ppm with coupling constants 11.7 Hz (J^3 diaxial) and 13.8 Hz (J^2 axial equatorial) and 2.88 ppm with coupling constants 2.7 Hz (J^3 axial equatorial) and 13.8 Hz (J^2 axial equatorial). The geminal coupling constant values suggest that those protons are present at same carbon which is assigned to methylenic protons at C-5. Furthermore, the vicinal coupling constant reveals that the double doublets at 2.23 and 2.88 ppm are due to H-5a and H-5e proton respectively. Consequently, the multiplet resonance at 2.57 ppm is ascribed to H-3a proton.

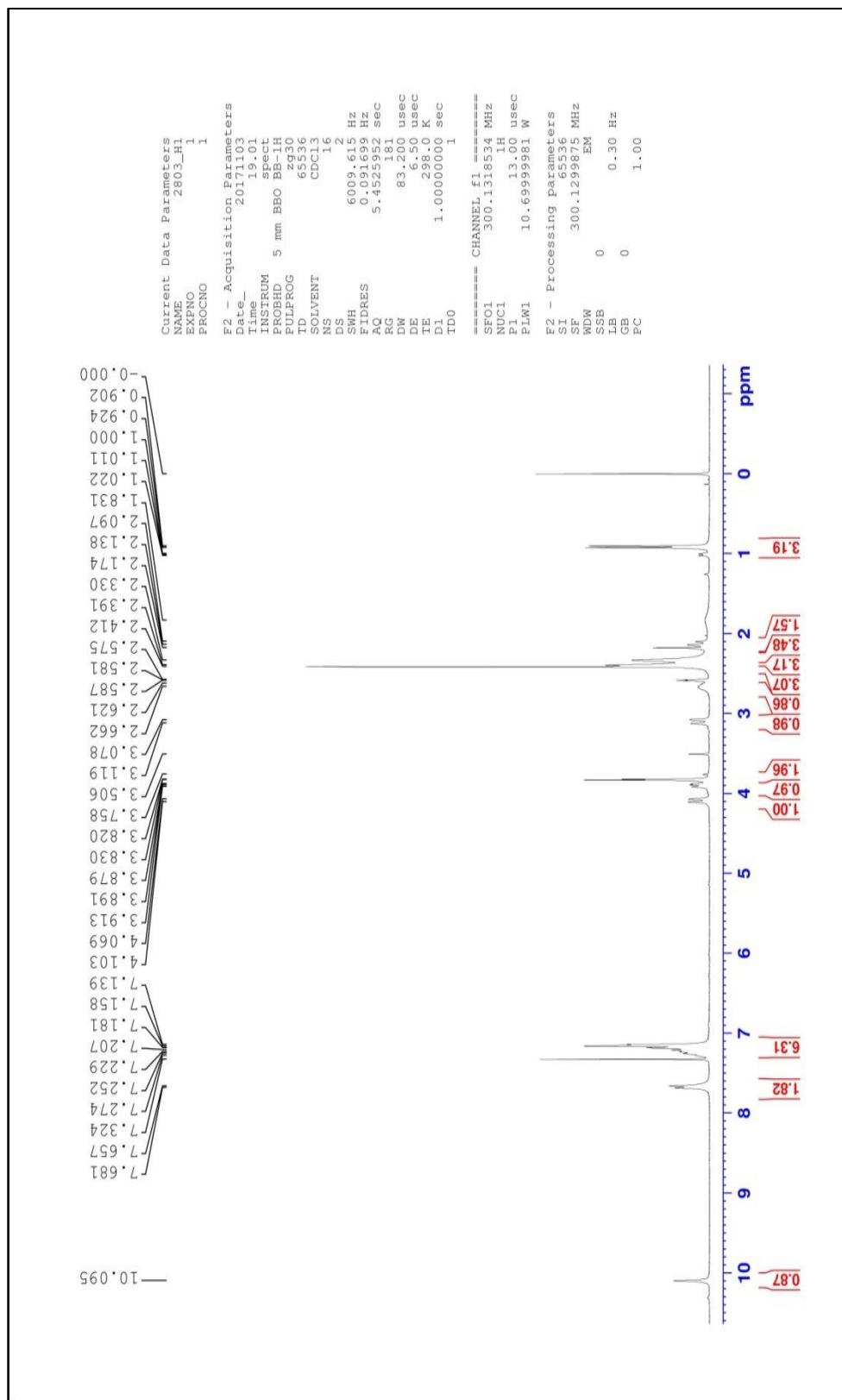


Fig. 26 ¹H NMR Spectrum of compound C7

5.9.3 ¹³C- NMR Spectral analysis

¹³C- NMR spectral assignment has been made based on characteristic signal positions of the functional groups and comparison with those of parent ketones.

¹³C- NMR spectra of the compound C7 depicted in (fig 27). As declared above, the ipso carbons of the phenyl rings could be simply eminent from rest of the ring carbons by their characteristic downfield absorption.

The signals at 140.90 ppm and 140.84 ppm is due to ipso carbons (C-2' and C-6' respectively) of compound C7. The signals at the region 126.75-131.45 ppm are due to other aromatic carbons. There are two less intense signals resonates at 210.30 and 174.24 ppm are characteristic for C=O (hydrazone moiety) and C=O (acetyl moiety). Hence, the signal at 172.49 and 126.22 ppm are characteristic for C=N and C≡N carbons, respectively.

The characteristic signals are appeared in the respective region for 156.34 and 114.29 ppm assigned for the CH₂ carbon for cyanoacetylhydrazone moiety. The 3-CH₃ proton signal appeared at 11.52 ppm and acetyl C-CH₃ resonance at 24.08 ppm.

There are four signals for piperidine ring has the chemical shifts at 68.48, 59.95, 50.04 and 40.18 ppm respectively. Among the four signals the downfield signals at 59.95 and 68.48 ppm assigned to C-2 and C-6 carbons where as the upfield signals at 50.04 and 44.29 ppm is due to C-3 and C-5 carbons. These characteristic signals are well supported our proposed structure.

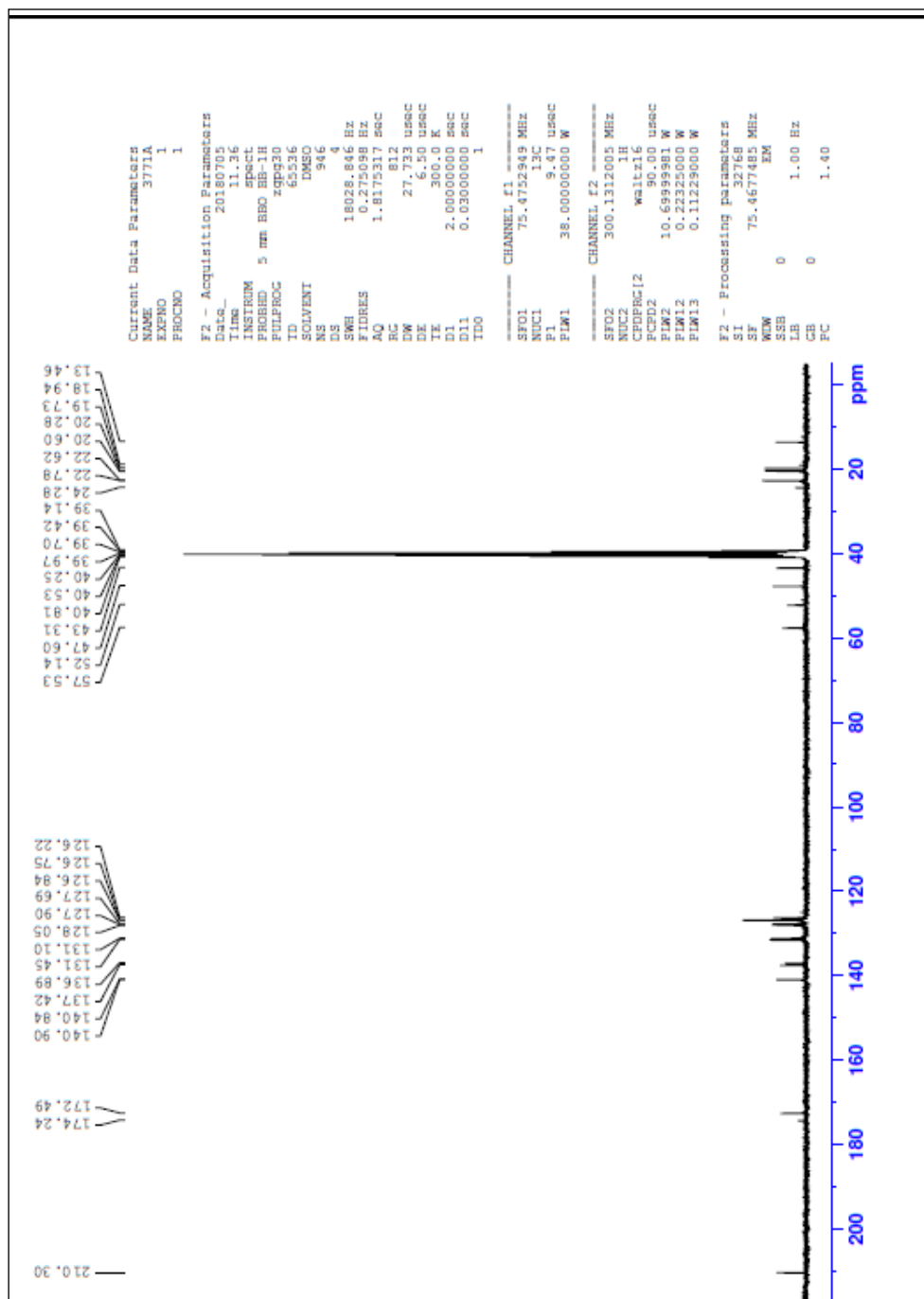


Fig. 27 ¹³C NMR Spectrum of compound C7

Analytical and spectral data of compound C7 is given in **Table.19**

TABLE.19 ANALYTICAL AND SPECTRAL DATA OF C7

MF: C ₂₅ H ₂₈ N ₄ O ₂	M.Pt. 139-141°C	Yield (%) : 80.56	M.W : 416
<p>IR (cm⁻¹): 3098-2936 (C-H Aliphatic & Aromatic stretching), 1674 (C=O), 1568 (C=O&C=N), 2267 (C≡N), 3184 (N-H).</p>			
<p>¹H NMR (δ ppm) : 7.32-7.13 (m, 8H, Aromatic Protons), 10.09 (b s, 1H, N-H, Hydrazone Moiety), 2.09 (b s, 1H, N-H Piperidin moiety), 3.50 (q, 2H, CH₂ –Protons in hydrazone moiety), 0.92 (d, J = 6Hz, 3H, 3-CH₃), 3.89 (dd, J³_{a,e} = 3Hz, J³_{a,a} = 10.2Hz, 1H, H-6a), 3.11 (d, J³_{a,a} = 10.2Hz, 1H, H-2a), 2.39 (dd, J³_{a,e} = 11.4Hz, J³_{a,a} = 11.7 Hz, 1H, H-5a), 3.07(dd, J³_{a,e} = 2.1 Hz, J²_{a,e} = 12Hz, 1H, H-5e), 2.57 (m, 1H, H-3a Proton), 2.33 (s, 3H, p-CH₃ protons).</p>			
<p>¹³C NMR (δ ppm) : 127.93(C-2 ipso carbon), 141.99(C-6 ipso carbon), 127.82-125.90 (Aromatic carbons),210.30 (C=O), 174.24(Ace C=O), 172.49 (C=N), 126.22 (C≡N), 39.14 (CH₂ carbon of cyanoacetyl hydrazone moiety) , 57.53 (C-2), 52.14 (C-6), 47.60 (C-3), 43.31 (C-5), 13.46 (3-CH₃)20.28(O=C-CH₃).</p>			

5.10 ANTI-OBESITY ACTIVITY

5.10.1 Pancreatic lipase inhibitory activity

In the current scenario, obesity is a major public health problem with approximately 1.9 billion adults (aged 18 years and older) worldwide and approximately 600 million of them are clinically obese. The disease is characterized by an increase in the size of the adipocytes, which leads to an increase in the amount of fat in the disease of adiposita. Microbes such as germline are cured in order to increase the adipocytes. Thus, inhibition of digestion and absorption of dietary fat is a first key to treating obesity. This inhibition involve lipase enzyme, the principle lipolytic enzyme synthezied and secreted by the pancreas. There is an increase in the amount of damage to the testes. The substrates for the lipase enzyme are long-chain triacylglycerols, which are separated from the surface phase by the aqueous medium. Thus, the lipase enzyme must be adsorbed on the substrate lipid surface and the nature of the substrate surface has an important role for lipase activity.

Inhibition of pancreatic lipase is an attractive targeted approach for the discovery of potent anti-obesity agents for the treatment of obesity. One of the screening strategies used in anti-obesity drug discovery is to search for potent lipase inhibitors from synthesized compounds. In this study, we screened synthesized compounds as potential anti-obesity agents by monitoring their anti-lipase activity. Concentration – dependently on the *invitro* assay.

The activity of the compounds was determined by comparison with the anti-obesity of pancreatic lipase. The test compound was measured for the decrease in clot weight at different concentrations. The different concentrations compared about orlistat as standard drug [2,3].

5.10.2 Invitro anti-obesity activity

The invitro Anti-obesity activity of the compound was investigated through pancreatic lipase inhibitory activity. The inhibitory activities of synthesized compounds are reported in **Table 20**. The synthesized compounds were comparable with standard obesity drug Orlistat. The compounds showed inhibitory effect on through pancreatic lipase with varying degrees of inhibition. Among the various concentrations (100 µg/ml, 200 µg/ml, 300 µg/ml, 400 µg/ml, 500 µg/ml) of synthesized compounds, the highest doses (500 µg/ml) of all synthesized compounds have greatest inhibition (lipase) activity.

Anti-obesity activity analysis of compound C1 was 14.25 ± 0.99 for 100 µg/mL, 23.56 ± 1.64 for 200 µg/mL, 39.69 ± 2.77 for 300 µg/mL, 60.81 ± 4.25 for 400 µg/mL, 76.45 ± 5.35 for 500 µg/mL for Lipase activity. The IC_{50} value is 343.49.

Anti-obesity activity analysis of compound C2 was 18.07 ± 1.26 for 100 µg/mL, 30.62 ± 2.14 for 200 µg/mL, 49.81 ± 3.48 for 300 µg/mL, 71.68 ± 5.01 for 400 µg/mL, 85.93 ± 6.01 for 500 µg/mL for Lipase activity. The IC_{50} value is 293.05.

Anti-obesity activity analysis of compound C3 was 19.54 ± 1.36 for 100 µg/mL, 33.29 ± 2.33 for 200 µg/mL, 51.65 ± 3.61 for 300 µg/mL, 72.43 ± 5.07 for 400 µg/mL, 87.45 ± 6.12 for 500 µg/mL for Lipase activity. The IC_{50} value is 283.52.

Anti-obesity activity analysis of compound C4 was 15.79 ± 1.10 for 100 µg/mL, 27.43 ± 1.92 for 200 µg/mL, 43.54 ± 3.04 for 300 µg/mL, 65.91 ± 4.61 for 400 µg/mL, 80.45 ± 5.63 for 500 µg/mL for Lipase activity. The IC_{50} value is 320.11.

Anti-obesity activity analysis of compound C5 was 16.94 ± 1.18 for 100 µg/mL, 29.46 ± 2.06 for 200 µg/mL, 45.98 ± 3.21 for 300 µg/mL, 66.49 ± 4.65 for 400 µg/mL, 81.26 ± 5.68 for 500 µg/mL for Lipase activity. The IC_{50} value is 311.85.

Anti-obesity activity analysis of compound C6 was 17.46 ± 1.22 for $100 \mu\text{g/mL}$, 30.21 ± 2.11 for $200 \mu\text{g/mL}$, 47.63 ± 3.33 for $300 \mu\text{g/mL}$, 68.95 ± 4.82 for $400 \mu\text{g/mL}$, 83.47 ± 5.84 for $500 \mu\text{g/mL}$ for Lipase activity. The IC_{50} value is 302.59.

Anti-obesity activity analysis of compound C7 was 14.39 ± 1.01 for $100 \mu\text{g/mL}$, 24.65 ± 1.72 for $200 \mu\text{g/mL}$, 40.98 ± 2.86 for $300 \mu\text{g/mL}$, 61.04 ± 4.27 for $400 \mu\text{g/mL}$, 78.05 ± 5.46 for $500 \mu\text{g/mL}$ for Lipase activity. The IC_{50} value is 337.75.

Anti-obesity activity of standard (Orlistst) 21.61 ± 1.51 for $100 \mu\text{g/mL}$, 37.48 ± 2.62 for $200 \mu\text{g/mL}$, 56.93 ± 3.98 for $300 \mu\text{g/mL}$, 78.52 ± 5.49 for $400 \mu\text{g/mL}$, 92.46 ± 6.476 for $500 \mu\text{g/mL}$ for Lipase activity. The IC_{50} value is 259.56.

Lipase involves inhibition of dietary triglyceride absorption, as this is the main sources of excess calories. The lowest inhibition of obesity activity of C1, C2, C3, C4, C5, C6, C7 and Orlistst were 14.25 ± 0.99 , 18.07 ± 1.26 , 19.54 ± 1.36 , 15.79 ± 1.10 , 16.94 ± 1.18 , 17.46 ± 1.22 , 14.39 ± 1.01 and 21.61 ± 1.51 in the concentration of $100 \mu\text{g/mL}$ respectively while the highest inhibition of obesity activity of C1, C2, C3, C4, C5, C6, C7 and Orlistat were 76.45 ± 5.35 , 85.93 ± 6.01 , 87.45 ± 6.12 , 80.45 ± 5.63 , 81.26 ± 5.68 , 83.47 ± 5.84 , 78.05 ± 5.46 and 92.46 ± 6.47 in the concentration of $500 \mu\text{g/mL}$ respectively [4].

Drug produced with chlorine chemistry are used to treat many medical conditions and diseases, including high cholesterol, diabetes, cancer, ulcer, high blood pressure and inflammation.

When chlorine is present in pharmaceuticals, it may appear in the form of a chloride (Cl) or hydro chloride salts. Alternatively, chlorine may be bonded to the pharmaceutical structure in a way that has a direct effect on its therapeutic activity. Although the amount of chlorine used in pharmaceutical production is very small, there are substantial health benefits.

Table. 20 Anti-obesity activities (Pancreatic lipase inhibitory activity) of Synthesized compound

Samples	Concentrations $\mu\text{g/ml}$					IC ₅₀ value ($\mu\text{g/ml}$)
	100 $\mu\text{g/ml}$	200 $\mu\text{g/ml}$	300 $\mu\text{g/ml}$	400 $\mu\text{g/ml}$	500 $\mu\text{g/ml}$	
C1 Parent	14.25±0.99	23.56±1.64	39.69±2.77	60.81±4.25	76.45±5.35	343.49
C2 O-Br	18.07±1.26	30.62±2.14	49.81±3.48	71.68±5.01	85.93±6.01	293.05
C3 O-Cl	19.54±1.36	33.29±2.33	51.65±3.61	72.43±5.07	87.45±6.12	283.52
C4 O-Me	15.79±1.10	27.43±1.92	43.54±3.04	65.91±4.61	80.45±5.63	320.11
C5 P-Br	16.94±1.18	29.46±2.06	45.98±3.21	66.49±4.65	81.26±5.68	311.85
C6 P-Cl	17.46±1.22	30.21±2.11	47.63±3.33	68.95±4.82	83.47±5.84	302.59
C7 P-Me	14.39±1.01	24.65±1.72	40.98±2.86	61.04±4.27	78.05±5.46	337.75
Std. (Orlistat)	21.61±1.51	37.48±2.62	56.93±3.98	78.52±5.49	92.46±6.47	259.56

Values were expressed as Mean \pm SD for triplicates

Lipase inhibition of synthesized compounds as shown in figures 28-34.

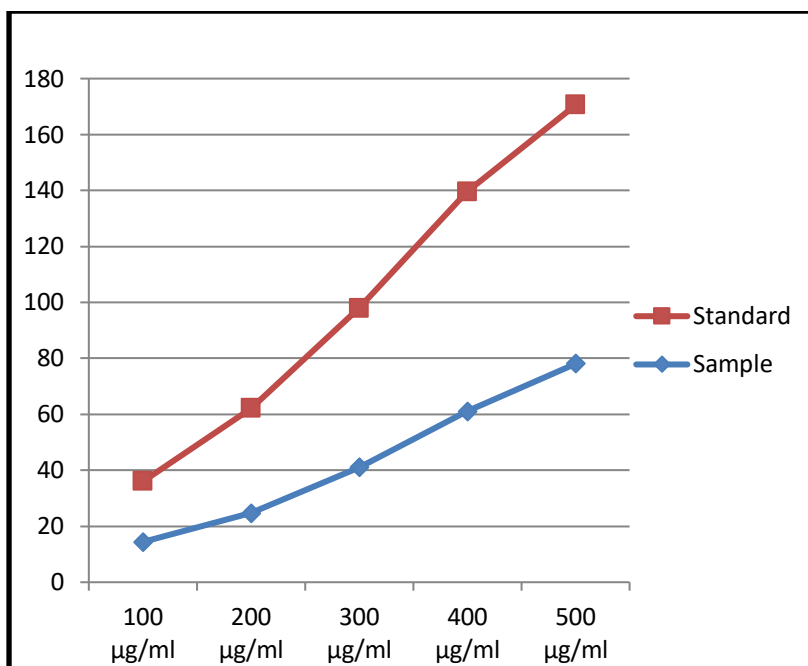


Figure 28. Pancreatic lipase inhibition of compound C1

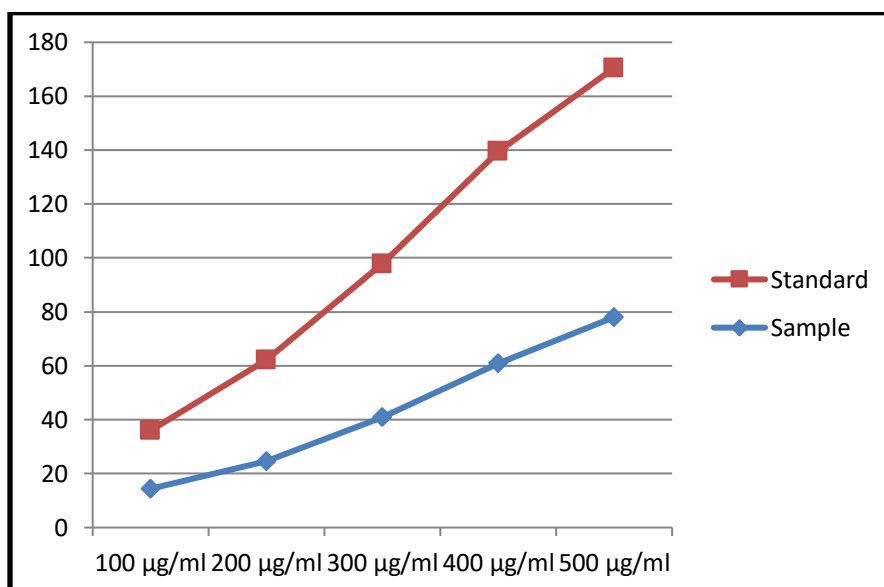


Figure 29. Pancreatic lipase inhibition of compound C2

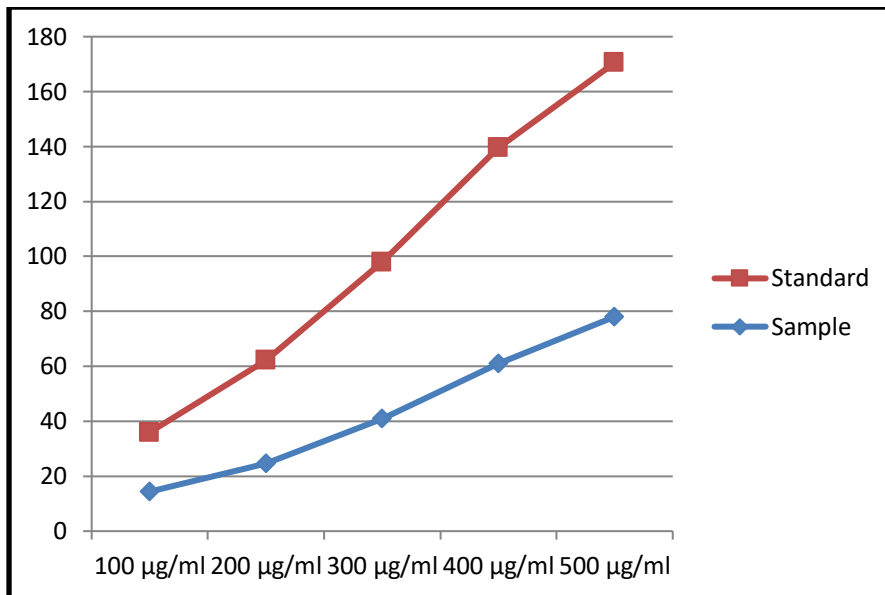


Figure 30. Pancreatic lipase inhibition of compound C3

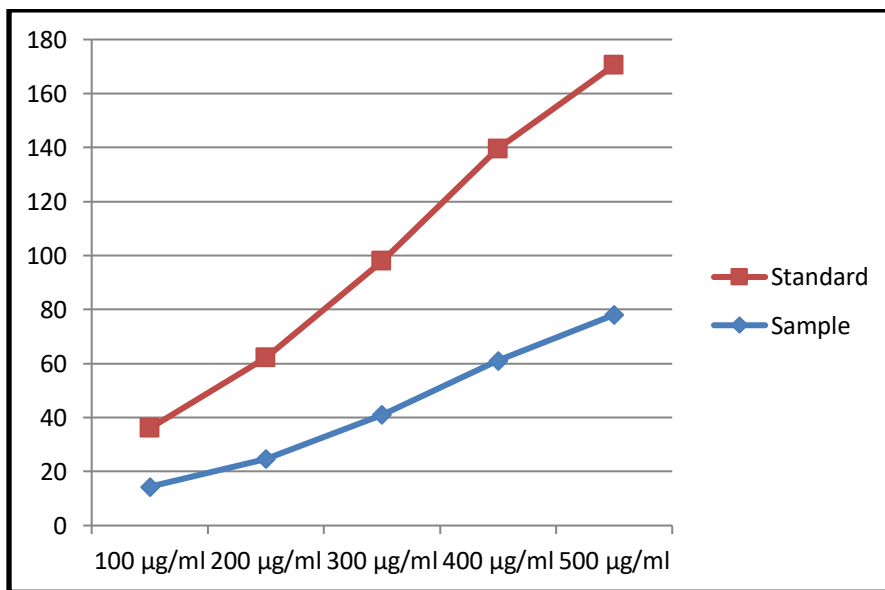


Figure 31. Pancreatic lipase inhibition of compound C4

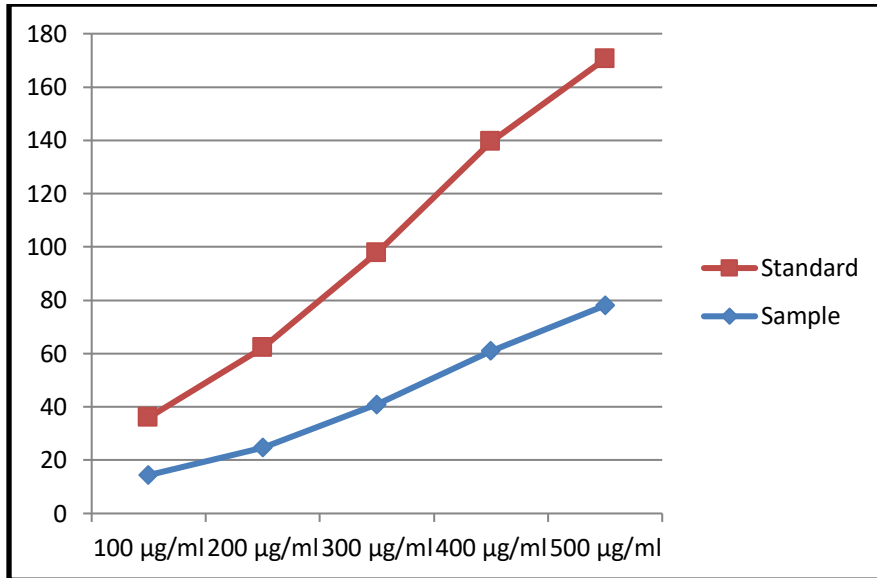


Figure 32. Pancreatic lipase inhibition of compound C5

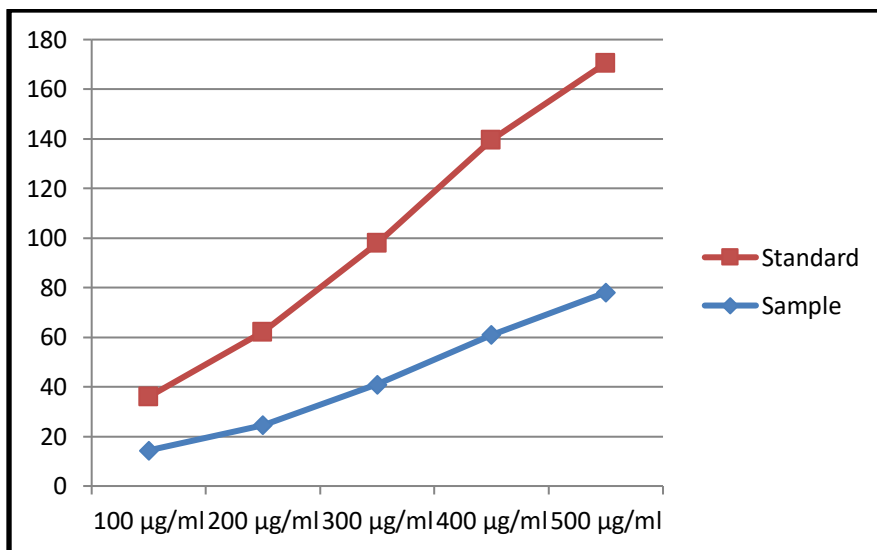


Figure 33. Pancreatic lipase inhibition of compound C6

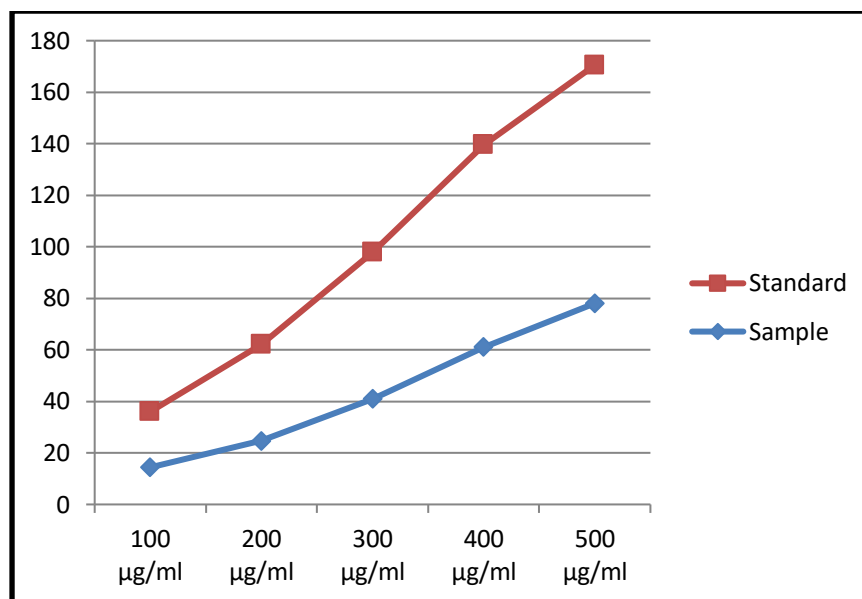


Figure 34. Pancreatic lipase inhibition of compound C7

Inhibition of pancreatic lipase is an attractive targeted approach for the discovery of potent anti-obesity agents for obesity treatment.

The result shows the o-substituted compounds have higher activity than p-substituted compounds. The order of activity for o-substituted compounds is C3>C2>C4 (o-Cl>o-Br>o-methyl). The order of activity for p-substituted compounds is C5>C6>C7 (p-Cl>p-Br>p-methyl). From the result it was observed that, compound C3 shows good anti-Obesity activity than other synthesized compounds due to the presence of electron with drawing group [5].

5.11 Insilico molecular docking study (Breast cancer activity)z

The most common form of tumour in women is breast cancer (BC), but metastasis are the primary cause of death. Metastasis is a complex mechanism in which cancer cells migrate into the vessels of the blood, invade other tissues, and identify secondary sites for a colony. Indeed, BC starts as a local disease but can spread to distant locations, such as lymph nodes

and various organs, with metastasis. This process includes the expression of a series of genes that control cancer cells' survival and invasion. As possible drug targets in the drug development phase, drugs that modulate the genes/proteins that control cancer cell survival, metastasis, apoptosis, and invasion are therefore of great importance [6]. However while new therapies have been developed to dramatically reduce metastatic BC mortality, resistance to anticancer agents can lead to treatment failure [7].

Big data, which provides a broad variety of biological and chemical knowledge, has been generated by the rapidly growing number of structures and is a recent opportunity to gain a deeper understanding of the relationships between drugs and targets (usually proteins), drugs and diseases, and targets and diseases. However, although the available data is often heterogeneous and incomplete, this information can be exploited by computational methods to deepen these interactions [8]. High-performance computational algorithms for drug discovery processes are needed, given the cost and time consumption of experimental methods. The "docking" computational technique can predict the binding of drug-target complexes as well as the ligand's conformation upon binding to a protein target. The binding free energy of target-drug interactions determines an association's affinity and the conditions for a complex to form. Rated binding free energies are not always reliable, but they can be used in a virtual screening method to pick new drugs such as small molecules to be tested experimentally [9-11].

5.11.1 Insilico molecular docking study synthesized compounds

Currently, the use of computers to predict the binding of ligands of small molecules to known target structures is an increasingly important component in the drug discovery process (12). Docking of small molecules in the receptor binding site and estimation of binding affinity of the complex is a vital part of structure based drug design (13).

Breast cancers are thought to be due to a hereditary predisposition to the disease. Two breast-cancer- susceptibility genes, *BRCA1* and *BRCA2*, have been identified, and mutations in these genes are responsible for most cases in families with a large number of early- onset breast cancers. The role of estrogen in affecting breast cancer risk during pre-menopausal years has remained largely unknown. Several factors related to reproduction appear to predispose women to breast cancer. *BRCA1* mutations confer high lifetime risk of both cancers, but there is evidence that the risk of ovarian cancer is heterogeneous. A second breast cancer gene, *BRCA2* has recently been localized to chromosome 13q (14). Mutations in the central part of the gene have been associated with a higher risk of ovarian cancer and a lower risk of prostate cancer than mutations in other parts of the gene (15).

Our *in silico* approach on include synthesized compounds and standard as Tamoxifen against breast cancer target *BRCA1* is carried out using virtual screening, molecular docking studies. Virtual screening of include synthesized compounds and Tamoxifen compound showed the binding affinity towards target *BRCA1*. The compound was screened with binding affinity and compound was selected as hits. Present study was to investigate the *in silico* anticancer effects of synthesized compounds and standard as Tamoxifen.

The docked ligand molecules were selected based on docking energy and good interaction with the active site residues and the results are shown in Table 21. The Plate 1 to 8 represents the docking of *BRCA1* with synthesized compounds and standard as Tamoxifen. Hydrogen bond was indicated by green dark lines in between atoms involved and rest of the interactions were hydrophobic. The docking score of 2Br, 2Cl, 2Me, 4Br, 4Cl, 4Me, Piperidone (Synthesized Compounds) and Tamoxifen was found be -6.1, -5.8, -5.8, -5.9, -6.3, -5.5, -5.4 and -5.3Kcal/mol respectively. The molecular docking of the hits showed the binding mode and interaction energy. The docking studies confirmed the inhibition of target protein *BRCA1* to show the anticancer activity of 2Br, 2Cl, 2Me, 4Br, 4Cl, 4Me, Piperidone

and standard as Tamoxifen. Among the various compounds, 4Cl has greatest binding energy followed by 2Br, 4Br, 2Cl, 2Me, 4Me, piperidone and highest than standard.

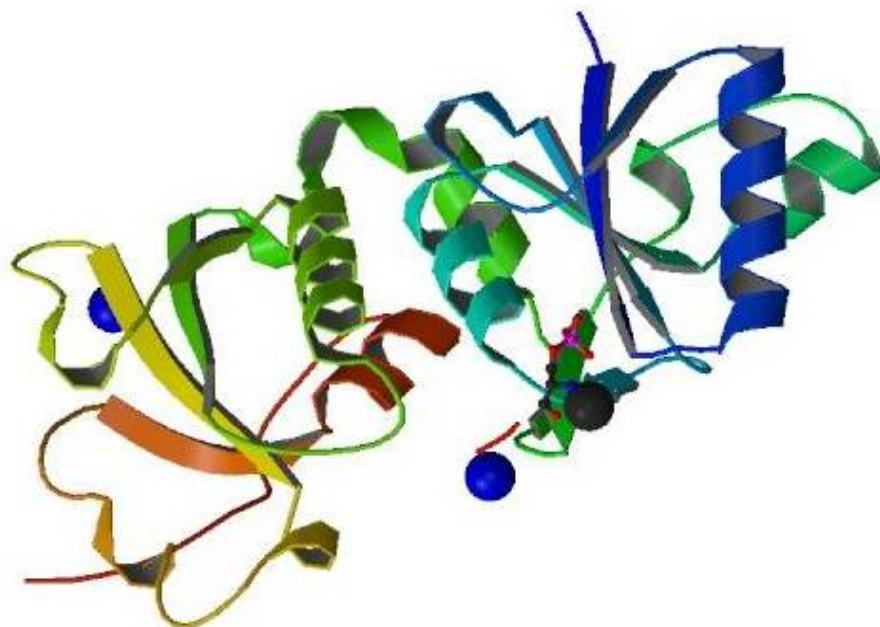
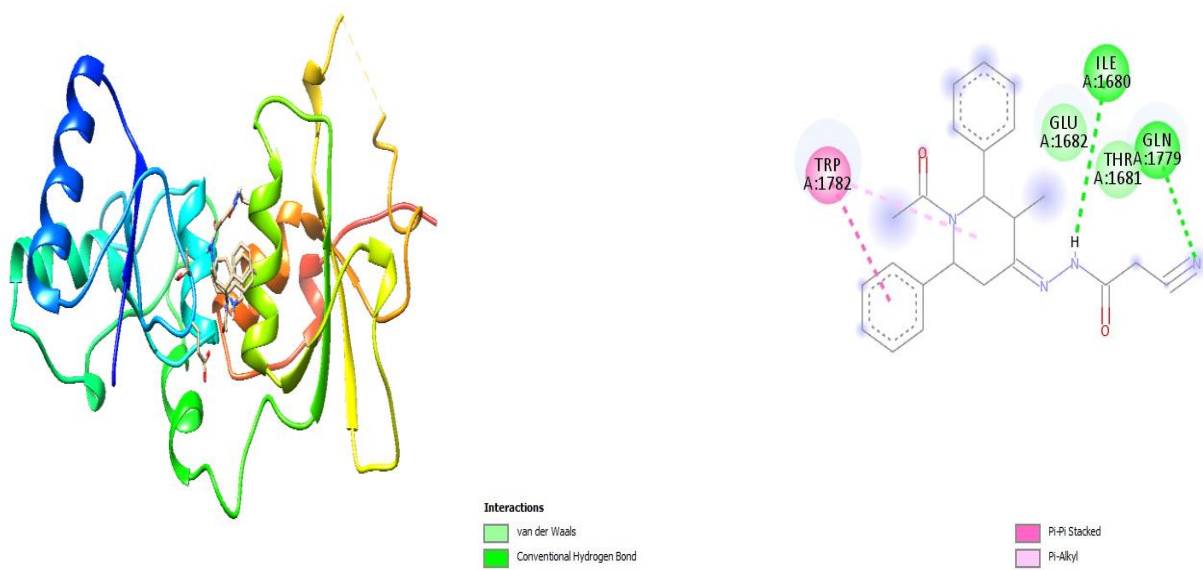


Fig.35 Three Dimensional Structure of BRACT1

Table. 21: Molecular docking with BRAC1 protein

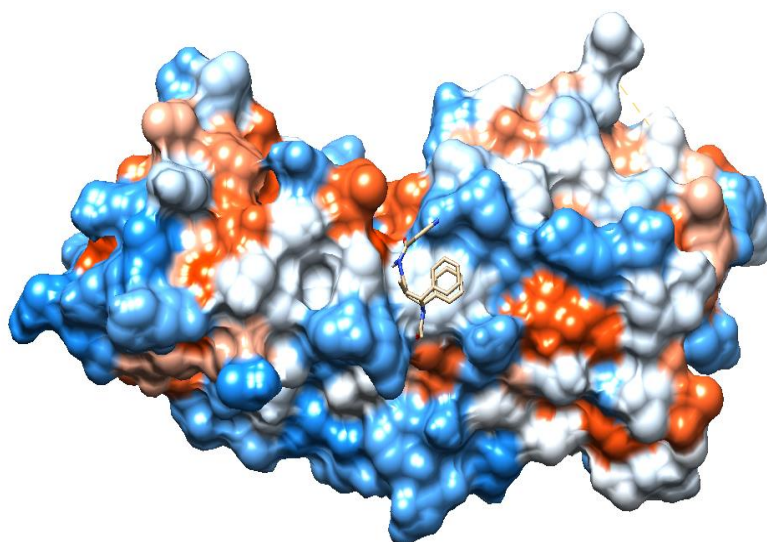
Ligands	H-bond acceptors / donors	Binding Affinity (kcal/mol)	BRAC1 -Amino acids binding to ligand	Binding site amino acids in the structural unit
C1	4/1	-5.4	TRP 1782, ILE 1680, GLU 1698,	Alpha helix
C2	4/1	-6.1	GLU 1698, ALA 1700, LEU 1701, ASN 1774,	Alpha helix
C3	4/1	-5.8	GLU 1698, LEU 1701, ASN 1774, ARG 1699	Alpha helix
C4	4/1	-5.8	TRP 1782, GLU 1682, GLU 1785	Alpha helix
C5	4/1	-5.9	ALA 1700, GLU 1698, ASN 1774, ARG 1699	Alpha helix
C6	4/1	-6.3	ALA 1700, LEU 1701, ASN 1774, ARG 1699	Alpha helix
C7	4/1	-5.5	ALA 1700, LEU 1701, ARG 1699	Alpha helix
Tamoxifen	2/0	-5.3	GLU 1698, ALA 1700, LEU 1701, ASN 1774, LEU 1839	Alpha helix



a

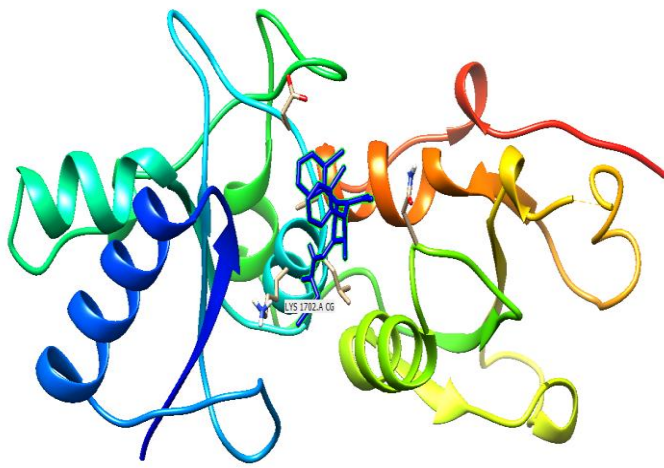
b

a) 3D cartoon structure and b) 2D structure of BRAC1 binding with C1

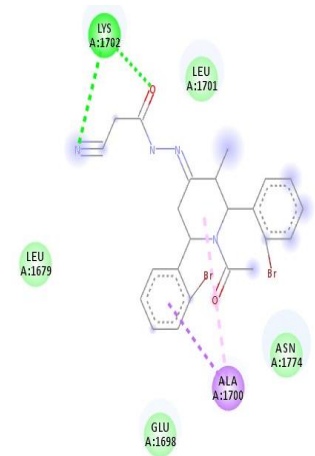


3D Surface structure of BRAC1 binding with C1

Plate.1



a

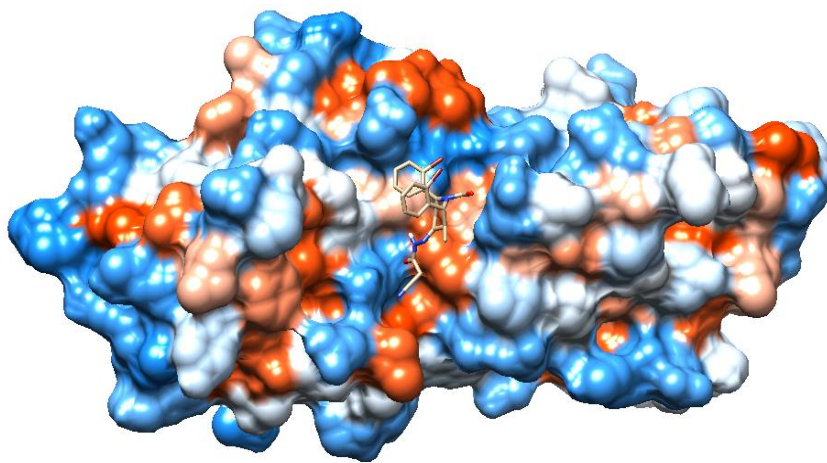


b

Interactions
 van der Waals
 Conventional Hydrogen Bond

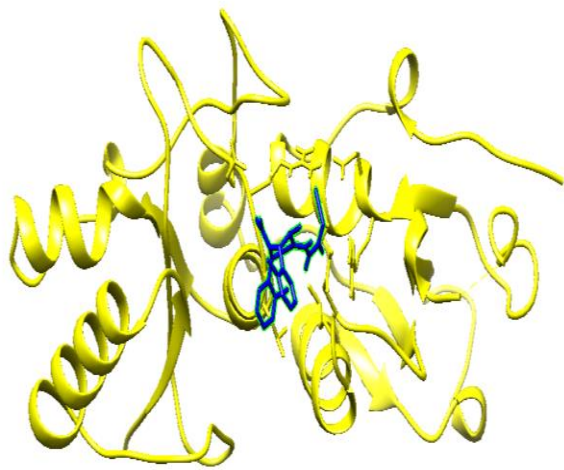
Pi-Sigma
 Alkyl

a) 3D cartoon structure and b) 2D structure of BRAC1 binding with C2

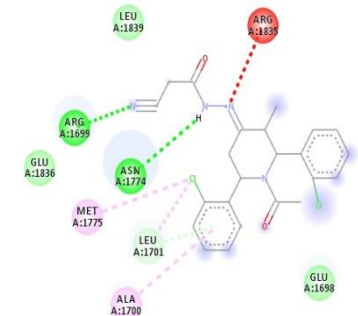


3D Surface structure of BRAC1 binding with C2

Plate.2

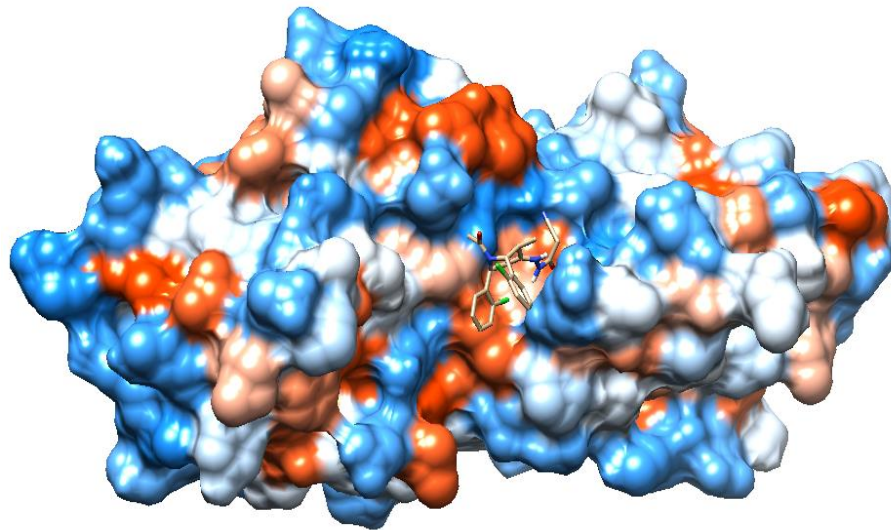


a



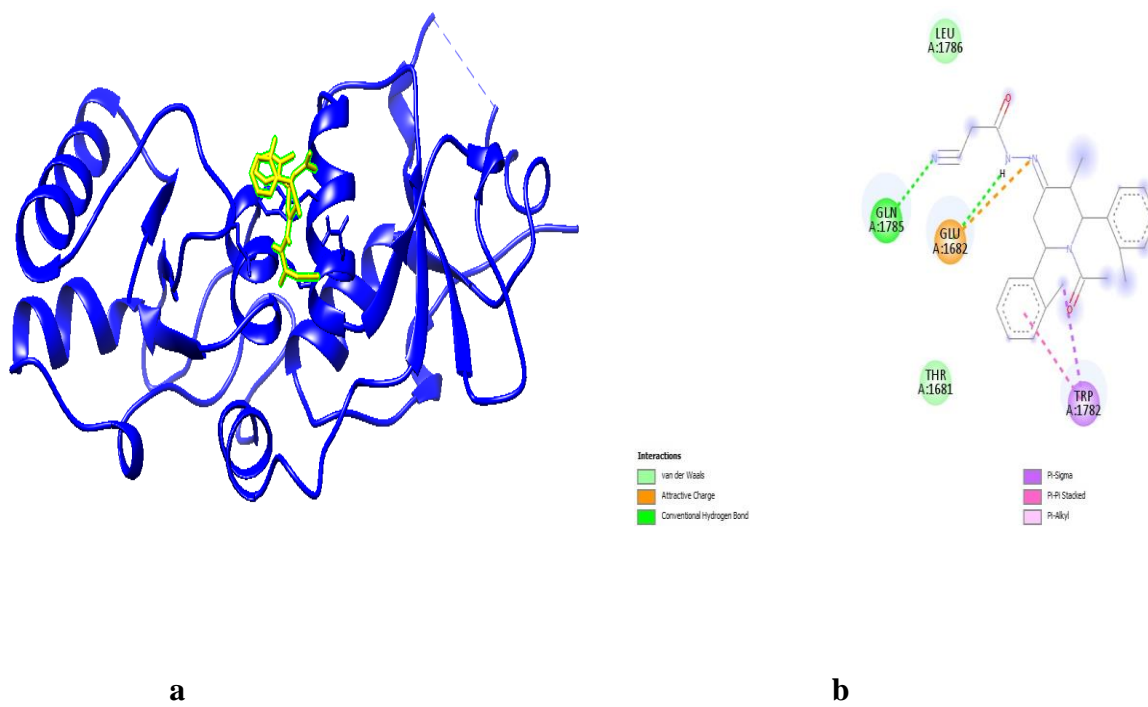
b

a) 3D cartoon structure and b) 2D structure of BRAC1 binding with C3

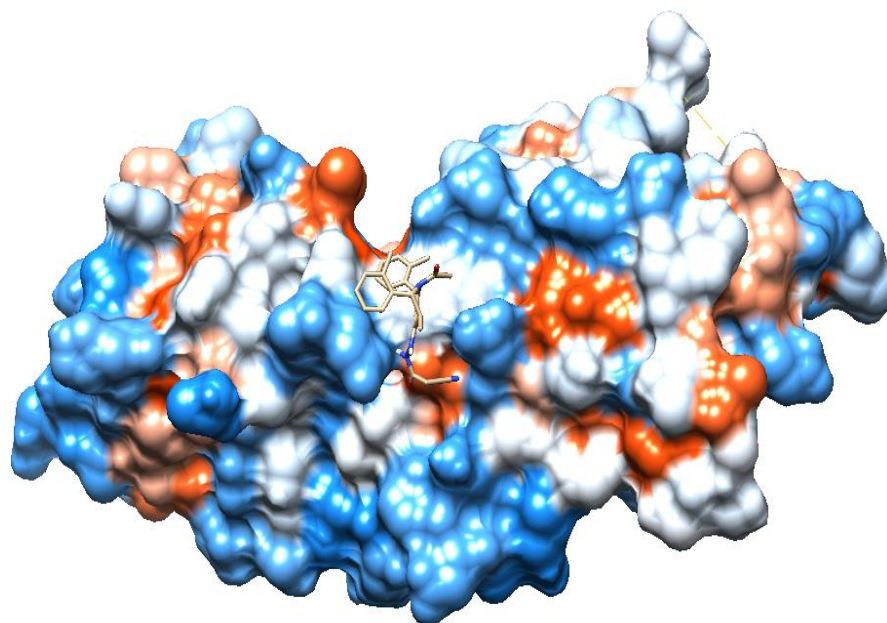


3D Surface structure of BRAC1 binding with C3

Plate 3

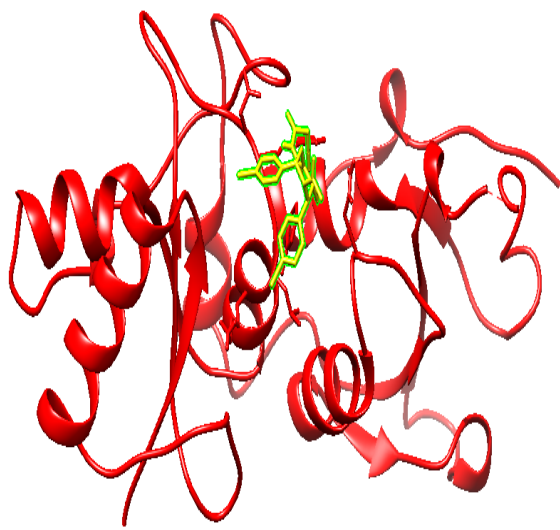


a) 3D cartoon structure and b) 2D structure of BRAC1 binding with C4

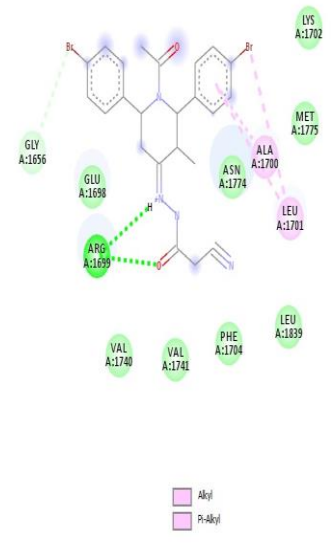


3D Surface structure of BRAC1 binding with C4

Plate 4

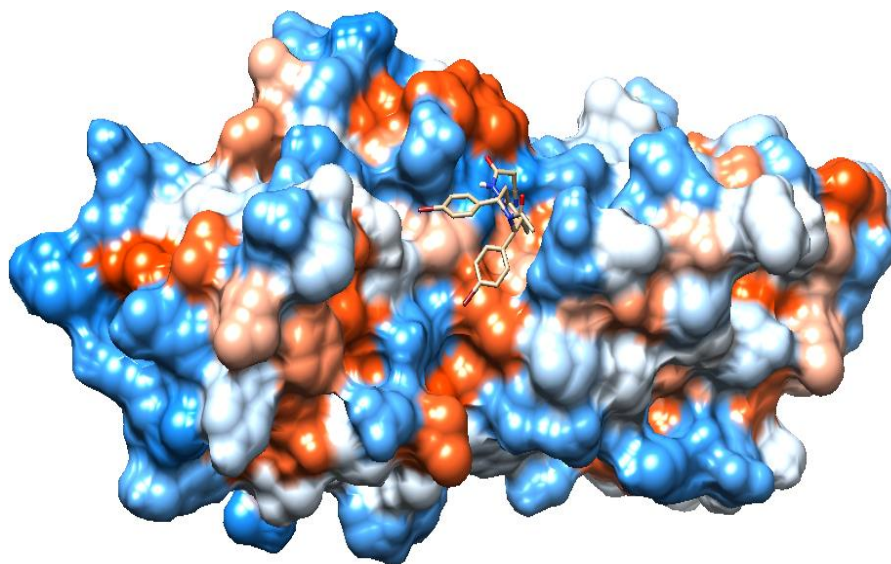


a



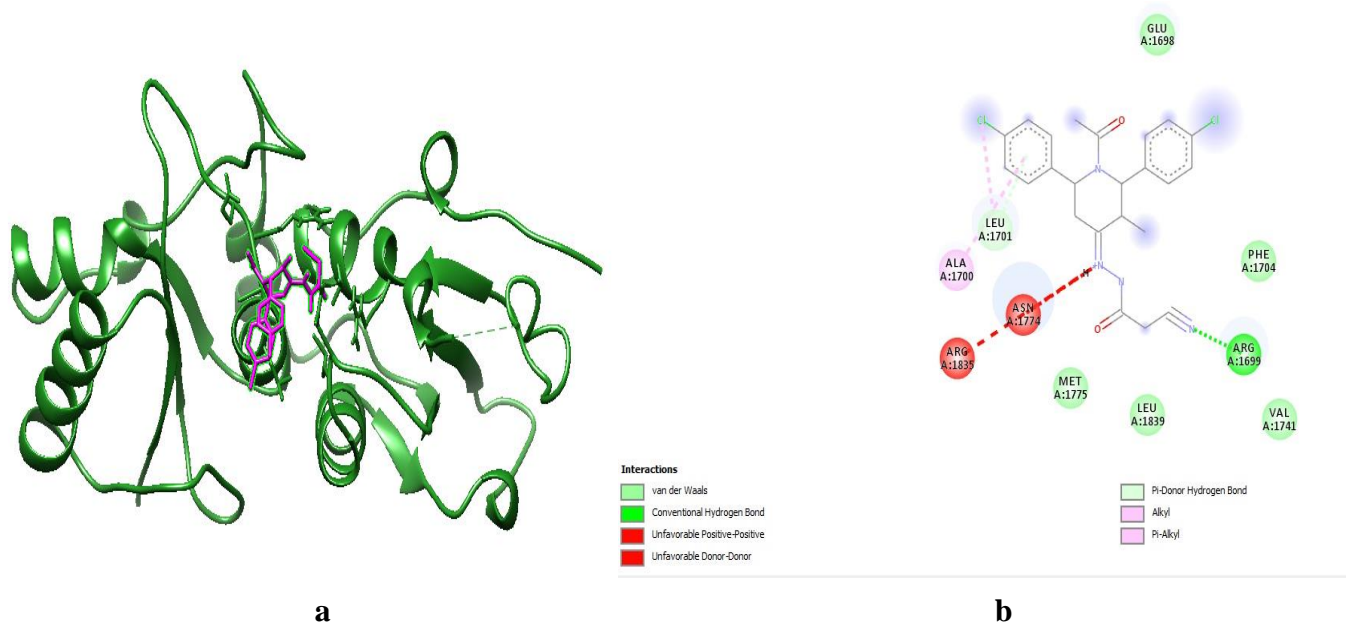
b

a) 3D cartoon structure and b) 2D structure of BRAC1 binding with C5

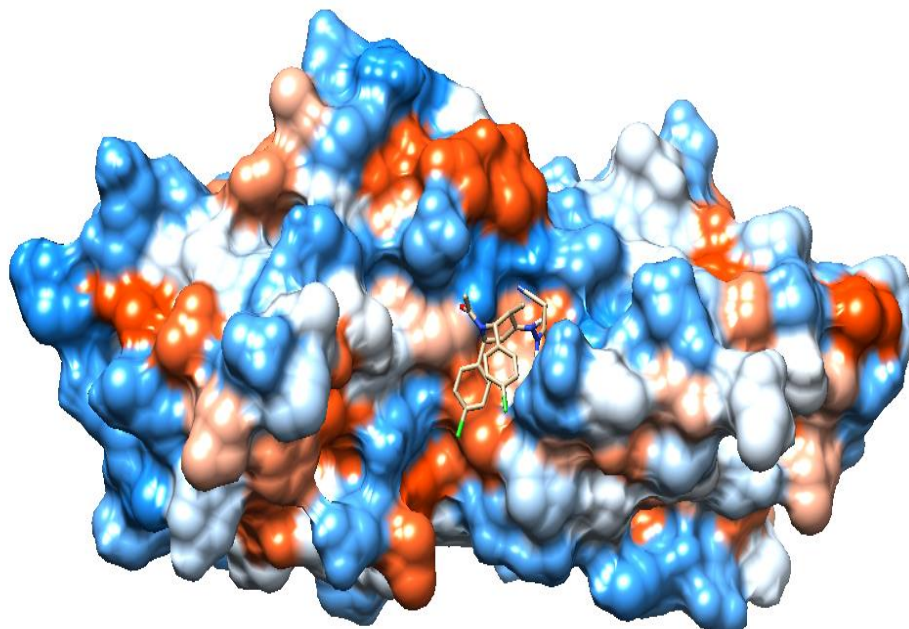


3D Surface structure of BRAC1 binding with C5

Plate 5

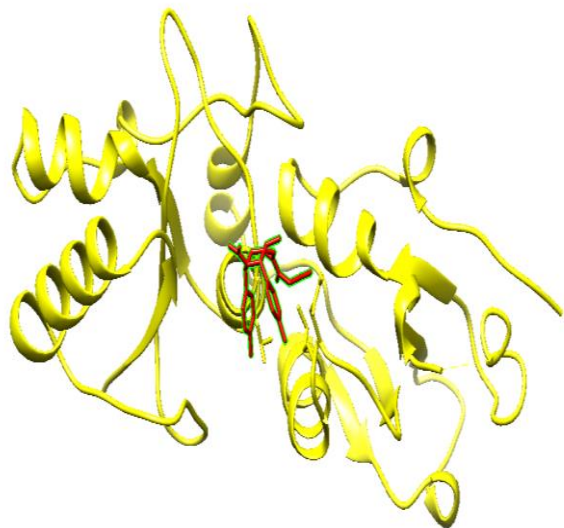


a) 3D cartoon structure and b) 2D structure of BRAC1 binding with C6

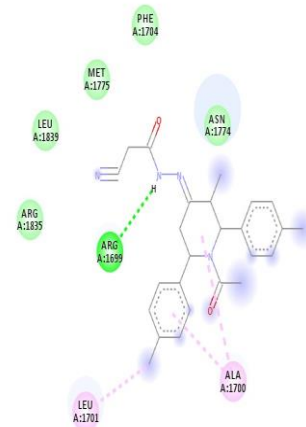


3D Surface structure of BRAC1 binding with C6

Plate 6



a

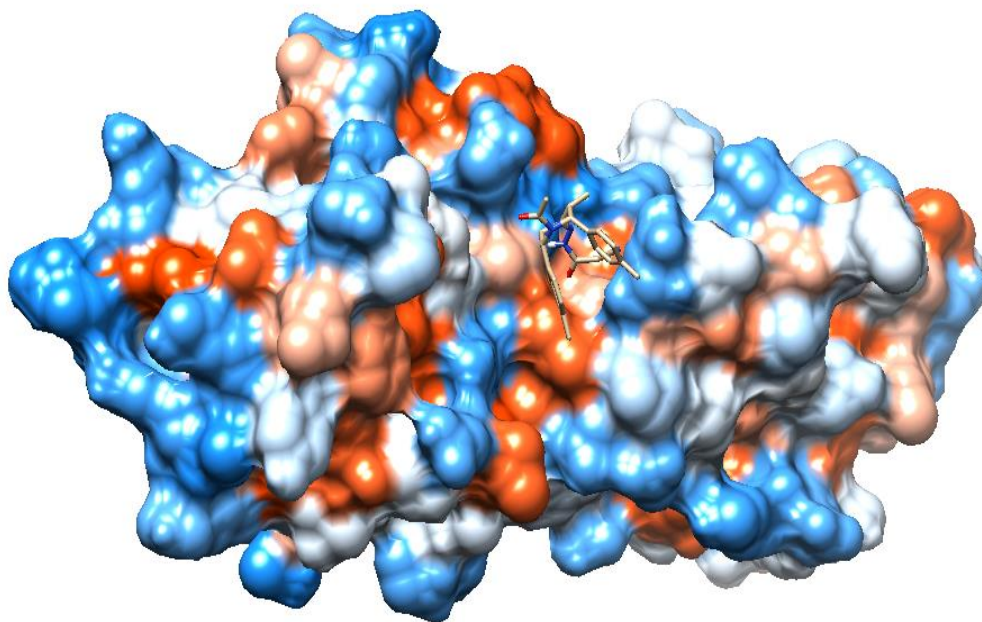


Interactions
 van der Waals
 Conventional Hydrogen Bond

alkyl
 pi-alkyl

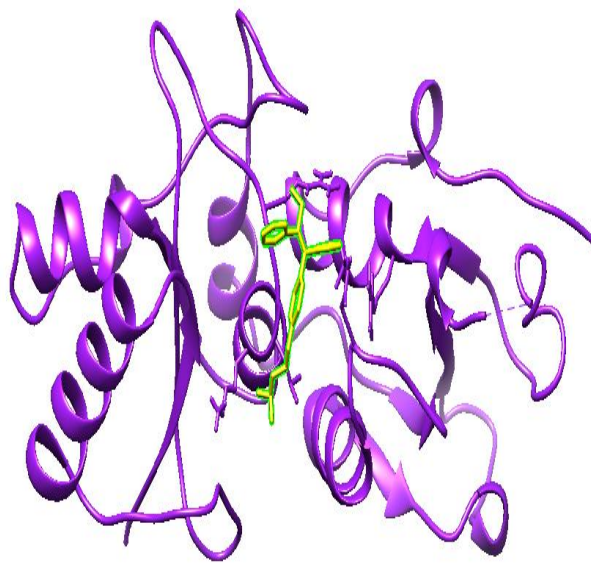
b

a) 3D cartoon structure b) 2D structure of BRAC1 binding with C7

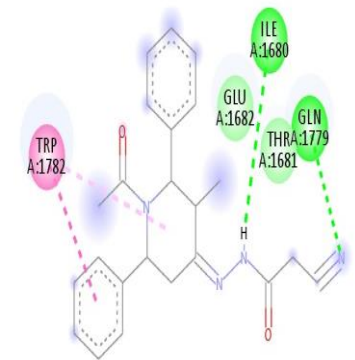


3D Surface structure of BRAC1 binding with C7

Plate. 7



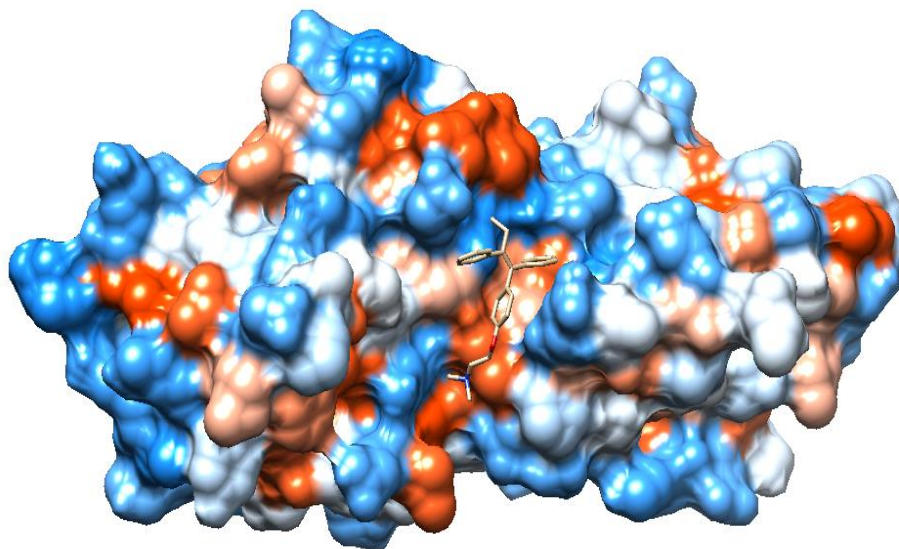
a



b



a)3D cartoon structure and b) of BRAC1 binding with Tamoxifen ligand



3D Surface structure of BRAC1 binding with Tamoxifen ligand

Plate.8

5.12 IN VITRO THROMBOLYTIC ACTIVITY

Thrombolytic therapy is the use of drugs to break up or dissolve blood clots, which are the main cause of both heart attacks and stroke. Thrombolytic therapy is the administration of drugs called lytics or clot buster to dissolve blood clots that have suddenly blocked your major arteries and pose potentially life threatening implications. Thrombolytic therapy is emergency treatment for patients completely blocked arteries or veins caused by blood clots

The in vitro thrombolytic activities of the compounds were determined by clot lysis study, the tested compounds were determined by comparison with the thrombolytic activity of streptokinase. The activity of the compounds was measured for the decrease in clot weight at different concentrations 100 and 200 ug/mL. respectively Streptokinase (30,000 IU) was positive control and water is negative control. The results were plotted concentration vs percentage of clot lysis. The result of in vitro thrombolytic activity were encouraging and the tested compounds exhibited considerable aggregation inhibition [16].

All the seven tested cyanoacetyl hydrazone derivatives exhibited substantial clot lysis value range from 40.5 to 78.45 % in comparison to 84.57 % clot lysis exhibited by the reference standard streptokinase (30,000 IU). Statistical representation of the effective clot lysis percentage by negative control (sterile distilled water) 26.74 ± 1.87 % and positive control (streptokinase) 84.57 ± 5.91 %. Values expressed as Mean \pm SD for triplicate. Effect of synthesized compounds on clot lysis percentage is given in Figures. 36-49

The activity of the compounds was determined by comparison with the thrombolytic activity of Streptokinase. The results of all synthesized compounds are presented in **Table 22**.

Table 22: In-vitro anti thrombolytic activity of synthesized compounds

Samples	% of clot lysis			
	Control	100 (µg/ml)	200 (µg/ml)	Standard
C1	26.74 ± 1.87	40.57 ± 2.83	69.19 ± 4.84	84.57 ± 5.91
C2	26.74 ± 1.87	47.62 ± 3.33	76.21 ± 5.33	84.57 ± 5.91
C3	26.74 ± 1.87	47.85 ± 3.85	78.45 ± 5.54	84.57 ± 5.91
C4	26.74 ± 1.87	44.28 ± 3.09	73.32 ± 5.13	84.57 ± 5.91
C5	26.74 ± 1.87	45.64 ± 3.19	74.21 ± 5.19	84.57 ± 5.91
C6	26.74 ± 1.87	46.59 ± 3.26	74.93 ± 5.24	84.57 ± 5.91
C7	26.74 ± 1.87	41.35 ± 2.89	72.83 ± 5.09	84.57 ± 5.91

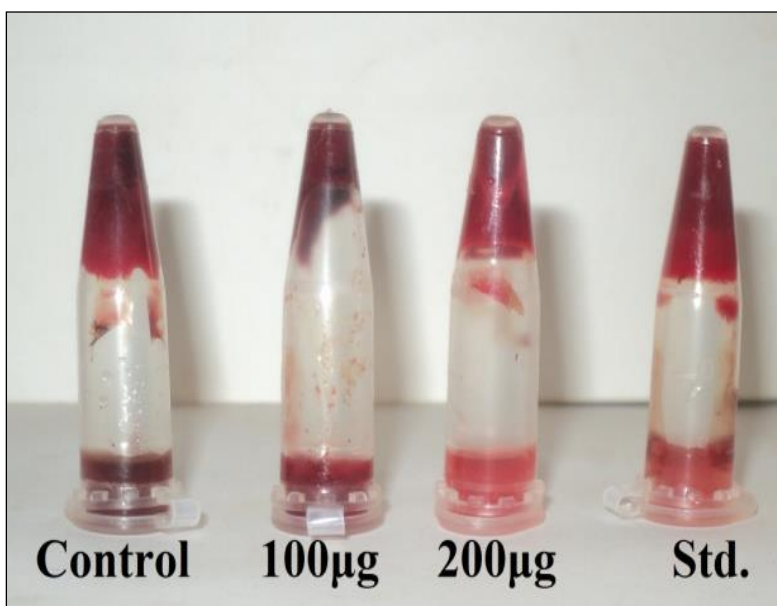


Fig.36 Clotlysis experiments with different concentrations of compound C1

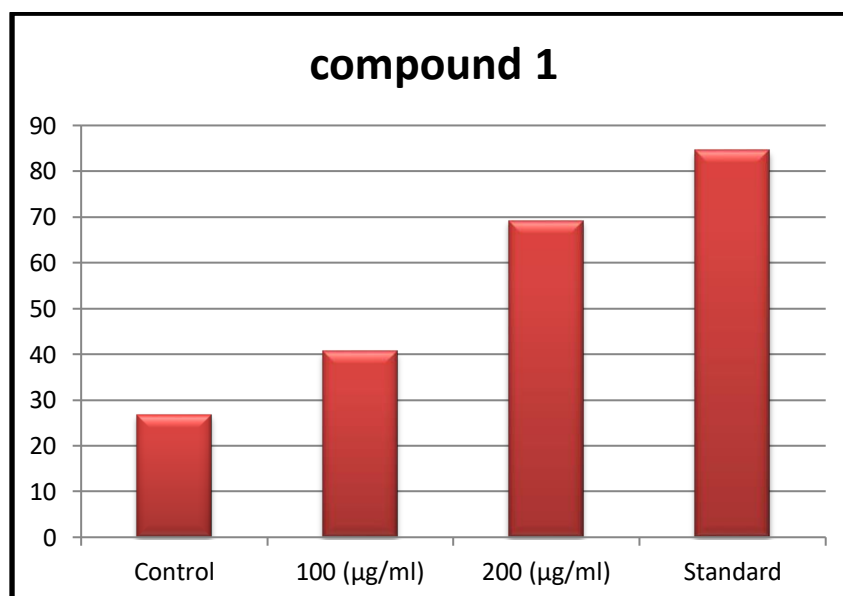


Fig .37 Clotlysis of compound C1 on Thrombolytic activity

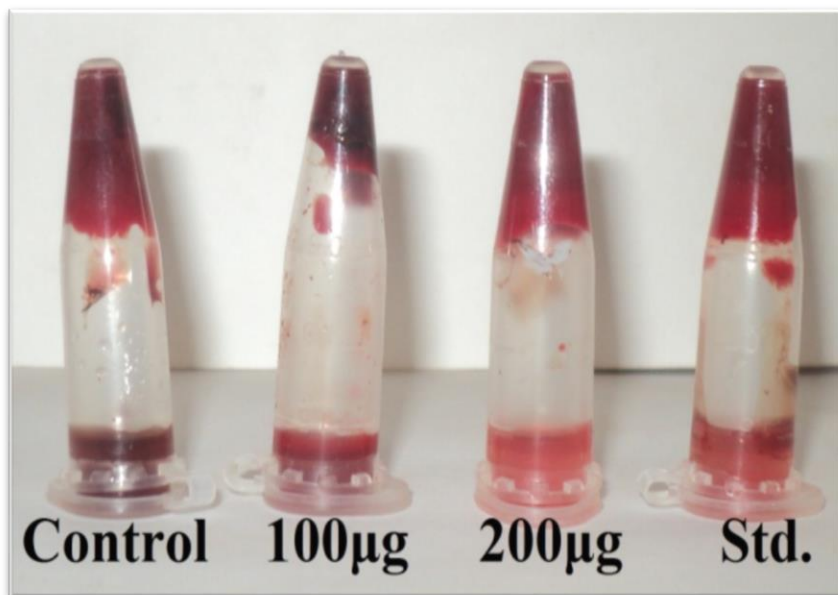


Fig.38 Clotlysis experiments with different concentrations of compound C2

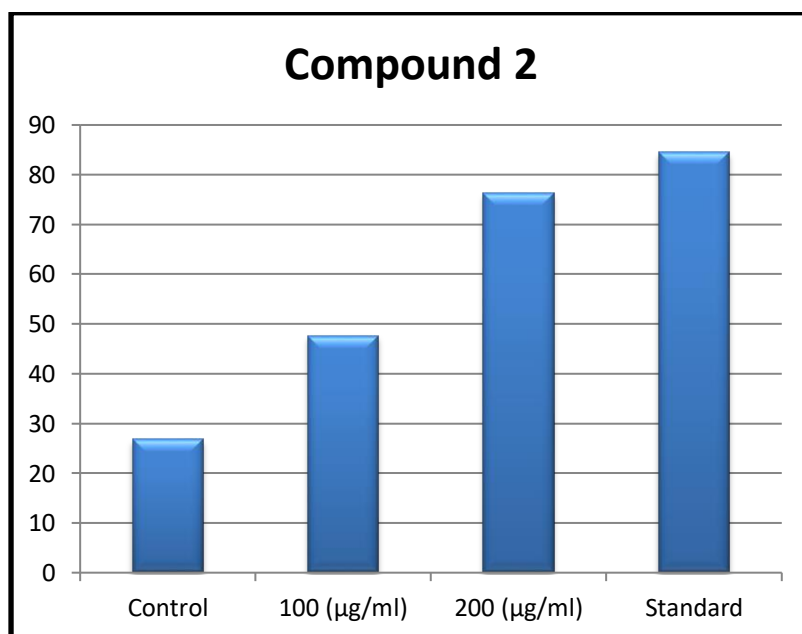


Fig .39 Clotlysis of compound C2 on Thrombolytic activity

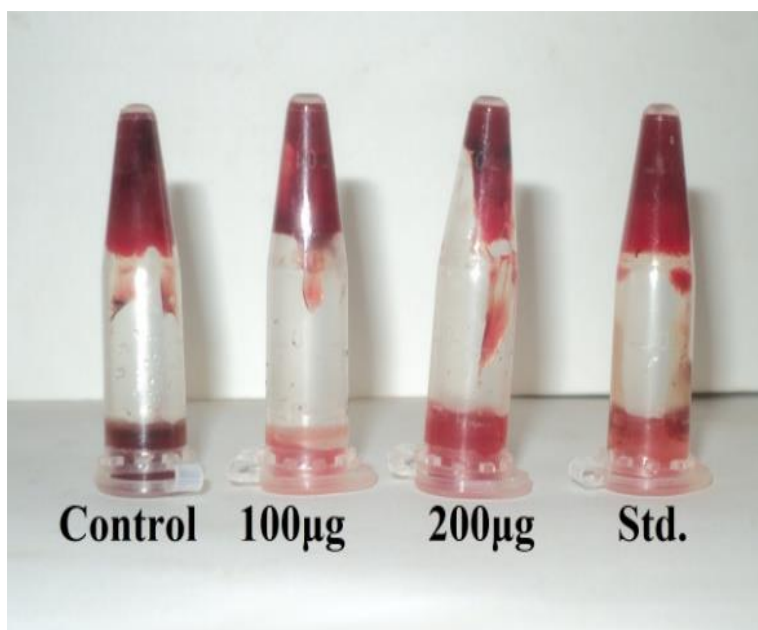


Fig.40 Clotlysis experiments with different concentrations of compound C3

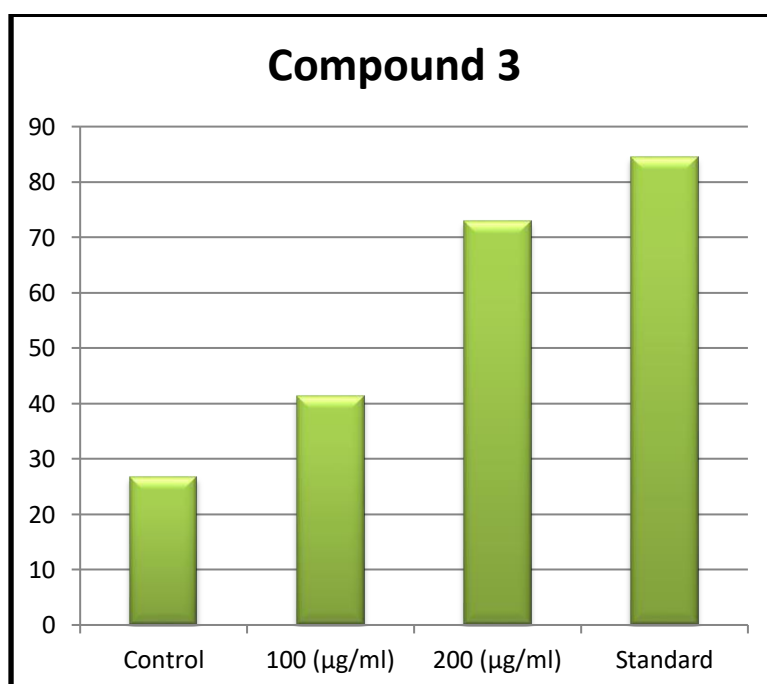


Fig .41 Clotlysis of compound C3 on Thrombolytic activity

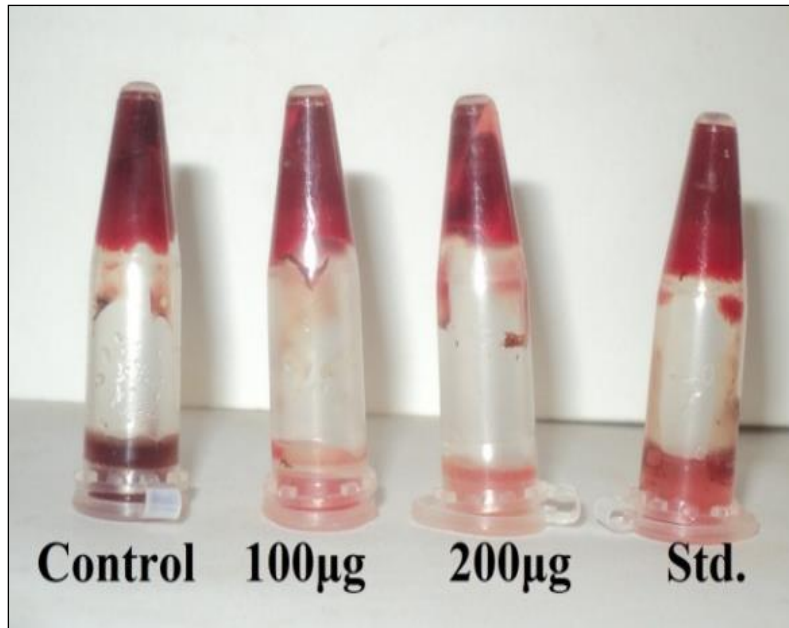


Fig .42 Clotlysis experiments with different concentrations of compound C4

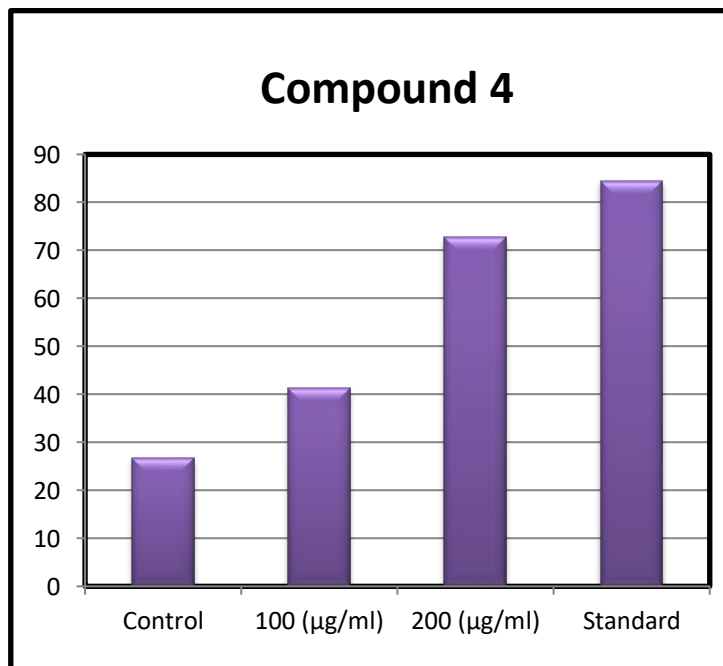


Fig .43 Clotlysis of compound C4 on Thrombolytic activity

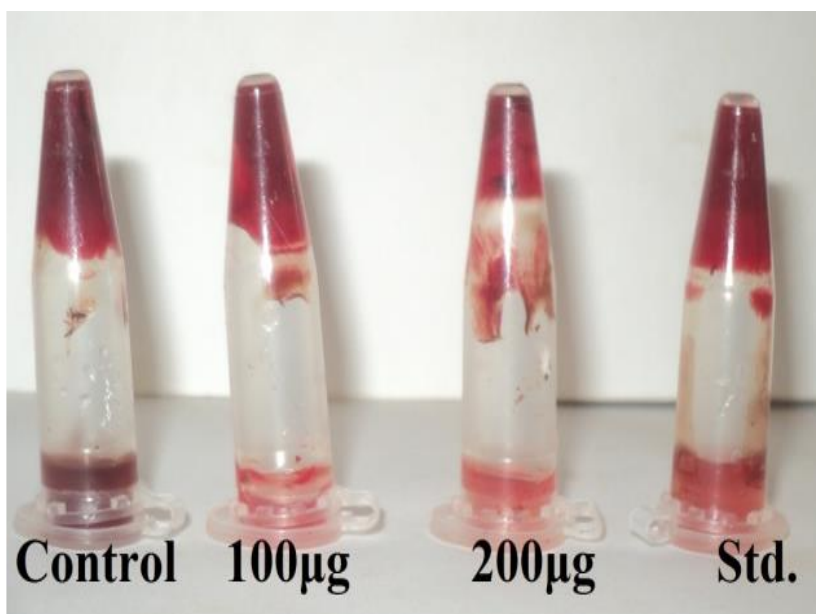


Fig .44 Clotlysis experiments with different concentrations of compound C5

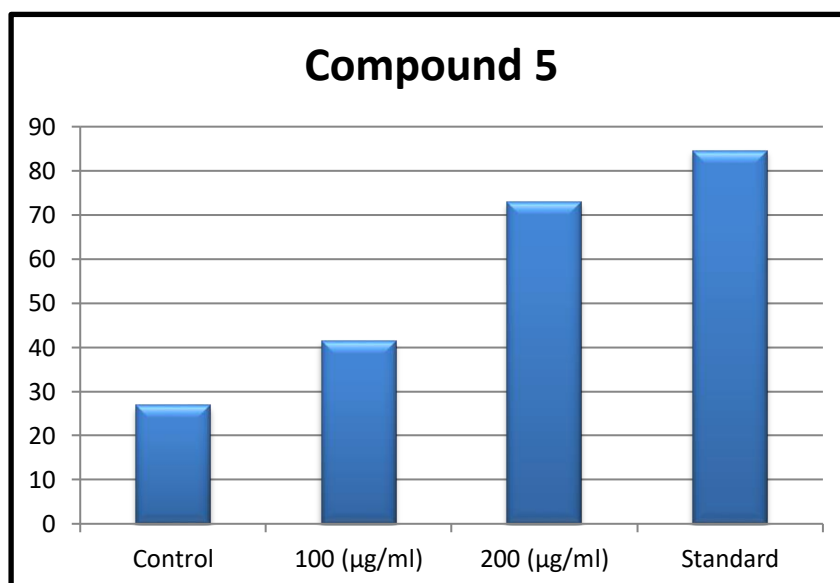


Fig .45 Clotlysis of compound C5 on Thrombolytic activity

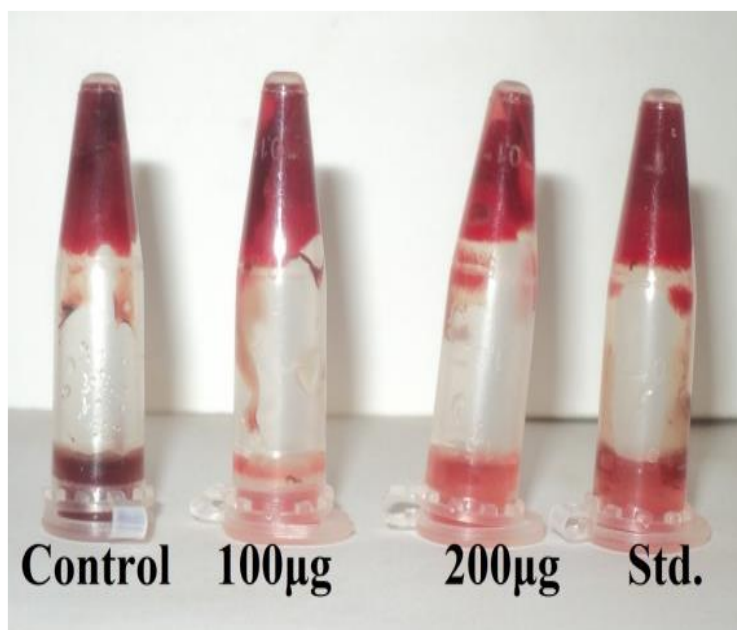


Fig.46 Clotlysis experiments with different concentrations of compound C6

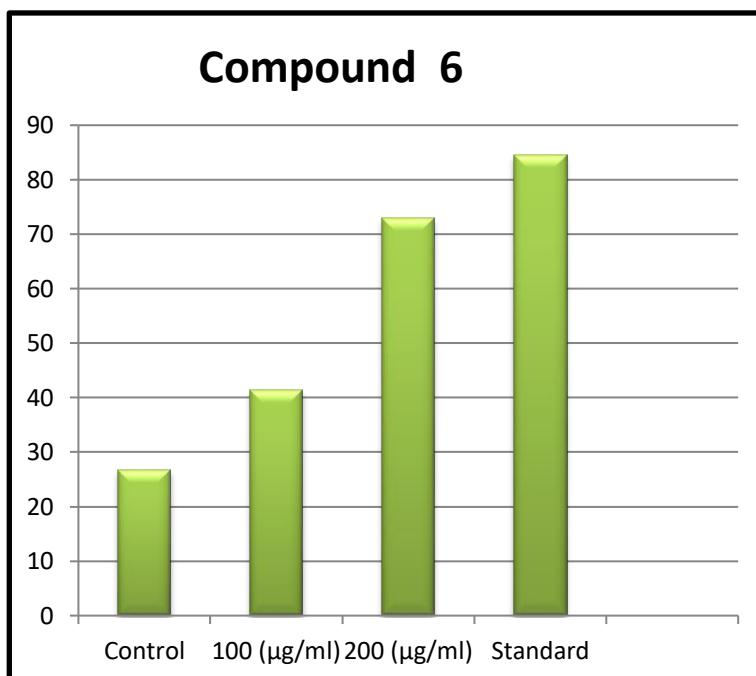


Fig .47 Clotlysis of compound C6 on Thrombolytic activity

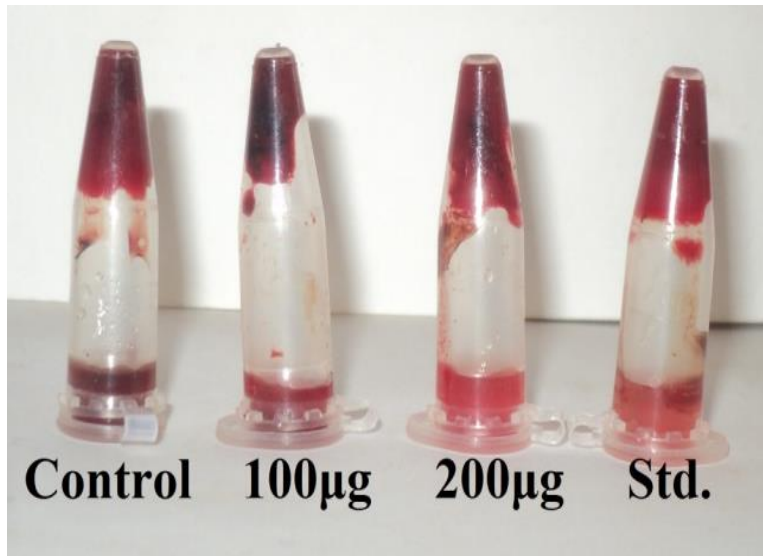


Fig.48 Clotlysis experiments with different concentrations of compound C7

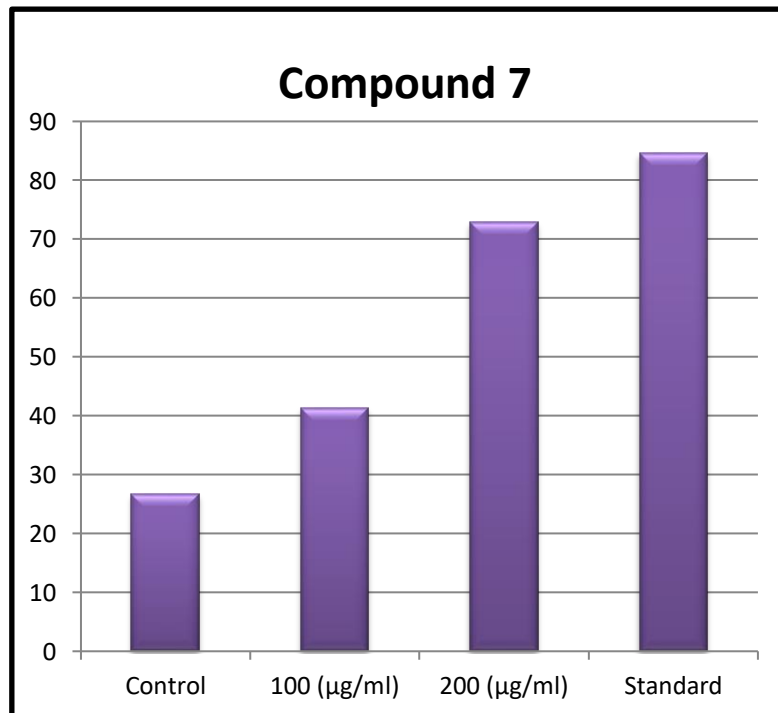


Fig . 49 Clotlysis of compound C7 on Thrombolytic activity

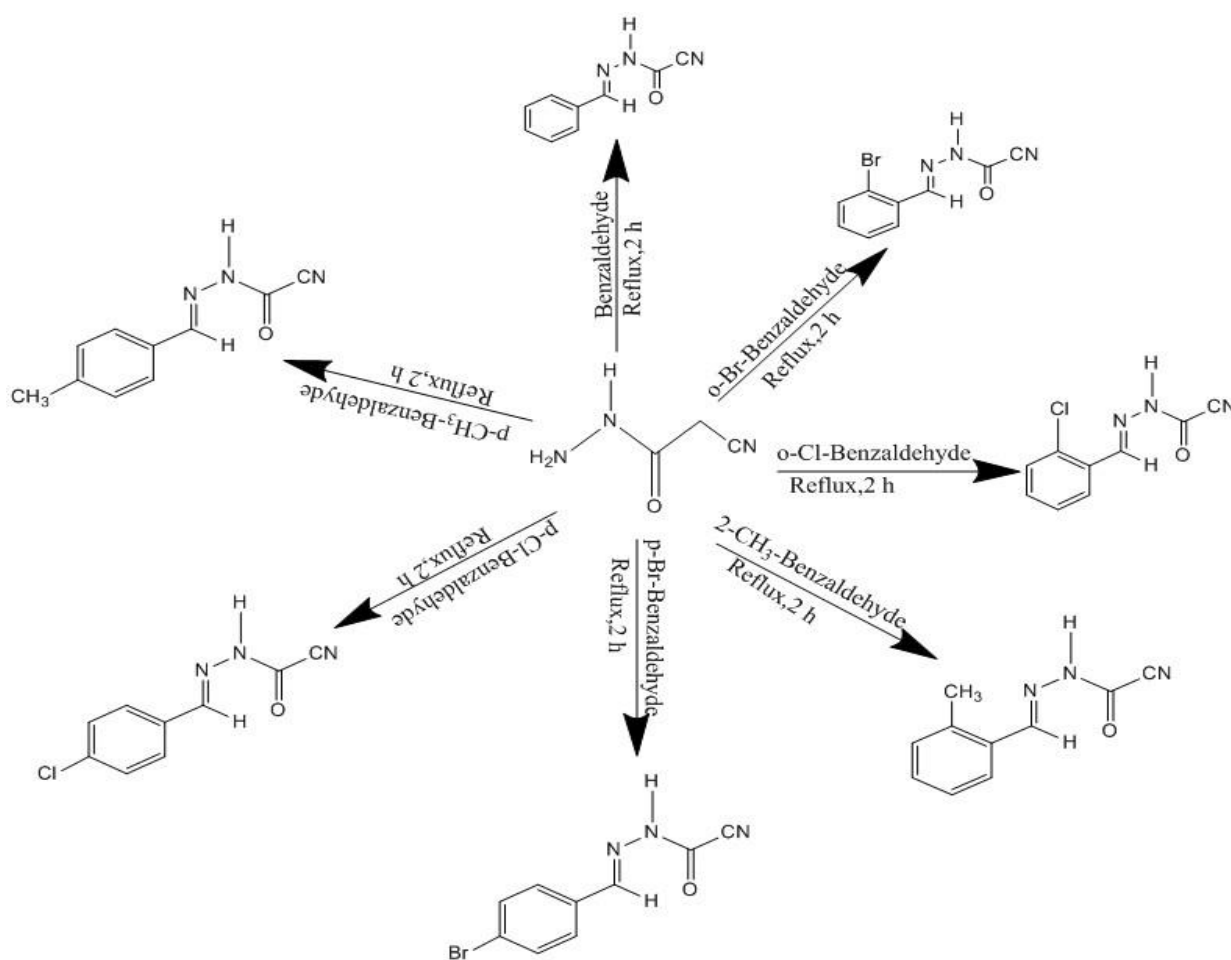
PART – II

5.13 Synthesis of compounds

5.13.1 Preparation of Benzaldehyde cyanoacetylhydrazone (BCAH)

In methanol, benzaldehyde (0.1mol), cyanoacetylhydrazide (0.1mol) and a few drops of glacial acetic acid were refluxed for two hours. The reaction mixture was cooled to room temperature once the reaction was completed. The solid product was separated by filtration and washed with warm water and recrystallized by methanol to afford Benzaldehyde cyanoacetyl hydrazone

The schematic representation of all the synthesized compounds are shown in **scheme 2**



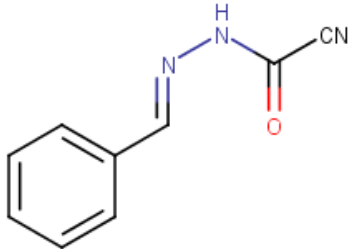
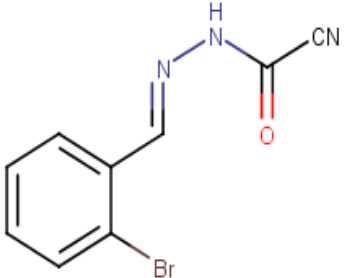
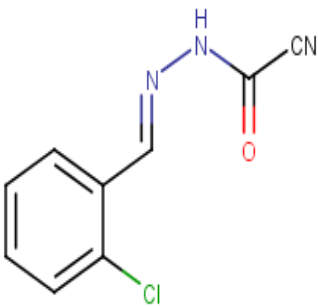
Scheme 2

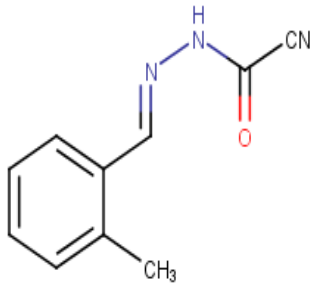
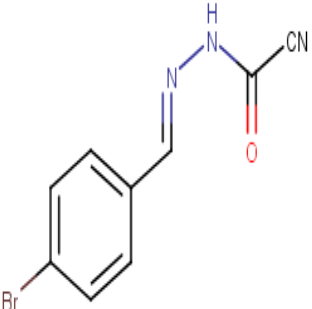
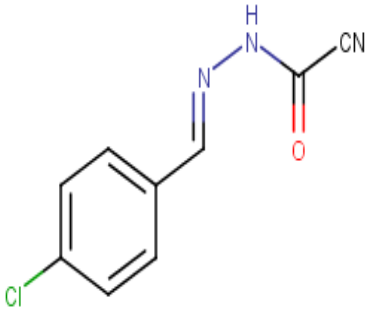
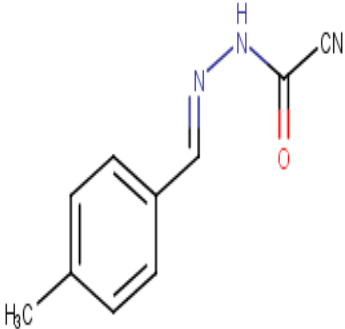
The structure of all the synthesized compounds viz., Benzaldehyde cyanoacetylhydrazone (C8), o-bromobenzaldehyde cyanoacetylhydrazone (C9), o-Chlorobenzaldehyde cyanoacetylhydrazone(C10), o-Methylbenzaldehyde cyanoacetylhydrazone(C11), p- Bromobenzaldehyde cyanoacetylhydrazone(12), p-Chlorobenzaldehyde cyanoacetylhydrazone(C13), p- Methylbenzaldehyde cyanoacetylhydrazone(C14) are characterized by IR,¹H,¹³C NMR spectral studies. The types of spectrum recorded for the synthesized compounds are listed in **Table.23**.

Table.23 Type of the spectrum recorded for the synthesized compounds.

Compounds	IR	¹ H NMR	¹³ C NMR
C8	✓	✓	✓
C9	✓	✓	✓
C10	✓	✓	✓
C11	✓	✓	✓
C12	✓	✓	✓
C13	✓	✓	✓
C14	✓	✓	✓

Table. 24 Physical data for the synthesized compounds

Compound	Structure	Molecular Formula	Molecular Weight	Melting point
C8		C ₉ H ₆ N ₃ O	172	103-105°C
C9		C ₉ H ₄ Br N ₃ O	249	109-111°C.
C10		C ₉ H ₄ Cl N ₃ O	205	122-125°C.

C11		$C_{11}H_7N_3O$	197	149-151°C
C12		$C_9H_4 Br N_3O$	249	156-159°C
C13		$C_9H_4 Cl N_3O$	454	188-131°C
C14		$C_{11}H_7N_3O$	416	119-121°C

5.14 SPECTRAL ANALYSIS OF COMPOUND BENZALDEHYDE CYANOACETYL HYDRAZONE (C8)

5.14.1 IR Spectral Analysis

IR spectrum of compound (C8) is reproduced in **Fig.50**. A strong absorption peak at 1706 cm^{-1} is characteristic peak for benzaldehyde. Hence a strong absorption band at 1683 cm^{-1} is due to carbonyl group present in the cyanoacetyl group of compound (C8).

An absorption band appeared at 1621 cm^{-1} is due to the stretching of C=N. The absorption band at 2261 cm^{-1} is due to the C≡N. Furthermore, the observed absorption band at 3195 cm^{-1} is assigned for N-H stretching.

A collection of medium bands in the region of $2963\text{-}2926\text{ cm}^{-1}$ is due to aliphatic and aromatic C-H stretching vibrations. All the observed IR bands are supporting evidences for the formation of compound C8.

IR spectral data of the compound C8 are shown in **Table 25**.

Table . 25 Characteristic IR stretching frequencies (cm^{-1}) of C8

Compound	Aliphatic and Aromatic C-H	C=O	C=N	C≡N	N-H
C8	2963-2926	1683	1621	2261	3195

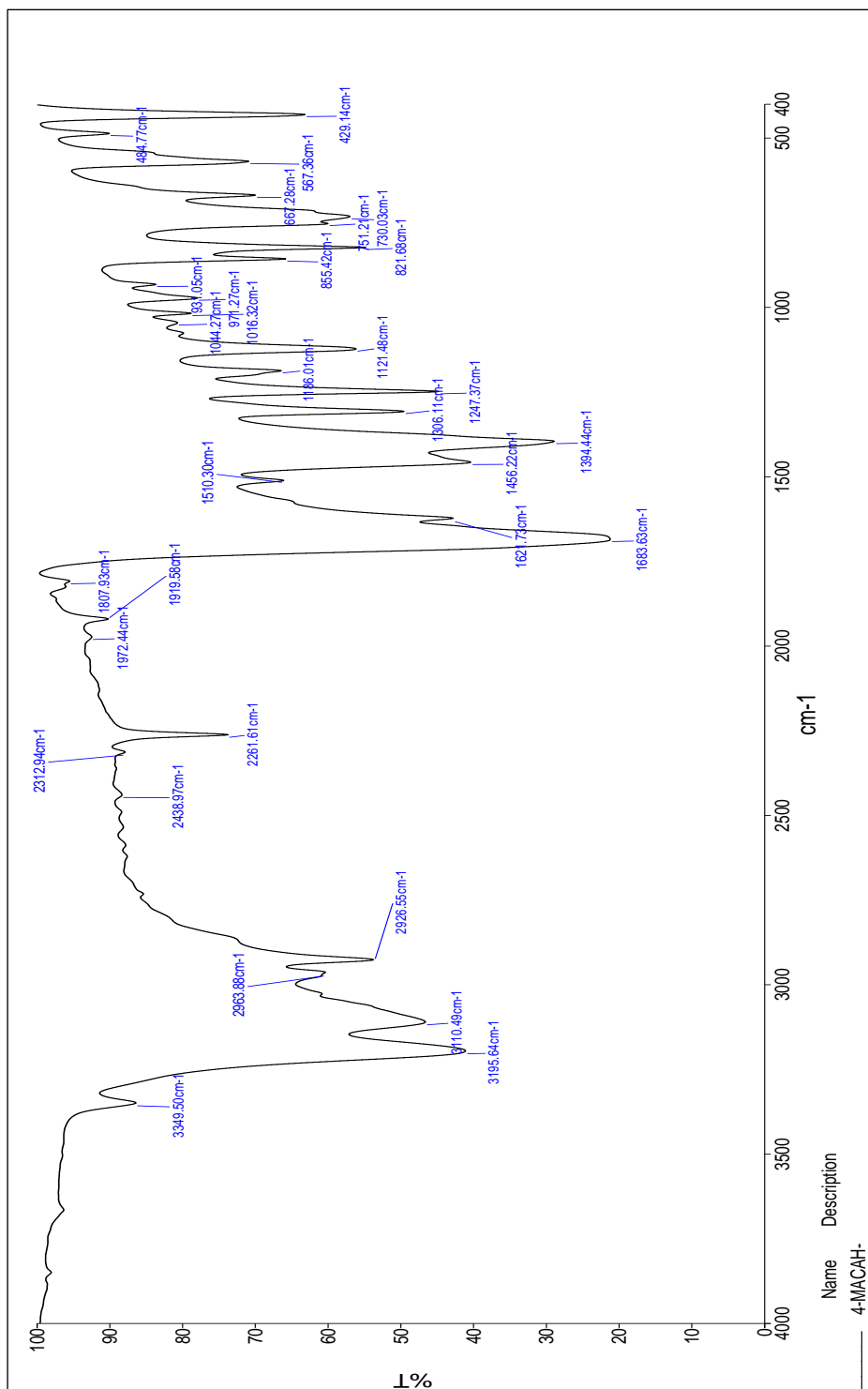


Fig. 50 IR Spectrum of compound C8

5.14.2 ¹H NMR Spectral Analysis

The ¹H NMR spectral signals are assigned by their position, multiplicity and integral values. The ¹H NMR spectrum of compound C8 is depicted in **Fig. 51a** and **Fig. 51b**.

In the NMR spectrum, there is a broad signal resonance at 9.46 ppm is due N-H proton. There are two signals at aromatic region centered at 7.45 ppm with two protons integral and a multiplet at 7.42 ppm with three proton integral values. Of the two signals, the most downfield signal at 7.45 ppm is due to the resonance of *ortho* protons of the phenyl ring and the remaining signal at 7.42 ppm is due to the resonance of *meta* and *para* protons.

In the upfield region there are two sharp singlets observed at 3.94 ppm and 2.32 ppm with two proton integrals and three proton integrals, respectively. The proton signal resonance at 3.94 ppm is due to the resonance of CH₂ protons. The proton signal resonance at 2.32 ppm is conveniently assigned for CH₂ protons.

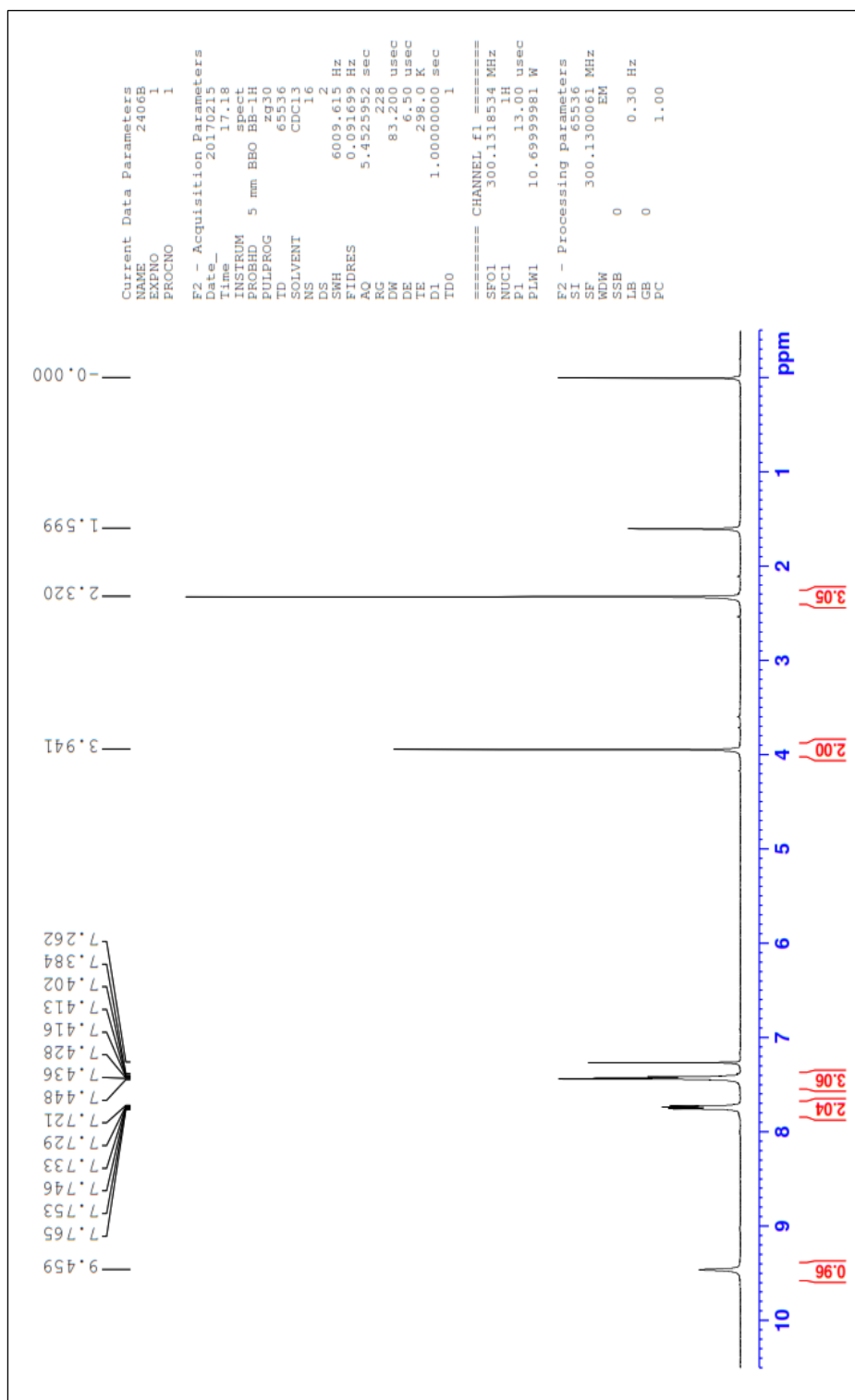


Fig. 51a ¹H NMR Spectrum of compound C8

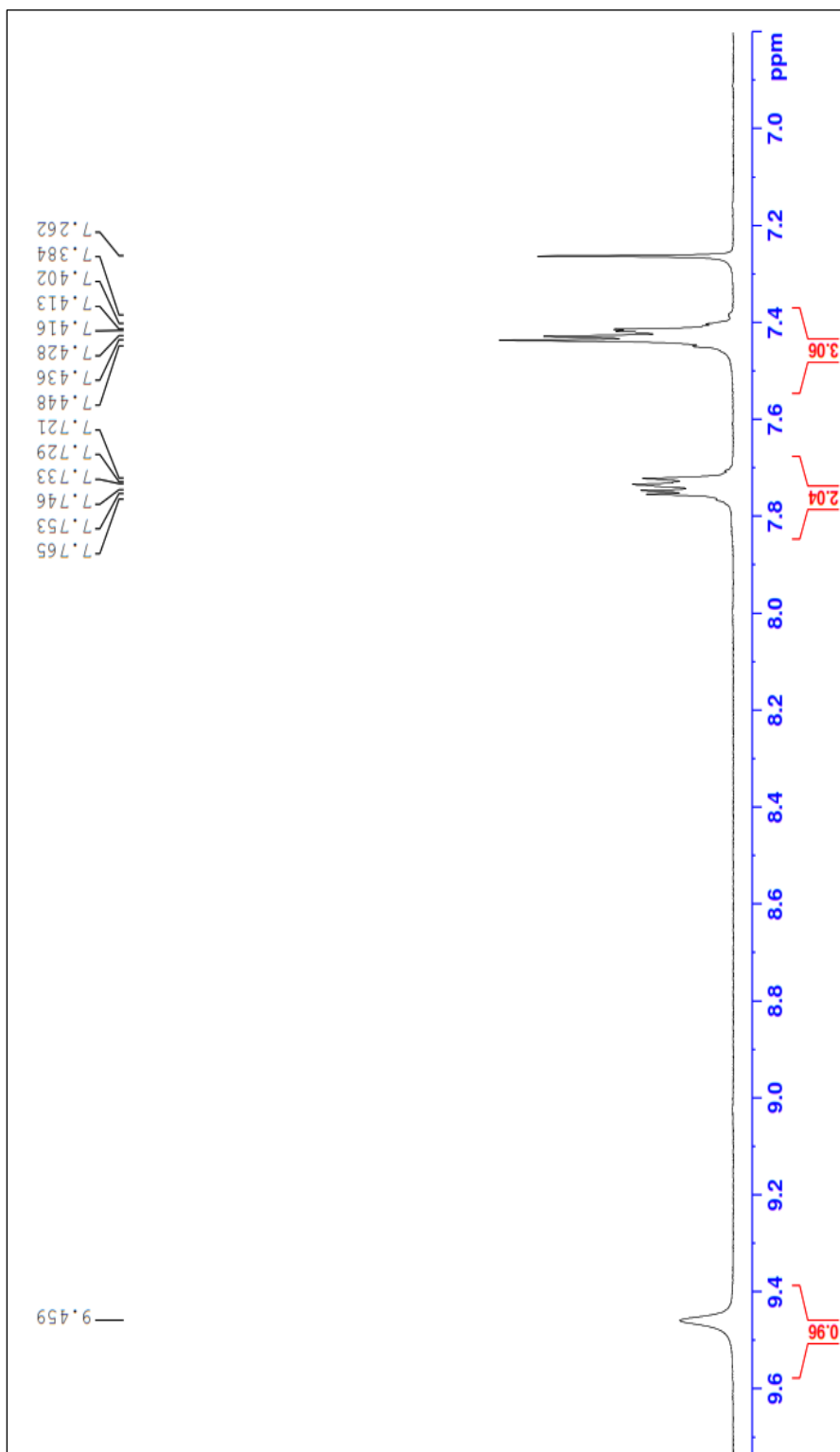


Fig. 51b ^1H NMR Spectrum of compound C8

5.14.3 ^{13}C NMR Spectral Analysis

^{13}C NMR spectroscopy is a well-established tool for the structural determination of wide-spectrum of organic compounds. The ^{13}C NMR spectral assignment has been made based on characteristic signal positions of the functional groups and comparison with those of parent ketones.

In general, the aromatic carbons present in a molecule could be very readily diagnosed from rest of the carbons due to their characteristic absorption in the region of around 120 ppm whereas the *ipso* carbons show their chemical shift at a further downfield region.

^{13}C NMR spectrum of the compound **C8** is reproduced in **Fig.52**. In the ^{13}C NMR spectrum, well resolved signals are obtained. As stated above, the *ipso* carbons of the phenyl rings could be simply distinguished from rest of the ring carbons by their characteristic downfield absorption. Hence, the signal at 137.17 ppm is due to *ipso* carbon of compound **C8** while the signals at aromatic region resonance at 130.07, 128.64 and 126.33 ppm are due to other phenyl carbons.

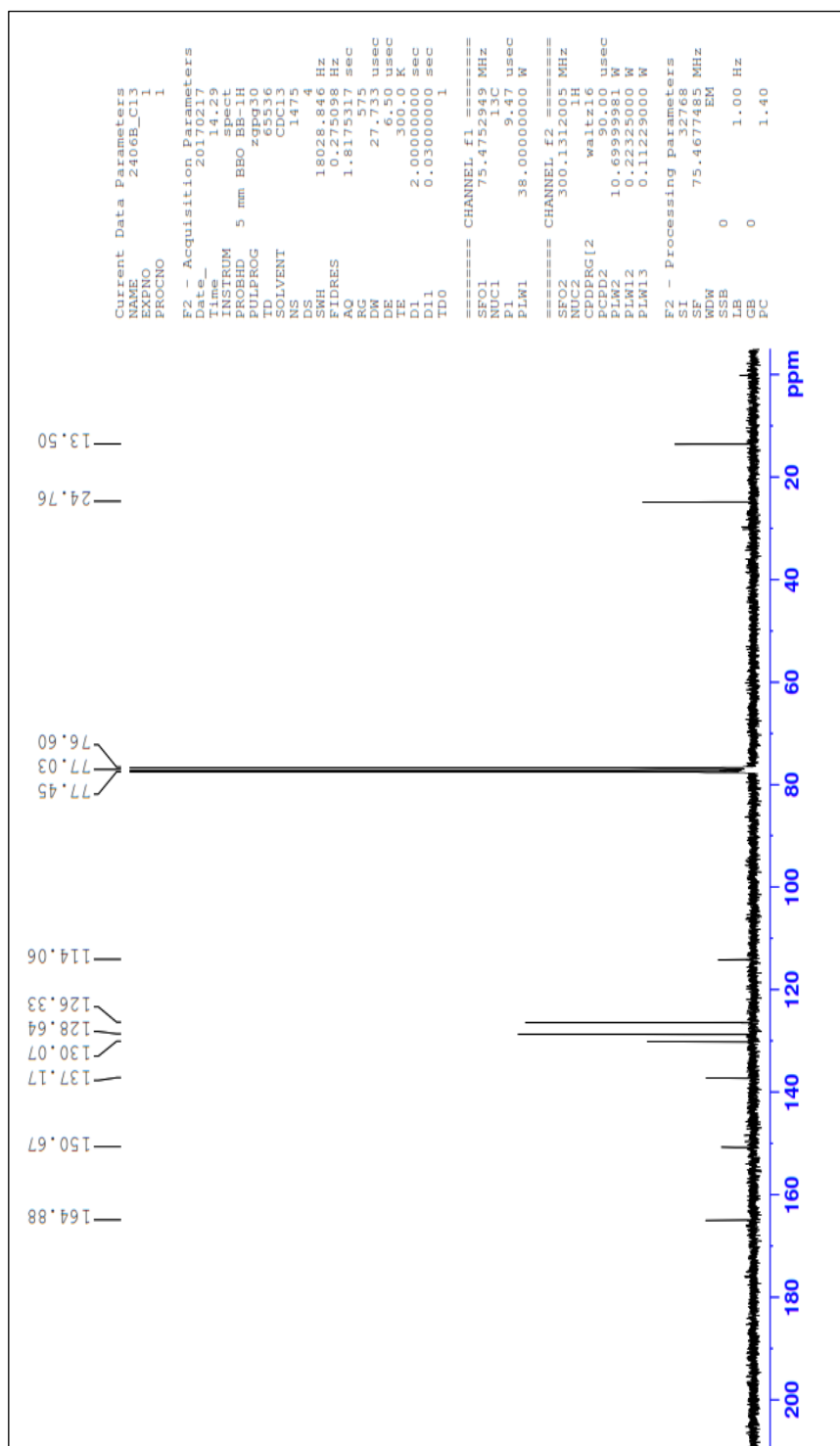


Fig. 52 ¹³C NMR Spectrum of compound C8

5.15. SPECTRAL ANALYSIS OF COMPOUND O-BROMOBENZALDEHYDE CYANOACETYL HYDRAZONE (C9)

5.15.1 IR Spectral Analysis

IR spectrum of compound (C9) is reproduced in **Fig. 53**. Hence a strong absorption band at 1683 cm^{-1} is due to carbonyl group present in the cyanoacetyl group of compound (C9).

An absorption band appeared at 1621 cm^{-1} is due to the stretching of C=N. The absorption band at 2261 cm^{-1} is due to the C≡N. Furthermore, the observed absorption band at 3195 cm^{-1} is assigned for N-H stretching.

A collection of medium bands in the region of $2963\text{-}2926\text{ cm}^{-1}$ is due to aliphatic and aromatic C-H stretching vibrations. All the observed IR bands are supporting evidences for the formation of compound C9.

IR spectral data of the compound C9 are shown in **Table 26**.

Table. 26 Characteristic IR stretching frequencies (cm^{-1}) of C9

Compound	Aliphatic and Aromatic C-H	C=O	C=N	C≡N	N-H
C9	2963-2926	1683	1621	2261	3195

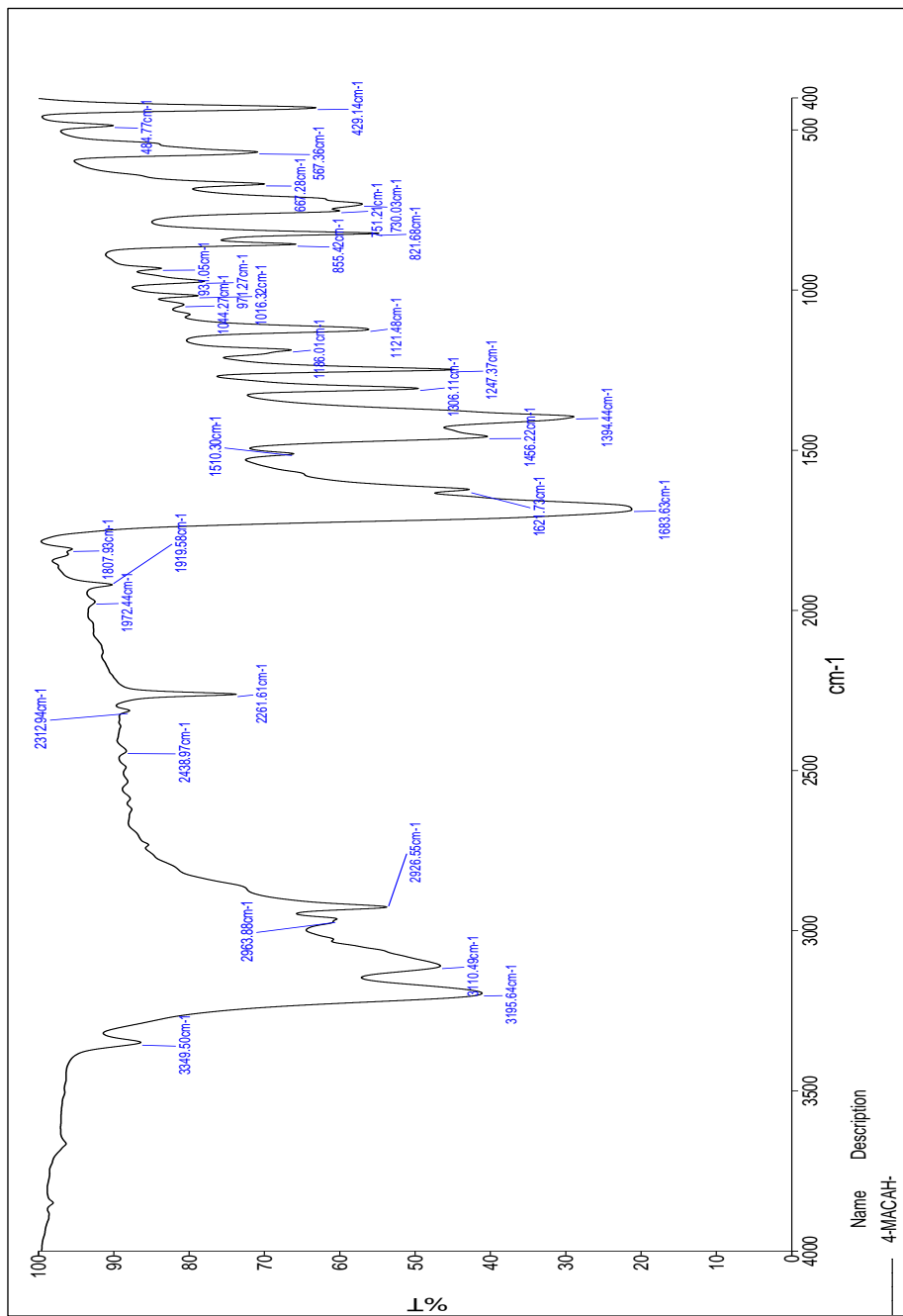


Fig. 53 IR Spectrum of compound C9

5.15.2 ^1H NMR Spectral Analysis

The ^1H NMR spectral signals are assigned by their position, multiplicity and integral values. The ^1H NMR spectrum of compound C9 is depicted in **Fig. 54**.

In the NMR spectrum, there a broad signal resonance at 9.12 ppm is due N-H proton. There are two signals at aromatic region centered at 7.43 ppm with two protons integral and a multiplet at 7.27 ppm with three proton integral values. Of the two signals, the most downfield signal at 7.43 ppm is due to the resonance of *ortho* protons of the phenyl ring and the remaining signal at 7.27 ppm is due to the resonance of *meta* and *para* protons.

In the upfield region there are two sharp singlets observed at 3.77 ppm and 2.50 ppm with two proton integrals and three proton integrals, respectively. The proton signal resonance at 3.77 ppm is due to the resonance of CH_2 protons. The proton signal resonance at 2.50 ppm is conveniently assigned for CH_2 protons.

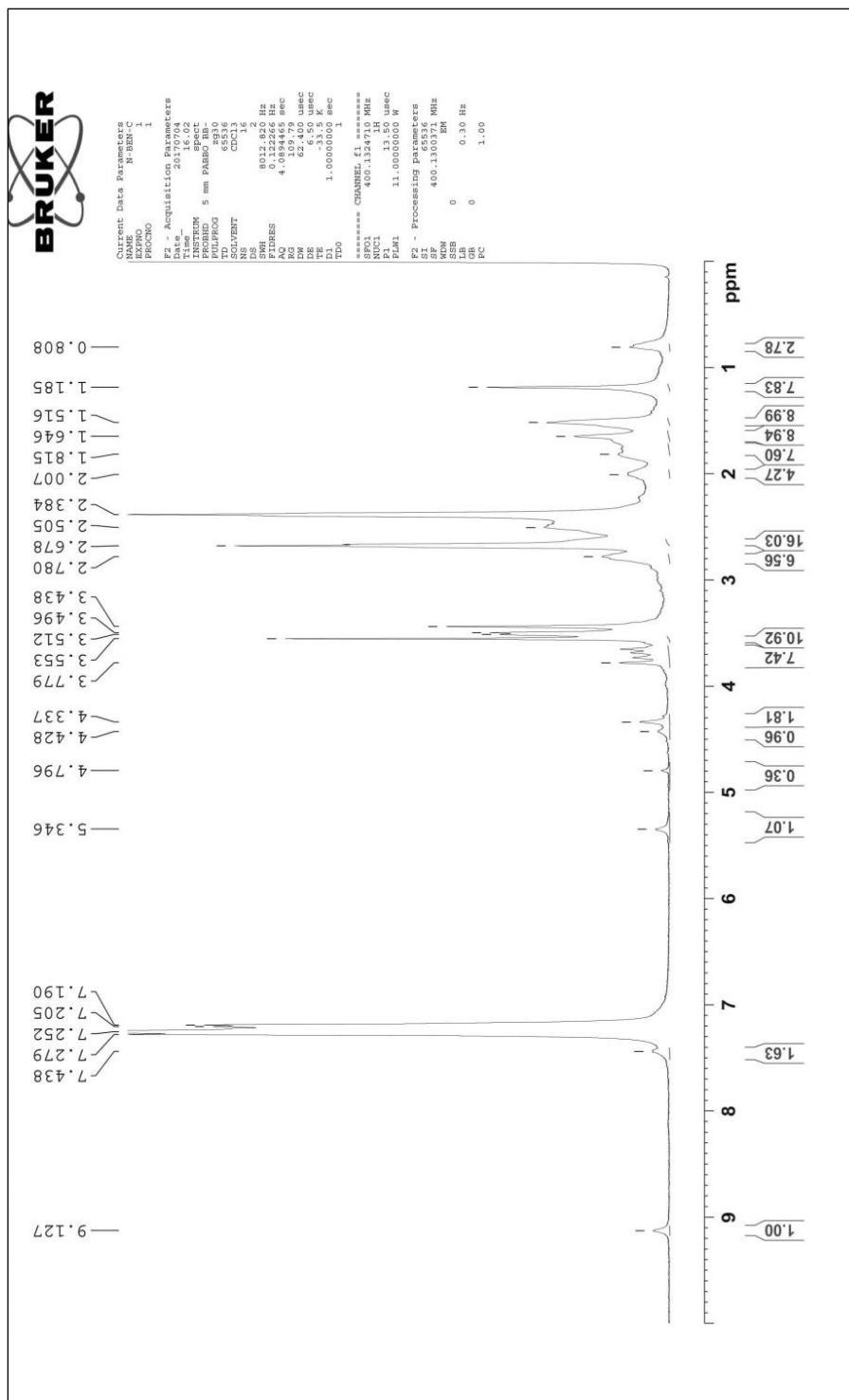


Fig. 54 ¹H NMR Spectrum of compound C9

5.15.3 ^{13}C NMR Spectral Analysis

^{13}C NMR spectroscopy is a well-established tool for the structural determination of wide-spectrum of organic compounds. The ^{13}C NMR spectral assignment has been made based on characteristic signal positions of the functional groups and comparison with those of parent ketones.

In general, the aromatic carbons present in a molecule could be very readily diagnosed from rest of the carbons due to their characteristic absorption in the region of around 120 ppm where as the *ipso* carbons show their chemical shift at a further downfield region.

^{13}C NMR spectrum of the compound **C9** is reproduced in **Fig.55**. In the ^{13}C NMR spectrum, well resolved signals are obtained. As stated above, the *ipso* carbons of the phenyl rings could be simply distinguished from rest of the ring carbons by their characteristic downfield absorption. Hence, the signal at 137.12 ppm is due to *ipso* carbon of compound **C9** while the signals at aromatic region resonance at 128.22, 128.04 and 127.90 ppm are due to other phenyl carbons.

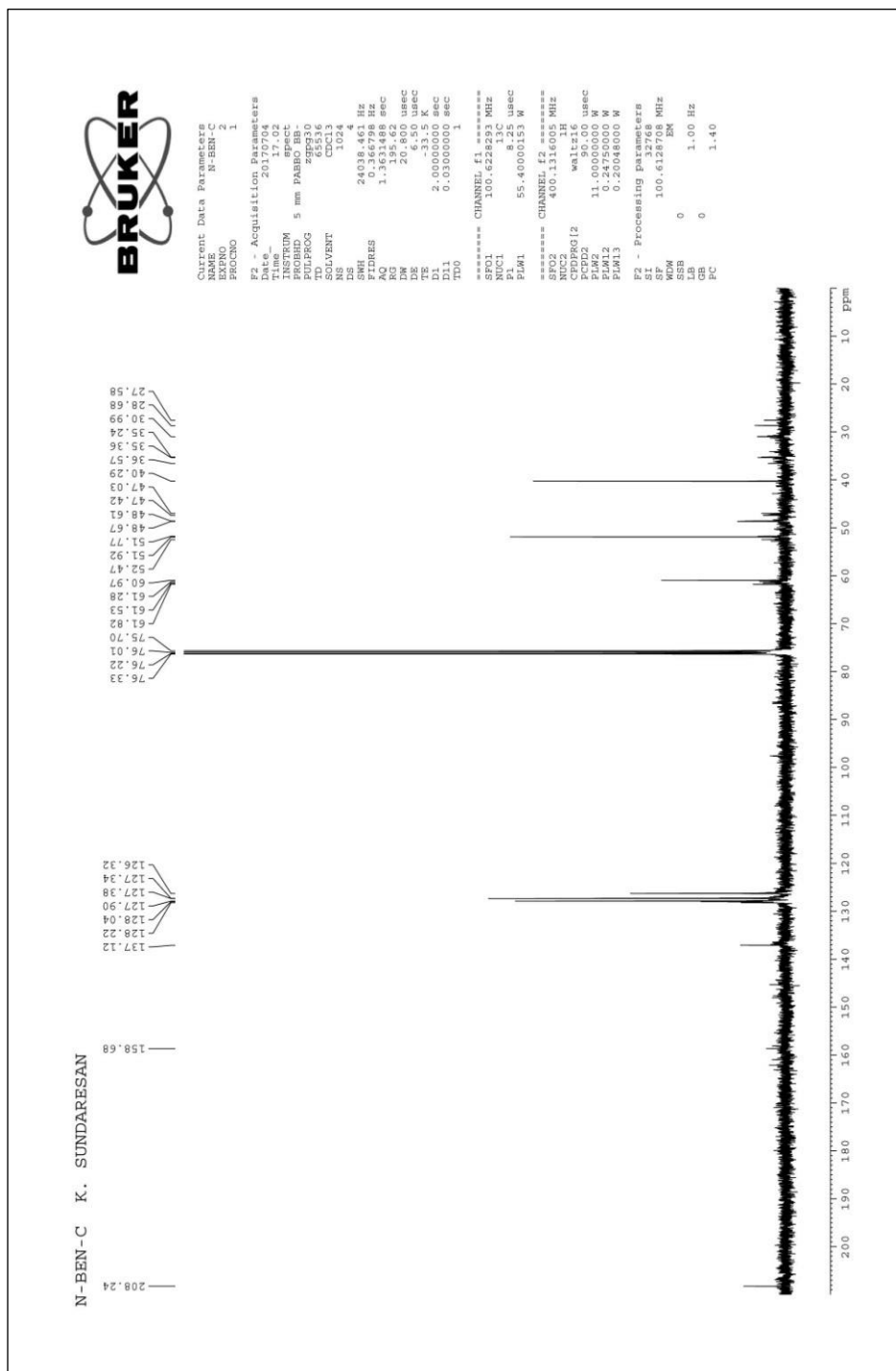


Fig. 55 ¹³C NMR Spectrum of compound C9

5.16 SPECTRAL ANALYSIS OF COMPOUND O-CHLOROBENZALDEHYDE CYANOACETYL HYDRAZONE (C10)

5.16.1 IR Spectral Analysis

IR spectrum of compound (C10) is reproduced in **Fig.56**. Hence a strong absorption band at 1716 cm^{-1} is due to carbonyl group present in the cyanoacetyl group of compound (C10).

An absorption band appeared at 1650 cm^{-1} is due to the stretching of C=N. The absorption band at 2261 cm^{-1} is due to the C≡N. Furthermore, the observed absorption band at 3066 cm^{-1} is assigned for N-H stretching.

A collection of medium bands in the region of $3024\text{-}2977\text{ cm}^{-1}$ is due to aliphatic and aromatic C-H stretching vibrations. All the observed IR bands are supporting evidences for the formation of compound C10.

IR spectral data of the compound C10 are shown in **Table 27**.

Table. 27 Characteristic IR stretching frequencies (cm^{-1}) of C10

Compound C10	Aliphatic and Aromatic C-H	C=O	C=N	C≡N	N-H
	3024-2977	1716	1650	2261	3066

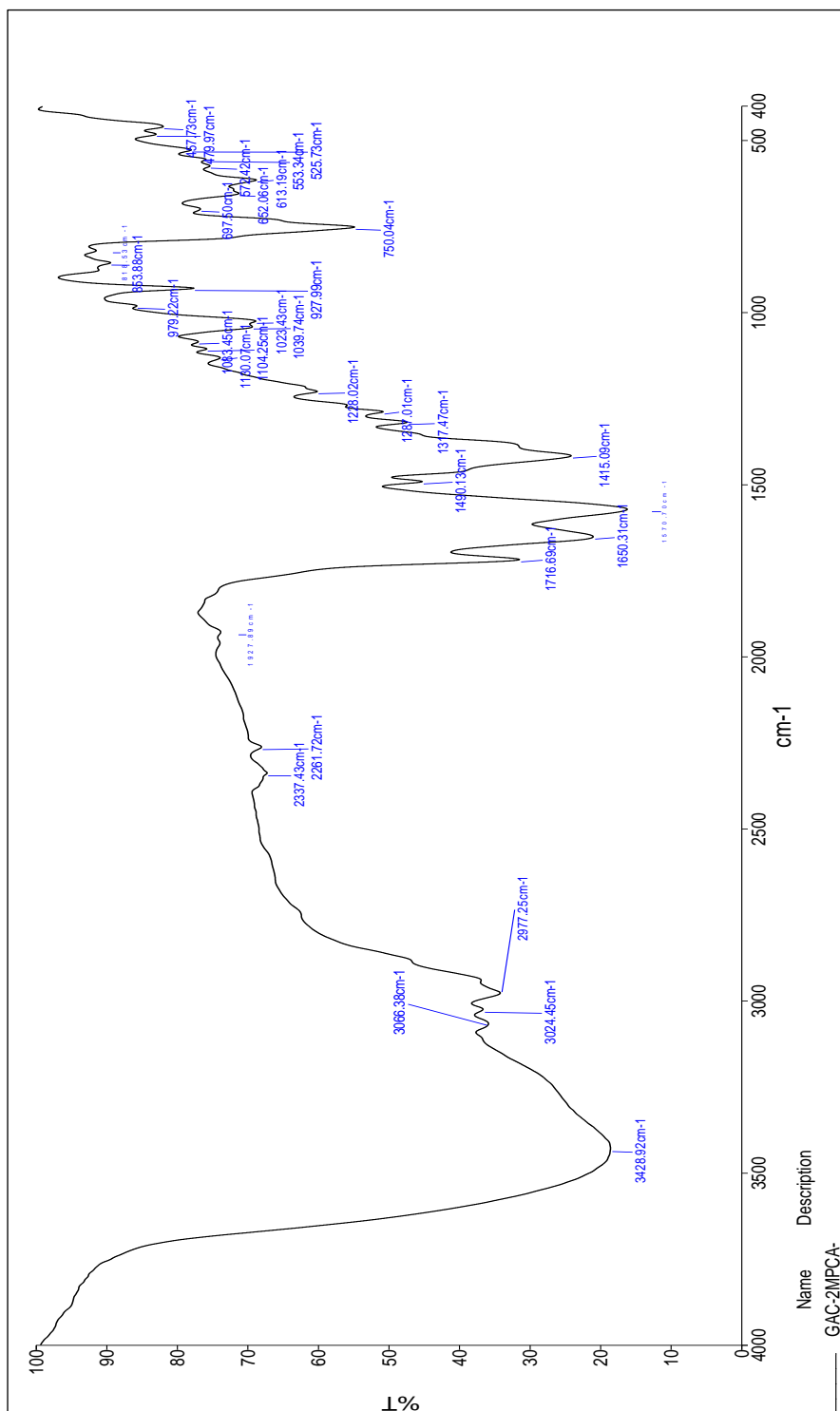


Fig. 56 ¹³C NMR Spectrum of compound C10

5.16.2 ^1H NMR Spectral Analysis

The ^1H NMR spectral signals are assigned by their position, multiplicity and integral values. The ^1H NMR spectrum of compound C10 is depicted in **Fig. 57**.

In the NMR spectrum, there a broad signal resonance at 10.59 ppm is due N-H proton. There are two signals at aromatic region centered at 7.34 ppm with two protons integral and a multiplet at 7.16 ppm with three proton integral values. Of the two signals, the most downfield signal at 7.34 ppm is due to the resonance of *ortho* protons of the phenyl ring and the remaining signal at 7.16 ppm is due to the resonance of *meta* and *para* protons.

In the upfield region there are two sharp singlets observed at 3.71 ppm and 2.36 ppm with two proton integrals and three proton integrals, respectively. The proton signal resonance at 3.71 ppm is due to the resonance of CH_2 protons. The proton signal resonance at 2.36 ppm is conveniently assigned for CH_2 protons.

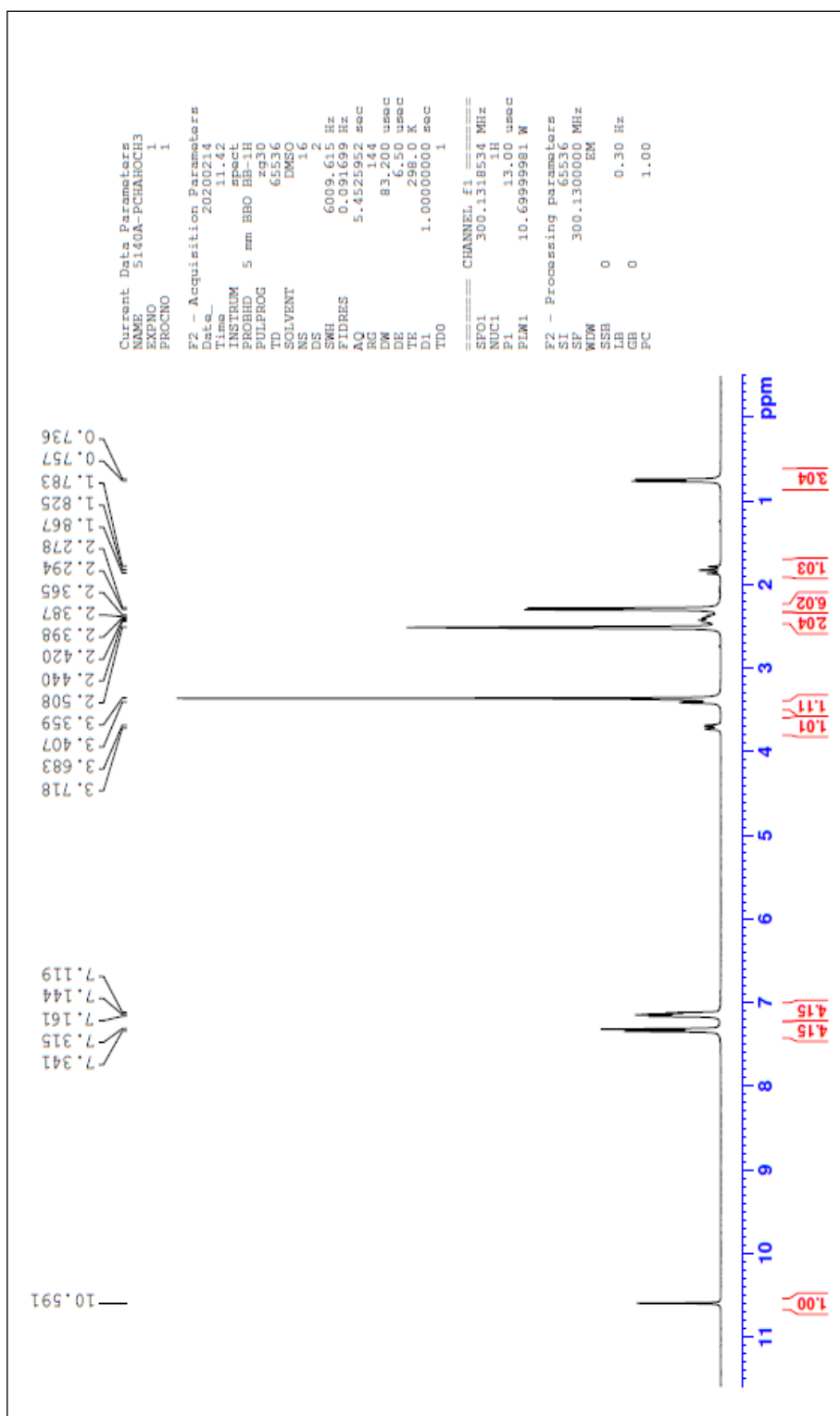


Fig. 57 ^1H NMR Spectrum of compound C10

5.16.3 ^{13}C NMR Spectral Analysis

^{13}C NMR spectroscopy is a well-established tool for the structural determination of wide-spectrum of organic compounds. The ^{13}C NMR spectral assignment has been made based on characteristic signal positions of the functional groups and comparison with those of parent ketones.

In general, the aromatic carbons present in a molecule could be very readily diagnosed from rest of the carbons due to their characteristic absorption in the region of around 120 ppm where as the *ipso* carbons show their chemical shift at a further downfield region.

^{13}C NMR spectrum of the compound **C10** is reproduced in **Fig. 58**. In the ^{13}C NMR spectrum, well resolved signals are obtained. As stated above, the *ipso* carbons of the phenyl rings could be simply distinguished from rest of the ring carbons by their characteristic downfield absorption. Hence, the signal at 163.07 ppm is due to *ipso* carbon of compound **C10** while the signals at aromatic region resonance at 161.73, 116.16 and 116.01 ppm are due to other phenyl carbons.

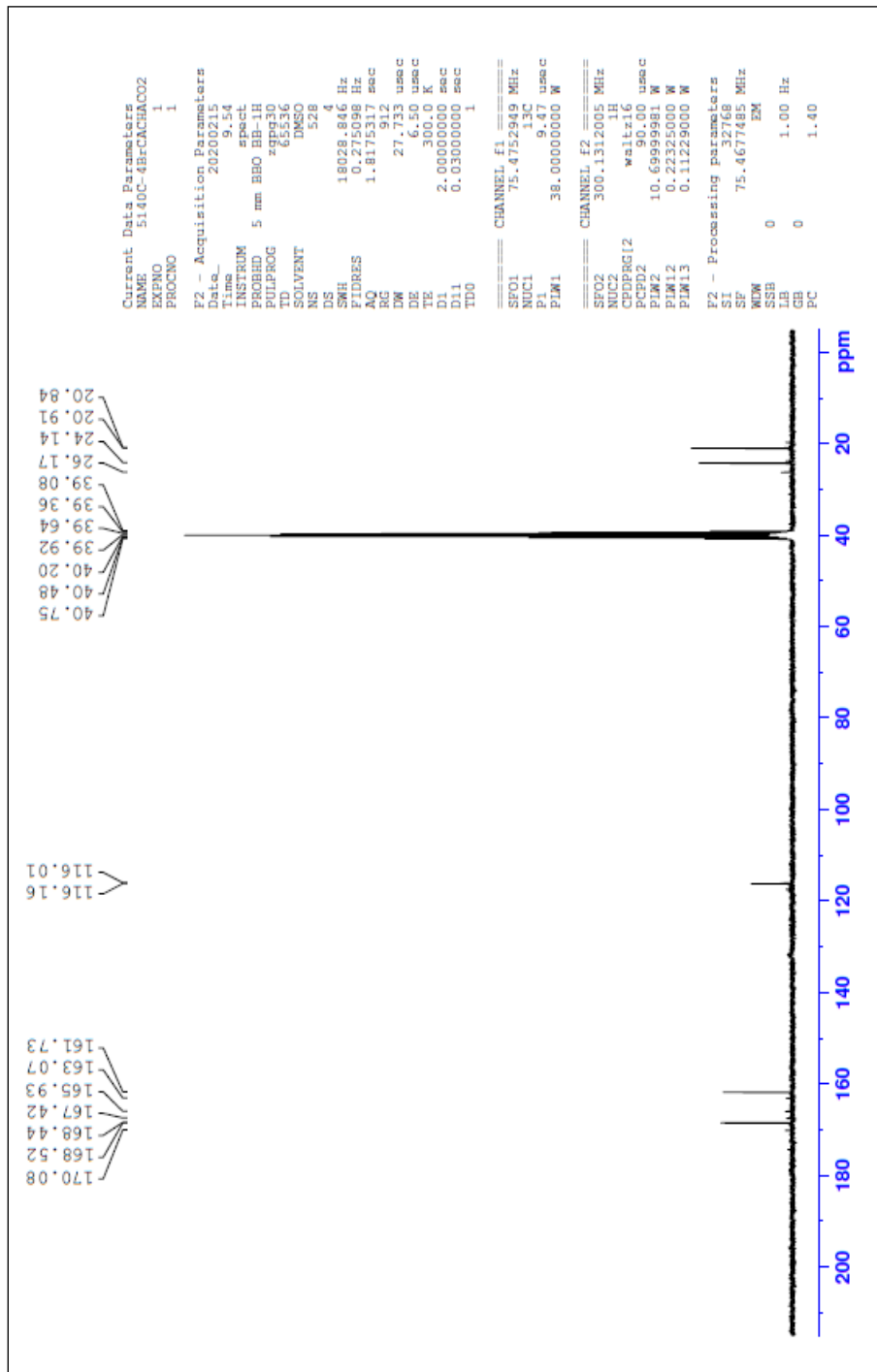


Fig. 58 ¹³C Spectrum of compound C10

5.17 SPECTRAL ANALYSIS OF COMPOUND O-METHYLBENZALDEHYDE CYANOACETYL HYDRAZONE (C11)

5.17.1 IR Spectral Analysis

IR spectrum of compound (C11) is reproduced in **Fig.59**. Hence a strong absorption band at 1647 cm^{-1} is due to carbonyl group present in the cyanoacetyl group of compound (C11).

An absorption band appeared at 1514 cm^{-1} is due to the stretching of C=N. The absorption band at 2260 cm^{-1} is due to the C≡N. Furthermore, the observed absorption band at 3026 cm^{-1} is assigned for N-H stretching.

A collection of medium bands in the region of $2977\text{-}2927\text{ cm}^{-1}$ is due to aliphatic and aromatic C-H stretching vibrations. All the observed IR bands are supporting evidences for the formation of compound C11.

IR spectral data of the compound C11 are shown in **Table 28**.

Table.28 Characteristic IR stretching frequencies (cm^{-1}) of C11

Compound C11	Aliphatic and Aromatic C-H	C=O	C=N	C≡N	N-H
	2977-2927	1647	1514	2260	3026

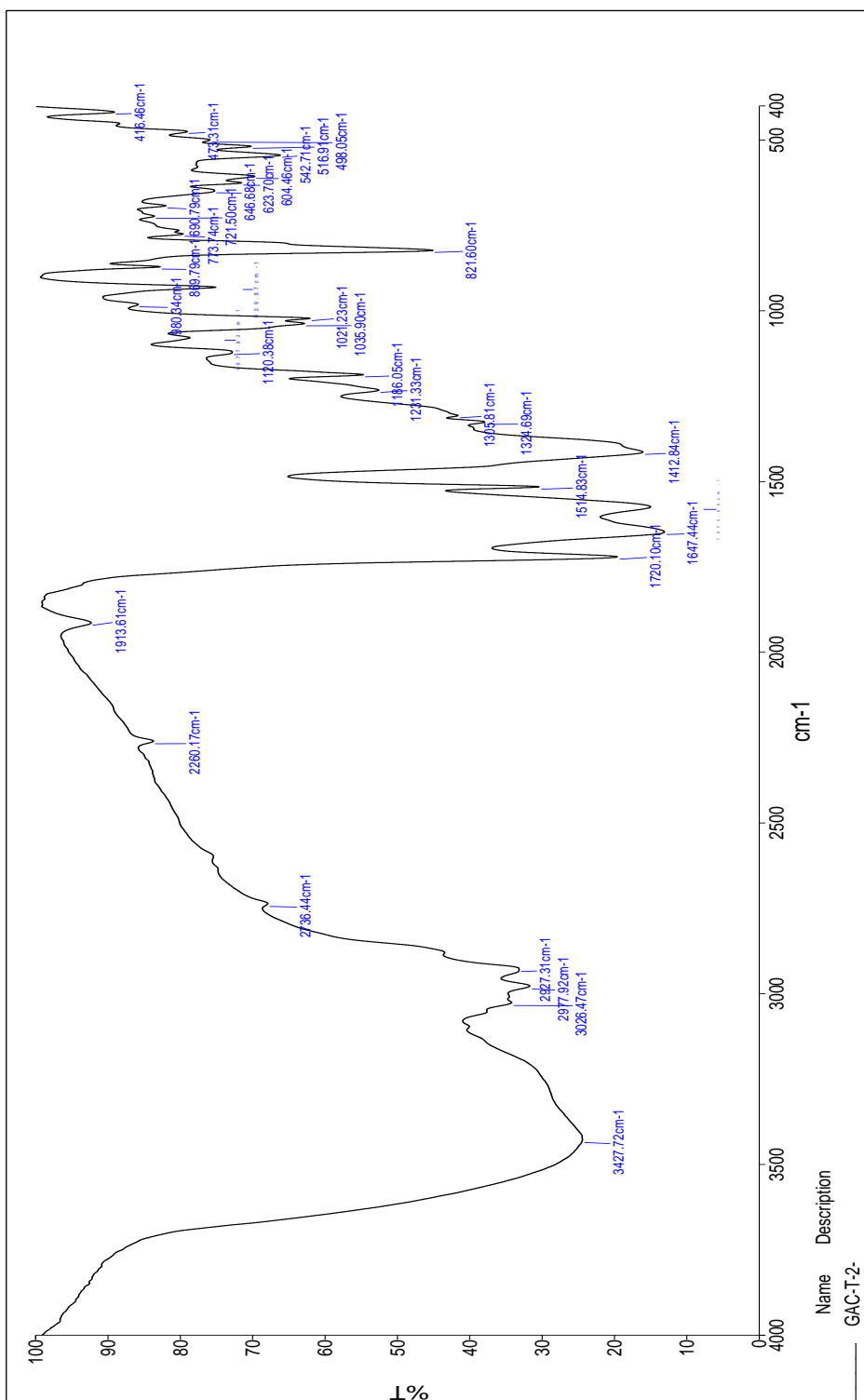


Fig. 59 IR Spectrum of compound C11

5.17.2 ¹H NMR Spectral Analysis

The ¹H NMR spectral signals are assigned by their position, multiplicity and integral values. The ¹H NMR spectrum of compound C11 is depicted in **Fig. 60**.

In the NMR spectrum, there a broad signal resonance at 8.41 ppm is due N-H proton. There are two signals at aromatic region centered at 7.21 ppm with two protons integral and a multiplet at 7.18 ppm with three proton integral values. Of the two signals, the most downfield signal at 7.21 ppm is due to the resonance of *ortho*protons of the phenyl ring and the remaining signal at 7.18 ppm is due to the resonance of *meta* and *para* protons.

In the upfield region there are two sharp singlets observed at 3.89 ppm and 2.50 ppm with two proton integrals and three proton integrals, respectively. The proton signal resonance at 3.89 ppm is due to the resonance of CH₂ protons. The proton signal resonance at 2.50 ppm is conveniently assigned for CH₂ protons.

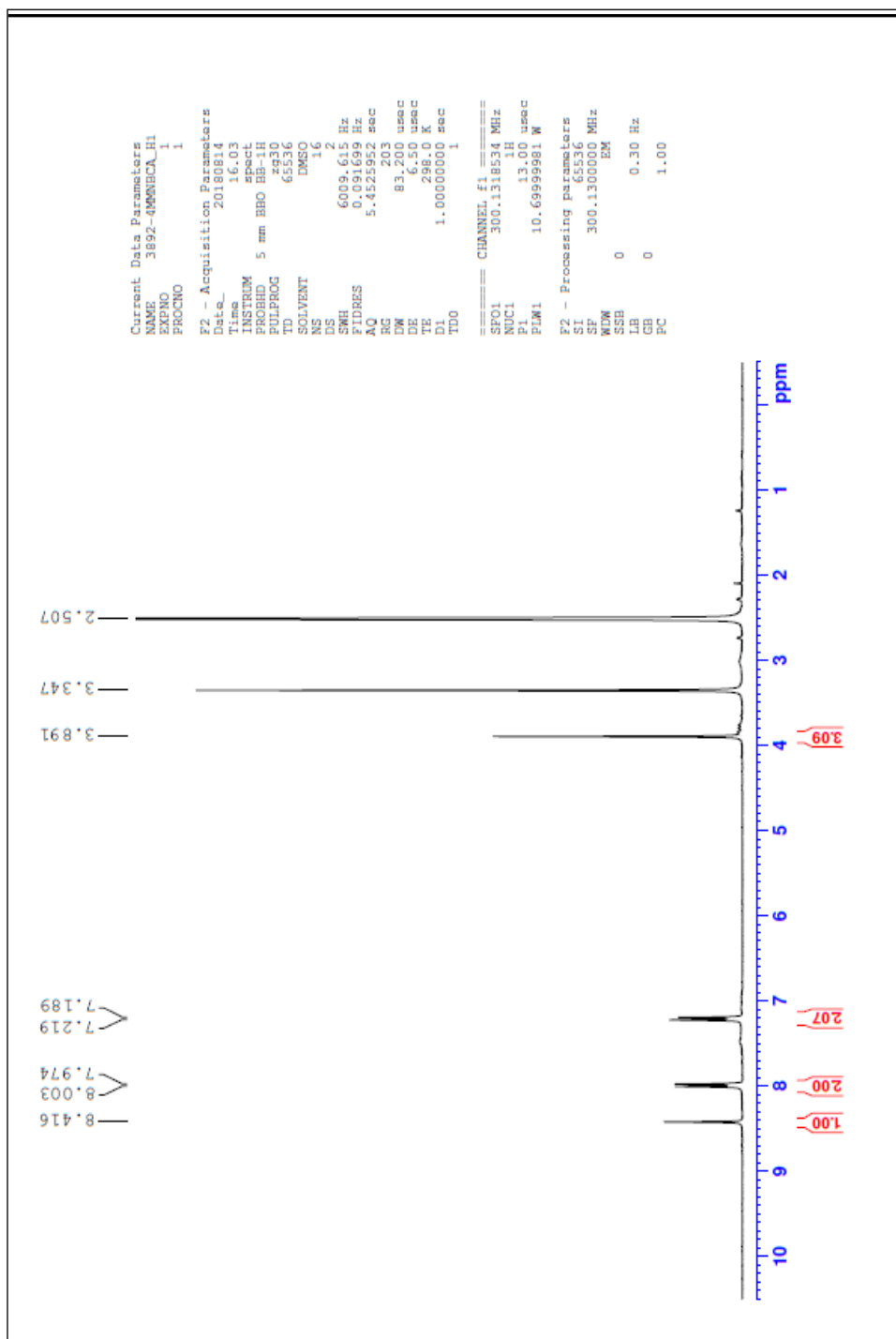


Fig. 60 ¹H NMR Spectrum of compound C11

5.17.3 ^{13}C NMR Spectral Analysis

^{13}C NMR spectroscopy is a well-established tool for the structural determination of wide-spectrum of organic compounds. The ^{13}C NMR spectral assignment has been made based on characteristic signal positions of the functional groups and comparison with those of parent ketones.

In general, the aromatic carbons present in a molecule could be very readily diagnosed from rest of the carbons due to their characteristic absorption in the region of around 120 ppm where as the *ipso* carbons show their chemical shift at a further downfield region.

^{13}C NMR spectrum of the compound **C11** is reproduced in **Fig.61**. In the ^{13}C NMR spectrum, well resolved signals are obtained. As stated above, the *ipso* carbons of the phenyl rings could be simply distinguished from rest of the ring carbons by their characteristic downfield absorption. Hence, the signal at 133.85 ppm is due to *ipso* carbon of compound **C11** while the signals at aromatic region resonance at 124.60, 128.64 and 115.68 ppm are due to other phenyl carbons.

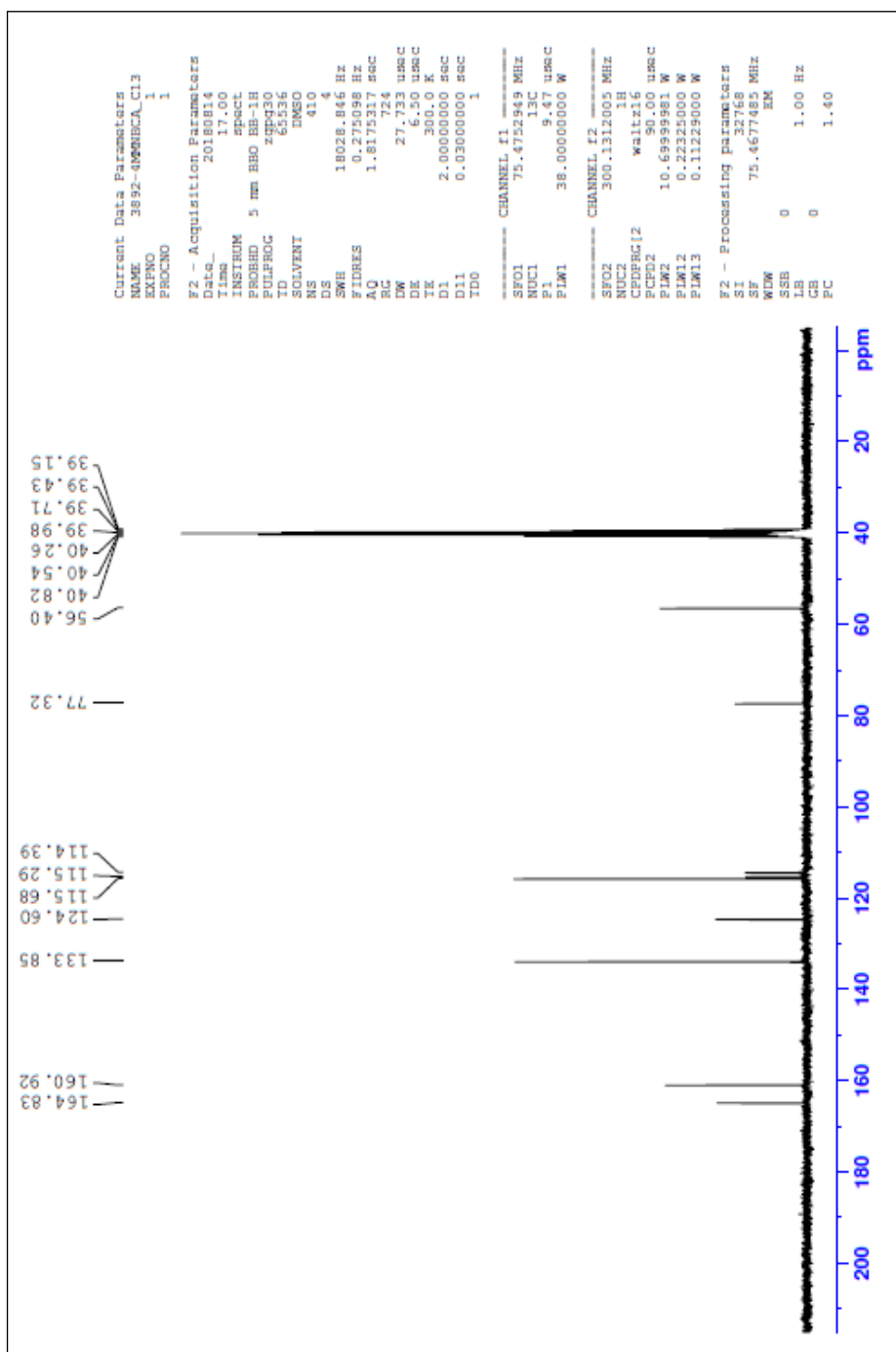


Fig. 61 ¹³C NMR Spectrum of compound C11

5.18 SPECTRAL ANALYSIS OF COMPOUND P-BROMOBENZALDEHYDE CYANOACETYLHYDRAZONE (C12)

5.18.1 IR Spectral Analysis

IR spectrum of compound (C12) is reproduced in **Fig.62**. Hence a strong absorption band at 1683 cm^{-1} is due to carbonyl group present in the cyanoacetyl group of compound (C12).

An absorption band appeared at 1573 cm^{-1} is due to the stretching of C=N. The absorption band at 2282 cm^{-1} is due to the C≡N. Furthermore, the observed absorption band at 3259 cm^{-1} is assigned for N-H stretching.

A collection of medium bands in the region of $3070\text{-}2938\text{ cm}^{-1}$ is due to aliphatic and aromatic C-H stretching vibrations. All the observed IR bands are supporting evidences for the formation of compound C12.

IR spectral data of the compound C12 are shown in **Table 29**.

Table. 29 Characteristic IR stretching frequencies (cm^{-1}) of C12

Compound C12	Aliphatic and Aromatic C-H	C=O	C=N	C≡N	N-H
	3070-2938	1683	1573	2282	3259

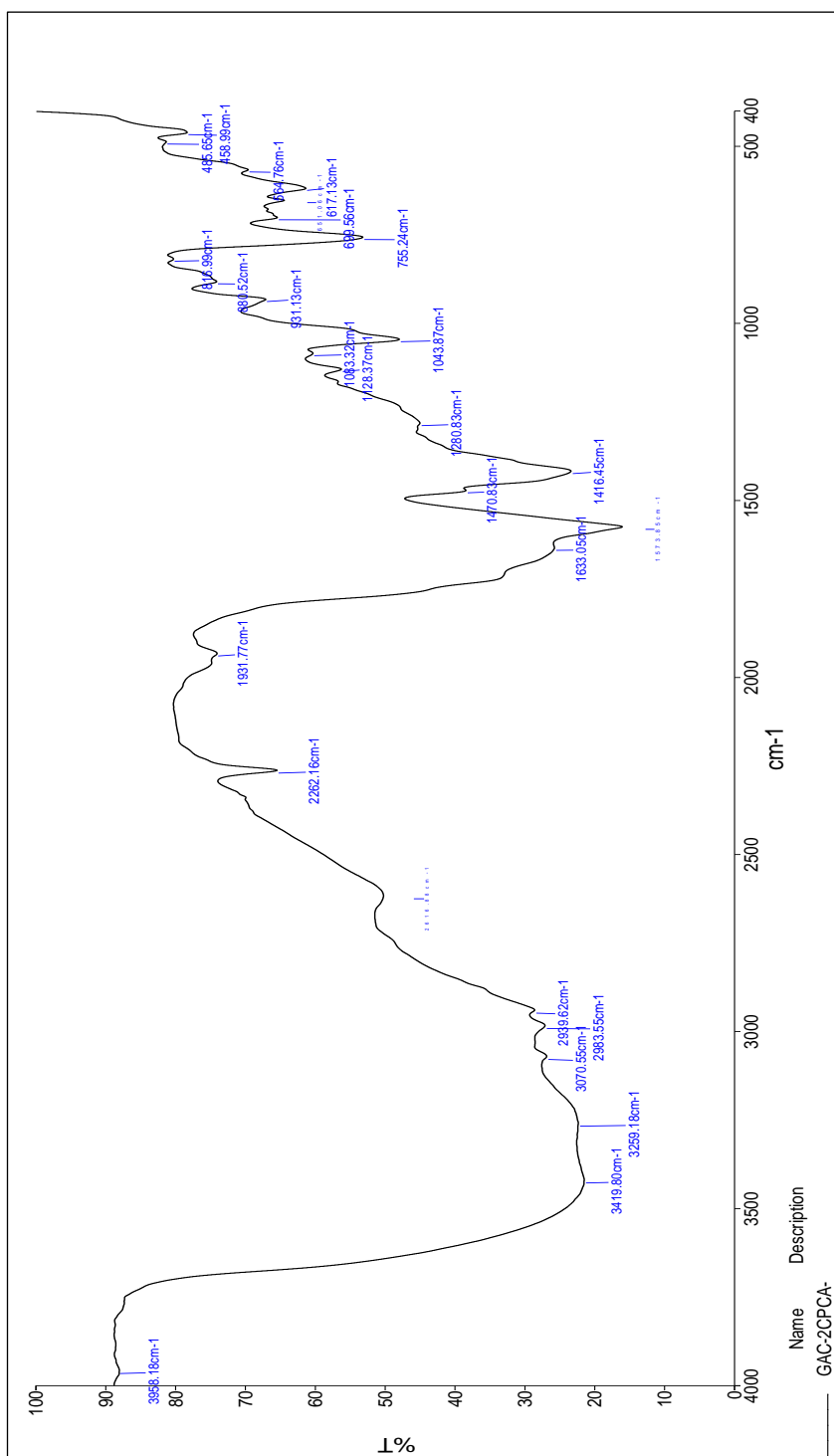


Fig. 62 IR Spectrum of compound C12

5.18.2 ¹H NMR Spectral Analysis

The ¹H NMR spectral signals are assigned by their position, multiplicity and integral values. The ¹H NMR spectrum of compound C12 is depicted in **Fig. 63**.

In the NMR spectrum, there a broad signal resonance at 7.26 ppm is due N-H proton. There are two signals at aromatic region centered at 7.12 ppm with two protons integral and a multiplet at 7.07 ppm with three proton integral values. Of the two signals, the most downfield signal at 7.12 ppm is due to the resonance of *ortho*protons of the phenyl ring and the remaining signal at 7.07 ppm is due to the resonance of *meta* and *para* protons.

In the upfield region there are two sharp singlets observed at 3.17 ppm and 2.31 ppm with two proton integrals and three proton integrals, respectively. The proton signal resonance at 3.17 ppm is due to the resonance of CH₂ protons. The proton signal resonance at 2.31 ppm is conveniently assigned for CH₂ protons.

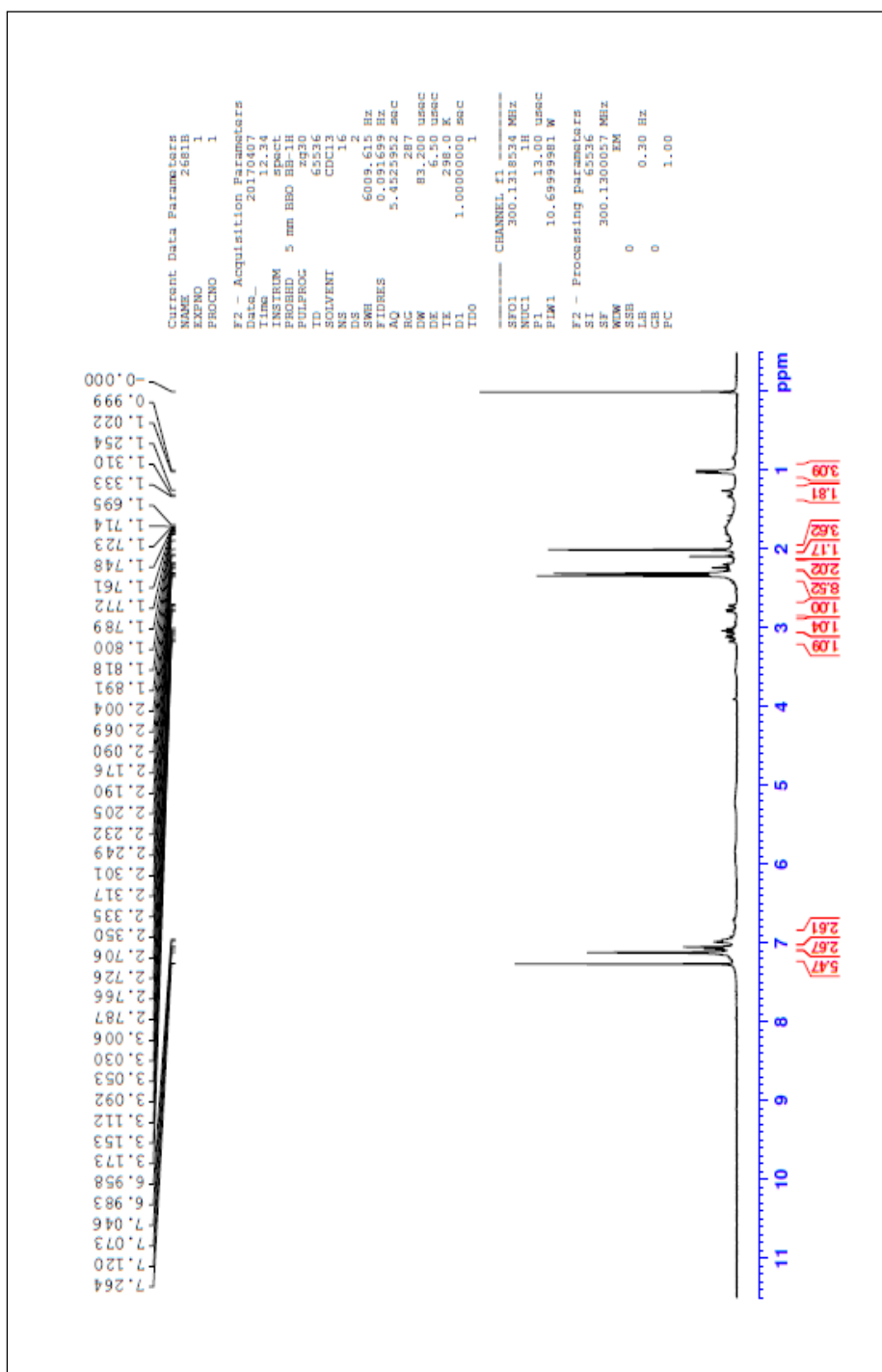


Fig. 63 ¹H NMR Spectrum of compound C12

5.18.3 ^{13}C NMR Spectral Analysis

^{13}C NMR spectroscopy is a well-established tool for the structural determination of wide-spectrum of organic compounds. The ^{13}C NMR spectral assignment has been made based on characteristic signal positions of the functional groups and comparison with those of parent ketones.

In general, the aromatic carbons present in a molecule could be very readily diagnosed from rest of the carbons due to their characteristic absorption in the region of around 120 ppm where as the *ipso* carbons show their chemical shift at a further downfield region.

^{13}C NMR spectrum of the compound **C12** is reproduced in **Fig.64**. In the ^{13}C NMR spectrum, well resolved signals are obtained. As stated above, the *ipso* carbons of the phenyl rings could be simply distinguished from rest of the ring carbons by their characteristic downfield absorption. Hence, the signal at 140.78 ppm is due to *ipso* carbon of compound **C12** while the signals at aromatic region resonance at 130.75, 128.89 and 127.72 ppm are due to other phenyl carbons.

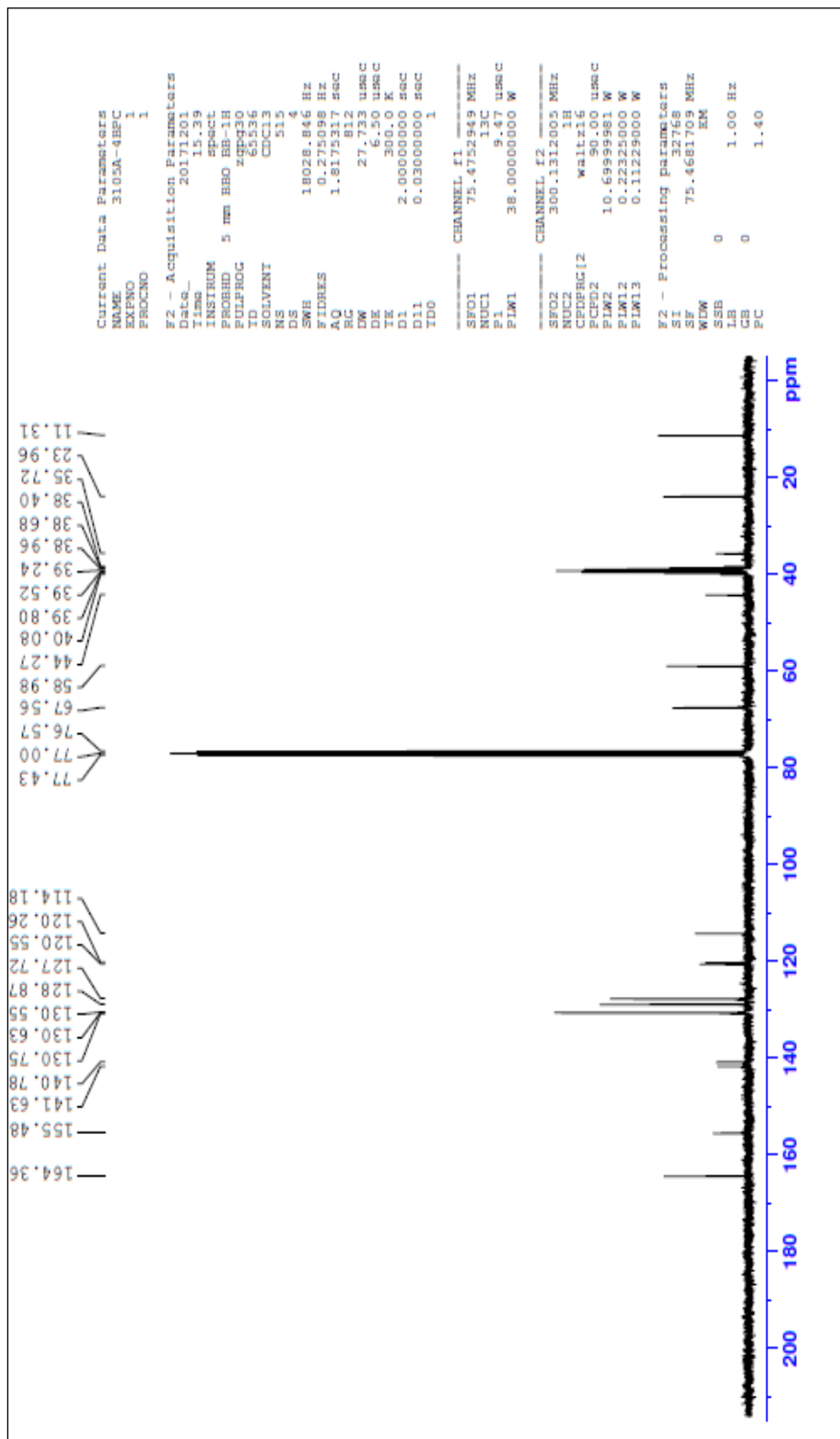


Fig . 64 ¹³C NMR Spectrum of compound C12

5.19 SPECTRAL ANALYSIS OF COMPOUND P-CHLOROBENZALDEHYDE CYANOACETYL HYDRAZONE (C13)

5.19.1 IR Spectral Analysis

IR spectrum of compound (C13) is reproduced in **Fig.65**. Hence a strong absorption band at 1708 cm^{-1} is due to carbonyl group present in the cyanoacetyl group of compound (C13).

An absorption band appeared at 1631 cm^{-1} is due to the stretching of C=N. The absorption band at 1951 cm^{-1} is due to the C≡N. Furthermore, the observed absorption band at 3251 cm^{-1} is assigned for N-H stretching.

A collection of medium bands in the region of $2978\text{-}2937\text{ cm}^{-1}$ is due to aliphatic and aromatic C-H stretching vibrations. All the observed IR bands are supporting evidences for the formation of compound C13.

IR spectral data of the compound C13 are shown in **Table 30**.

Table.30 Characteristic IR stretching frequencies (cm^{-1}) of C13

Compound C13	Aliphatic and Aromatic C-H	C=O	C=N	C≡N	N-H
	2978-2937	1708	1631	1951	3251

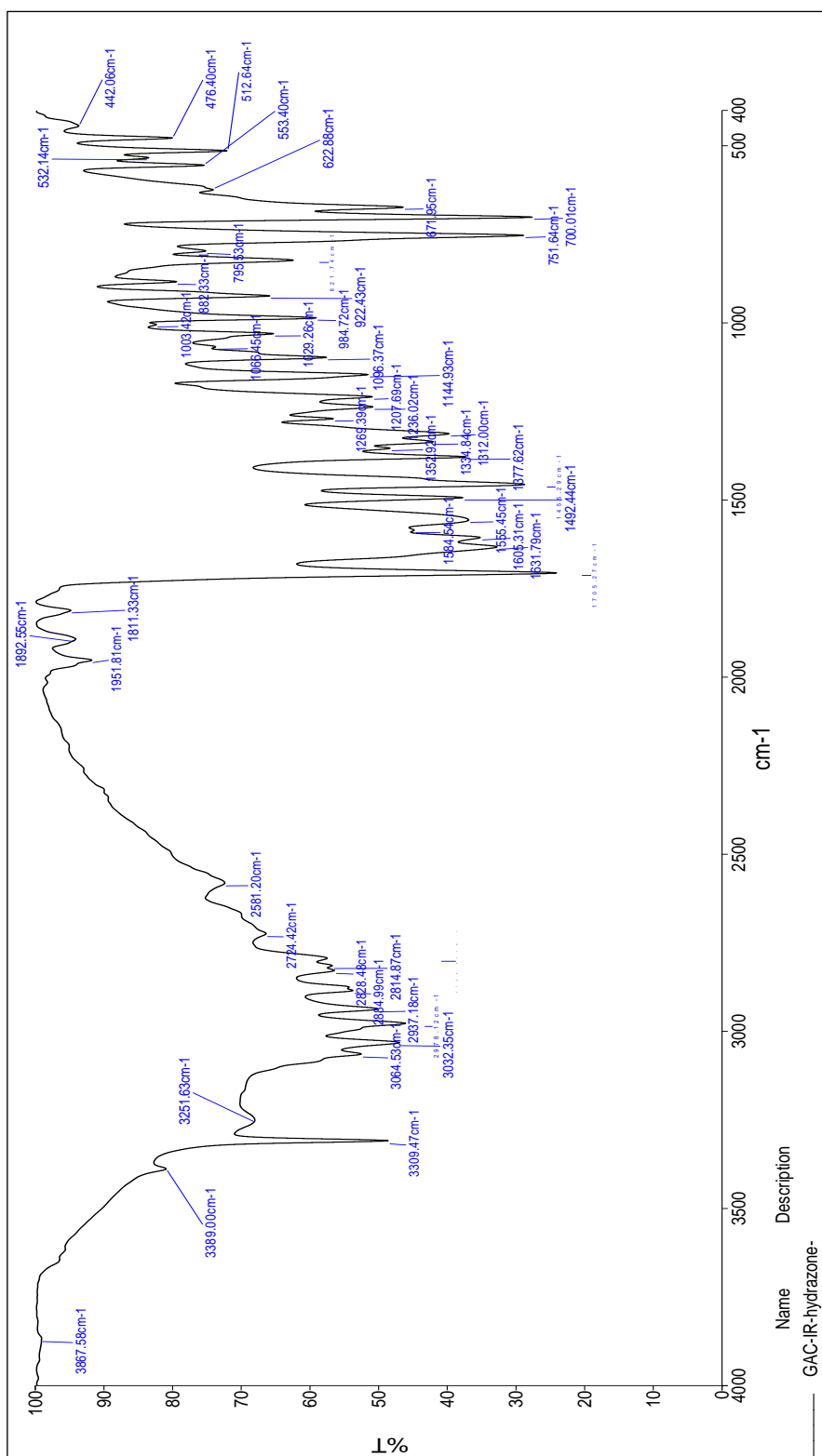


Fig. 65 IR Spectrum of compound C13

5.19.2 ¹H NMR Spectral Analysis

The ¹H NMR spectral signals are assigned by their position, multiplicity and integral values. The ¹H NMR spectrum of compound C13 is depicted in **Fig. 66**.

In the NMR spectrum, there a broad signal resonance at 10.59 ppm is due N-H proton. There are two signals at aromatic region centered at 7.34 ppm with two proton integral and a multiplet at 7.16 ppm with three proton integral value. Of the two signals, the most downfield signal at 7.34 ppm is due to the resonance of *ortho*protons of the phenyl ring and the remaining signal at 7.16 ppm is due to the resonance of *meta* and *para* protons.

In the upfield region there are two sharp singlet observed at 3.71 ppm and 2.36 ppm with two proton integrals and three proton integrals, respectively. The proton signal resonance at 3.71 ppm is due to the resonance of CH₂ protons. The proton signal resonance at 2.36 ppm is conveniently assigned for CH₂ protons.

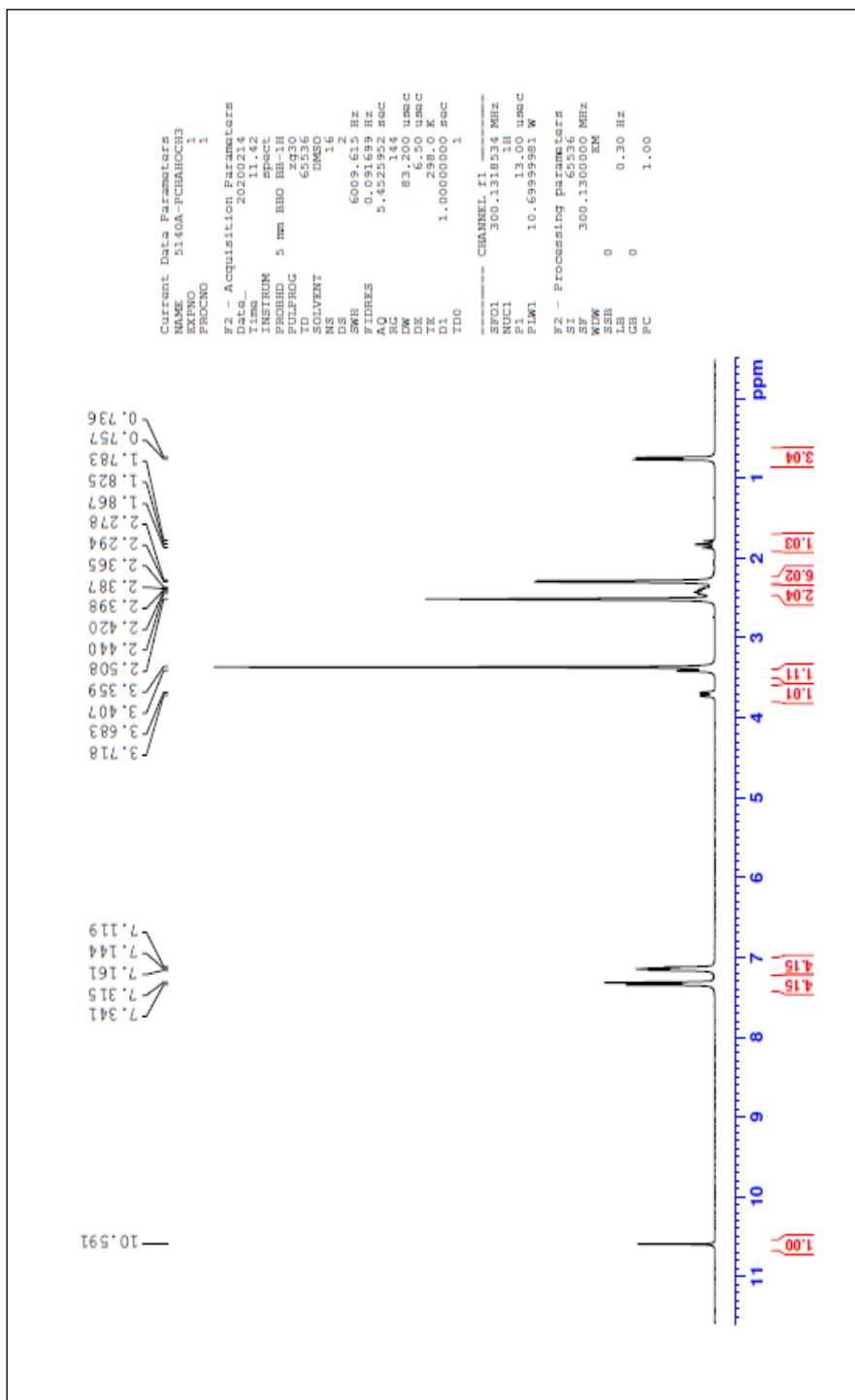


Fig. 66 ¹H NMR Spectrum of compound C13

5.19.3 ^{13}C NMR Spectral Analysis

^{13}C NMR spectroscopy is a well-established tool for the structural determination of wide-spectrum of organic compounds. The ^{13}C NMR spectral assignment has been made based on characteristic signal positions of the functional groups and comparison with those of parent ketones.

In general, the aromatic carbons present in a molecule could be very readily diagnosed from rest of the carbons due to their characteristic absorption in the region of around 120 ppm where as the *ipso* carbons show their chemical shift at a further downfield region.

^{13}C NMR spectrum of the compound **C13** is reproduced in **Fig.67**. In the ^{13}C NMR spectrum, well resolved signals are obtained. As stated above, the *ipso* carbons of the phenyl rings could be simply distinguished from rest of the ring carbons by their characteristic downfield absorption. Hence, the signal at 141.06 ppm is due to *ipso* carbon of compound **C13** while the signals at aromatic region resonance at 133.36, 129.76 and 128.75 ppm are due to other phenyl carbons.

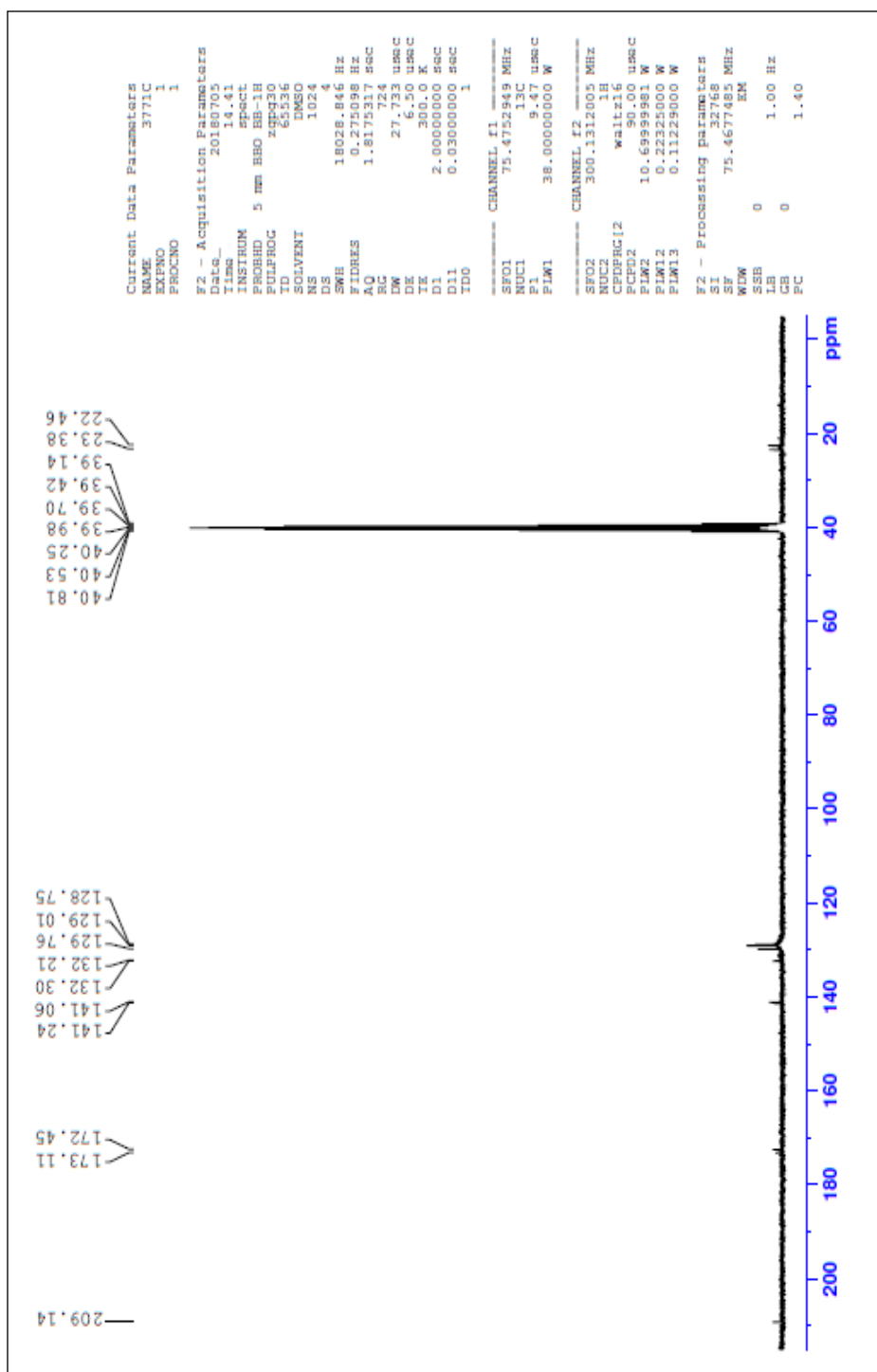


Fig. 67 ¹³C NMR Spectrum of compound C13

5.20 SPECTRAL ANALYSIS OF COMPOUND P-METHYLBENZALDEHYDE CYANOACETYL HYDRAZONE (C14)

5.20.1 IR Spectral Analysis

IR spectrum of compound (C14) is reproduced in **Fig.68**. Hence a strong absorption band at 1630 cm^{-1} is due to carbonyl group present in the cyanoacetyl group of compound (C14).

An absorption band appeared at 1455 cm^{-1} is due to the stretching of C=N. The absorption band at 2209 cm^{-1} is due to the C≡N. Furthermore, the observed absorption band at 3358 cm^{-1} is assigned for N-H stretching.

A collection of medium bands in the region of $2924\text{-}2856\text{ cm}^{-1}$ is due to aliphatic and aromatic C-H stretching vibrations. All the observed IR bands are supporting evidences for the formation of compound C14.

IR spectral data of the compound C14 are shown in **Table 31**.

Table.31 Characteristic IR stretching frequencies (cm^{-1}) of C14

Compound C14	Aliphatic and Aromatic C-H	C=O	C=N	C≡N	N-H
	2924-2856	1630	1455	2209	3358

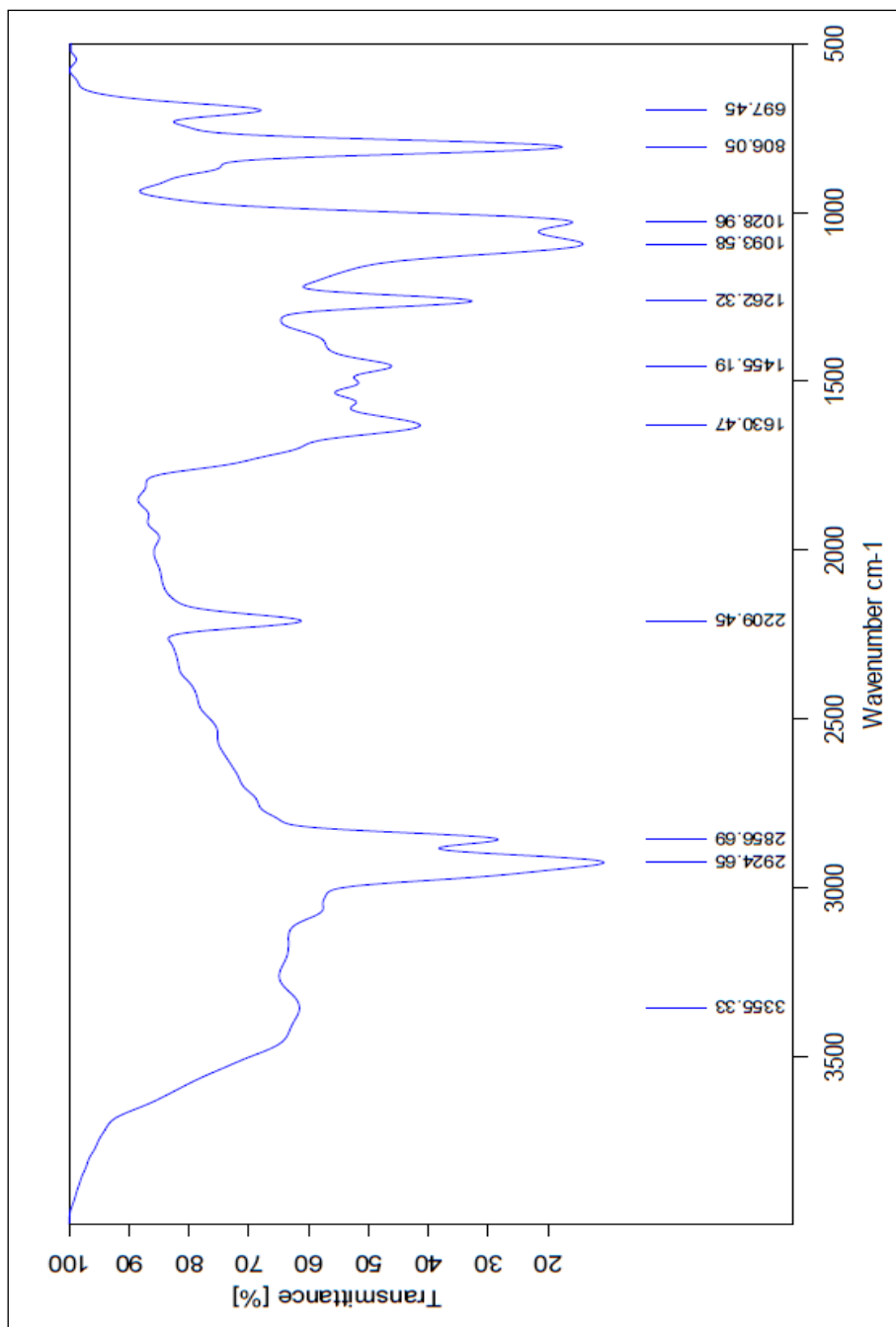


Fig. 68 IR Spectrum of compound C14

5.20.2 ¹H NMR Spectral Analysis

The ¹H NMR spectral signals are assigned by their position, multiplicity and integral values. The ¹H NMR spectrum of compound C14 is depicted in **Fig. 69**.

In the NMR spectrum, there a broad signal resonance at 7.25 ppm is due N-H proton. There are two signals at aromatic region centered at 7.10 ppm with two protons integral and a multiplet at 6.17 ppm with three proton integral values. Of the two signals, the most downfield signal at 7.10 ppm is due to the resonance of *ortho* protons of the phenyl ring and the remaining signal at 6.17 ppm is due to the resonance of *meta* and *para* protons.

In the upfield region there are two sharp singlets observed at 3.93 ppm and 2.32 ppm with two proton integrals and three proton integrals, respectively. The proton signal resonance at 3.93 ppm is due to the resonance of CH₂ protons. The proton signal resonance at 2.32 ppm is conveniently assigned for CH₂ protons.

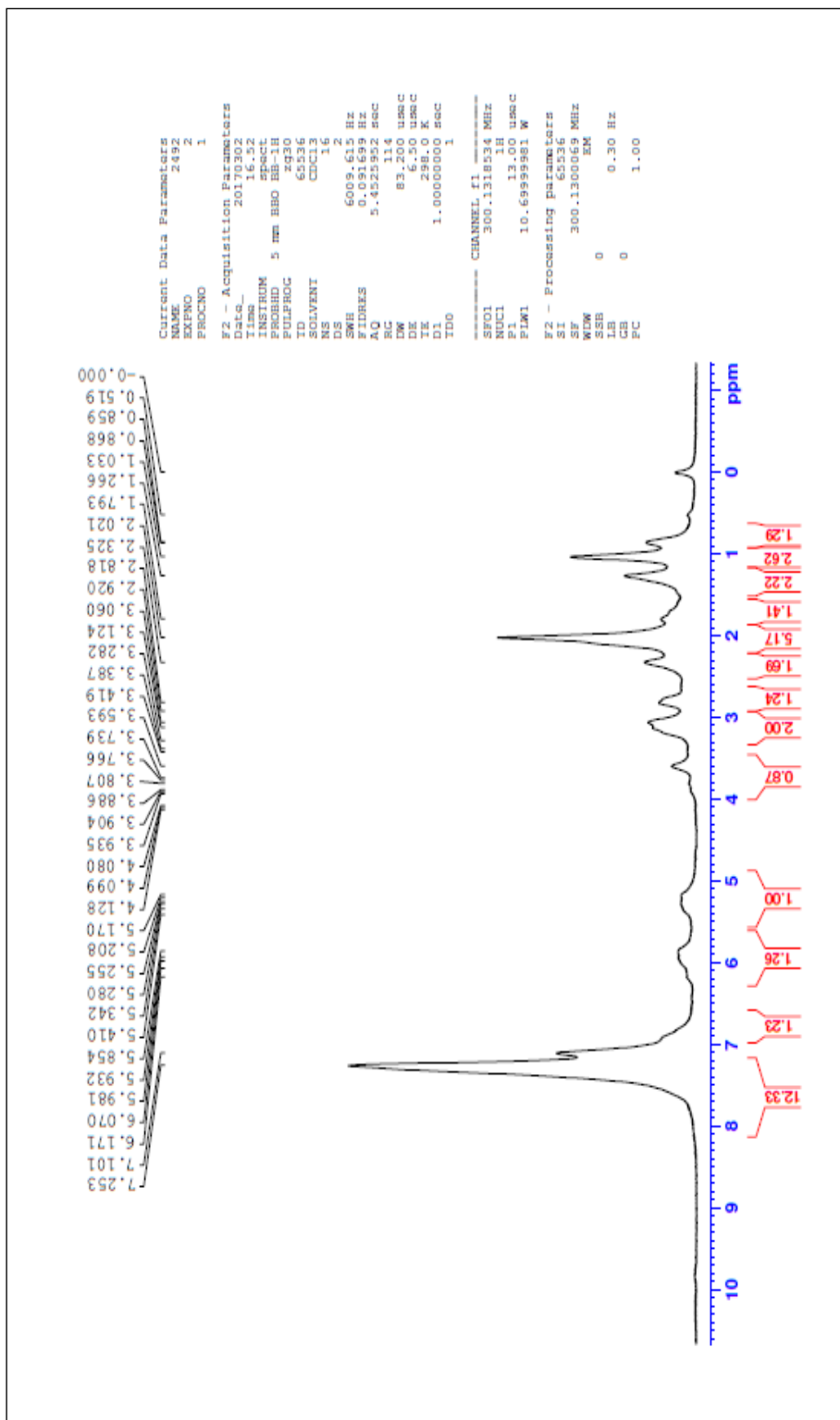


Fig. 69 ¹H NMR Spectrum of compound C14

5.20.3 ^{13}C NMR Spectral Analysis

^{13}C NMR spectroscopy is a well-established tool for the structural determination of wide-spectrum of organic compounds. The ^{13}C NMR spectral assignment has been made based on characteristic signal positions of the functional groups and comparison with those of parent ketones.

In general, the aromatic carbons present in a molecule could be very readily diagnosed from rest of the carbons due to their characteristic absorption in the region of around 120 ppm where as the *ipso* carbons show their chemical shift at a further downfield region.

^{13}C NMR spectrum of the compound **C14** is reproduced in **Fig.70**. In the ^{13}C NMR spectrum, well resolved signals are obtained. As stated above, the *ipso* carbons of the phenyl rings could be simply distinguished from rest of the ring carbons by their characteristic downfield absorption. Hence, the signal at 141.17 ppm is due to *ipso* carbon of compound **C14** while the signals at aromatic region resonance at 128.92, 128.66 and 126.82 ppm are due to other phenyl carbons.

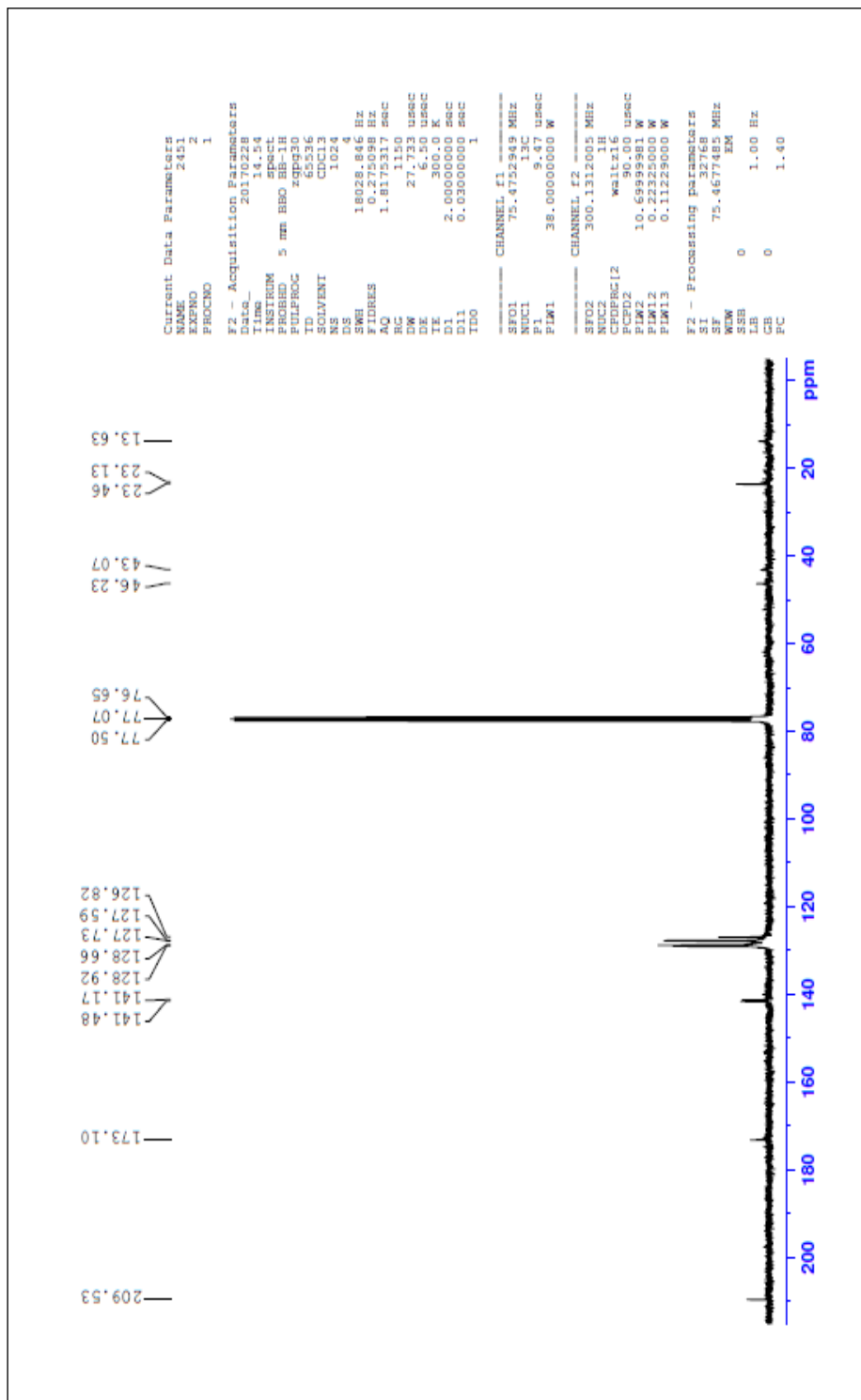


Fig . 70 ¹³C NMR Spectrum of compound C14

5.21 Invitro anti –Obesity activity

Among the various concentrations (100 µg/ml, 200 µg/ml, 300 µg/ml, 400 µg/ml, 500 µg/ml) of synthesized compounds, the highest doses (500 µg/ml) of all synthesized compounds have greatest inhibition (lipase) activity shown in **Table 32**.

Anti-obesity activity analysis of compound C8 was 13.93±0.97 for 100 µg/mL, 19.66±3.64 for 200 µg/mL, 29.29±3.37 for 300 µg/mL, 53.81±3.35 for 400 µg/mL, 71.15±4.35 for 500 µg/mL for Lipase activity. The IC₅₀ value is 337.49.

Anti-obesity activity analysis of compound C9 was 16.27±1.91 for 100 µg/mL, 23.56±4.14 for 200 µg/mL, 39.81±3.48 for 300 µg/mL, 68.17±5.81 for 400 µg/mL, 79.63±7.01 for 500 µg/mL for Lipase activity. The IC₅₀ value is 301.01.

Anti-obesity activity analysis of compound C10 was 18.64±1.36 for 100 µg/mL, 31.49±3.33 for 200 µg/mL, 51.65±3.61 for 300 µg/mL, 72.43±5.07 for 400 µg/mL, 86.32±6.04 for 500 µg/mL for Lipase activity. The IC₅₀ value is 277.81.

Anti-obesity activity analysis of compound C11 was 14.19±1.10 for 100 µg/mL, 26.43±1.92 for 200 µg/mL, 44.54±2.04 for 300 µg/mL, 65.91±4.61 for 400 µg/mL, 80.45±5.63 for 500 µg/mL for Lipase activity. The IC₅₀ value is 290.11.

Anti-obesity activity analysis of compound C12 was 16.94±1.18 for 100 µg/mL, 28.41±1.98 for 200 µg/mL, 53.26±3.72 for 300 µg/mL, 65.37±4.57 for 400 µg/mL, 80.45±5.35 for 500 µg/mL for Lipase activity. The IC₅₀ value is 290.11.

Anti-obesity activity analysis of compound C13 was 17.46±1.22 for 100 µg/mL, 31.26±2.18 for 200 µg/mL, 55.41±3.87 for 300 µg/mL, 68.37±4.57 for 400 µg/mL, 83.04±5.81 for 500 µg/mL for Lipase activity. The IC₅₀ value is 293.93.

Anti-obesity activity analysis of compound C14 was 14.39 ± 1.01 for $100 \mu\text{g/mL}$, 24.65 ± 1.72 for $200 \mu\text{g/mL}$, 40.98 ± 2.86 for $300 \mu\text{g/mL}$, 61.04 ± 4.27 for $400 \mu\text{g/mL}$, 78.05 ± 5.46 for $500 \mu\text{g/mL}$ for Lipase activity. The IC_{50} value is 347.49.

Anti-obesity activity (lipase activity) of standard (Orlistst) 20.63 ± 1.44 for $100 \mu\text{g/mL}$, 37.41 ± 2.61 for $200 \mu\text{g/mL}$, 60.02 ± 4.20 for $300 \mu\text{g/mL}$, 75.34 ± 5.27 for $400 \mu\text{g/mL}$, 94.67 ± 6.62 for $500 \mu\text{g/mL}$ for Lipase activity. The IC_{50} value is 259.08.

Lipase are involves inhibition of dietary triglyceride absorption, as this is the main sources of excess calories. The lowest inhibition of obesity activity of C8, C9, C10, C11, C12, C13, C14 and Orlistst were 13.93 ± 0.97 , 16.27 ± 1.91 , 18.64 ± 1.36 , 14.19 ± 1.10 , 16.94 ± 1.18 , 17.46 ± 1.22 , 14.39 ± 1.01 and 20.63 ± 1.44 in the concentration of $100 \mu\text{g/mL}$ respectively while the highest inhibition of obesity activity of C8, C9, C10, C11, C12, C13, C14 and Orlistat were 71.15 ± 4.35 , 79.63 ± 7.01 , 86.32 ± 6.04 , 80.45 ± 5.63 , 80.45 ± 5.35 , 83.04 ± 5.81 , 78.05 ± 5.46 and 94.67 ± 6.62 in the concentration of $500 \mu\text{g/mL}$ respectively.

Table . 32 Anti-obesity activity (Pancreatic lipase inhibitory activity) of Synthesized compound

Samples	Concentrations $\mu\text{g/ml}$					IC ₅₀ value ($\mu\text{g/ml}$)
	100 $\mu\text{g/ml}$	200 $\mu\text{g/ml}$	300 $\mu\text{g/ml}$	400 $\mu\text{g/ml}$	500 $\mu\text{g/ml}$	
C8 Parent	13.93±0.97	19.66±3.64	29.29±3.37	53.81±3.35	71.15±4.35	337.49
C9 O-Br	16.27±1.91	23.56±4.14	39.81±3.48	68.17±5.81	79.63±7.01	301.01
C10 O-Cl	18.64±1.36	31.49±3.33	51.65±3.61	72.43±5.07	86.32±6.04	277.81
C11 O-Me	14.19±1.10	26.43±1.92	44.54±2.04	65.91±4.61	80.45±5.63	290.11
C12 P-Br	16.94±1.18	28.41±1.98	53.26±3.72	65.37±4.57	80.48±5.63	308.50
C13 P-Cl	17.46±1.22	31.26±2.18	55.41±3.87	65.37±4.57	83.04±5.81	293.93
C14 P-Me	14.39±1.01	24.65±1.72	40.98±2.86	61.04±4.27	78.05±5.46	347.75
Std. (Orlistat)	20.63±1.44	37.41±2.61	60.02±4.20	75.34±5.27	94.67±6.62	259.08

Values were expressed as Mean \pm SD for triplicates

Lipase inhibition of synthesized compounds as shown in **figures 71-77**.

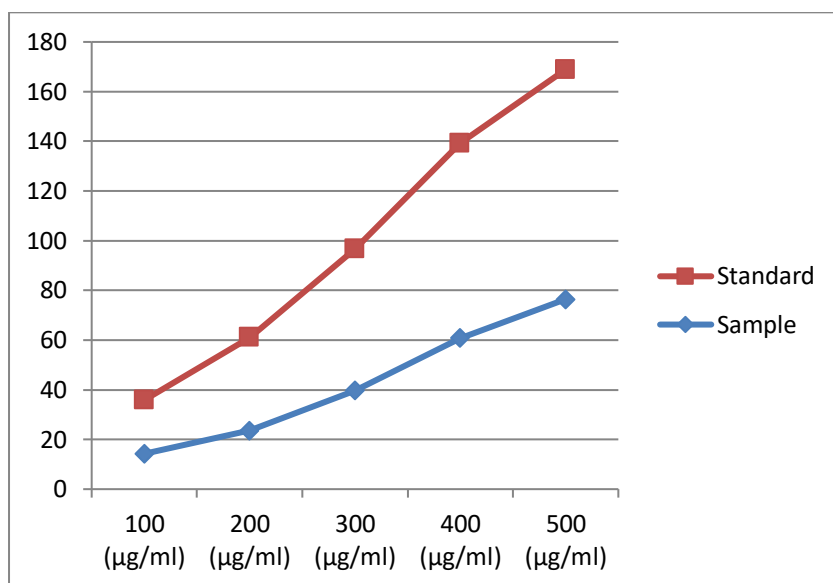


Figure 71. Pancreatic lipase inhibition of compound C8

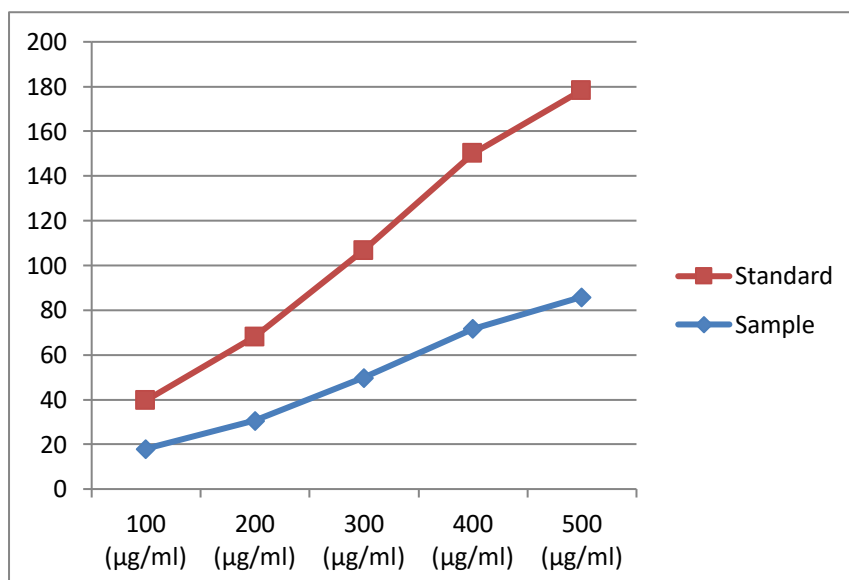


Figure 72. Pancreatic lipase inhibition of compound C9

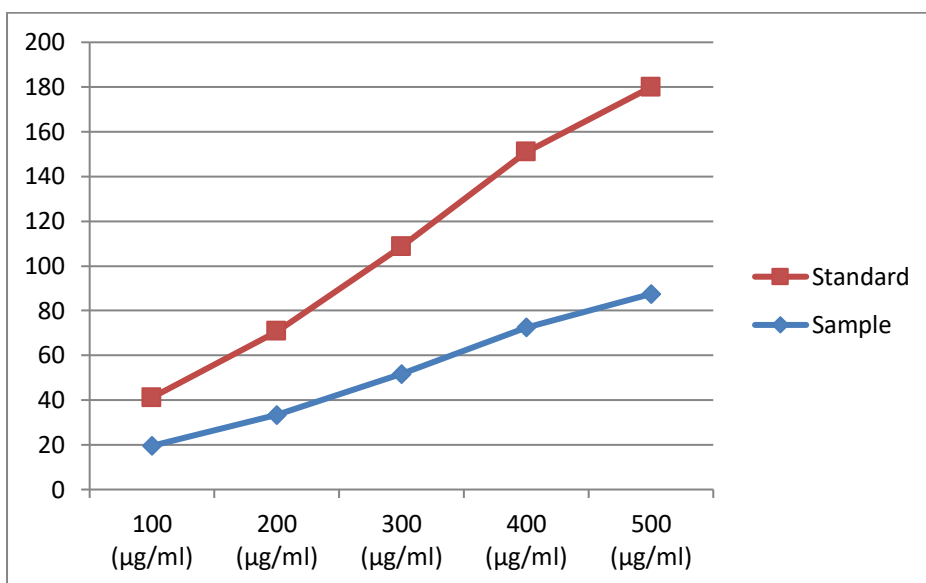


Figure 73. Pancreatic lipase inhibition of compound C10

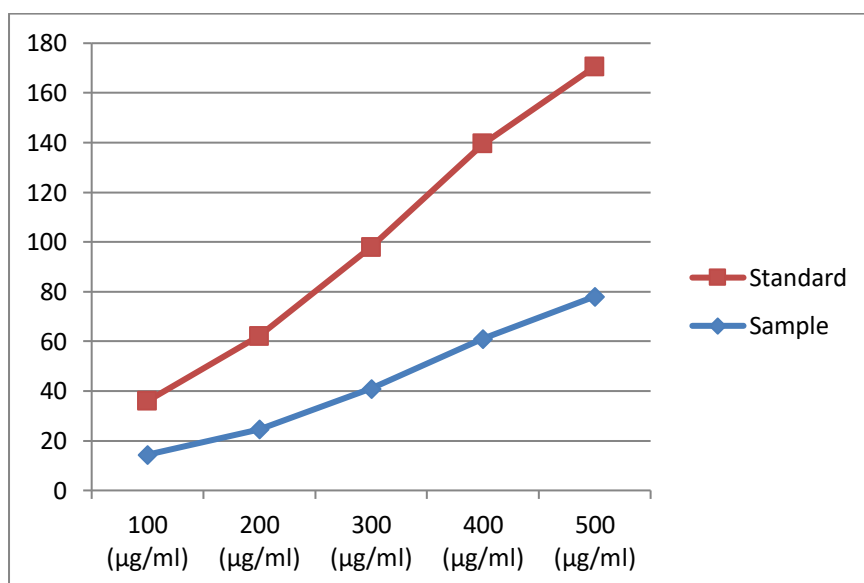


Figure 74. Pancreatic lipase inhibition of compound C11

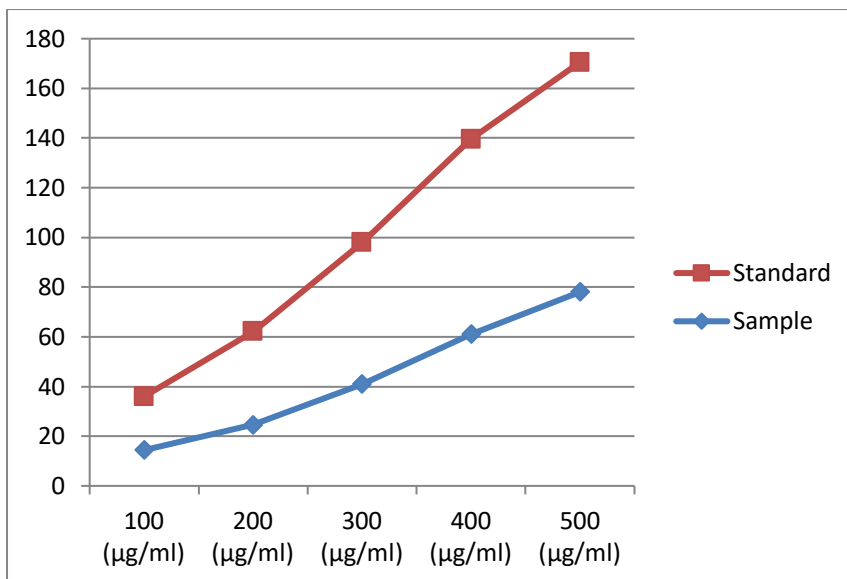


Figure 75. Pancreatic lipase inhibition of compound C12

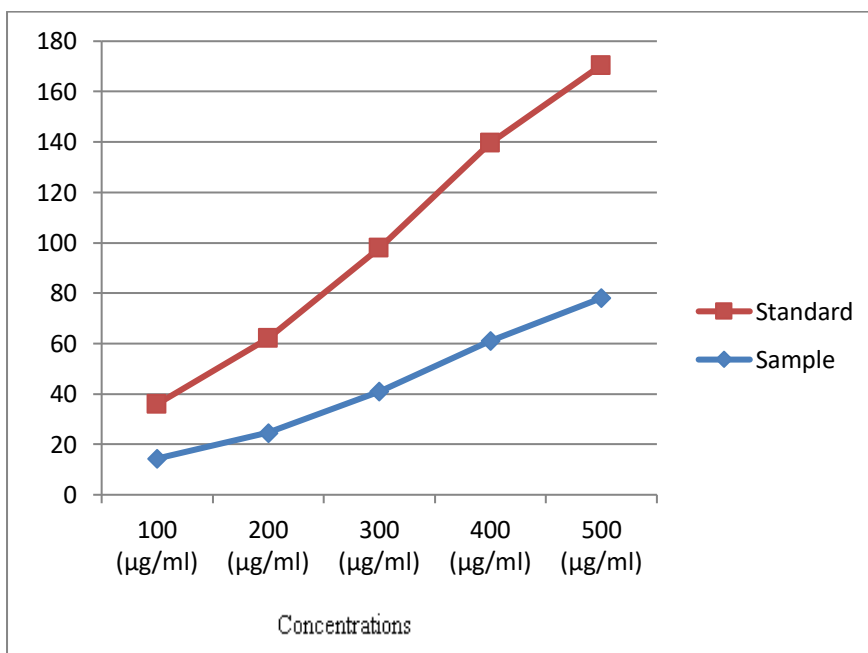


Figure 76. Pancreatic lipase inhibition of compound C13

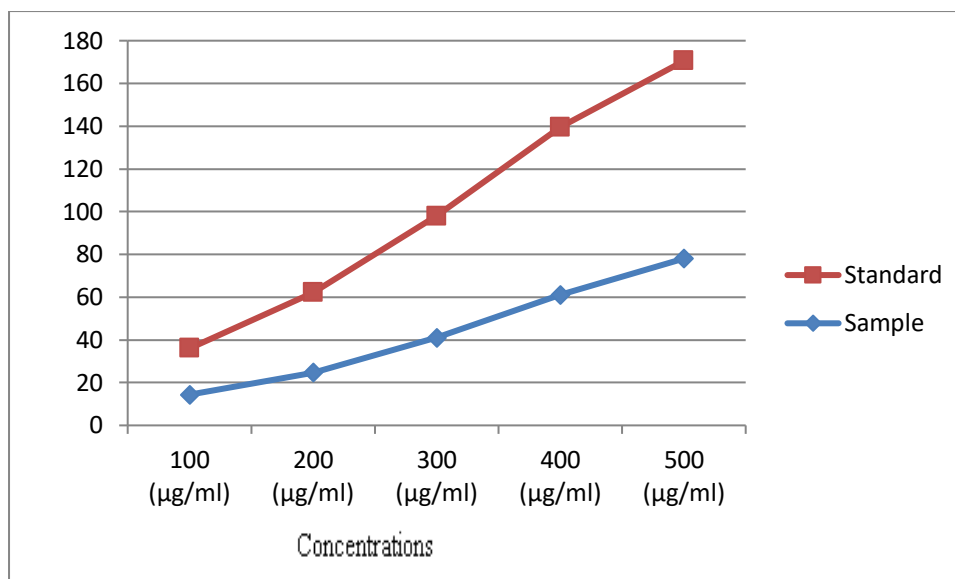


Figure 77. Pancreatic lipase inhibition of compound C14

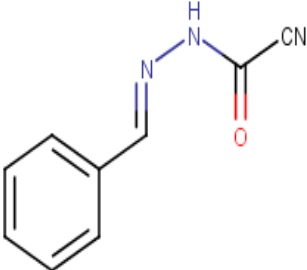
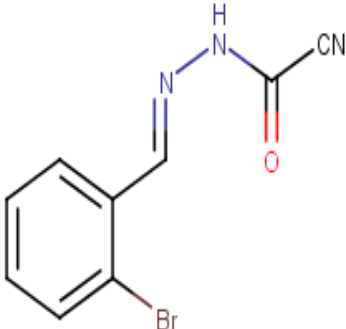
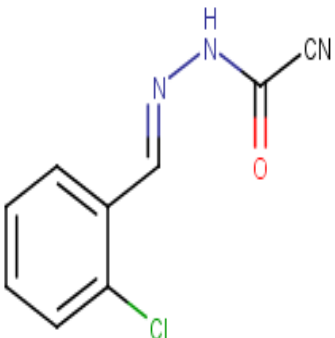
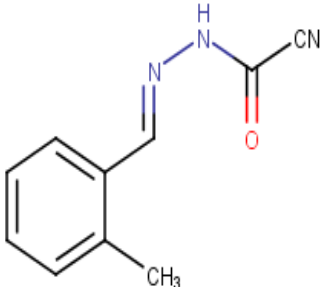
The result from the study showed that the Benzaldehyde cyano acetyl hydrazone derivatives had excellent anti-obesity activity that was comparable to the activity of Orlistat. The study revealed that few of the synthesized such as Benzaldehyde cyano acetyl hydrazone derivatives exhibited high total potent pancreatic lipase inhibitory effects. Strong positive correlation between synthesized bioactives and that of the anti - lipase activity was observed. It can be concluded from the present study that Benzaldehyde cyano acetyl hydrazone derivatives provide convincing anti-obesity. This research may provide a basic for in vivo study and strong foundation for future development of synthesized compounds with great applications in prevention and treatment of obesity.

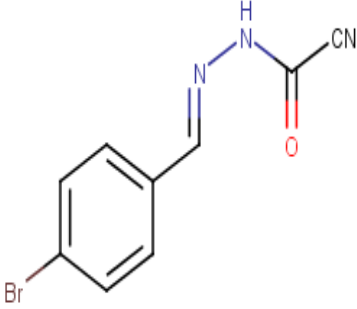
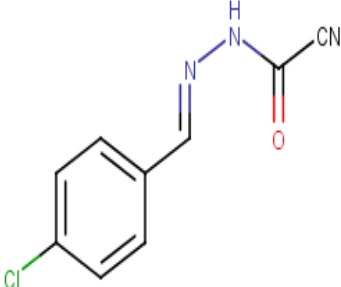
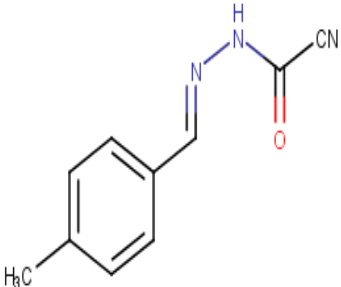
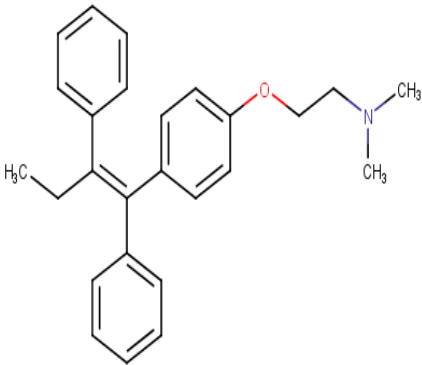
5.22 In silico Molecular Docking study

In the hope that effective and selective inhibitors will constitute a new class of therapeutics for cancers as well as other proliferative diseases, both pharmaceutical companies and university laboratories were involved in developing compounds that could inhibit the action of tyrosine kinase. As a new mode of cancer treatment, 3COJ inhibitors may also be implemented appropriately. To classify successful anti-breast cancer compounds, the current in silico research was conducted. The seven compounds (C8-C14) and standard drug Tamoxifen were also evaluated for their binding interactions in 3COJ active site. After being tested via in vitro experiments, the virtual hits found in this study can be used as an alternative targeting agent for breast cancer. The secondary structure of the active-site sphere target protein (radius 9) is shown in **Figure 78**. The -CDOCKER energy of each molecule with the target protein is described in **Table 33** as a result of the docking analysis.

The binding analysis indicates that the Human Estrogen Receptor was successfully docked with the seven compounds. From the docking results, the Mol.1 forms one strong Hydrogen bond with Arg 394 and Alkyl and Pi-Alkyl interactions with Leu 346, Met 421 and Leu 525 respectively. The -CDOCKER energy of this interaction is $-19.0777 \text{ kcal/mole}^{-1}$. Out of seven molecules the Mol.1 shows higher binding affinity in receptor 3COJ compare to standard drug Tamoxifen (-CDOCKER energy $-18.2547 \text{ Kcal/mol}^{-1}$) due to forms Pi-Alkyl and Pi-Pi T-shaped interactions. The remaining all compounds of 2D results are depicted in Figure 4. Here, the Mol. 4 revealed the poor binding affinity with binding energy being (is $-19.0777 \text{ kcal/mole}^{-1}$) which predict its weak biological breast cancer activity (not measured yet), but it may be similar activity to Tamoxifen drug. Therefore it is easily seen that it is predicted that all compounds would have almost identical activity against Human Estrogen Receptor.

Table 33. CDOCKER energy of the molecules (C8 to C14)

S. No	Molecule Number	Structure	-CDOCKER Energy (Kcal/mol ⁻¹)
1	Compound C8 (Mol-7)		22.2919
2	Compound C9 (Mol-3)		20.3915
3	Compound C10 (Mol-1)		19.0777
4	Compound C11 (Mol-5)		22.2153

5	Compound C12 (Mol-2)		23.3452
6	Compound C13 (Mol-6)		22.7068
7	Compound C14 (Mol-4)		23.9721
8	Tamoxifen		18.2547

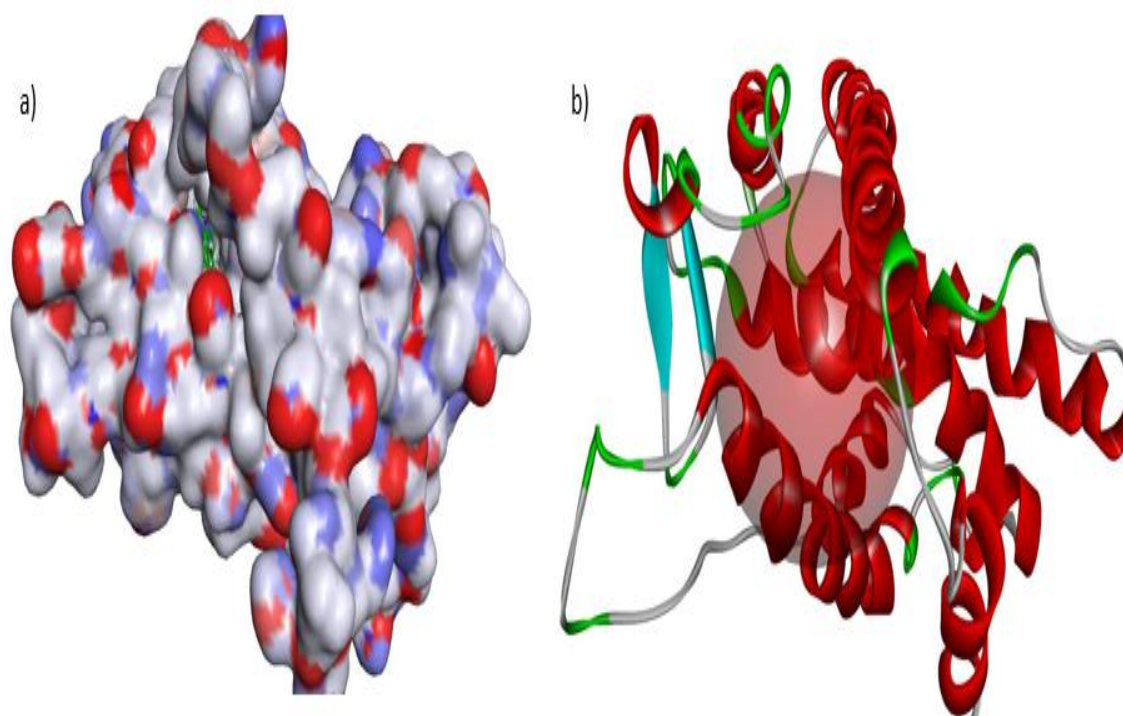


Figure 78. a) The secondary 3D structure of the target 3COJ protein with molecules and b) active site sphere of the protein.

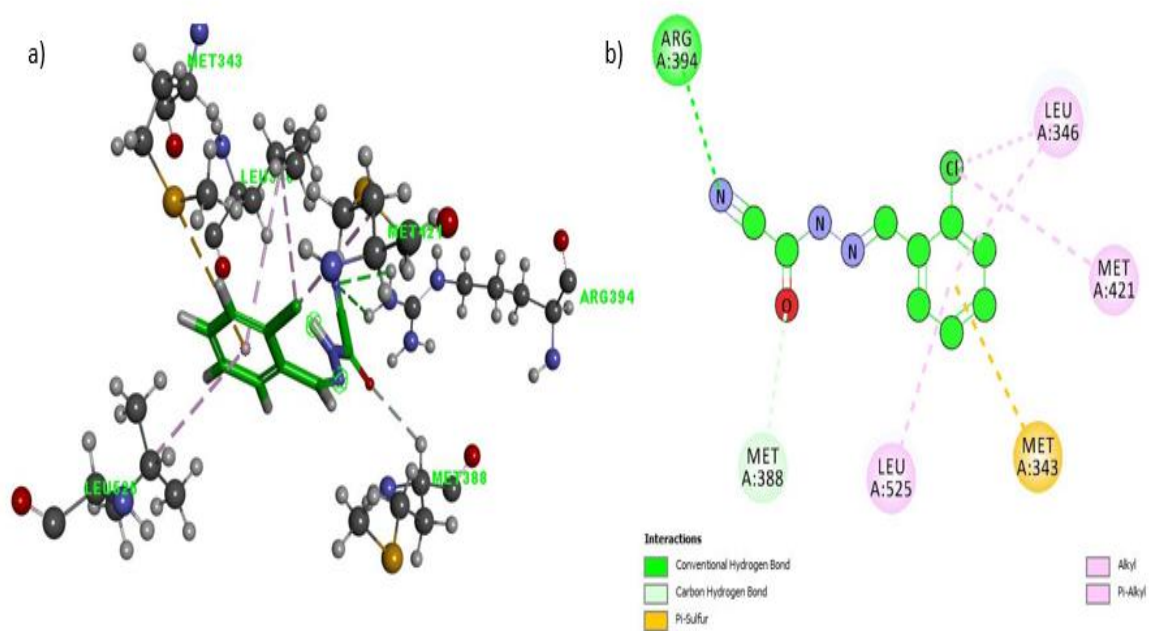


Figure 79. a) 3D and b) 2D binding site interaction of C8 in receptor 3COJ active site.

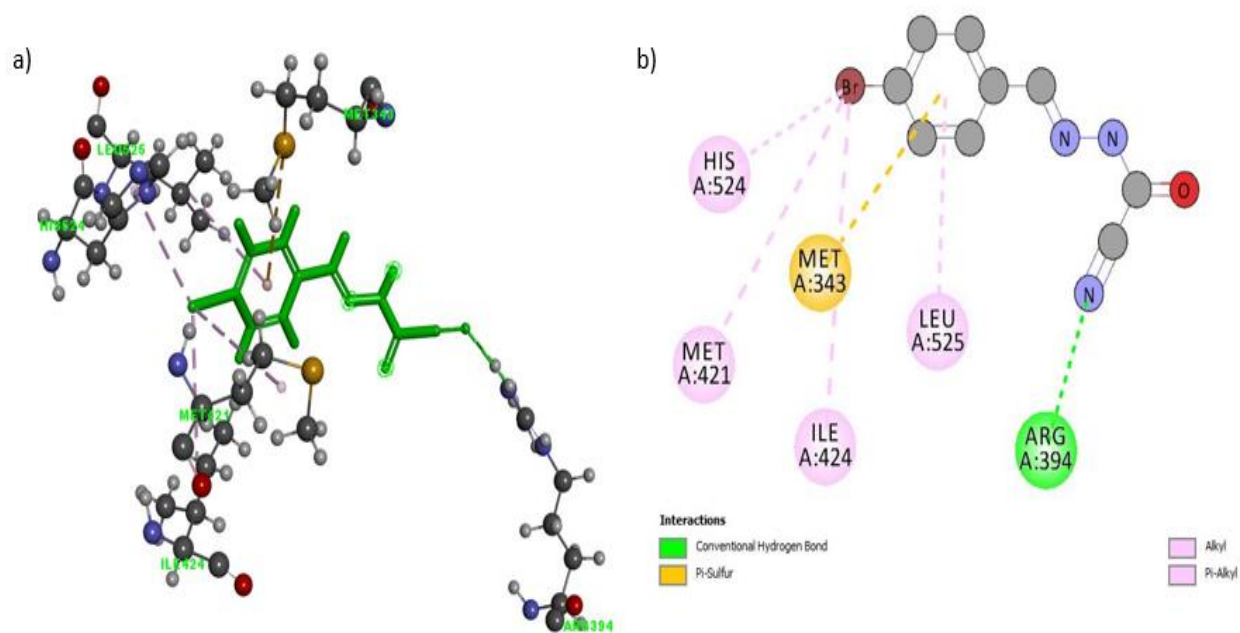


Figure 80. a) 3D and b) 2D binding site interaction of (E)-2-(4-bromobenzylidene)hydrazine-1-carbonyl cyanide [Mol.2] in receptor 3COJ active site.

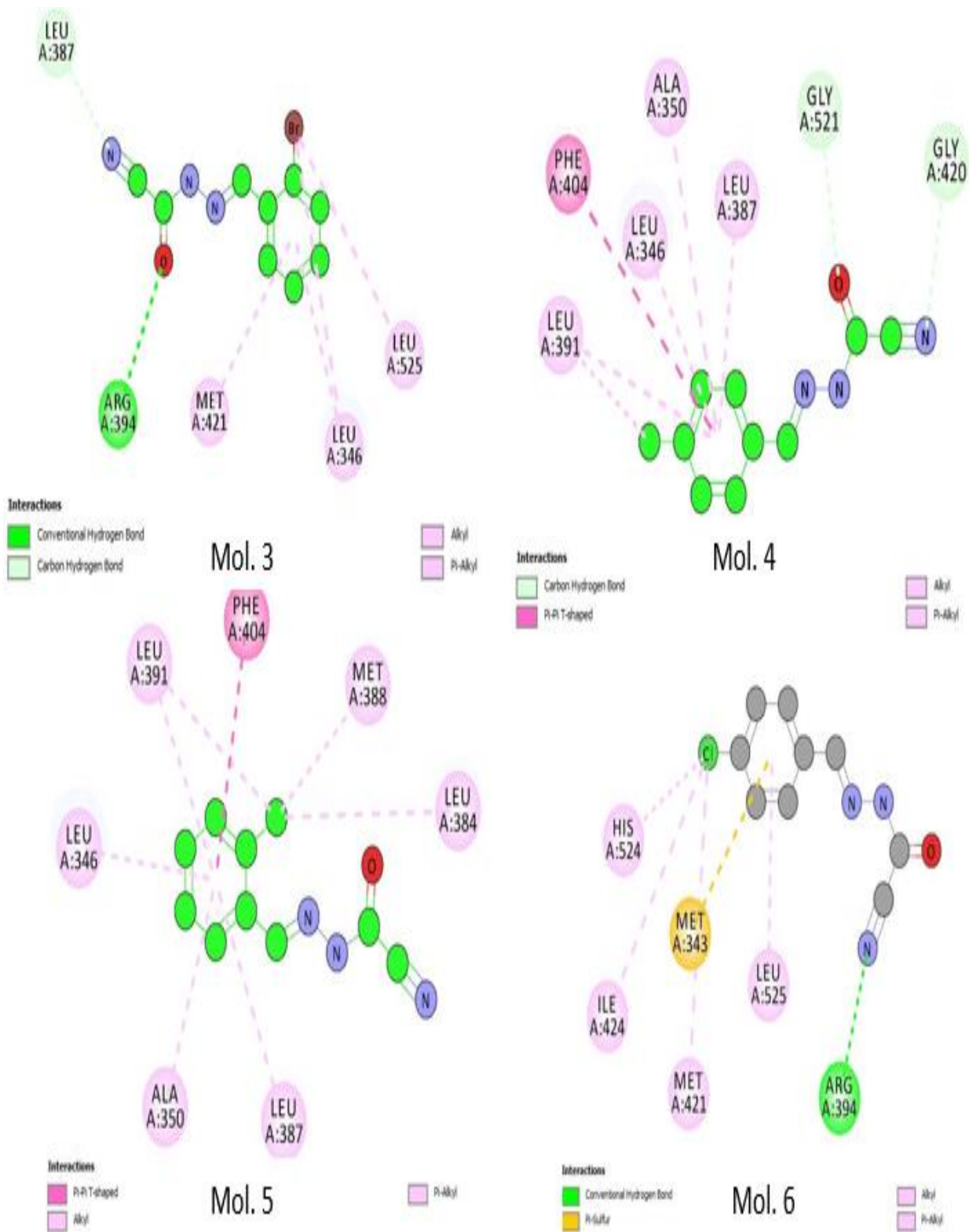


Figure 81. 2D interactions analysis of Mol.3, Mol.4, Mol.5 and Mol. 6 in receptor 3COJ active site.

5.23 Thrombolytic activity

All the seven tested cyanoacetyl hydrazone derivatives exhibited substantial clot lysis value range from 40.5 to 78.45 % in comparison to 84.57 % clot lysis exhibited by the reference standard streptokinase (30,000 IU). Statistical representation of the effective clot lysis percentage by negative control (sterile distilled water) is 26.74 ± 1.87 % and positive control (streptokinase) is 84.57 ± 5.91 %.

The clot lysis activity of compound C8 was 36.63 ± 4.77 % for 100 $\mu\text{g/mL}$ and 61.06 ± 6.65 % for 200 $\mu\text{g/mL}$. The clot lysis activity of compound C9 was 44.94 ± 3.14 % for 100 $\mu\text{g/mL}$ and 80.17 ± 5.61 % for 200 $\mu\text{g/mL}$. The clot lysis activity of compound C10 was 46.81 ± 3.27 % for 100 $\mu\text{g/mL}$ and 83.01 ± 5.81 % for 200 $\mu\text{g/mL}$. The clot lysis activity of compound C11 was 36.73 ± 3.43 % for 100 $\mu\text{g/mL}$ and 72.07 ± 5.15 % for 200 $\mu\text{g/mL}$. The clot lysis activity of compound C12 was 37.49 ± 2.62 % for 100 $\mu\text{g/mL}$ and 75.36 ± 5.27 % for 200 $\mu\text{g/mL}$. The clot lysis activity of compound C13 was 42.47 ± 3.27 % for 100 $\mu\text{g/mL}$ and 76.07 ± 5.10 % for 200 $\mu\text{g/mL}$. The clot lysis activity of compound C14 was 34.57 ± 2.41 % for 100 $\mu\text{g/mL}$ and 71.62 ± 5.01 % for 200 $\mu\text{g/mL}$.

The results of all synthesized compounds are presented in Tables **34**.

Table 39: In-vitro anti thrombolytic activity of the compounds

Samples	% of clot lysis			
	Control	100 (µg/ml)	200 (µg/ml)	Standard
C8	26.74 ± 1.87	36.63 ± 4.77	61.06 ± 6.65	84.57 ± 5.91
C9	26.74 ± 1.87	44.94 ± 3.14	80.17 ± 5.61	84.57 ± 5.91
C10	26.74 ± 1.87	46.81 ± 3.27	83.04 ± 5.81	84.57 ± 5.91
C11	26.74 ± 1.87	36.73 ± 3.14	72.07 ± 5.15	84.57 ± 5.91
C12	26.74 ± 1.87	37.49 ± 2.62	75.36 ± 5.27	84.57 ± 5.91
C13	26.74 ± 1.87	42.47 ± 3.27	76.07 ± 5.10	84.57 ± 5.91
C14	26.74 ± 1.87	34.57 ± 2.41	71.62 ± 5.01	84.57 ± 5.91

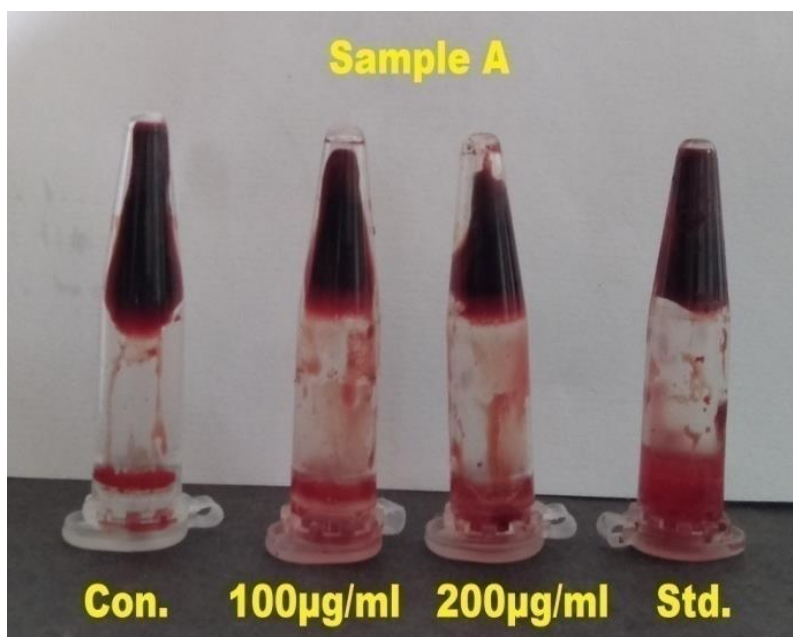


Fig. 82 Clotlysis experiments with different concentrations of compound C8

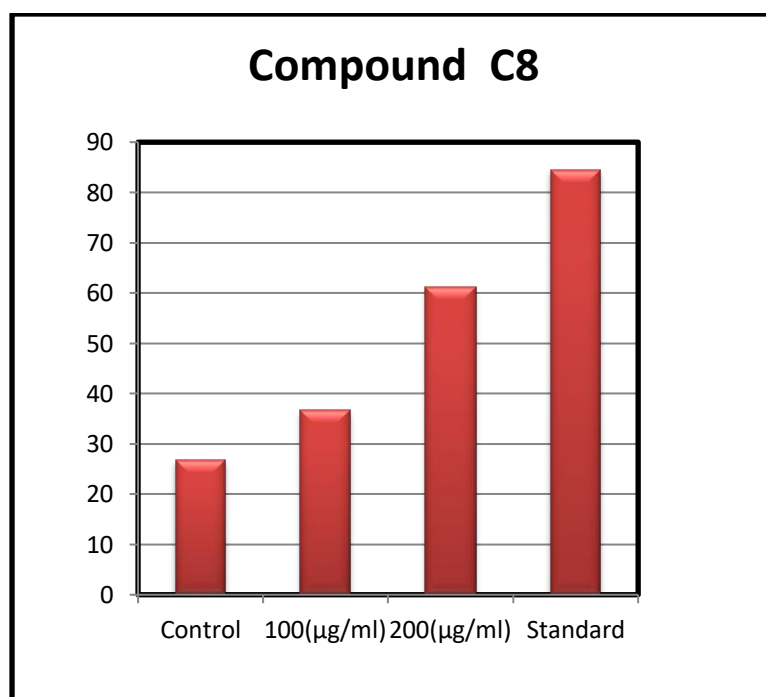


Fig. 83 Clotlysis of compound C8 on Thrombolytic activity

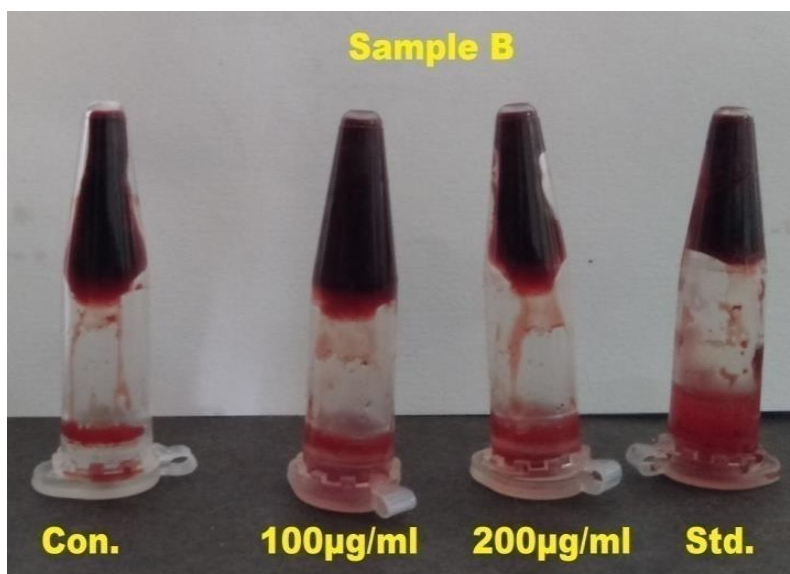


Fig. 84 Clotlysis experiments with different concentrations of compound C9

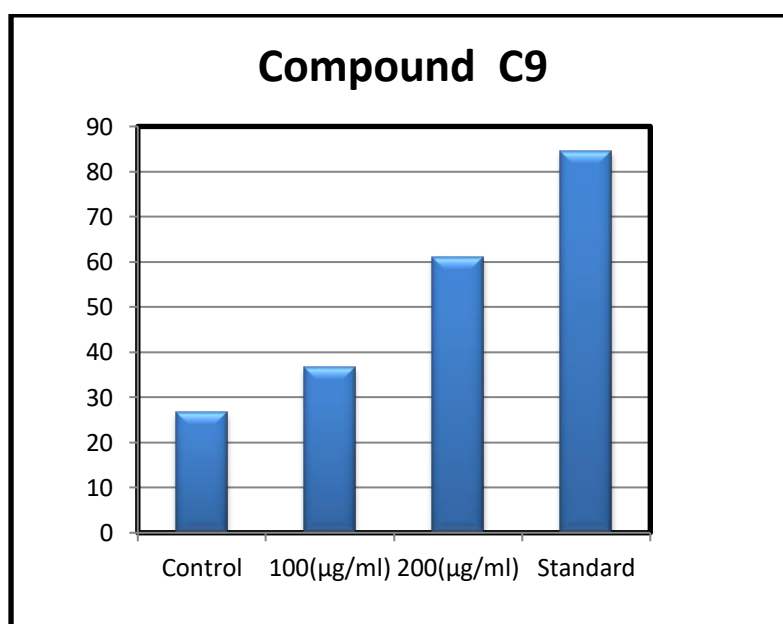


Fig. 85 Clotlysis of compound C9 on Thrombolytic activity

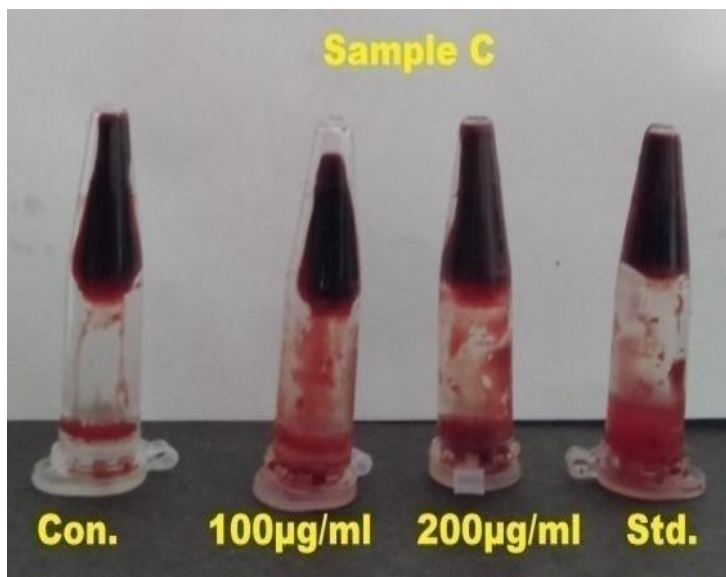


Fig. 86 Clotlysis experiments with different concentrations of compound C10

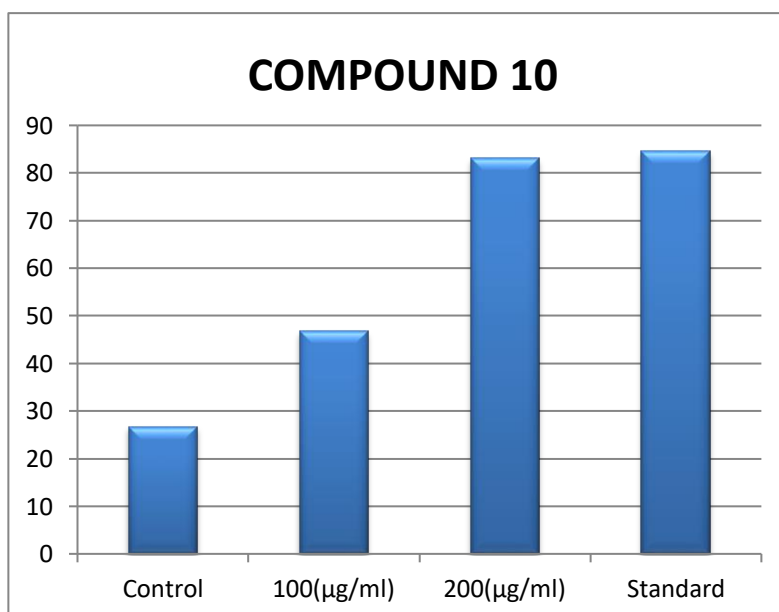


Fig. 87 Clotlysis of compound C10 on Thrombolytic activity

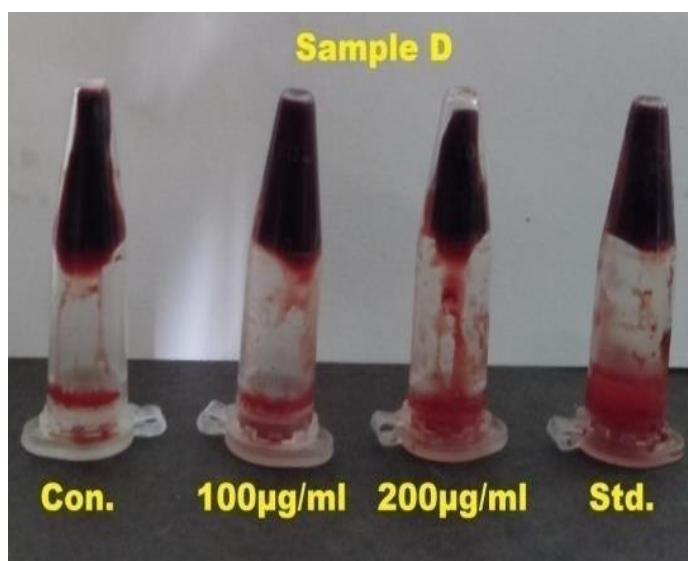


Fig. 88 Clotlysis experiments with different concentrations of compound C11

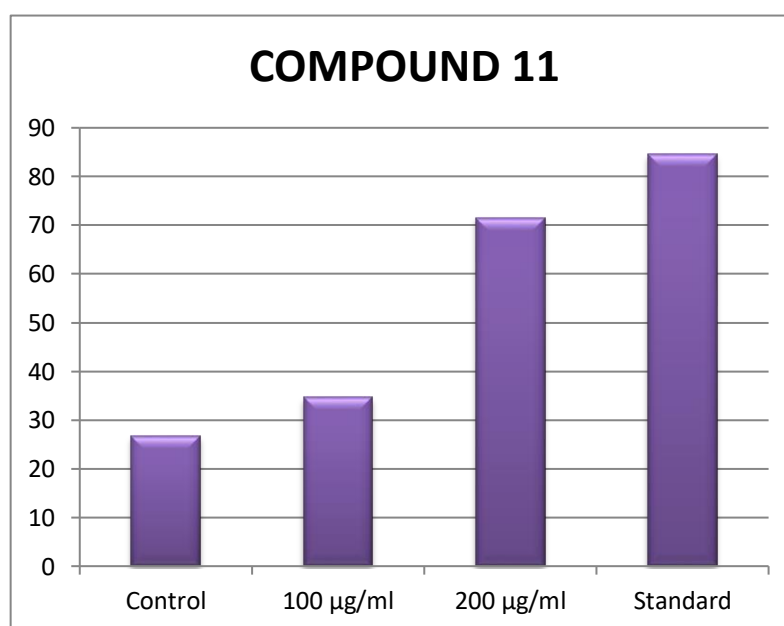


Fig. 89 Clotlysis of compound C11 on Thrombolytic activity

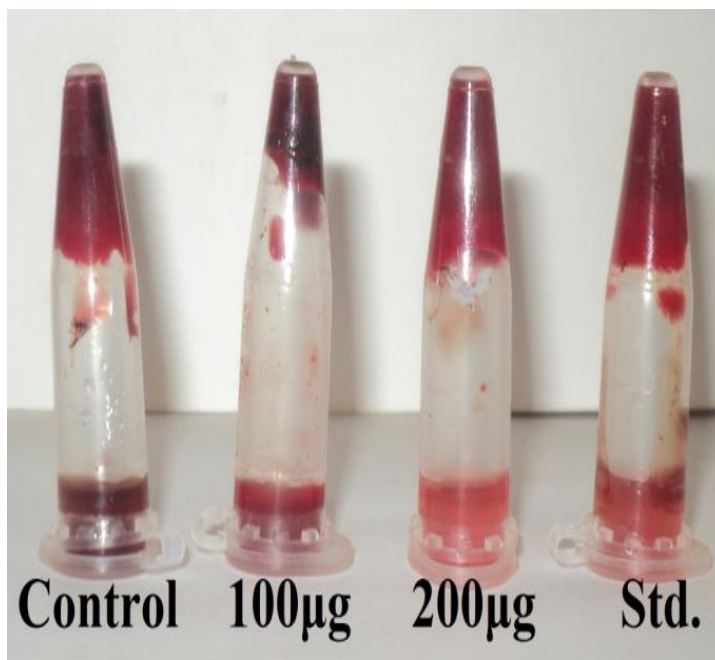


Fig. 90 Clotlysis experiments with different concentrations of compound C12

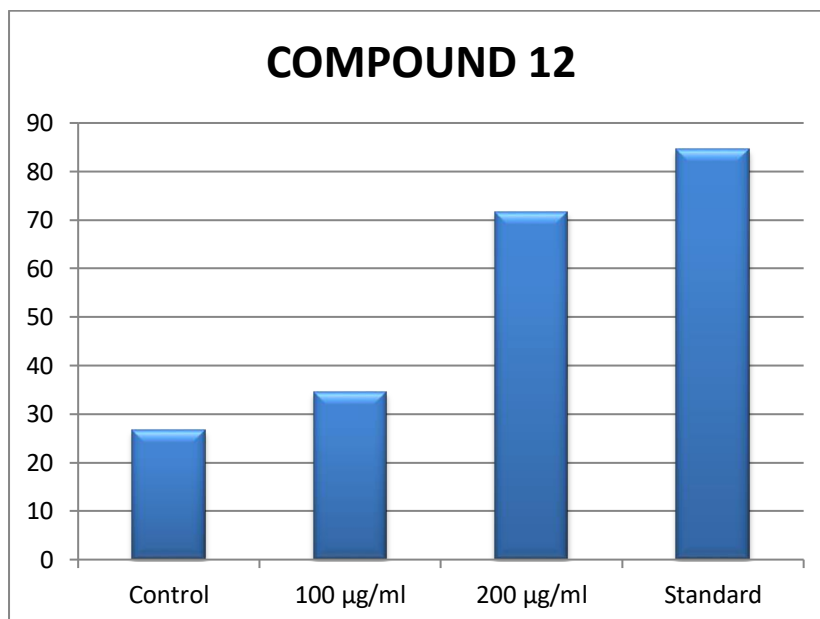


Fig. 91 Clotlysis of compound C12 on Thrombolytic activity

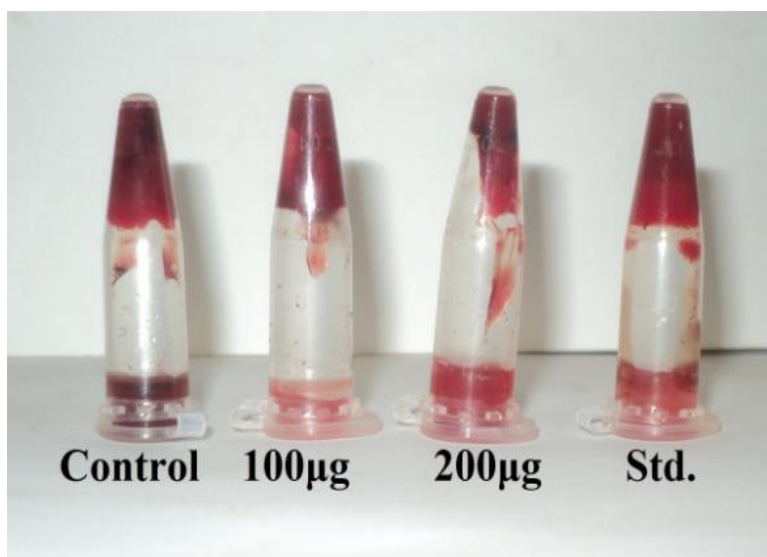


Fig. 92 Clotlysis experiments with different concentrations of compound C3

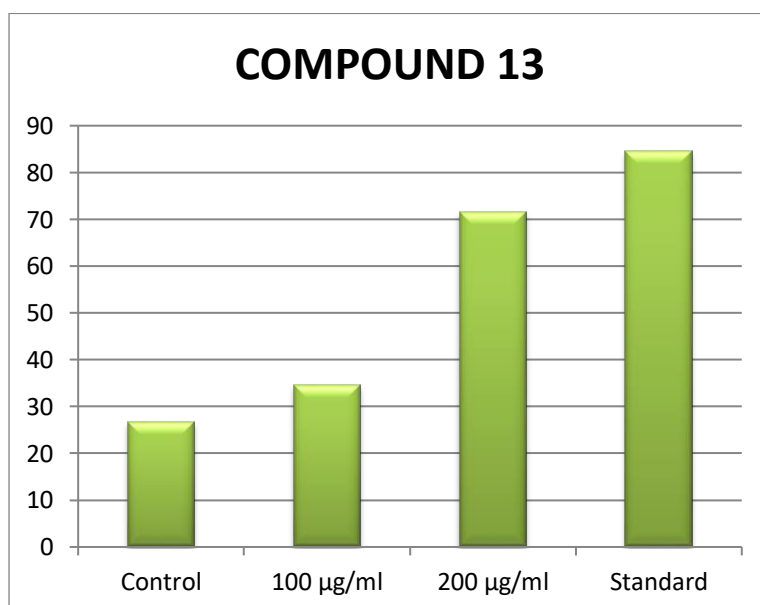


Fig. 93 Clotlysis of compound C9 on Thrombolytic activity

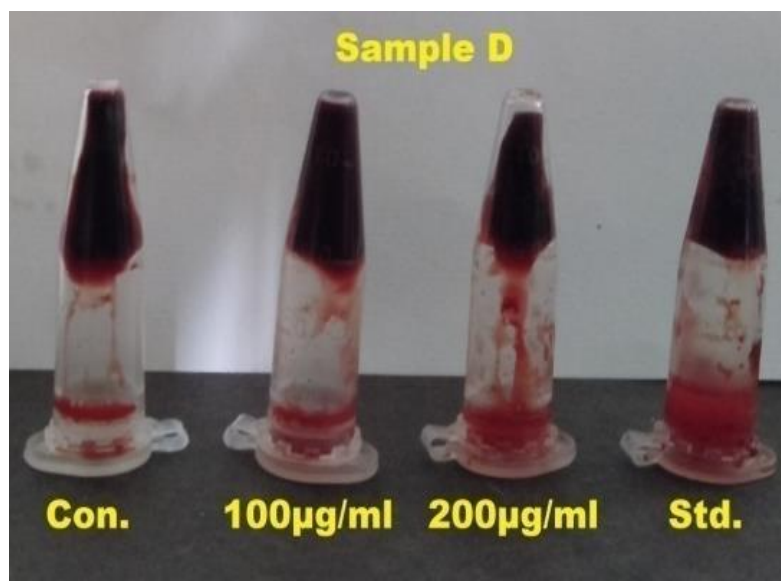


Fig. 94 Clotlysis experiments with different concentrations of compound C14

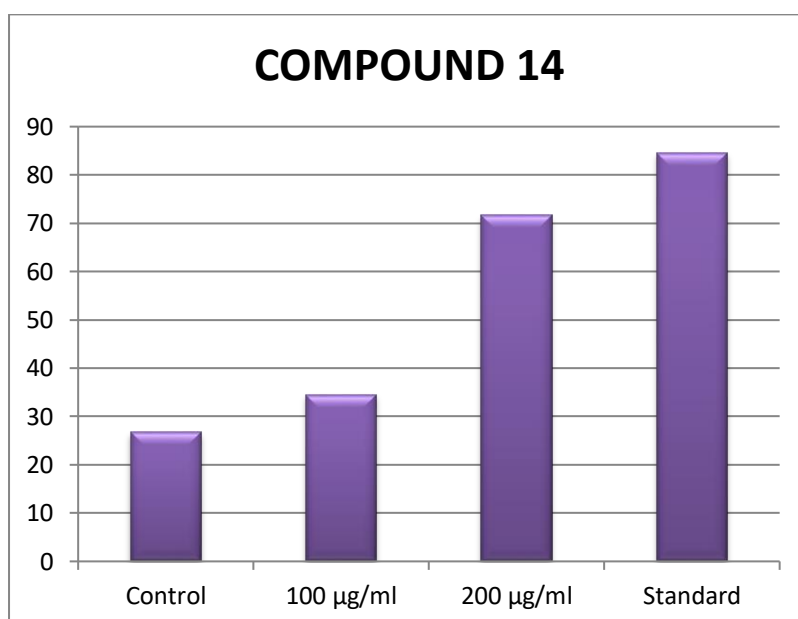


Fig. 95 Clotlysis of compound C14 on Thrombolytic activity

Results demonstrated that compound **C10** has impressive clot lysis activity (83%) compared to SK (84%). While compound **C8** depicted less clot lysis activity (36%), and the order of the in vitro clot lysis effect of all tested compounds is **C10 > C9 > C13 > C12 > C11 > C14 > C8**.

References

1. Maheshwari R, Manjula J. Synthesis, Characterization and Biological Applications of Benzohydrazide derivatives, *International journal of applied research* 1,1(10) (2015) p587-592.
2. Shizhen L, Xiwen L. Compendium of Materia Medica. *Foreign Languages Press; Beijing, China*. 6 (2003) p410-416.
3. Rahul B, Birari A, Shikhar Gupta C, Gopi Mohan B, Kamlesh K and Bhutania. Antiobesity and lipid lowering effects of Glycyrrhizachalcones Experimental and computational studies. *Phytomedicine*. 18 (2011) p795-801.
4. Manimegalai B and Velavan S, Evaluation of anti-obesity activity of gymnema sylvestre leaves extract, *Journal of Pharmacognosy and Phytochemistry*. 8(3) (2019) p.2170-2173.
5. Hughes, J.; Rees, S.; Kalindjian, S.; Philpott, K. Principles of early drug discovery. *Br. J. Pharmacol*. 162 (2011) p 1239–1249.
6. Cava, C.; Colaprico, A.; Bertoli, G.; Bontempi, G.; Mauri, G.; Castiglioni, I. How interacting pathways are regulated by miRNAs in breast cancer subtypes. *BMC Bioinform*. 17 (2016) p 111–133.
7. Cava, C.; Novello, C.; Martelli, C.; Lodico, A.; Ottobrini, L.; Piccotti, F.; Truffi, M.; Corsi, F.; Bertoli, G.; Castiglioni, I. Theranostic application of miR-429 in HER2+ breast cancer. *Theranostics* 10(2020) p 50–61.
8. Yang, Y.; Adelstein, S.J.; Kassis, I.A. Target discovery from data mining approaches. *Drug Discov. Today* 14 (2009) p147–154.
9. Meng, X.-Y.; Zhang, H.-X.; Mezei, M.; Cui, M. Molecular docking: A powerful approach for structure-based drug discovery. *Curr. Comput. Drug Des*. 7 (2011) p 146–157.

10. McConkey, B.J.; Sobolev, V.; Edelman, M. The performance of current methods in ligand-protein docking. *Curr. Sci.* 83 (2002) p845–855.
11. Csermely, P.; Korcsmáros, T.; Kiss, H.J.; London, G.; Nussinov, R. Structure and dynamics of molecular networks: A novel paradigm of drug discovery: A *comprehensive review*. *Pharmacol. Ther.* 138(2013) p333–408.
12. Koppen H. Virtual screening – what does it give us? *Curr Opin Drug Disc Dev.* 12 (2009) p 397-407.
13. Seeliger D, Groot BL. Ligand docking and binding site analysis with PyMOL and Autodock/Vina. *J Comput Aided Mol. Des.* 24 (2010) p417-24.
14. Senthilraja P, Senthil Vinoth K, Sindhuraj M and Prak. (2012) Potential of marine derived compounds against breast cancer (BRCA1): an in-silico docking study. *IJRAP* 3(4), 5701-572.
15. Lubinski J, Phelan C M, Ghadirian P, Lynch H T, Garber J, Weber B, Tung N, Horsman D, Isaacs C, Monteiro A N, Sun P, Narod S A 2004 Cancer variation associated with the position of the mutation in the BRCA2 gene. *Fam Cancer* 3(1): 1–10
16. B. Vishwanathan B.M. Gurupadayya Thrombolytic activity of 1,3,4-oxadizole derivatives , *World Journal of Pharmaceutical Sciences* 3(10) (2015)p 2004-2008.

Chapter-6

Summary and Conclusion

The work embodied in this thesis entitled “**SYNTHESIS, CHARACTERIZATION AND BIOLOGICAL EVALUATION OF SOME NOVEL BIOACTIVE HYDRAZONE DERIVATIVES**” comprises of six chapters.

Chapter one: This chapter is divided into four sections. Section – I deals with Hetero cyclic compounds and hydrazone derivatives and its applications in different fields. Section – II describes the anti-obesity studies and its classification, treatments. Section – III deals with insilico molecular docking, structure based drug design in the pharmaceutical fields. Section-IV explains the thrombolytic activity and treatments.

Chapter two: This chapter involves a review of literature on the synthesis of hydrazone derivatives and its applications in the various fields, invitro anti-obesity study by pancreatic activity, insilico molecular docking studies and finally thrombolytic activity of the hydrazone derivatives.

The structures of all the synthesized compounds are established on the basis of their analytical and spectral studies.

Chapter three: This chapter describes the scope of the present work.

Chapter four: This chapter gives the materials and methods used. It includes

- ❖ Preparation of various substituted N-acetyl-3-methyl 2,6-diaryl piperidin-4-one cyanoacetylhydrazones derivatives using condensation reaction in the presence of ammonium acetate as catalyst and various substituted benzaldehyde cyanoacetylhydrazones derivatives .
- ❖ Characterization of synthesized compounds using advanced analytical and spectral methods such as FT-IR, ¹H and ¹³C NMR.
- ❖ In vitro (anti-obesity activity) pancreatic lipase inhibitory activity was carried out by the method of apostolidis.
- ❖ *In silico* molecular docking studies were carried out using BIOVIA Discovery Studio (DS) 2017 software.
- ❖ Thrombolytic activity was determined by comparison with Streptokinase.

Chapter five: This chapter deals with discussion on experimental results, obtained for the synthesized compounds, such as characterization of synthesized compounds, evaluation of *in vitro* anti-obesity activity by pancreatic lipase inhibition activity, *in silico* molecular docking studies using BIOVIA Discovery Studio (DS) 2017 software and evaluation of thrombolytic activity using Streptokinase.

Chapter six: In this chapter result of chapter V was summarized.

1. A novel piperidones in combination with cyanoacetylhydrazone derivatives were synthesized using Mannich followed by condensation reactions.

The synthesized compounds are N-acetyl 3-methyl-2,6-diphenylpiperidin-4-one cyanoacetyl hydrazone (C1), N-acetyl 3-methyl-2,6- bis(*o*-bromo phenyl) piperidin-4-one cyanoacetyl hydrazone (C2), N-acetyl 3-methyl-2,6- bis(*o*-chloro phenyl) piperidin-4-one cyanoacetyl hydrazone (C3), N-acetyl 3-methyl-2,6- bis(*o*-methyl phenyl) piperidin-4-one

cyanoacetyl hydrazone (C4), N-acetyl 3-methyl-2,6- bis(*p*-bromo phenyl) piperidin-4-one cyanoacetyl hydrazone (C5), N-acetyl 3-methyl-2,6- bis(*p*-chloro phenyl) piperidin-4-one cyanoacetyl hydrazone (C6), N-acetyl 3-methyl-2,6- bis(*p*-methyl phenyl) piperidin-4-one cyanoacetyl hydrazone (C7).

2. Synthesized compounds are Benzaldehyde cyanoacetylhydrazone(C8), *o*-bromo Benzaldehyde cyanoacetyl hydrazone(C9), *o*- Chloro Benzaldehyde cyanoacetylhydrazone(C10), *o*-Methyl Benzaldehyde cyanoacetylhydrazone(C11), *p*- Bromo Benzaldehyde cyanoacetylhydrazone (12), *p* - Chloro Benzaldehyde cyanoacetylhydrazone(C13), *p*- Methyl Benzaldehyde cyanoacetylhydrazone(C14)

3. The melting points of the compounds (**C1-C14**) were noted.
4. The synthesized compounds (**C1-C14**) are characterized by analytical and spectral studies (IR, ¹H NMR and ¹³C NMR).
5. All the spectral data are consistent with the assigned structures of the desired product and the progress of the reactions was monitored on silica gel G plates using iodine vapour as visualizing agent.
6. Structure of all the synthesized compounds (**C1-C14**) are established on the basis of their IR, ¹H NMR and ¹³C NMR spectral studies.
7. The observed chemical shifts, coupling constants indicate that the synthesized compounds (**C1-C7**) are adopting the chair conformation.

8. **Invitro Anti-obesity activity**

Inhibition of pancreatic lipase is an attractive targeted approach for the treatment of obesity. For instance, orlistat, a hydrogenated derivative of lipstatin, which is obtained from *Streptomyces toxytricini*, is the only pancreatic lipase inhibitor currently approved for long-term treatment of obesity.

The various concentrations of the synthesized compounds (100µg/mL, 200µg/mL, 300µg/mL, 400µg/mL, 500µg/mL). Similar concentrations of positive control as Orlistat (Standard) are used.

The result(C1-C7) shows the o-substituted compounds have higher activity than p-substituted compounds. The order of activity for o-substituted compounds is **C3>C2>C4(o-Cl>o-Br>o-methyl)**. The order of activity for p-substituted compounds is **C5>C6>C7(p-Cl>p-Br>p-methyl)** and (C8-C14) C10 > C9 > C13 > C11 > C12 > C14 > C8.

From the result it was observed that, compound C3 and C10 shows good anti-Obesity activity than other synthesized compounds.

9. In silico molecular docking studies

The RCSB PDB (Research Collaboratory for Structural Bioinformatics, Protein Data Bank) is a repository for the 3D structural data of large biological macromolecules such as proteins and nucleic acids. It provides simple and advanced searches based on annotations related to sequence structure and function. The crystal structure of the drug targets BRCA1 was downloaded from the Protein Data Bank (PDB ID-3KOH) (<http://www.pdb.org>).

In silico molecular docking is one of the most powerful techniques to discover novel ligand for proteins of known structure and thus play key role in structure based drug. Investigators often use docking computer programs to find the binding affinity for molecules that fit a binding site on the protein. Hence in this present work we have carried out *in silico* molecules docking to analyze the binding properties of the mediator called BRCA1 with synthesized compounds. So the present study might act as supportive evidence for *in vivo* cancer activity of synthesized compounds and surely help these molecules in reaching the market as commercial drug. Among the various synthesized compounds (C1-C7), 4Cl has greatest binding energy followed by 2Br, 4Br, 2Cl, 2Me, 4Me, piperidone and highest than

standard. The results of the *in silico* study further supported the *in vitro* pharmacological activity.

In this analysis, the X-ray diffraction-based Crystal Structure of the BRCT Domains of Human BRCA1 in Complex with a Phosphorylated Peptide from Human Acetyl-CoA Carboxylase 1(PDB ID: 3COJ) with a resolution of 1.90 Å was selected. Hydrogens were applied to the 3COJ protein by applying the Forcefield algorithm and then using CHARM forcefield in DS, the protein energy was reduced.

For molecular docking of II series research, The investigator followed previously mentioned parameter. The binding analysis indicates that the Human Estrogen Receptor was successfully docked with the seven compounds (C8-C14). Out of seven molecules the C10 shows higher binding affinity in receptor 3COJ compare to standard drug Tamoxifen (-CDOCKER energy -19.0777 Kcal/mol⁻¹) due to forms Pi-Alkyl and Pi-Pi T-shaped interactions.

In the future, further development and modification of these analogues may lead to the production of new, highly potent anti-breast cancer drugs.

10. Thrombolytic activity

The *in-vitro* thrombolytic activity of the synthesized compounds was determined by clot lysis study. The activity of the compounds was determined by comparison with the thrombolytic activity of Streptokinase. The test compound was measured for the decrease in clot weight at different concentrations. The *in-vitro* thrombolytic activity of the N-acetyl cyanoacetyl hydrazone derivatives were determined by clot lysis study. The activity of the compounds was determined by comparison with the thrombolytic activity of Streptokinase. The test compounds were measured for the decrease in clot weight at different concentrations 100 and 200 µl, respectively, Streptokinase (30,000 IU) was employed as positive control

and distilled water as negative control. The results were plotted conc. Vs percentage clot lysis was obtained by regression analysis.

The results of the *in vitro* thrombolytic activity were encouraging and the tested compounds exhibited substantial aggregation inhibition. Synthesized compounds (C1-C7), N-acetyl cyanoacetyl hydrazone derivative exhibited substantial clot lysis, with percentage value ranging from 40.5 to 78.45% in comparison to 84.57 % clot lysis exhibited by the reference standard streptokinase (30,000 IU).

The result shows (C1-C7) the o- substituted compounds have higher activity than p substituted compounds. The order of activity of o-substituted **C10 > C9 > C11 (o-Cl > o-Br > o-methyl)**. The order of activity of p-substituted compounds **C13 > C12 > C14 (p-Cl > p-Br > p-methyl)**.

The result shows the Chloro substituted compounds have higher clot lysis activity than Bromo and Methyl substituted compounds.

Following are the scope for future work

The outcomes of these studies may be useful for the clinical applications in humans and may open up a new therapeutic avenue.

- ♣ Showing hope of discovering new molecules based on these structures with different substitutions would result in highly biologically active compounds.
- ♣ Screening for different biological activities and conformational analysis.
- ♣ Synthesis of new 2, 6-diarylpiperidin-4-one derivatives using a various groups at the 3rd position of the piperidine ring.

PUBLICATIONS



**International Journal of Biology, Pharmacy
and Allied Sciences (IJBPAS)**

'A Bridge Between Laboratory and Reader'

www.ijbpas.com

SYNTHESIS, CHARACTERIZATION AND ANTI-OBESITY ACTIVITY OF N-ACETYLCYANOACETYL HYDRAZONE DERIVATIVE

V.PRIYADARSHINI¹, K.SUNDARESAN² AND K.THARINI^{1*}

1: Department of Chemistry, Government Arts College, Trichy-22, (Affiliated to
Bharathidasan University)

2: Department of Chemistry, Meenakshi Ramaswamy College, Thathanur, Tamil Nadu, India.

Corresponding Author:

*Corresponding Author: K.Tharini; E Mail: tharinilenin@gmail.com

Received 19th July 2021; Revised 20th Aug. 2021; Accepted 29th Sept. 2021; Available online 1st Nov. 2021

<https://doi.org/10.31032/IJBPAS/2021/10.11.1022>

ABSTRACT

Pancreatic lipase or triglycerol acylhydrolase, the major lipolytic enzyme synthesized and secreted by the pancreas, plays an important role in the efficient digestion of triglycerides.

Pancreatic lipase is responsible for the hydrolysis of 50-70% of the total dietary fats. It removes fatty acids from the α -apdsitions of dietary triglycerides, yielding β -monoglycerides and long chain saturated and poly unsaturated fatty acids as the lipolytic products. The bioactive heterocyclic compounds present an exciting opportunity. Inhibition of digestive enzymes is one of the most widely studied mechanisms used to determine the potential efficacy of anti-obesity agents. The majority of pharmaceutical products that mimic heterocyclic compounds can and do participate in chemical reactions in the humanbody. The present study describes about the synthesis and the present study describes about the synthesis and characterization and biological studies of novel alkyl/halo substituted cyanoacetyl hydrazone derivatives. The synthesized compounds were characterized by FT-IR, ¹H-NMR and ¹³C-NMR spectral studies. From this study it is obvious that the compounds inhibit the activity of pancreatic lipase, which indicates its protective role in treating obesity. The present study also confirmed that the ease of nucleophilic substitution depends on nucleophilicity. All these observations gave impetus to start a research program for the synthesis of new hydroazone derivatives containing the heterocyclic fraction.

Keywords: cyanoacetyl hydrazone, pancreaticlipase, anti-obesity

INTRODUCTION

Organic chemistry and medicinal chemistry are becoming very important chemicals. The primary objective of an organic chemist is to work towards the isolation, characterization and synthesis of new compounds that are suitable for use as drugs. Pharmaceutical chemistry is a discipline on the incorporation of chemistry and pharmacology, the chemistry, incorporation and development of pharmaceuticals shaped. However their derivatives with N–C linkages have been used in the fields of medicinal and pharmaceutical chemistry and have been reported to exhibit a variety of biological activities [1].

Medicinal chemistry always leads to drug discovery and development. The introduction of synthetic substances as drugs began in the late nineteenth and early twentieth century's. Initially this development focused on isolated natural products from plant and animal sources but as knowledge increased, a wide range of synthetic compounds such as drugs developed. The original pharmacologically active compound from which these synthetic analogs are developed is known as the lead compound [2].

The work of a medicinal chemist is focused on the discovery of lead compounds with specific medicinal properties. This includes the development of more effective and safer analogues of these existing and new lead compounds. Molecular manipulation of a promising lead is a major approach for the discovery of a new drug. This involves attempts to remove, replace, or replace individual groups with similar activity in a compound, or add a new fraction to the original lead compound. This could potentially result in enhancing activity, warding off unwanted side effects, and preventing the development of resistance, particularly by infectious micro-organisms [3].

Hydrazones and their derivatives form an important class of compounds that have found widespread utility in organic synthesis. The chemistry of the carbon–nitrogen double bond of hydrazones is becoming the backbone of the condensation reaction in benzo – fused N-heterocyclics, also forming an important class of compounds for new drug development. Studies in heterocyclic compounds are two particular sources of interest Subject. First these are their steady streams of discovery of new heterocyclic compounds playing

important roles in the metabolism of all living cells and secondly the increasing availability of suitable intermediates for large-scale production of heterocyclic compounds. Many important compounds contain heterocyclic rings, for example most vitamins B-complex, alkaloids, antibiotics chlorophyll, hemin, plant pigments, amino acids, drugs, enzymes, DNA, RNA etc. A lot of research has been done to synthesize New heterocycles with therapeutic value and industrial applications [4-9].

Obesity is defined as excessive fat accumulation of impair health. Body mass index (BMI) is a crude population measure of obesity commonly used to classify overweight and obesity in adults; Classified as the weight of a person, which is worse than the square of the height in meters (kg/m^2). A person with a BMI of 30 or greater is generally considered obese, while a person with a BMI equal to or greater than 25 is considered overweight [10].

The prevalence of obesity varies from country to country and depends on a number of factors, including gender, age, educational achievement, annual household income, employment status, and social class [11-12]. Obesity is regarded as an extremely costly health problem, with the direct medical costs of being overweight and obesity accounting

for approximately 5.0% to 10% of United States health care spending [13].

Obesity is a common disorder usually caused by the interaction of genetic, nutritional and environmental factors [14]. It has now become one of the most important health issues of modern society around the world. It is often associated with other diseases such as arteriosclerosis, high blood pressure, cancer, diabetes and osteoarthritis [15, 16]. The incidence of obesity is increasing rapidly, and it is revealed that around 500 million adults worldwide are obese [17].

Pancreatic lipase (PL) is an enzyme, which is secreted from the pancreas and plays an excellent role in the absorption of triglyceride in the small intestine. Dietary fat is made up of about 95% triacylglycerol (TG). Pancreatic lipase hydrolyzes water-insoluble triacylglycerol in the intestinal lumen and is thus used for dietary fat absorption. Pancreatic lipase inhibitors considered a valuable therapeutic agent for the treatment of diet-induced obesity [18].

One of the screening strategies used in anti-obesity drug discovery is to search for potent lipase inhibitors from natural products. Medicines that come from natural sources are safer and more efficient, even if they are toxic, but less harmful than pure

synthetic ones. Attention is being paid to the discovery of novel natural bioactive compounds as the foundation of new drug discovery as previously reliable standard drugs become less effective against emerging new strains of many drug-resistant strains [19].

MATERIALS AND METHODS

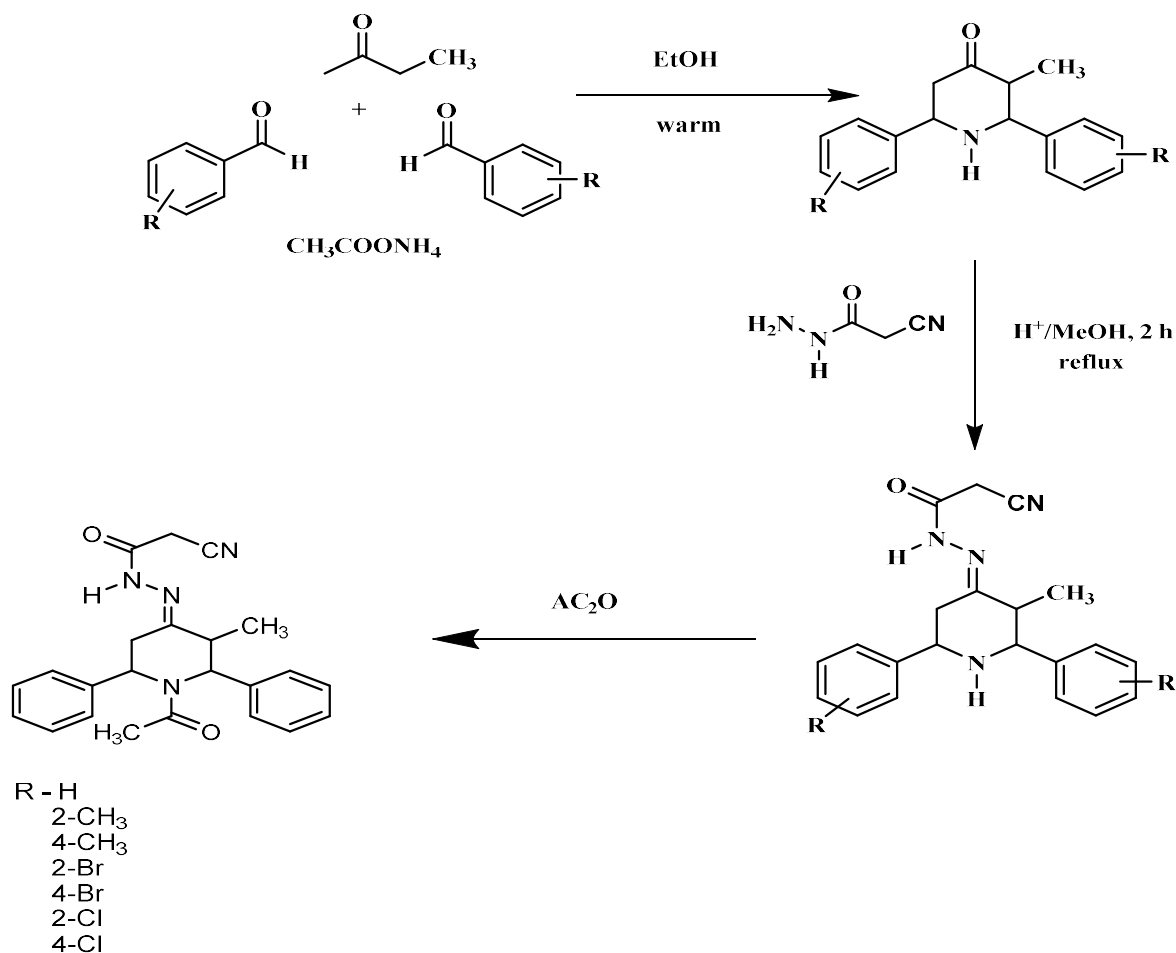
All chemicals (solvents and reagents) were obtained from AR grade Sigma/Aldrich and Merck. was purchased from foreign companies (Hi-Media and Sigma/Aldrich) and was not used with further purification and distillation. Local chemicals have not been used in the research work. The purity of these chemicals was 98–99.9%. Other reagents used were ammonium acetate and cyanoacetic hydrazide (Merck). Analytical grade solvents such as ethanol, methanol, ethyl acetate, chloroform (CHCl₃) and n-hexane were used without further distillation. The synthesized compounds were increased to yield and purified by recrystallization with the appropriate solvent system.

IR spectra were recorded in an AVATAR-330 FT-IR spectrophotometer (Thermo Nicolet) and only notable absorption levels (mutual centimeter) are listed. ¹H NMR spectra were recorded on a

BRUKER AMX 300 MHz and 300 MHz NMR was performed on a BRUKER AMX 300 MHz NMR spectrometer operating at 100 MHz. For recording ¹H NMR spectrum of compound solution were prepared by dissolving about 10mg of the compound in 0.5 ml of CDCl₃ was used as solvent while for ¹³C NMR spectra, about 50 mg of the compound was dissolved in the same volume of the respective solvents. TMS (Tetra methyl silane) was used as a internal standard.

Preparation of N-acetyl 3-methyl-2,6-diphenylpiperidin-4-one cyanoacetyl hydrazone derivatives

A mixture of 3-methyl-2,6-diphenylpiperidin-4-one (0.1 mol), cyanoacetic hydrazide (0.1 mol) in the presence of few drops of concentrated acetic acid in methanol was refluxed for 2 hours. After the completion of reaction, the reaction mixture was cooled to room temperature. The solid product was separated by filtration and washed with warm water and recrystallized by methanol to afford 3-methyl-2,6-diphenylpiperidin-4-one cyanoacetyl hydrazone. Then cyclized by 0.1 mol of acetic anhydride.



In vitro Anti-obesity activity

Anti-obesity activity determined by the method of

Pancreatic lipase inhibitory (Anti-obesity) activity of compounds

Pancreatic lipase activity was modified from that previously described by Kim *et al.* (2010) and Anil Kumar *et al* (2011) method.

Reagents

1. Olive oil
2. Phosphate Buffer (pH 6)

3. Porcine pancreatic lipase (1 mg/ml; 0.1 mm potassium phosphate buffer (pH 6.0))
4. Acetone
5. Ethanol
6. Sodium hydroxide (0.02M)
7. Oxalic acid ((0.01M)
8. Standard: Orlistat

Procedure

Different concentrations (100, 200, 300, 400 and 500 $\mu\text{g}/\text{ml}$) of sample were taken and each concentration of the sample (100 μl) was mixed with 8 ml of olive oil,

0.4 ml phosphate buffer and 1 ml of Porcine pancreatic lipase and it were incubated for 60 min. The reaction was stopped by the addition of 1.5 ml of a mixture containing acetone and 95 % ethanol (1:1). The appearance of pink colour from yellow colour shows the liberated fatty acids, which was determined by titrating the solution against 0.02 M sodium hydroxide (standardized by 0.01 M oxalic acid) using phenolphthalein as an indicator. Similar concentrations of positive control as Orlistat (Standard) are used. The Lipase activity of the control was checked without inhibitor (sample). Percentage inhibition of lipase activity was calculated using the formula:

$$\text{Lipase inhibition} = \frac{A - B}{A} \times 100$$

Where A is lipase activity, B is activity of lipase when incubated with the sample.

Orlistat was used with the same concentrations as a positive control. The data were expressed as percentage inhibition, which was calculated using the formula,

Lipase Inhibition = $\frac{A - B}{A} \times 100$ where, A is the lipase activity B is activity of lipase when incubated with the sample.

The concentration of the synthesized compounds which inhibits 50% of enzyme activity is termed as the IC50. orlistat were used as controls. A standard

dose response curve was plotted at all the different concentrations. From the plotted curves, the IC50 value for each of the synthesized compounds was calculated. The data were combined and identified as mean \pm standard deviation (SD).

RESULT AND DISCUSSION

N-acetyl 3-methyl-2,6-diphenylpiperidin-4-one cyanoacetylhydrazone (S1): Yield. 79.65%.

Mp. 160-163°C. FT-IR (KBr) ν_{max} (cm⁻¹): 3062-2935(C-H Aliphatic & Aromatic stretching), 1720(C=O), 1495 (C=O piperidin moiety), 1647(C=N), 2261 (C≡N), 3424-3269(N-H).

¹³C NMR(300 MHz, CDCl₃) δ ppm :141.48(C-2 ipso carbon), 141.17 (C-6 ipsocarbon), 127.59-128.72(Aromatic carbons), 209.53(C=O Piperidin moiety), 23.13 (CH₃ carbon of Piperidin moiety),173.10(C=N), 126.82(C≡N), 43.07(CH₂ carbon of cyanoacetylhydrazone moiety) , 76.65(C-2), 77.50(C-6), 46.23(C-3),23.46(C-5), 13.63(3-CH₃).¹H NMR(300 MHz, CDCl₃),

δ ppm: 7.25-7.10 (Aromatic Protons), 6.17 (N-H HydrazoneMoiety), 3.59 (CH₃ – Protons in Piperidin moiety), 3.28 (CH₂ – Protons in hydrazone moiety), 0.86 (3-CH₃), 3.90 (H-6a), 3.53

(H-2a), 2.23 (H-5a), 2.90 (H-5e), 2.58 (H-3a Proton).

N-acetyl 3-methyl-2, 6 (bis-*o*-bromo phenyl) piperidin-4-one cyanoacetyl hydrazone (S2): Yield. 79.65%. Mp.179-181°C. FT-IR (KBr) ν_{\max} (cm⁻¹): 3099-2931 (C-H Aliphatic &Aromatic stretching), 1681 (C=O), 1567 (C=N), 2265 (C≡N), 3308-3179 (N-H).

¹³C NMR(300 MHz, CDCl₃) δ ppm: 130.10 (C-2 ipso carbon), 130.62 (C-6 ipso carbon), 128.59-129.54(Aromatic carbons), 166.34 (C=O), 159.54 (C=N), 125.18 (C≡N), 25.11 (CH₂ carbon of cyanoacetohydrazone moiety),65.86 (C-2), 59.64 (C-6), 39.14 (C-3), 25.23 (C-5), 12.19 (3-CH₃). ¹H NMR (300 MHz, CDCl₃), δ ppm: 7.53- 7.31 (Aromatic protons) 10.79 (N-H, Hydrazone Moiety), 2.50 (N-H Piperidin moiety), 3.35 (CH₂ –Protons in hydrazone moiety), 0.91((3-CH₃), 3.88 (H-6a), 3.35(H-2a), 2.50 (H-5a), 3.35 (H-5e), 2.51(H-3a Proton).

N-acetyl 3-methyl-2, 6 (bis-*o*-chloro phenyl) piperidin-4-one cyanoacetyl hydrazone (S3) : Yield. 80.69%. Mp.142-145°C. FT-IR(KBr) ν_{\max} (cm⁻¹): 3070-2939((C-H Aliphatic &Aromatic stretching), 1633 (C=O),1470 (C=O piperidinmoiety) 1416(C=N), 2262 (C≡N), 3419-3259 (N-H). ¹³C NMR(300 MHz, CDCl₃) δ ppm: 139.58 (C-2 ipso carbon),133.81(C-6 ipso carbon),

128.17-132.84 (Aromatic carbons), 172.49(C=O Piperidin moiety), 21.55(CH₃ carbon of Piperidin moiety), 139.79(C=N), 128.17(C≡N), 22.97(CH₂ carbon of cyanoacetohydrazone moiety) , 48.05(C-2), 58.59(C-6), 39.15(C-3), 39.43(C-5), 13.52(3-CH₃). ¹H NMR(300 MHz, CDCl₃), δ ppm: 7.237-4.8(Aromatic Protons), 7.50 (N-H Hydrazone Moiety), 3.17 (CH₃ –Protons in Piperidin moiety), 3.20 (CH₂ –Protons in hydrazone moiety), 1.17 (3-CH₃)3.73(H-6a), 3.3(H-2a), 2.98 (H-5a), 3.4(H-5e), 2.67(H-3a Proton).

N-acetyl 3-methyl-2,6 (bis-*o*-methyl phenyl) piperidin-4-one cyanacetyl hydrazone (S4): Yield. 82.6%. Mp. 179-181°C.FT-IR(KBr) ν_{\max} (cm⁻¹): 3024-2977((C-H Aliphatic &Aromatic stretching), 1716 (C=O),1490 (C=O piperidin moiety)1650(C=N), 2337 (C≡N), 3428-3066 (N-H). ¹³C NMR(300 MHz, CDCl₃) δ ppm: 137.42 (C-2 ipso carbon), 136.89(C-6 ipso carbon), 126.75-131.45(Aromatic carbons), 172.49(C=O Piperidin moiety), 22.62(CH₃ carbon of Piperidin moiety),140.90(C=N), 126.22(C≡N), 24.28(CH₂ carbon of cyanoacetohydrazone moiety) , 52.14(C-2), 57.53(C-6), 39.14(C-3),22.78(C-5), 18.94(3-CH₃). ¹H NMR(300 MHz, CDCl₃), δ ppm: 6.88-7.31(Aromatic Protons), 7.42 (N-H Hydrazone Moiety),

2.32(CH₃ –Protons in Piperidin moiety), 3.21 (CH₂ –Protons in hydrazone moiety), 1.106 (3-CH₃) 3.73(H-6a),3.3(H-2a), 2.98 (H-5a), 3.4(H-5e), 2.67(H-3a Proton).(3-CH₃), 3.89 (H-6a), 3.11 (H-2a), 2.39 (H-5a), 3.07(H-5e), 2.57(H-3a Proton), 2.33 (*o*-CH₃ protons).

N-acetyl 3-methyl-2,6 (bis-*p*-bromo phenyl) piperidin-4-one cyanoacetyl hydrazone (S5): Yield. 79.65%. Mp. 186-189°C. IR (cm⁻¹): 3025-2852 (C-H Aliphatic & Aromatic stretching), 1674 (C=O), 1568 (C=N), 2267 (C≡N), 3440-3184 (N-H).¹³C NMR (δ ppm): 139.98 (C-2 ipso carbon), 140.49(C-6 ipso carbon), 126.49-129.77 (Aromatic carbons), 164.48 (C=O), 158.05 (C=N), 114.35 (C≡N), 24.16 (CH₂ carbon of cyanoacetohydrazone moiety), 76.57 (C-2), 56.12 (C-6), 44.89 (C-3), 34.56 (C-5), 11.15 (3-CH₃) 19.20 (*o*-CH₃). ¹H NMR (δ ppm) : 7.32-7.13 (Aromatic Protons), 10.09 (Hydrazone Moiety), 2.09 (N-H Piperidin moiety), 3.50 (CH₂ –Protons in hydrazone moiety), 0.92 (3-CH₃), 3.89 (H-6a), 3.11 (H-2a), 2.39(H-5a), 3.07(H-5e), 2.57 (H-3a Proton), 2.33 (*o*-CH₃ protons).

3-methyl-2,6 (bis-*p*-chloro phenyl) piperidin-4-one cyanoacetyl hydrazone (S6) : Yield. 80.69% . Mp.118-120°C. IR (cm⁻¹): 3100-2875(C-H Aliphatic & Aromatic stretching), 1687 (C=O), 1592

(C=N), 2261 (C≡N), 3295-3198 (N-H). ¹³C NMR (δ ppm): 140.78 (C-2 ipso carbon), 141.63(C-6 ipso carbon), 130.55-130.75 (Aromatic carbons), 164.36 (C=O), 155.48 (C=N), 114.18 (C≡N), 23.96 (CH₂ carbon of cyanoacetohydrazone moiety), 67.56 (C-2), 58.98 (C-6), 44.27 (C-3), 35.72 (C-5), 11.31 (3-CH₃). ¹H NMR (δ ppm) :7.26-7.51(Aromatic Protons), 9.83 (N-H Hydrazone Moiety), 2.09 (N-H Piperidin moiety), 3.77 (CH₂ –Protons in hydrazone moiety), 0.89 (3-CH₃), 3.90 (H-6a), 3.51 (H-2a), 2.18 (H-5a), 2.97 (H-5e), 2.55 (H-3a Proton).

3-methyl-2,6 (bis-*p*-methyl phenyl) piperidin-4-one cyanoacetyl hydrazone (S7) :Yield. 78.69%. Mp. 120-122 °C. FT-IR(KBr) ν_{\max} (cm⁻¹): 3026-2963(C-H Aliphatic & Aromatic stretching), 1701 (C=O), 1638 (C=N), 2266 (C≡N), 3195-3097(N-H). ¹³C NMR(300 MHz, CDCl₃) δ ppm: 139.33 (C-2 ipso carbon), 139.83 (C-6 ipso carbon), 126.42-129.38 (Aromatic carbons), 164.87 (C=O), 158.07 (C=N), 114.13 (C≡N), 24.56 (CH₂ carbon of cyanoacetohydrazone moiety), 68.92 (C-2), 60.46 (C-6), 45.34 (C-5), 36.16 (C-3), 12.10 (3-CH₃), 21.13(*p*-CH₃) . ¹H NMR(300 MHz, CDCl₃) δ ppm : 7.14-7.36 (Aromatic Protons), 9.01(N-H, Hydrazone Moiety), 2.06 (N-H Piperidin moiety), 3.73 (CH₂ –

Protons in hydrazone moiety), 0.89 (3-CH₃), 3.87 (H-6a), 3.49 (H-2a), 2.24 (H-5a), 2.83 (H-5e), 2.57 (H-3a Proton), 2.06 (p-CH₃ protons).

Anti obesity activity

In the current scenario, obesity is a major public health problem with approximately 1.9 billion adults (aged 18 years and older) worldwide and approximately 600 million of them are clinically obese. The disease is characterized by an increase in the size of the adipocytes, which leads to an increase in the amount of fat in the disease of adipota. Microbes such as germline are cured in order to increase the adipocytes. Thus, inhibition of digestion and absorption of dietary fat is a first key to treating obesity. This inhibition involve lipase enzyme, the principle lipolytic enzyme synthezied and secreted by the pancreas. There is an increase in the amount of damage to the testes. The substrates for the lipase enzyme are long-chain triacylglycerols, which are separated from the surface phase by the aqueous medium. Thus, the lipase enzyme must be adsorbed on the substrate lipid surface and the nature of the substrate surface has an important role for lipase activity.

Inhibition of pancreatic lipase is an attractive targeted approach for the

discovery of potent anti-obesity agents for the treatment of obesity. One of the screening strategies used in anti-obesity drug discovery is to search for potent lipase inhibitors from synthesized compounds. In this study, we screened synthesized compounds as potential anti-obesity agents by monitoring their anti-lipase activity. Concentration – dependently on the *in vitro* assay.

The activity of the compounds was determined by comparison with the anti-obesity of Pancreatic lipase. The test compound was measured for the decrease in clot weight at different concentrations. The different concentrations compared about or list at as standard drug [20-22].

Pancreatic lipase inhibitory activity of synthesized compound is given in **Figure 1**.

In the present study, anti-obesity activity analysis of compounds (low concentration

(100 µg/ml) to higher concentration (500 µg/ml).

Synthesized compoundBCAHACO₂ (S1) significantly inhibited lipase with low concentration was 14.25% while the higher concentration was 76.45%.Anti-obesity activity analysis of compounds (low concentration (100 µg/ml) to higher concentration(500 µg/ml). Synthesized compound 2-BrCAHACO₂(S2)

significantly inhibited lipase with low concentration was 17.46% while the higher concentration was 83.47%.

anti-obesity activity analysis of compounds (low concentration (100 $\mu\text{g/ml}$) to higher concentration (500 $\mu\text{g/ml}$). Synthesized compound 2- ClCAHACO₂(S3) significantly inhibited lipase with low concentration was 18.07% while the higher concentration was 85.93%. anti-obesity activity analysis of compounds (low concentration(100 $\mu\text{g/ml}$) to higher concentration(500 $\mu\text{g/ml}$). Synthesized compound 2-MeCAHACO₂ (S4) significantly inhibited lipase with low concentration was 19.54% while the higher concentration was 87.45%.

anti-obesity activity analysis of compounds (low concentration (100 $\mu\text{g/ml}$) to higher

concentration (500 $\mu\text{g/ml}$). Synthesized compound 4-BrCAHACO₂(S5) significantly inhibited lipase with low concentration was 14.39% while the higher concentration was 78.05%.

Anti-obesity activity analysis of compounds (low concentration (100 $\mu\text{g/ml}$) to higher concentration (500 $\mu\text{g/ml}$). Synthesized compound 4-ClCAHACO₂(S6) significantly inhibited lipase with low concentration was 16.94% while the higher concentration was 81.26%.

anti-obesity activity analysis of compounds (low concentration(100 $\mu\text{g/ml}$) to higher concentration(500 $\mu\text{g/ml}$). Synthesized compound 4-MeCAHACO₂(S7) significantly inhibited lipase with low concentration was 15.79% while the higher concentration was 80.45%.

Table 1: Anti-obesity activity (Pancreatic lipase inhibitory activity) of Synthesized compound

Samples	Concentrations ($\mu\text{g/ml}$)					IC ₅₀ value ($\mu\text{g/ml}$)
	100	200	300	400	500	
S1	14.25±0.99	23.56±1.64	39.69±2.77	60.81±4.25	76.45±5.35	343.49
S2	17.46±1.22	30.21±2.11	47.63±3.33	68.95±4.82	83.47±5.84	302.59
S3	18.07±1.26	30.62±2.14	49.81±3.48	71.68±5.01	85.93±6.01	293.05
S4	19.54±1.36	33.29±2.33	51.65±3.61	72.43±5.07	87.45±6.12	283.52
S5	14.39±1.01	24.65±1.72	40.98±2.86	61.04±4.27	78.05±5.46	337.75
S6	16.94±1.18	29.46±2.06	45.98±3.21	66.49±4.65	81.26±5.68	311.85
S7	15.79±1.10	27.43±1.92	43.54±3.04	65.91±4.61	80.45±5.63	320.11
Std. (Orlistat)	21.61±1.51	37.48±2.62	56.93±3.98	78.52±5.49	92.46±6.47	259.56

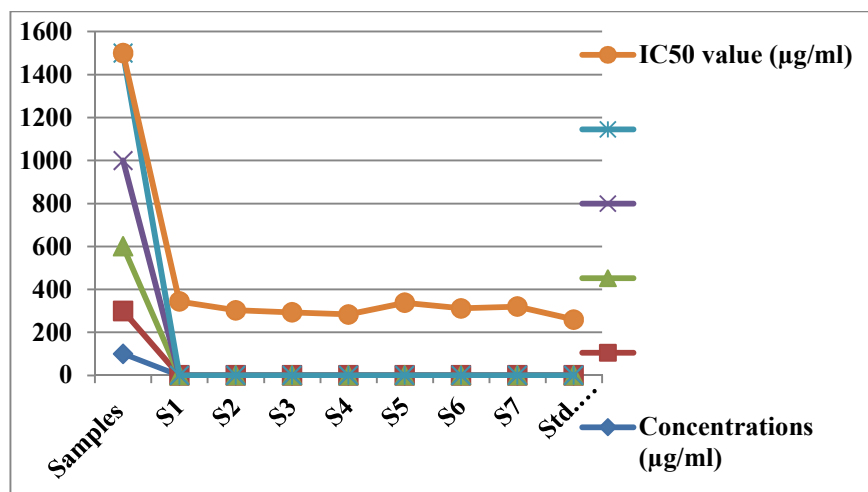


Figure 1: Anti-Obesity activity Graph

CONCLUSION

The structure of the synthesized compound is established on the basis of their analytical and spectral data (IR, ^1H NMR, ^{13}C NMR). The synthesized compound was subjected to preliminary anti-obesity by pancreatic lipase inhibitory activity. The result from the study showed that the N-acetyl -3-methyl cyano acetyl hydrazone derivatives had excellent anti-obesity activity that was comparable to the activity of Orlistat. The study revealed that few of the synthesized such as N- acetyl -3-methyl cyano acetyl hydrazone derivatives exhibited high total potent pancreatic lipase inhibitory effects. Strong positive correlation between synthesized bioactives and that of the anti - lipase activity was observed. It can be concluded from the present study that N-acetyl -3-methyl cyano acetyl hydrazone derivatives provide convincing anti-obesity.

This research may provide a basic for in vivo study and strong foundation for future development of synthesized compounds with great applications in prevention and treatment of obesity.

Acknowledgements

The authors wish to thank Government Arts Cllege, Trichy-22 for letting us use his laboratory equipment in the process of Synthesizing compounds. Dr. Velavan Director of Harman Institute, Thanjavur-613005, Tamilnadu for providing lab facilities.

REFERENCE

- [1] Hasan, M.U.; Arab, M.; Pandiarajan, K.; Sekar, R.; Marko, D. *Magn. Reson. Chem.* 1985, 23, 292.
- [2] Thomas G. In *Fundamentals of Medicinal Chemistry-An Introduction*. John Wiley and Sons. West Sussex: 2000; pp 1-6.

- [3] Thomas L. Gilchrist In Heterocyclic Chemistry. 3rd ed.; Pearson Education (Singapore) Pvt. Ltd. 2005 pp 319-328.
- [4] V.Karthikeyan, K. Sivakumar, Aishwarya Gokuldass and S.MohanaSundaram (2012). Studies on Larvicidal Activity of *Leucas aspera*, *Vitex negundo* and *Eucalyptus* against *Culex quinquefasciatus* collected from Coovum River of Chennai, India. Asian J Pharmaceutical Sci. and Clin. Res. Vol 5 Suppl 3, 1-4.
- [5] Mohanasundaram, S., Ramirez-Asis, E., Quispe-Talla, A. *et al.* Experimental replacement of hops by mango in beer: production and comparison of total phenolics, flavonoids, minerals, carbohydrates, proteins and toxic substances. Int J Syst Assur Eng Manag (2021). <https://doi.org/10.1007/s13198-021-01308-3>.
- [6] Clack HT, Johnson JR, & Robinson R. The chemistry of penicillin's. Princeton University. New York. 1949.
- [7] Victor Arokia Doss, Prasad Maddisetty, Mohanasundaram.S (2016). Biological active compounds with various medicinal values of *Strychnos Nux-vomica* – A Pharmacological summary. J Global Trends Pharm Sci 7(1): 3044-3047.
- [8] Mohanasundaram.S, N.Rangarajan, V.Sampath, K.Porkodi, M.Pennarasi (2021). GC-MS and HPLC analysis of Antiglycogenolytic and Glycogenic compounds in Kaempferol 3 – O – gentiobioside containing *Senna alata* L leaves in experimental rats. Translational Metabolic Syndrome Research., 4(2021):10-17..
- [9] Victor Arokia Doss, Mohanasundaram.S, Prasad Maddisetty (2016). Analysis of hydroethanolic extract of *Senna alata* (L.) to screen bioactive compounds with inhibitory activity on lipid peroxidation, in vitro antibacterial and antidiabetic efficacy. Int J Pharma Sci., 6(1): 1360-1366.
- [10] World Health Organization (WHO), World Health Organization Factsheets, Obesity and overweight, 2017, <http://www.who>

- .int/mediacentre/factsheets/fs311/en/.
- [11] C.K. Cheung, J.F. Wyman, and L.L. Halcon, “Use of complementary and alternative therapies in community-dwelling older adults,” *The Journal of Alternative and Complementary Medicine*, vol.13, no.9, pp. 997–1006, 2007.
- [12] S.K.N dao Brumblay and C.R. Green, “Predictors of complementary and alternative medicine use in chronic pain patients,” *PainMedicine*, vol. 11, no. 1, pp. 16–24, 2010.
- [13] A. G. Tsai, D. F. Williamson, and H. A. Glick, “Direct medical cost of overweight and obesity in the USA: a quantitative systematic review,” *Obesity Reviews*, vol. 12, no.1, pp. 50–61, 2011.
- [14] Poulos, S.P.; Dodson, M.V.; Hausman, G.J. Cell Line Models for Differentiation: Preadipocytes and Adipocytes. *Experimental Biology and Medicine* 2010, 235, 1185–1193.
- [15] Sweeting. A.N.; Hocking, S.L.; Markovic, T.P. Pharmacotherapy for the Treatment of Obesity. *Molecular Cell Endocrinology* 2015, 418, 173–183.
- [16] Hanefeld, M.; Sachse, G. The Effects of Orlistat on Bodyweight and Glycaemic Control in Overweight Patients with Type 2 Diabetes: A Randomized, Placebo-Controlled Trial. *Diabetes, Obesity and Metabolism* 2002, 4, 415–423.
- [17] Chakrabarti, R. Pharmacotherapy of Obesity: Emerging Drugs and Targets. *Expert Opinion on Therapeutic Targets* 2009, 13, 195–207.
- [18] Kusunoki, M.; Tsutsumi, K.; Tana, C.; Sato, D.; Nakamura, T. Lipoprotein Lipase Activation Improves the Cachexia and Obesity. *Journal of Obesity and Weight Loss Therapy* 2013, 3, Article ID 1000177.
- [19] Muller K. Pharmaceutically relevant metabolites from lichens. *Appl Microbiol Biotechnol* 2002; 56: 9-16.
- [20] Tsujita T, Ninomiya H, Okuda H. p-Nitrophenyl butyrate hydrolyzing activity of hormone-sensitive lipase from bovine adipose tissue. *J Lipid Res.* 1989; 30:997-1004.

[21] Shizhen L, Xiwen L. Compendium of Materia Medica. Foreign Languages Press; Beijing, China. 2003; 6:410-416.

[22] Rahul B, Birari A, Shikhar Gupta
C. Gopi Mohanb, Kamlesh K and

Bhutania. Antiobesity and lipid lowering effects of Glycyrrhizachalcones Experimental and computational studies. Phyto-medicine. 2011; 18: 795-801.



**International Journal of Biology, Pharmacy
and Allied Sciences (IJBPAS)**

'A Bridge Between Laboratory and Reader'

www.ijbpas.com

INSILICO MOLECULAR DOCKING OF N-ACETYL CYANOACETY HYDRAZONE DERIVATIVES SCAFFOLDS AS PROSPECTIVE ANTI- BREAST CANCER AGENT

V.PRIYADARSHINI¹, K.SUNDARESAN² AND K.THARINI^{1*}

1: Department of Chemistry, Government Arts College, Trichy-22, (Affiliated to Bharathidasan University)

2: Department of Chemistry, Meenakshi Ramaswamy College, Thathanur, Tamil Nadu, India

*Corresponding Author: K.Tharini; E Mail: tharinilenin@gmail.com

Received 26th July 2021; Revised 27th Aug. 2021; Accepted 1st Oct. 2021; Available online 1st Nov. 2021

<https://doi.org/10.31032/IJBPAS/2021/10.11.1113>

ABSTRACT

The present study is concerned with the docking of synthesized molecules ((E)-2-(2-chlorobenzylidene) hydrazine-1-carbonyl cyanide [1], (E)-2-(4-bromobenzylidene) hydrazine-1-carbonyl cyanide [2], (E)-2-(2-bromobenzylidene) hydrazine-1-carbonyl cyanide [3], (E)-2-(4-methylbenzylidene) hydrazine-1-carbonyl cyanide [4], (E)-2-(2-methylbenzylidene) hydrazine-1-carbonyl cyanide [5], (E)-2-(4-chlorobenzylidene) hydrazine-1-carbonyl cyanide [6], (E)-2-benzylidene hydrazine-1-carbonyl cyanide [7] and in order to arrive at an effective drug such as a molecule targeting the Crystal Structure of the BRCT Domains of Human BRCA1 primarily responsible for Breast Cancer, this application as an anticancer agent. Protein Data Bank, to retrieve the protein structure; Pubchem compound database, to retrieve the chemical structure of estrogen receptor inhibitors; Discovery Studio 2017 for docking and ADMET research are the methods and applications used. The findings indicate that both compounds have a strong binding affinity with the Human Estrogen Receptor protein's active site and can be used in breast cancer as a possible estrogen receptor inhibitor.

Key words: Molecular docking, Breast cancer, ADMET, BRCA1, Schiff base

1. INTRODUCTION

Breast cancer is characterized by the uncontrolled growth of cells in the breast tissue forming a hard-painless lump, typically in the milk ducts or lobules supplying milk to them [1]. The status of three unique cell surface receptors is the most common practice for classifying breast tumours: the estrogen receptor (ER), the progesterone receptor, and the HER2/neu receptor for the human epidermal growth factor (EGF) receptor. Of all breast cancers, approximately 75 percent are hormone receptor-positive. HER2-positive breast cancer accounts for 20% to 30% of hormone receptor-positive breast cancer associated with HER2/neu protein overexpression [2]. Triple-negative breast cancer (TNBC), a rare type of breast cancer, contains tumour cells that lack estrogen and progesterone receptors and do not over-express the protein HER2 [3]. One of the factors shown to raise the risk of a woman getting breast cancer is age. In women, breast cancer has been found to develop at or above the age of 50. It is also understood that a good personal or family history presents an increased risk of developing breast cancer. Moreover, long menstrual life or the use of hormone replacement therapy after menopause raises the risk of breast cancer growth [4].

The most common form of tumour in women is breast cancer (BC), but metastases are the primary cause of death. Metastasis is a complex mechanism in which cancer cells migrate into the vessels of the blood, invade other tissues, and identify secondary sites for a colony. Indeed, BC starts as a local disease but can spread to distant locations, such as lymph nodes and various organs, with metastases [5]. This process includes the expression of a series of genes that control cancer cells' survival and invasion. As possible drug targets in the drug development phase, drugs that modulate the genes/proteins that control cancer cell survival, metastasis, apoptosis, and invasion are therefore of great importance [6]. However while new therapies have been developed to dramatically reduce metastatic BC mortality, resistance to anticancer agents can lead to treatment failure [7].

When there is a chronic disorder without an adequate cure, a drug discovery phase occurs. In academia, where a hypothesis is developed, the first phase of research always begins; for example, the inhibition or induction of a protein or pathway as a therapeutic effect in a condition of illness. Indeed, the selection of a target, which can be a variety of biological entities

such as proteins, RNA, and genes that can be selected through bioinformatics analysis, is a crucial point of the research process [7]. The putative drug molecule must have an ideal target available and the binding drug-target complex should induce a biological response [5] that can be quantified by in vitro models. Cell lines are the most used in vitro BC models, since they share many BC molecular and genomic features. With molecular docking, the binding affinity between the drug and the target can be computed in silico. In silico and in vitro screening can also help to determine the toxicity of the drugs/molecules examined rapidly, thus preventing further steps, such as in vivo and preclinical trials (in case of adverse effects of in silico and in vitro methods [5]. At least two components are needed in silico approaches with docking studies: a protein/drug database and a molecular docking algorithm. Protein and drug databases are a list of protein and drug structures.

Big data, which provides a broad variety of biological and chemical knowledge, has been generated by the rapidly growing number of structures and is a recent opportunity to gain a deeper understanding of the relationships between drugs and targets (usually proteins), drugs and diseases, and

targets and diseases. However, although the available data is often heterogeneous and incomplete, this information can be exploited by computational methods to deepen these interactions [8]. High-performance computational algorithms for drug discovery processes are needed, given the cost and time consumption of experimental methods. The "docking" computational technique can predict the binding of drug-target complexes as well as the ligand's conformation upon binding to a protein target. The binding free energy of target-drug interactions determines an association's affinity and the conditions for a complex to form. Rated binding free energies are not always reliable, but they can be used in a virtual screening method to pick new drugs such as small molecules to be tested experimentally [9-11]. New drugs with a low molecular weight that allow them to easily penetrate cells are promising small molecules [12]. Molecular docking may also be used to predict the effects of a drug, such as detecting an unintended reaction between a compound and off-targets. 57,000 abstracts/papers on molecular docking have been published to date, showing the importance of this analytical approach in drug production [13].

In silico methods have opened the way for a variety of biological problems to

be solved, leading to the discovery of novel inhibitors for multiple diseases. In this research, structure-based virtual screening (VS) screened active compounds against breast cancer targets to identify possible virtual hits. In addition, the ligands were examined for their absorption, delivery, metabolism, excretion, and toxicity (ADMET) profile, which determined the drug's ADMET efficacy. Potential hits have a greater chance of being potential drugs that suggest successful pharmacokinetic (PK) and pharmacodynamic (PD) properties. The results of the current study concluded that after testing through in vitro experiments, five multi-targeted compounds with high binding energies and a strong ADMET profile against all three targets were taken into account, suggesting them as possible hits for drug production against breast cancer.

2. METHODOLOGY

In our present study, *in silico* molecular docking and ADMET toxicity studies were carried out using BIOVIA Discovery Studio (DS) 2017 software.

2.1.Preparation of protein

In this analysis, the X-ray diffraction-based Crystal Structure of the BRCT Domains of Human BRCA1 in Complex with a Phosphorylated Peptide from Human Acetyl-CoA Carboxylase 1(PDB ID: 3COJ)

with a resolution of 1.90 Å was selected. Hydrogens were applied to the 3COJ protein by applying the Forcefield algorithm and then using CHARM forcefield in DS, the protein energy was reduced. For molecular docking research, we followed previously mentioned parameter [14].

2.2.Ligand preparation

The molecules ((E)-2-(2-chlorobenzylidene)hydrazine-1-carbonyl cyanide [1], (E)-2-(4-bromobenzylidene)hydrazine-1-carbonyl cyanide [2], (E)-2-(2-bromobenzylidene)hydrazine-1-carbonyl cyanide [3], (E)-2-(4-methylbenzylidene)hydrazine-1-carbonyl cyanide [4], (E)-2-(2-methylbenzylidene)hydrazine-1-carbonyl cyanide [5], (E)-2-(4-chlorobenzylidene)hydrazine-1-carbonyl cyanide [6], (E)-2-benzylidene hydrazine-1-carbonyl cyanide [7] and standard drug Tamoxifen were drawn in chemdraw software, subsequently, energy of the all the molecules were minimized and saved in SDF file format for further docking studies.

2.3. Docking study

In order to analyse the most common geometry of the protein-ligand complex, a molecular docking analysis was carried out. To understand the structural basis of these target proteins, a computational docking

study was used to analyse structural complexes of the 3COJ with 7 molecules along with Schiff base compounds. The CDOCKER (CHARMm-based DOCKER) protocol integrated within DS has examined potential binding modes between the ligands and these target proteins. The CDOCKER parameter to be run was tabulated in **Table 1**. The algorithm flexibly provides complete ligand and employs fields of CHARMm

power. Using CDOCKER energy, CDOCKER Interaction energy, Hydrogen bonds, binding energies, protein energy and ligand-protein complex energy, ligand binding affinity was measured. The energy of CDOCKER is stated in negative values. More negative value energy is seen as the ligands' higher binding affinity to the target protein protein [15, 16].

Table 1: Parameter of CDOCKER protocol

Input Receptor	Input/3COJ.dsv
Input Ligands	/Input/Total_min_ligands.sd
Input Site Sphere	-23.9454, 29.2003, 7.29961, 9
Top Hits	1
Random Conformations	10
Random Conformations Dynamics Steps	1000
Random Conformations Dynamics Target Temperature	1000
Include Electrostatic Interactions	True
Orientations to Refine	10
Maximum Bad Orientations	800
Orientation vdW Energy Threshold	300
Simulated Annealing	True
Heating Steps	2000
Heating Target Temperature	700
Cooling Steps	5000
Cooling Target Temperature	300
Forcefield	CHARMm
Use Full Potential	Yes
Grid Extension	8.0
Ligand Partial Charge Method	CHARMm
Random Number Seed	314159
Final Minimization	Full Potential
Final Minimization Gradient Tolerance	0
Parallel Processing	False
Parallel Processing Batch Size	25
Parallel Processing Server	localhost
Parallel Processing Server Processes	2
Parallel Processing Preserve Order	True
Random Dynamics Time Step	0.002

2.4.ADMET Toxicity Analysis

In drug development and environmental hazard assessment, prediction of the ADMET profile for drug candidates

and environmental chemicals plays a major role. The ADMET properties of the filtered compounds were predicted using DS software in order to classify the potential

adverse effects of these compounds in humans. Solubility, Absorption, BBB, HIA, and ADMET parameters are included. Risks and toxicity. 95% and 99% confidence ellipses in the ADMET PSA 2D, ADMET AlogP98 aircraft are described by the absorption levels of the HIA model [16].

3. RESULTS AND DISCUSSION

3.1. Molecular docking study

In the hope that effective and selective inhibitors will constitute a new class of therapeutics for cancers as well as other proliferative diseases, both pharmaceutical companies and university laboratories were involved in developing compounds that could inhibit the action of tyrosine kinase. As a new mode of cancer treatment, 3COJ inhibitors may also be implemented appropriately. To classify successful anti-breast cancer compounds, the current in silico research was conducted. The seven compounds such as ((E)-2-(2-chlorobenzylidene) hydrazine-1-carbonyl cyanide [Mol.1], (E)-2-(4-bromobenzylidene) hydrazine-1-carbonyl cyanide [Mol.2], (E)-2-(2-bromobenzylidene) hydrazine-1-carbonyl cyanide [Mol.3], (E)-2-(4-methylbenzylidene) hydrazine-1-carbonyl cyanide [Mol.4], (E)-2-(2-methylbenzylidene) hydrazine-1-carbonyl cyanide [Mol.5], (E)-2-(4-chlorobenzylidene) hydrazine-1-carbonyl cyanide [Mol.6], (E)-

2-benzylidene hydrazine-1-carbonyl cyanide [Mol.7] and standard drug Tamoxifen were also evaluated for their binding interactions in 3COJ active site. After being tested via in vitro experiments, the virtual hits found in this study can be used as an alternative targeting agent for breast cancer. In addition, to philtre top hits to identify acceptable virtual hit candidate compounds, the ADMET profile was analysed. By extracting water molecules and repeating coordinates, the crystal structures have been refined. Atoms of hydrogen were added and charges were allocated to the atoms of proteins. The secondary structure of the active-site sphere target protein (radius 9) is shown in **Figure 1**. The -CDOCKER energy of each molecule with the target protein is described in **Table 2** as a result of the docking analysis.

The binding analysis indicates that the Human Estrogen Receptor was successfully docked with the seven compounds. From the docking results, the Mol.1 forms one strong Hydrogen bond with Arg 394 and Alkyl and Pi-Alkyl interactions with Leu 346, Met 421 and Leu 525 respectively. The -CDOCKER energy of this interaction is $-19.0777 \text{ kcal/mole}^{-1}$. Out of seven molecules the Mol. 4 shows higher binding affinity in receptor 3COJ compare to standard drug Tamoxifen (-CDOCKER

energy $-18.2547 \text{ Kcal/mol}^{-1}$) due to forms Pi-Alkyl and Pi-Pi T-shaped interactions. The remaining all compounds of 2D results are depicted in **Figure 4**. Here, the Mol. 1 revealed the poor binding affinity with binding energy being (is $-19.0777 \text{ kcal/mole}^{-1}$) which predict its weak biological breast cancer activity (not measured yet), but it may be similar activity to Tamoxifen drug. Therefore it is easily seen that it is predicted that all compounds would have almost identical activity against Human Estrogen Receptor.

3.2.ADMET analysis

The good absorption or permeation of the compound through the blood brain barrier is measured by its LogP, which must be lower than 5 [17, 18]. Pharmacokinetic screening results showed the Mol. 1 to Mol.7 adopted the law of five for oral

bioavailability of Lipinski. **Table 3** summarizes these ADMET screening findings. For drug likeness research, the ADMET descriptors of all the molecules were determined. Intestinal absorption and penetration of the blood brain barrier is predicted by the development of an ADMET model using 2D PSA and AlogP98 descriptors that include 95% and 99% confidence ellipses. These ellipses describe regions in which it is predicted that well-absorbed compounds will be contained. ADMET model screening findings have shown that all the compounds have 99 percent confidence levels for human intestinal absorption and penetration of the blood brain barrier (BBB). The polar surface area plot and ALogP for Mol.1 to Mol.7 are shown in **Figure 5**.

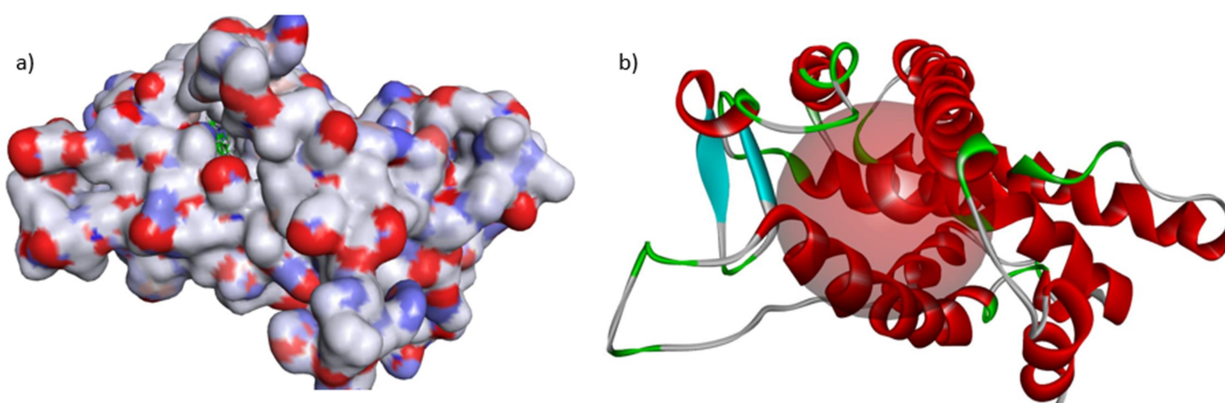
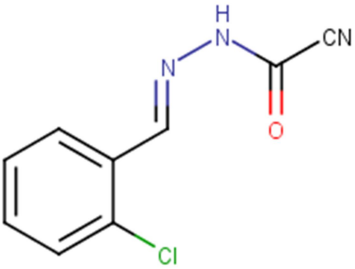
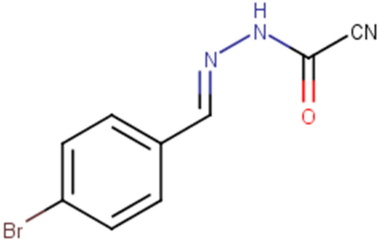
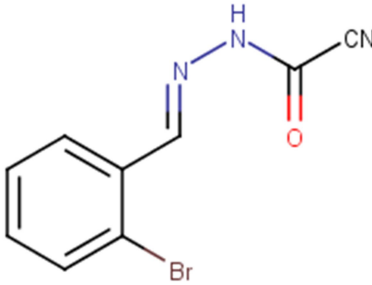
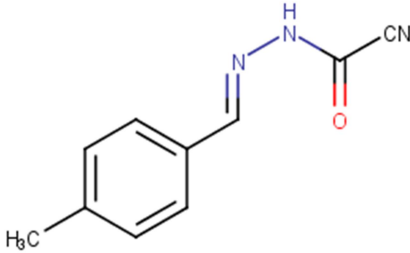
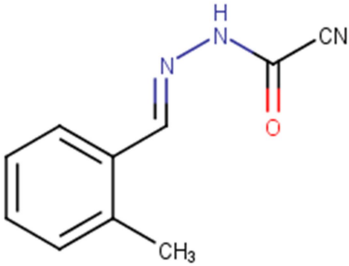
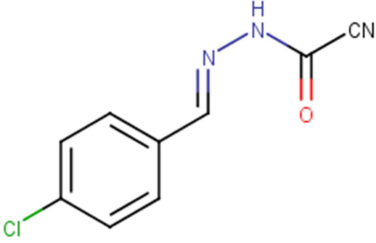
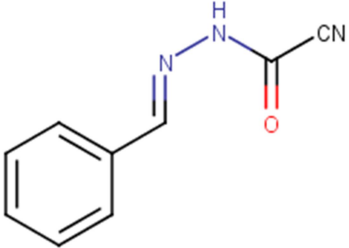
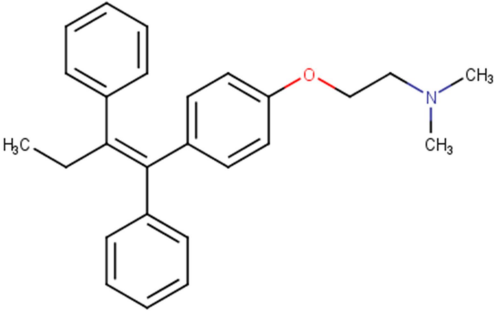


Figure 1: a) The secondary 3D structure of the target 3COJ protein with molecules and b) active site sphere of the protein

Table 2: CDOCKER energy of the molecules (Mol 1 to Mol.7)

S. No	Molecule Number	Structure	-CDOCKER Energy (Kcal/ mol ¹)
1	Mol. 1		19.0777
2	Mol. 2		23.3452
3	Mol. 3		20.3915
4	Mol. 4		23.9721
5	Mol. 5		22.2153

6	Mol. 6		22.7068
7	Mol. 7		22.2919
8	Tamoxifen		18.2547

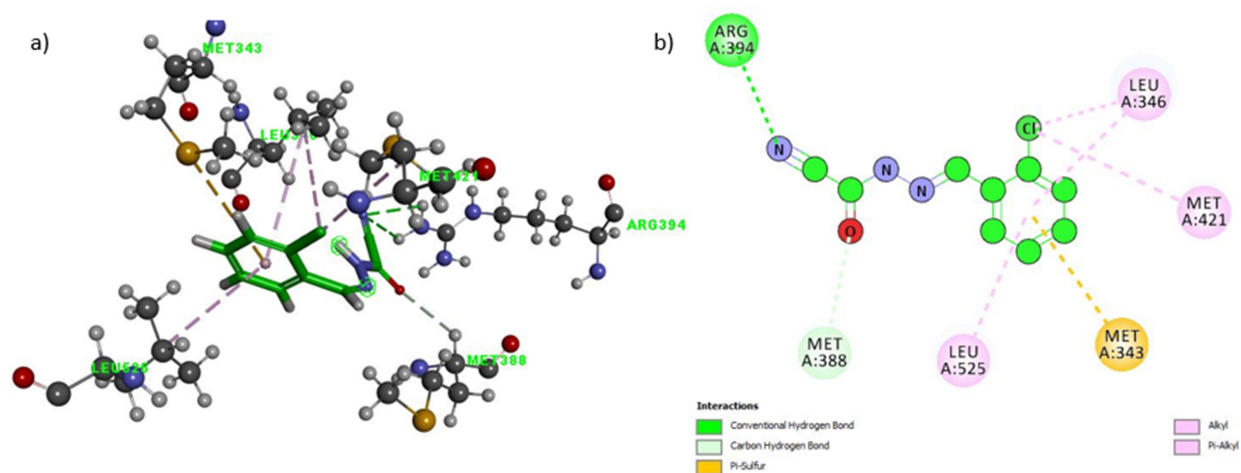


Figure 2: a) 3D and b) 2D binding site interaction of (E)-2-(2-chlorobenzylidene) hydrazine-1-carbonyl cyanide [Mol.1] in receptor 3COJ active site.

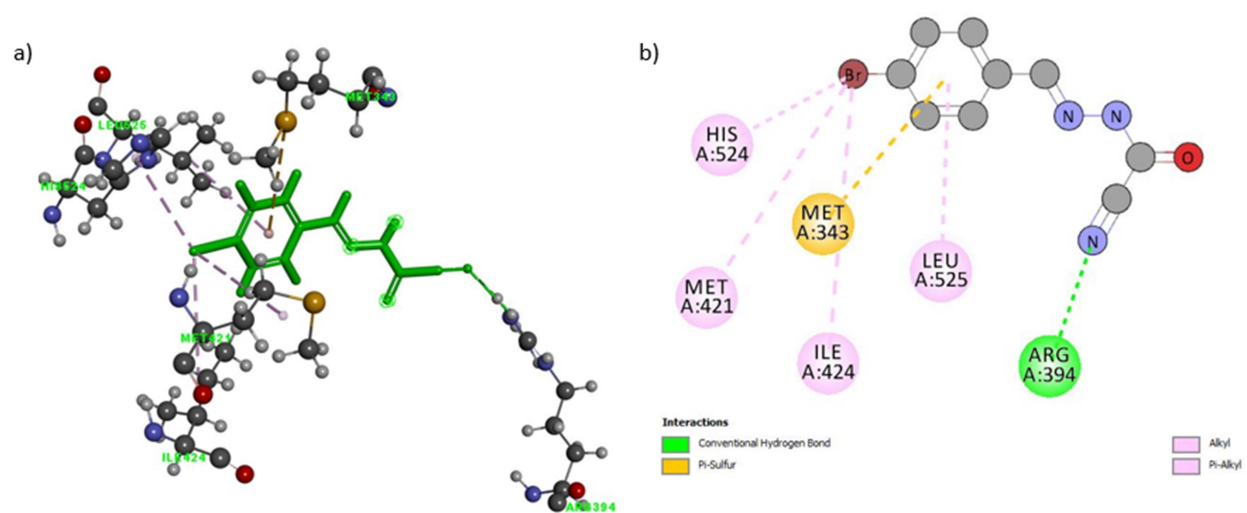


Figure 3: a) 3D and b) 2D binding site interaction of (E)-2-(4-bromobenzylidene) hydrazine-1-carbonyl cyanide [Mol.2] in receptor 3COJ active site

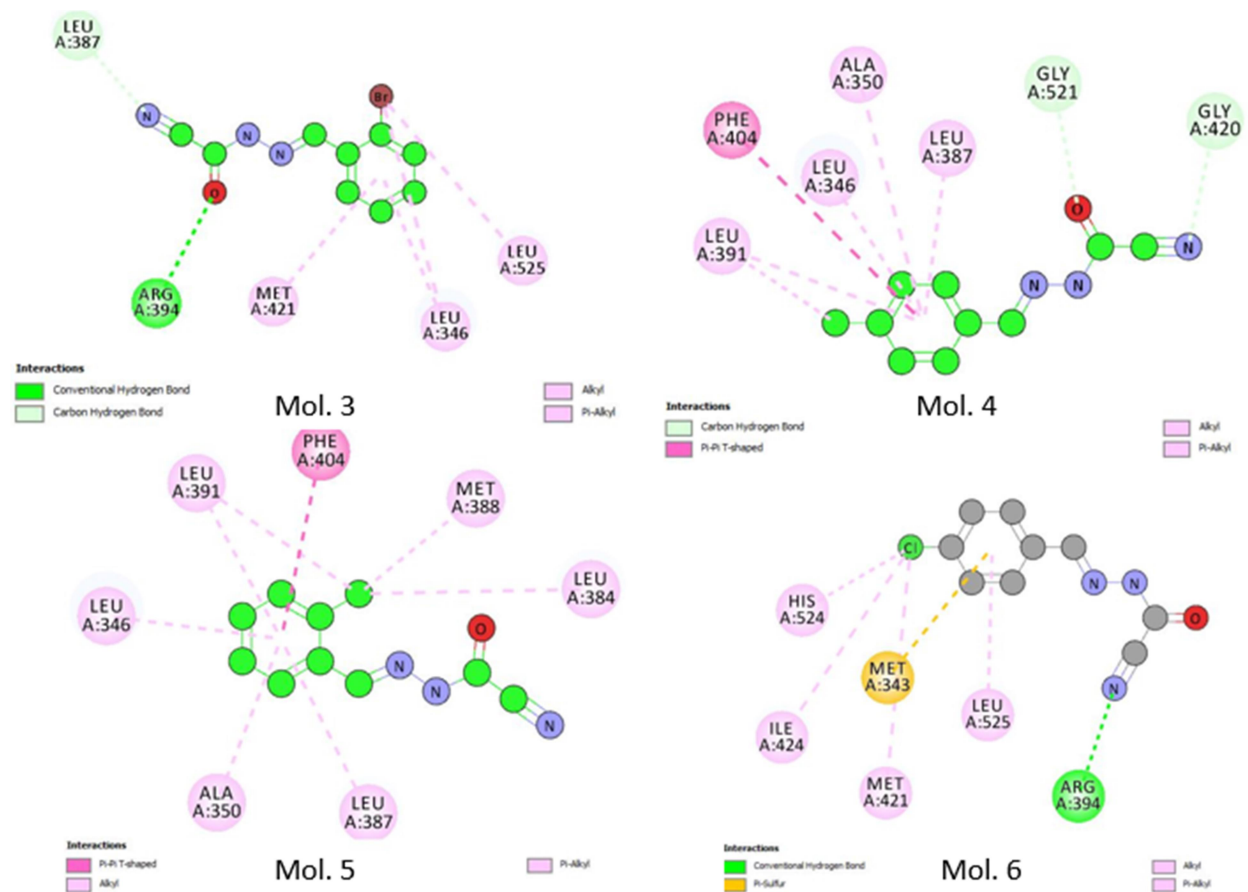


Figure 4: 2D interactions analysis of Mol.3, Mol.4, Mol.5 and Mol. 6 in receptor 3COJ active site

Table 3: ADMET properties of the compound Mol. 1 to Mol. 7

Name	Absorption level	Solubility level	BBB level	PPB level	Hepatotoxic level	CYP 2D6	PSA 2D	AlogP98
Mol. 1	Good	good	Very Low	0	<90%	Non inhibitor	64.369	4.46
Mol. 2	Moderate	good	Very Low	0	<90%	Non inhibitor	64.369	4
Mol. 3	Moderate	good	Very Low	0	<90%	Non inhibitor	64.369	4
Mol. 4	Moderate	good	Very Low	0	<90%	Non inhibitor	64.369	4.66
Mol. 5	good	good	Very Low	1	<90%	Non inhibitor	64.369	5.48
Mol. 5	good	good	Very Low	0	<90%	Non inhibitor	64.369	4.539
Mol. 6	good	good	Very Low	1	<90%	Non inhibitor	64.369	4.492
Mol. 7	good	good	Very low	1	<90%	Non inhibitor	64.369	4.85
Tamoxifen	good	good	Very low	1	<90%	Non inhibitor	64.369	4.91

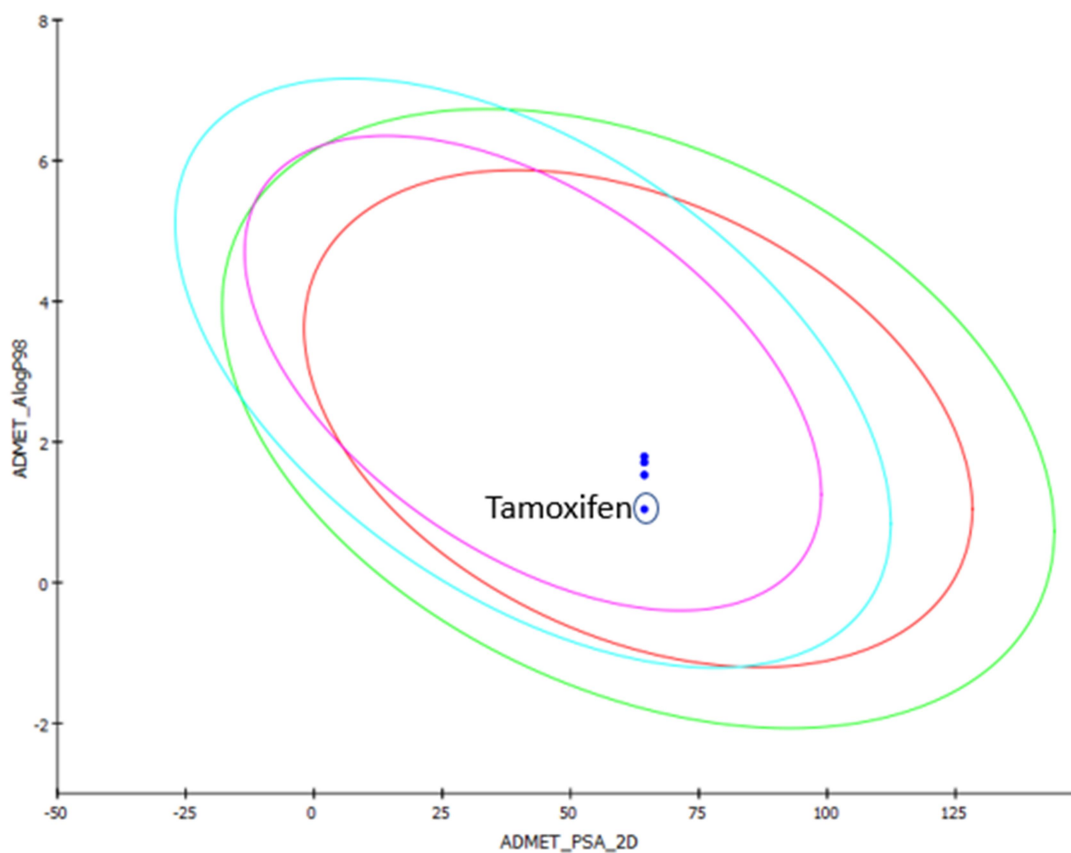


Figure 5: Plot of polar surface area (PSA) versus ALogP for capsazepine and its derivatives showing the 95% and 99% confidence limit ellipses corresponding to the blood brain barrier (BBB) and intestinal absorption

3.3.CONCLUSION

It can be concluded that ((E)-2-(2-chlorobenzylidene) hydrazine-1-carbonyl cyanide [Mol.1], (E)-2-(4-bromobenzylidene) hydrazine-1-carbonyl cyanide [Mol.2], (E)-2-(2-bromobenzylidene) hydrazine-1-carbonyl cyanide [Mol.3], (E)-2-(4-methylbenzylidene) hydrazine-1-carbonyl cyanide [Mol.4], (E)-2-(2-methylbenzylidene) hydrazine-1-carbonyl cyanide [Mol.5], (E)-2-(4-chlorobenzylidene) hydrazine-1-carbonyl cyanide [Mol.6], (E)-2-benzylidene hydrazine-1-carbonyl cyanide [Mol.7] have better binding interactions with crystal Structure of the BRCT Domains of Human BRCA1 in Complex with a Phosphorylated Peptide from Human Acetyl-CoA Carboxylase 1(PDB: 3COJ.) The protein-ligand interactions' binding energies also confirm that the ligands are fitted tightly into the receptor's active pockets. The Silico ADMET study concludes that when compared to myricetin, both analogues have better profiles. As drug candidates that inhibit the human estrogen receptor, these can hold better promise. In the future, further development and modification of these analogues may lead to the production of new, highly potent anti-breast cancer drugs.

REFERENCES

[1] Salomon DS, Brandt R, Ciardiello F, Normanno N. Epidermal growth factor-related peptides and their

receptors in human malignancies. *Crit Rev Oncol Hematol.* 1995;19(3):183–232.

- [2] Goldsmith YB, Roistacher N, Baum MS. Capecitabine-induced coronary vasospasm. *J Clin Oncol.* 2008;26(22):3802–3804.
- [3] DeSantis C, Ma J, Bryan L, Jemal A. Breast cancer statistics, 2013. *CA Cancer J Clin.* 2014;64(1):52–62.
- [4] Li CI, Beaver EF, Tang MT, Porter PL, Daling JR, Malone KE. Reproductive factors and risk of estrogen receptor positive, triple-negative, and HER2-neu overexpressing breast cancer among women 20-44 years of age. *Breast Cancer Res Treat.* 2013;137(2):579–587.
- [5] Hughes, J.; Rees, S.; Kalindjian, S.; Philpott, K. Principles of early drug discovery. *Br. J. Pharmacol.* 2011, 162, 1239–1249.
- [6] Cava, C.; Colaprico, A.; Bertoli, G.; Bontempi, G.; Mauri, G.; Castiglioni, I. How interacting pathways are regulated by miRNAs in breast cancer subtypes. *BMC Bioinform.* 2016, 17, 111–133.
- [7] Cava, C.; Novello, C.; Martelli, C.; Lodico, A.; Ottobrini, L.; Piccotti, F.;

- Truffi, M.; Corsi, F.; Bertoli, G.; Castiglioni, I. Theranostic application of miR-429 in HER2+ breast cancer. *Theranostics* 2020, 10, 50–61.
- [8] Yang, Y.; Adelstein, S.J.; Kassis, I.A. Target discovery from data mining approaches. *Drug Discov. Today* 2009, 14, 147–154.
- [9] Meng, X.-Y.; Zhang, H.-X.; Mezei, M.; Cui, M. Molecular docking: A powerful approach for structure-based drug discovery. *Curr. Comput. Drug Des.* 2011, 7, 146–157.
- [10] McConkey, B.J.; Sobolev, V.; Edelman, M. The performance of current methods in ligand-protein docking. *Curr. Sci.* 2002, 83, 845–855.
- [11] Csermely, P.; Korcsmáros, T.; Kiss, H.J.; London, G.; Nussinov, R. Structure and dynamics of molecular networks: A novel paradigm of drug discovery: A comprehensive review. *Pharmacol. Ther.* 2013, 138, 333–408.
- [12] Ngo, H.X.; Garneau-Tsodikova, S. What are the drugs of the future? *MedChemComm* 2018, 9, 757–758.
- [13] Lin, X.; Li, X.; Lin, X. A Review on Applications of Computational Methods in Drug Screening and Design. *Molecules* 2020, 25, 1375.
- [14] Puratchikody A, Irfan N, Balasubramaniyan S. Conceptual design of hybrid PCSK9 lead inhibitors against coronary artery disease. *Biocatalysis and Agricultural Biotechnology.* 2019 Jan 1;17:427-40.
- [15] Balasubramaniyan S, Irfan N, Senthilkumar C, Umamaheswari A, Puratchikody A. The synthesis and biological evaluation of virtually designed fluoroquinolone analogs against fluoroquinolone-resistant *Escherichia coli* intended for UTI treatment. *New Journal of Chemistry.* 2020;44(31):13308-18.
- [16] Balasubramaniyan S, Irfan N, Umamaheswari A, Puratchikody A. Design and virtual screening of novel fluoroquinolone analogs as effective mutant DNA Gyrase inhibitors against urinary tract infection-causing fluoroquinolone resistant *Escherichia coli*. *RSC advances.* 2018;8(42):23629-47.
- [17] Ramalakshmi N, Arunkumar S, Balasubramaniyan S. QSAR and Lead Optimization. In *Computer Applications in Drug Discovery and*

Development 2019 (pp. 80-100).

IGI Global.

- [18] Umamaheswari A, Puratchikody A, Balasubramaniyan S. Target Identification of HDAC8 Isoform for the Treatment of Cancer. In Computer Applications in Drug Discovery and Development 2019 (pp. 140-172). IGI Global.
- [19] Balasubramaniyan S, Irfan N, Umamaheswari A, Puratchikody A. Design and virtual screening of novel fluoroquinolone analogs as effective mutant DNA GyrA inhibitors against urinary tract infection-causing fluoroquinolone resistant *Escherichia coli*. RSC advances. 2018;8(42):23629-47.